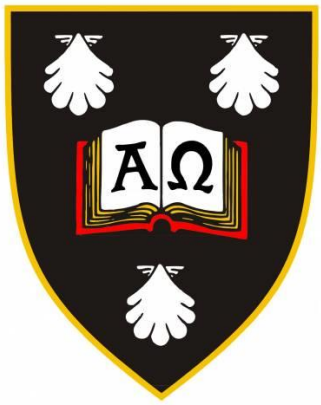
The evolution and role of Natural Killer (NK) cell subsets during acute HIV-1 infection and emerging SARS-CoV-2 infection

---

Submitted by: Aljawharah Alrubayyi

Candidate Number: 1210285





University of Oxford, Linacre College

Submitted in partial fulfilment of the requirements of the degree of

Doctor of Philosophy

in

Clinical Medicine

Trinity Term 2023

Supervised by: Professor Sarah Rowland-Jones, Associate Professor Dimitra Peppa, Professor Eduard J Sanders, and Associate Professor Joakim Esbjörnsson

The evolution and role of Natural Killer (NK) cell subsets during acute HIV-1 infection and emerging SARS-CoV-2 infection.

Aljawharah Alrubayyi, Trinity Term 2023

Abstract.

Natural killer (NK) cells are innate lymphocytes with potent antiviral capacities and are capable of mediating early protection against viral infections. In this thesis, I investigated NK cell responses in acute human immunodeficiency virus type 1 (HIV-1) infection and the newly emerged severe acute respiratory syndrome coronavirus 2 (SARS-CoV-2) infection. In the first part of this thesis, I performed an in-depth analysis of NK cell responses, including their phenotypic characteristics, antibody-dependent cellular cytotoxicity (ADCC) functions, and their relationship with T-cell activation, in a well-characterised cohort of patients acutely infected with different HIV-1 subtypes. This analysis demonstrated that subtype A infection is associated with a preferential increase in adaptive NK cells, characterised by an enhanced metabolic profile and a superior capacity for ADCC. The increased frequencies of adaptive NK cells were associated with lower HIV-1 viral load and higher $CD4^+$ T-cell counts, suggesting that adaptive NK cells could confer better HIV-1 control. In the second part of this thesis, I performed a comprehensive assessment of the NK cell repertoire, including their adaptive properties and their potential for Fc-dependent activation, in people living with HIV-1 (PLWH) following SARS-CoV-2 infection and/or vaccination. I evaluated NK cell responses in relation to the magnitude and breadth of T-cell and antibody responses to assess the interplay between NK cells and virus-specific T-cells. This analysis shows that adaptive NK cells contribute to vaccine-mediated responses in PLWH, so could be promoted to potentiate vaccine efficiency. Overall, the findings of this thesis contribute significantly to our understanding of the early innate and adaptive immune responses that occur during acute viral infections, their sustained responses after the viral resolution, and their role in promoting viral clearance following vaccination.

Acknowledgement

I have had the privilege to work with so many great people before and during my doctoral studies at Oxford. Without whom, this thesis would not have been made possible. Thank you! The list below acknowledges everyone involved.

Supervision

Sarah Rowland-Jones (Primary supervision)
Dimitra Peppa (Primary supervision)
Eduard J Sanders (Supervision)
Joakim Esbjörnsson (Supervision)

Funding

Saudi Ministry of Education (**Main funding**: Course fees & Research funding)
British HIV Association (Research funding)
UK Research and Innovation (Research funding)

University of Oxford

Elia Moreno-Cubero (Mentoring, Lab)
Jakub Kopycinski (Data, Collaboration)
Dan Hameiri-Bowen (Data, Collaboration)
Ester Gea-Mallorquí (Data, Collaboration)
Bethany Charlton (Data, Collaboration)
Karen Poxon (Lab Facilitation)

Kenya Medical Research Institute (KEMRI)

Amin Hassan (Data & Collaboration)

University College London

Emma Touizer (Data & Collaboration)
Laura E. McCoy (Collaboration)

Examiners

Tao Dong (Transfer, Confirmation & D.Phil *Viva*)
Susanna Dunachie (Transfer & Confirmation)
Upkar S. Gill (D.Phil *Viva*)

IAVI HIV Immunology Laboratories (HIL), Imperial college

Jill Gilmour (Collaboration)
Jonathan Hare (Collaboration)
Lucas Black (Assistance)
Julia Makinde (Assistance)
Liam Fletcher (Assistance)
Sarah Joseph (Assistance)

Scientific Career

Jeffrey E Teigler (Supervision, Pre-D.Phil.)
Dominic Paquin-Proulx (Supervision, Pre-D.Phil.)
Michael A Eller (Supervision, Pre-D.Phil.)

Friends & Family

Norah Alkannan (Support)
Saleh Alrubayyi (Support)
Hadeel Alrubayyi (Support)
Alaa Alrubayyi (Support)
Renad Alrubayyi (Support)
Hind Alrubayyi (Support)
Zaid Alrubayyi (Support)
Abeer Alharbi (Support)
Tayyaba Komal (Support)
And all other family members and friends

A final thanks to all study participants and clinical staff. Without whom, no science would be possible.

Statement of originality

I declare that the work presented within this thesis entitled “The evolution and role of Natural Killer (NK) cell subsets during acute HIV-1 infection and emerging SARS-CoV-2 infection” is my own. Contributions made by collaborators have been clearly acknowledged. I have not submitted this thesis in whole or in part for any other degree or qualification at The University of Oxford.

Aljawharah Alrubayyi

Trinity Term 2023

Table of Contents

Abstract. **1**

Acknowledgement **2**

Statement of originality **3**

List of abbreviations. **8**

Terminology / Glossary. **11**

Chapter 1: Introduction. **12**

1.1 Section 1: Acute HIV-1 infection. *13*
1.1.1 The human immunodeficiency virus. 13
1.1.2 Public health significance of HIV-1 infection and lack of effective vaccine. 14
1.1.3 Clinical outcomes and infection with different HIV-1 subtypes. 16
1.1.4 Dynamics of AHI. 19
1.1.5 The evolution of innate immune responses during AHI. 21
1.1.6 NK cells in viral infections. 23
1.1.7 NK cells in AHI. 33
1.1.8 T cells in viral infections. 38
1.1.9 T cells in AHI. 41

1.2 Section 2: SARS-CoV-2 infection in people living with HIV-1. ..... *44*
1.2.1 COVID-19 outcomes in PLWH. 44
1.2.2 Impact of HIV-1 infection on immune responses to SARS-CoV-2. 45
1.2.3 T-cell responses to SARS-CoV-2 in PLWH. 47
1.2.4 NK cell responses in SARS-CoV-2 infection. 49

1.3 Overall study aims *52*
1.3.1 Specific aims. 52

Chapter 2: Methods. **53**

2.1 General methods. *55*
2.1.1 Peripheral blood mononuclear cells (PBMC) and plasma sample preparation. 55
2.1.2 Serum isolation. 55
2.1.3 Thawing PBMCs samples. 56
2.1.4 NK and T-cell phenotypic flow cytometric analysis. 56
2.1.5 Statistical analyses. 60
2.1.6 High-dimensional data analysis. 61
2.1.7 Correlation analysis and heatmap visualisations. 61
2.1.8 Figure visualisations. 62

2.2 Methods for acute HIV-1 infection study (Chapters 3 and 4) *63*
2.2.1 Chapters 3 and 4 ethics statement. 63
2.2.3 Chapters 3 and 4 study subjects. 64
2.2.4 NK cell functional assay. 65
2.2.5 Measurement of soluble biomarkers. 68
2.2.6 Extracellular flux assays. 70
2.2.7 Mitochondrial membrane potential measurement. 71

2.3 Methods for SARS-CoV-2 infection study (Chapters 5 and 6). *72*
2.3.1 Chapters 5 and 6 ethics statement. 72
2.3.2 Chapters 5 and 6 study subjects. 73
2.3.3 IgG purification. 75
2.3.4 Semiquantitative S1 ELISA. 75
2.3.5 Pseudovirus production and neutralisation assays. 76
2.3.6 Standardised ELISA for measurement of CMV-specific IgG levels in plasma. 77
2.3.7 Production and purification of recombinant Spike. 77
2.3.8 Antibody-dependent NK activation assay. 78
2.3.9 *Ex vivo* IFN-γ ELISpot assay. 79
2.3.10 Intracellular cytokine stimulation (ICS) functional assay. 82
2.3.11 Cytokine bead assays. 84

Chapter 3: The NK cell landscape during acute HIV-1 infection with different subtypes. 85

Chapter 3 graphical abstract. *85*

Chapter 3 written abstract. *86*

3.1 Introduction. *87*

3.2 Results. *90*
3.2.1 The study cohort 90
3.2.2 Subtype A is associated with slower disease progression in treatment-naïve participants. 94
3.2.3 Distinct NK cell signatures in subtype A and non-A subtype infection during AHI 98
3.2.4 The early antibody-dependent NK cell-mediated cytotoxicity response is associated with low viral load in AHI. 105
3.2.5 Enhanced mitochondrial oxidative phosphorylation is associated with ADCC capacity. 107
3.2.6 Subtype A future controllers exhibit higher frequencies of $CD38^{+}NKG2A^{-}$ adaptive NK cells 1 month after EDI. 112

3.3 Discussion. *116*

Chapter 4: The evolution of T-cell responses during acute HIV-1 infection. 122

Chapter 4 graphical abstract. *122*

Chapter 4 written abstract. *123*

4.1 Introduction. *124*

4.2 Results. *127*
4.2.1 The magnitude of $CD8^{+}$ T-cell activation correlated with HIV-1 viraemia during the first month of infection. 127
4.2.2 $CD4^{+}$ T-cell activation correlated with $CD4^{+}$ T-cell count. 130
4.2.3 Future viral controllers demonstrated an expansion of $CD127^{+}TCF\text{-}1^{+}CCR7^{+}CD45RA^{+}$ $CD8^{+}$ T cells. 132
4.2.4 Distinct NK and T-cell relationships between subtype A and non-A subtype infections during early HIV-1 infection. 136

4.3 Discussion. *139*

Chapter 5: Characterisation of T-cell responses in PLWH following SARS-CoV-2 infection and vaccination. . 143

Chapter 5 graphical abstract. *143*

Chapter 5 written abstract. *144*

5.1 Introduction. *145*

5.2 Results. *149*

5.2.1 Section 1: Adaptive immune responses in convalescent SARS-CoV-2 infection. 149
5.2.1.1 Study cohort. 149
[C] Participants who had organ transplantation, including renal or liver transplantation. 151
5.2.1.2 Levels of SARS-CoV-2 antibodies during the convalescent phase. 152
5.2.1.3 The magnitude of SARS-CoV-2-specific T-cell responses in the convalescent infection. 154
5.2.1.4 T-cell and antibody response complementarity in the convalescent infection. 157
5.2.1.5 SARS-CoV-2-specific T-cell responses are dominated by $CD4^+$ T cells in convalescent individuals. 160
5.2.1.6 Immune profile relationships between convalescent PLWH and HIV-negative individuals. 164

5.2.2 Section 2: Adaptive immune responses in SARS-CoV-2 vaccination. 167
5.2.2.1 Study cohort. 167
5.2.2.2 Levels of SARS-CoV-2 antibodies after SARS-CoV-2 immunisation. 170
5.2.2.3 The magnitude of SARS-CoV-2-specific T-cell responses after SARS-CoV-2 vaccination. 173
5.2.2.4 T-cell responses are induced in a proportion of PLWH who had low or absent nAbs (ID_{50} <150) following vaccination. 182
5.2.2.5 PLWH with suboptimal antibody responses demonstrate an expansion of $CXCR3^+CD127^+$ $CD8^+$ T cells after two doses of SARS-CoV-2 vaccination. 184
5.3 Discussion. 191

Chapter 6: NK cell responses during SARS-CoV-2 infection and vaccination in PLWH. 201

Chapter 6 graphical abstract. 201

Chapter 6 written abstract. 202

6.1 Introduction. 203

6.2 Results. 205
6.2.1 Study cohort. 205
6.2.2 Increased frequencies of adaptive NK cells following SARS-CoV-2 infection in PLWH 207
6.2.3 Longitudinal assessment of NK cells in PLWH following SARS-CoV-2 vaccination. 214
6.2.4 Antibodies induced by SARS-CoV-2 vaccination can trigger antibody-mediated NK cell responses in PLWH. 219
6.2.5 Antibody-dependent NK cell responses are enriched in adaptive NK cell subsets. 224

6.3 Discussion. 230

Chapter 7: Concluding remarks and future directions. 236

7.1 Section 1: acute HIV-1 infection. 237
7.1.1 Engaging innate immunity in HIV-1 vaccine and cure strategies. 237
7.1.2 Future directions in studies of NK cell responses during AHI. 240
7.1.3 Antigen-specific NK cell responses in AHI, so much more to learn. 242
7.1.4 Implications for vaccine design. 244
7.1.4 Implication for therapeutic strategies. 245
7.1.5 Virus-specific T-cell responses to different HIV-1 subtypes. 249
7.1.6 The interaction of NK cells with other immune cells and their impact on lymphoid organs. 252
7.1.7 Defining the balance between protective versus pathological/ immunoregulatory responses of NK cells. 254

7.2 Section 2: SARS-CoV-2 infection and vaccination in PLWH. 258
7.2.1 Future studies in T-cell responses to SARS-CoV-2 in PLWH. 258
7.2.2 NK cell responses in the context of introducing another virus in PLWH. 260
7.2.3 Remaining questions in NK cell responses during SARS-CoV-2 infection. 261
7.2.4 Adaptive NK cell responses: implication for future vaccine strategies. 264

7.3 Overall contribution. 266

7.4 Conferences, symposiums and publications during D.Phil. studies. *266*
7.4.1 Publications. 266
7.4.2 Conferences and workshops. 267
7.4.3 Awards. 269

References. **270**

List of abbreviations.

2-DG - 2-Deoxy-Glucose
ADCC - Antibody-Dependent Cellular Cytotoxicity
AHI - Acute HIV-1 Infection
AIDS - Acquired Immune Deficiency Syndrom
ANOVA - Analysis of Variance
APC - Antigen Presenting Cells
ART - Anti-Retroviral Therapy
AZ - AstraZeneca
bnAbs - Broadly Neutralising Antibodies
CCL3 - Chemokine (C-C motif) Ligand 3
CCL4 - Chemokine (C-C motif) Ligand 4
CCL5 - Chemokine (C-C motif) Ligand 5
CCR5 - C-C Chemokine Receptor type 5
CCR7 - C-C Chemokine Receptor type 7
CD - Cluster of Differentiation
CIML - Cytokine-Induced Memory-Like NK cells
CM - Central Memory
CMV - Cytomegalovirus
COVID-19 - Coronavirus Disease 2019
CTL - Cytotoxic T Lymphocytes
CXCL10 - C-X-C motif Chemokine Ligand 10

CXCR3 - Chemokine Receptor 3
CXCR31 - CX3C Motif Chemokine Receptor 1
CXCR4 - C-X-C Chemokine Receptor Type 4
CXCR5 - C-X-C Chemokine Receptor Type 5
DC - Dendritic Cell
DMEM - Dulbecco's Modified Eagle Medium
DNA - Deoxyribonucleic Acid
DPSO - Days Post-Symptom Onset
EAT-2 - EWS Activated Transcript 2
ECAR - Extracellular Acidification Rate
ECDC - European Centre for Disease Prevention
EDI - Estimated Date of Infection
EDTA - Ethylene Diamine Tetra Acetic Acid
EM - Effector Memory
Env -Envelope
ETC- Electron Transport Channel
FAB - Fragment Antigen Binding
FasL - Fas Ligand
FBS - Foetal Bovine Serum
FCCP - Carbonyl Cyanide-4 (Rrifluoromethoxy) Phenylhydrazone
FcεRγ - FcεRI Gamma Chain
FlowSOM - Flow Clustering and Visualisation Algorithm based on a Self-Organising Map

FRESH - Females Rising through Education, Support, and Health
GCP - Good Clinical Practice
GP - Glycoprotein
GRAP2 - GRB2 Related Adaptor Protein 2
GZMB - Granzyme B
HBV - Hepatitis B
HEPES - N-2-Hydroxyethyl Piperazine-N-2 Ethane Sulfonic Acid
HIL - Human Immunology Laboratory
HIV-1 - Human Immunodeficiency Virus Type 1
HLA - Human Leukocyte Antigens
HLA-DR - Human Leukocyte Antigen – DR Isotype
HLA-E - HLA Class I Histocompatibility Antigen, alpha Chain E
HCMV - Human Cytomegalovirus
IAVI - International AIDS Vaccine Initiative
ICAM2 - Intercellular Adhesion Molecule 2
ID_{50} - 50% Inhibitory Serum Dilution
IFI44 - Interferon (IFN)-Inducible Protein 44
IFI6 - Interferon-alpha Inducible Protein 6
IFN - Interferon
IFN-I - Type I Interferon
Ig - Immunoglobulin
IL - Interleukin

IL-7Rα - IL-7 Receptor Alpha Expressing
ILC - Innate Lymphoid Cell
ISG - Interferon-Stimulated Genes
KIR- Killer Immunoglobulin-Like Receptors
KLRG1 - Killer Cell Lectin-Like Receptor G1
(LRAs) - Latency Reversing Agents
LTR - Long Terminal Repeats
LPS - Lipo-Poly Saccharide
M - Membrane
MHC - Major Histocompatibility Complex Class I
MM - Mitochondrial Mass
MSD - Meso Scale Discovery
MSM - Men who Have Sex with Men
MX1 - MX Dynamin Like GTPase 1
N - Nucleocapsid
NCR- Natural Cytotoxicity Receptors
nAbs - Neutralising Antibodies
NHP - Non-Human Primates
NK - Natural Killer
NKG2 - Natural Killer Group 2
OCR - Oxygen Consumption Rate
ORF - Open Reading Frame
OXPHOS - Oxidative Phosphorylation
PBMC - Peripheral Blood Mononuclear Cell
PBS - Phosphate Buffered Saline
PD-1 - Programmed Cell Death 1

PLWH - People Living With HIV-1
PLZF - Promyelocytic Leukaemia Zinc Finger
Pol - Polymerase
PRF1 - Perforin
RNA- Ribonucleic Acid
S - Spike
SARS-CoV-2 - Severe Acute Respiratory Syndrome Coronavirus 2
Siglec-7- Sialic Acid Binding Ig-like Lectin 7
SIV - Simian Immunodeficiency Virus
SHIV - Simian Human Immunodeficiency Virus
SPICE - Simplified Presentation of Incredibly Complex Evaluations
SRC - Spare Respiratory Capacity
SYK - Spleen Tyrosine Kinase
T/F- Transmitted Founder
TCF-1 – T-cell Factor 1
TCF-7 – T-cell Factor 7
TEMRA - Terminally Differentiated Effector Memory
T_{FH} - Follicular Helper T cells
TGF-β1- Transforming Growth Factor-β1
T_H1 - T Helper Cell Type 1

T_H2 - T Helper Cell Type 2
TIGIT – T-cell Immunoreceptor with Ig and ITIM Domains
TIM-3 – T-cell Immunoglobulin and Mucin-domain Containing-3
TMRM – Tetra-Methyl-Rhodamine, Methyl Ester
TNF-α - Tumour Necrosis Factor-Alpha
TRAIL - Tumour Necrosis Factor (TNF)- Related Apoptosis-Inducing Ligand
Tregs - T Regulatory Cells
USA - United States of America
VA – Virginia State
VISCONTI - Viro-Immunological Sustained Control after Treatment Interruption
viSNE - Visual Interactive Stochastic Neighbour Embedding
VL- Viral Load
VOC - Variants of Concern
WHO - World Health Organisation
WT – Wild Type
XAF1 – XIAP Associated Factor 1
ZAP70 – Zeta Chain Associated Protein Kinase 70

Terminology / Glossary.

The following terms will be used throughout this thesis:

Chapters 3 and 4:

Hyperacute HIV-1 infection*: The period between HIV-1 acquisition and the development of anti-HIV-1 antibodies (detected by enzyme-linked immunosorbent assay (ELISA) or on western immunoblot) (Fiebig stage I and II)

Acute HIV-1 infection*: The stage following seroconversion and during the first few months of HIV-1 infection (Fiebig stages III-V). In studies presented in Chapters 3 and 4, AHI was defined as the period between the first detectable virus and up to three months post-infection.

Chronic HIV-1 infection: The stage between acute and the onset of AIDS.

Chapters 5 and 6:

The convalescent phase of SARS-CoV-2 infection: The stage after recovery from COVID-19 infection where viral RNA becomes undetectable in the peripheral blood.

Prior SARS-CoV-2 infection: Individuals who had confirmed SARS-CoV-2 diagnosis (SARS-CoV-2 PCR and/or Roche antibody tests) prior to their vaccination.

SARS-CoV-2 naïve: Individuals who had no history of SARS-CoV-2 infection prior to their vaccination.

* A limitation to these definitions is that there is no clear or widely accepted definition of AHI. The definitions here are based on published literature defining the stages of AHI and on published work in the IAVI Protocol C cohort (cohort used in this thesis) and other similar AHI cohorts (1–6).

Chapter 1: Introduction.

Publication.

Alrubayyi A, *et al.* Natural killer cells during acute HIV-1 infection: clues for HIV-1 prevention and therapy. AIDS Lond Engl. 2022 July 11.

- Figures were reproduced under license (a Creative Commons Attribution 4.0 International License)

Chapter 1

1.1 Section 1: Acute HIV-1 infection.

1.1.1 The human immunodeficiency virus.

HIV is a lentivirus of the retrovirus family with a genome that consists of two single-stranded RNA molecules enclosed within the core of each virus particle. There are two main strains of HIV: HIV-1 and HIV-2. In this thesis, I focus on HIV-1 as it is the more dominant and pathogenic strain (7). The HIV-1 genome is approximately 9.2 kb and consists of two open reading frames (ORF), which code for the promotor for transcription of the viral genes (8). The reading frame of the *gag* gene encodes the outer core membrane proteins, capsid protein (p24), nucleocapsid, and a smaller nucleic acid-stabilising protein. Following the *gag* reading frame, the *pol* reading frame codes for protease, reverse transcriptase, and integrase. The *env* reading frame is adjacent to the *pol* gene, and it encodes the two envelope glycoproteins gp120 (surface protein) and gp41 (transmembrane protein). In addition to the structural proteins, the HIV-1 genome encodes regulatory proteins, including Nef (negative regulating factor), Tat (trans-activator protein), and Vpr/Vpu (virus protein r/unique), which have an important role in HIV-1 replication and immune evasion (8).

Life cycle: HIV-1 is a retrovirus and is, therefore, able to integrate its DNA into the host genome, making it challenging to eradicate with current treatments. Despite its limited number of proteins, the virus is highly efficient in its structure. After entering a host cell, the single-strand RNA is reverse-transcribed into HIV-1 DNA which is then integrated into the host DNA (1,6,7). Using host enzymes,

HIV-1 RNA is transcribed, viral proteins are produced, and mature HIV-1 virions are released. These steps can be inhibited therapeutically using available inhibitors that target HIV-1 entry, reverse transcriptase, integrase, and protease.

1.1.2 Public health significance of HIV-1 infection and lack of effective vaccine.

The global outbreak of HIV-1 in 1980s has resulted in more than 39 million HIV/AIDS-related deaths; currently, an estimated 38 million people are now living with HIV-1 worldwide (9). Despite significant progress made in worldwide treatment coverage and preventive measures, approximately 1.5 million people become newly infected with HIV-1 every year (10,11). HIV-1 infection remains a significant contributor to global morbidity and mortality, with a disproportionate burden of disease concentrated in sub-Saharan Africa (12). Its toll on human health and global healthcare systems cannot be readily quantified (7).

On the individual level, If untreated, HIV-1 infection causes progressive depletion of $CD4^+$ T cells, multiple immunological dysfunctions and major tissue damage, leading to an increased risk of clinical complications (7). The natural history of untreated HIV-1 infection varies between individuals, with multiple factors contributing to these variations, including both viral and host factors (13). After HIV-1 exposure, HIV-1 spreads within days to the lymphoid organs and becomes detectable in blood within 1-2 weeks (14). The viral peak is often achieved within 3-5 weeks, followed by the induction of immune responses mediating some degree of control, leading to a stable level of viraemia, known as the ‘set-point’

(15). During the early stages of the infection, HIV-1 integrates into the host genome through mechanisms that are not fully defined and establishes a long-lived viral reservoir (16). After several years, profound immunodeficiency emerges in untreated individuals, leading to the development of infectious or oncological clinical complications (7), known as AIDS. The rate of progression to AIDS or AIDS-related death varies among HIV-1 individuals, with a rare subset of patients that can mediate natural control of infection (7).

Combination anti-retroviral treatment (ART) has transformed the prognosis of HIV-1 infection, transforming it from a life-threatening illness to a manageable chronic condition. Adherence to ART effectively suppresses viral replication, enhances the lifespan of infected individuals, prevents progression to AIDS, and reduces the risk of transmission (17). However, despite these advantages, limitations in medication access and challenges with adherence remain significant barriers to ending the HIV-1 epidemic through ART alone. Additionally, the risk of disease progression and increased virus transmission re-emerge in the majority of people with HIV-1 upon cessation of ART, due to the viral rebound from persistent reservoirs, requiring lifelong adherence to ART (2). Such key limitations highlight the critical need for an effective and durable HIV-1 vaccine, in addition, to cure strategies. Thus, there is an urgent need to redirect efforts towards understanding the determinants of HIV-1 immune control, especially during the early stage of infection, and the mechanisms underlying the failure of such control to inform the development of novel HIV-1 preventive and therapeutic strategies.

1.1.3 Clinical outcomes and infection with different HIV-1 subtypes.

A main challenge to immune containment and vaccine development is the high genetic diversity within the HIV-1 genome, which is known to be steadily increasing over time, both within and between subtypes (18–21). In light of such variation, different HIV-1 subtypes have been identified and were classified into three HIV-1 groups: major (M), outlier (O), and nonmajor and nonoutlier (N), with the group M being the predominant circulating form (22). Group M has been divided into subtypes, also called clades, denoted with letters (A, B, C, D, F, G, H, J, K) and circulating recombinant forms. HIV-1 subtypes are phylogenetically linked variants of HIV-1 with 25-35% and 15%-20% genetic variation between and within HIV-1 subtypes, respectively (23). These HIV-1 subtypes have expanded rapidly, leading to multiple regional epidemics **(Figure. 1.1)** (23). The global distribution of HIV-1 subtypes across the world varies, with subtype B being the dominant variant in North America and Europe and subtypes A, C, and D, and inter-subtype recombinants are most prevalent in the African continent (21). The highest HIV-1 genetic diversity has been reported in West and Central Africa; however, other African regions show an assortment of diverse viral subtypes (21). Subtype C generally predominates in Southern Africa, whereas subtype A is most prevalent in Eastern Africa, although co-circulation of subtypes D and C have also been reported in this region (24,25).

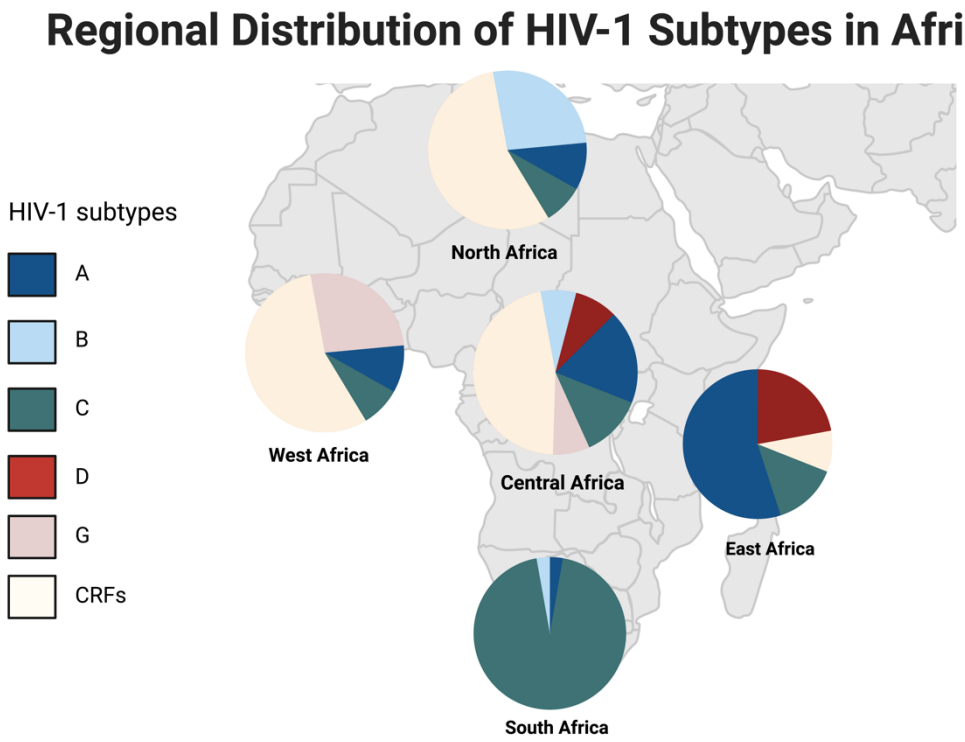


Figure 1.1. Regional distributions of HIV-1 subtypes in Africa.

Map representing four different regions (North, East, Central, and West Africa). Each pie chart represents the proportion of people living with HIV-1 infected with a certain subtype in each region. HIV-1 subtypes are colour-coded. CRFs = Circulating Recombinant Forms, including CRF01_AE, CRF01_AG, and other CRFs. Adapted from (19).

Differences in the rates of transmission and disease progression between HIV-1 subtypes could potentially account for their distinct prevalence and expansion patterns. Studies in East Africa, where subtypes A and D co-circulate, demonstrated that subtype A is associated with lower disease progression compared to subtype D (26–30). Additional study in International AIDS Vaccine Initiative (IAVI) Protocol C cohort (the cohort used in the analysis presented in future chapters) showed that individuals infected with subtypes D and C reached

a high viral load (log_{10} VL> 5) more rapidly and progressed faster to AIDS compared to subtype A (31). Additionally, subtype A infection is associated with a slower rate of $CD4^+$ T-cell count decline to 350 cells/mm^3 (in the absence of ART) and a lower risk of mortality compared to subtypes D and C (29,31–33). A follow-up analysis in the IAVI Protocol C cohort showed that individuals with subtype A infection had increased odds of long-term viral control compared to subtypes C and D (33). More recently, Professor Eduard J Sanders (Kilifi, Kenya), one of the principal investigators in the study, and colleagues demonstrated that acute retroviral syndrome (ARS) symptoms were significantly more prevalent during acute and early infection with subtype A virus than with either subtype C or D infections (34). Hassan and Esbjörnsson *et al*., also collaborators and a principal investigator in the study, showed that stronger innate immune responses during hyperacute HIV-1 infection were associated with ARS (5), suggesting that clinical presentations and outcomes reflect differences in virus-host interactions.

Differential disease progression rates and the prevalence of subtypes have important implications for future projections of the pandemic and for the development of preventative or therapeutic strategies. Variations in the structural and regulatory gene sequences between different HIV-1 subtypes can lead to functional and biological differences (35). *Ex vivo* competition assays of limited numbers of HIV-1 viral isolates have indicated that subtype C (from Africa) is less fit than subtype A and B (36–38), and recombinant viruses are fitter than their parental forms (39,40). More recently, analysis of more than 100 clinical isolates

showed that subtype D had higher Pol-driven replication capacity than subtype A, and these differences were linked with disease progression (41). Subtype-specific differences in Nef function have been reported in AHI and showed that Nef functional differences correlated with the down-regulation of CD4 and HLA class I molecules (42,43). Taken together, these results suggest that genetic variation within HIV-1 subtypes could contribute to subtype-specific differences in protein function; however, the implications of these factors on host immune responses and disease progression remain unclear.

1.1.4 Dynamics of AHI.

The initial exposure to an HIV-1 subtype, the so-called transmitted founder (T/F) virus strain(s), results in the establishment of a new infection. New HIV-1 infections are mostly established by sexual exposure through the mucosa of the genital tract or rectum, although small proportions of new infections can occur by percutaneous or intravenous inoculations (1,44). The inoculum, such as semen, cervicovaginal secretions, or infected blood, contains a complex genetic quasi-species of HIV-1 variants, of which a small number are likely to breach mucosal barriers and establish a new infection (1). The vast majority of new infections in heterosexuals and men who have sex with men are established by a single virion (T/F virus) despite the presence of multiple variants in the donor (45). Certain genetic and phenotypic characteristics which can facilitate viral transmission are selected for in the T/F viruses, including some genetic signatures in the *env* region, which plays a key role in the internalisation of the infecting virus (45). The *env* sequence in the chronically infected sexual partner was shown to be identical

to that of the T/F virus identified in the newly infected partner (46), although it is not always the most common variant in the partner. In subtype C, the T/F *env* protein can skew innate inflammatory responses in their favour to facilitate viral transmission (47).

Following HIV-1 transmission, there is a period of 3-10 days, known as the eclipse phase, in which the viral RNA is undetectable in the plasma, but the virus is actively replicating in the mucosal and lymphoid tissues **(Figure. 1.2)** (48). At the end of the eclipse phase, HIV-1 reaches the draining lymph node and interacts with activated $CD4^+$ T cells, which are one of the main targets for further HIV-1 infection, resulting in an increased viral replication and rapid spread of the virus throughout the body (48). While HIV-1 is replicating in the lymphoid tissues, there is an exponential increase in the plasma viral load, generally, to more than a million viral RNA copies, reaching a peak at 14-28 days after HIV-1 transmission, representing a period that is known as peak viraemia (48). Following peak viraemia, the viral load declines to reach a more stable level, plasma viral load (pVL) set-point (49,50). In the absence of ART, the cumulative virus and host balance following these early events are critical to determine and maintain the level of viral replication, which strongly predicts the long-term outcomes of HIV-1 infection **(Figure. 1.2)** (48).

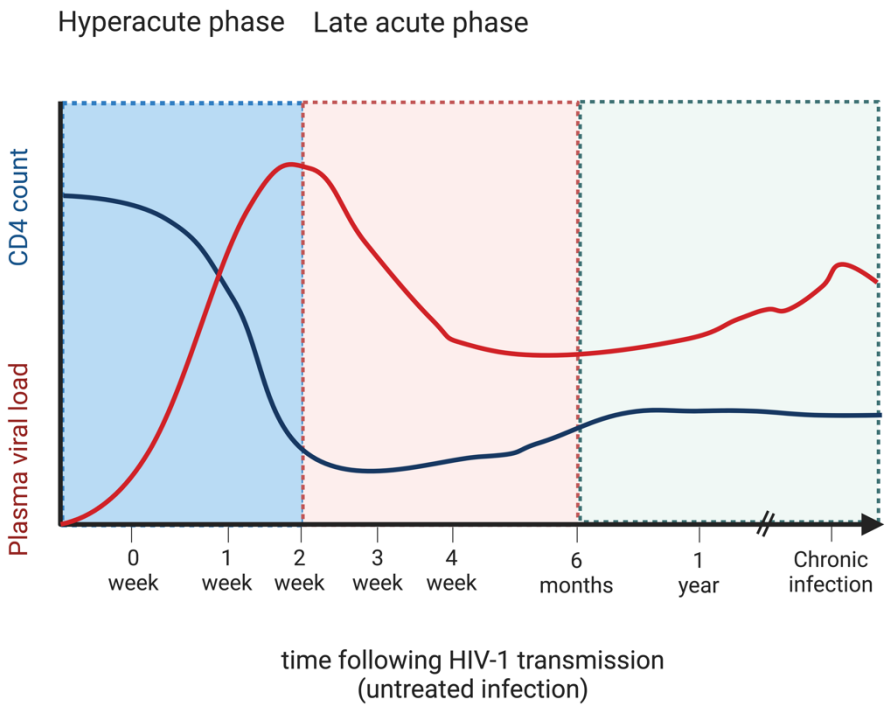


Figure 1.2. Dynamics of acute HIV-1 infection.

Graph representing the dynamics of plasma viral load and peripheral $CD4^+$ T-cell counts during early HIV-1 infection in untreated individuals. The time between infection and the first detection of viral RNA in the plasma is referred to as the eclipse phase. The level of plasma viral load then increases exponentially, peaking at 2-3 weeks following infection, and then gradually declines, reaching the VL set-point.

1.1.5 The evolution of innate immune responses during AHI.

Our knowledge of immune responses during acute infection has been hampered by the fact that identifying infected individuals within the first weeks of infection is challenging. Most of our understanding of the evolution of the early immune response has largely been drawn from studies in non-human primates (NHPs), such as macaques with simian immunodeficiency virus (SIV) or simian-human

immunodeficiency virus (SHIV) infection, which recapitulate many of the immunological and clinical hallmarks of HIV-1 infection in humans (51). However, some studies in sub-Saharan Africa or other regions of high HIV-1 incidence have provided unique opportunities for understanding the early human immune responses and viral evolution that emerge after the onset of HIV-1 viraemia (6). Examples include the RV217 and RV254 studies in Thailand and Africa and the Females Rising through Education, Support, and Health (FRESH) study in South Africa, in which uninfected persons at high risk of infection were screened twice weekly and monitored for HIV-1 incidence (3,52). Additionally, the IAVI Protocol C study, which enrolled recently infected HIV-1 individuals across five sub-Saharan African countries with various risks for HIV-1 infection and diverse HIV-1 subtypes, represents a unique opportunity to characterise early immune responses to different HIV-1 subtypes. In addition to frequent testing of individuals at high risk of HIV-1 infection, one strategy that was used in the Protocol C study to identify AHI was testing young adults (<30 years) who met pre-defined AHI criteria, including fever, sexually transmitted disease symptoms, diarrhoea, body pains or multiple partners, and sought care at pharmacies and health facilities (53). This approach allowed for the identification of individuals with AHI and demonstrated that AHI was as prevalent as malaria in coastal Kenya (one of the most highly malaria-endemic regions of the world) (53). Together, close monitoring and employing AHI detection strategies targeting key populations in high-transmission settings facilitated the establishment of unique cohorts of AHI to identify and address unmet needs for health care, counselling and prevention among these key populations and to understand host-virus

interactions both shortly after virus acquisition and in the longer-term (more details of the IAVI Protocol C cohort are provided in Chapter 2, section 2.2.3) (4).

In NHP models, the initial exposure to SIV leads to local viral replication within hours with a rapid systemic spread of the virus (within 1-3 days) (54,55). This is combined with robust systemic inflammation, upregulation of type I interferon (IFN-I) signalling, and induction of pro-inflammatory and antiviral cytokine and chemokines, including IFN-α, CXCL10 (also known as IP-10) (54,56,57). Comparisons between pathogenic SIV infection (leads to AIDS) in rhesus macaques and non-pathogenic SIV infection in African green monkeys demonstrated that the timing of pro-inflammatory and antiviral responses in both the tissues and periphery is linked to disease progression (6,57). While these inflammatory responses, along with the upregulation of IFN-stimulated genes (ISG), gradually decline and, in some cases, return to the baseline level within the first few months in non-pathogenic SIV, such responses persist for weeks and years in pathogenic SIV infection (57). Similarly, longitudinal analysis of immune responses in the FRESH cohort showed a persistent ISG response (58). The level and profile of the induced cytokines in early infection can significantly impact subsequent immune activation and directly or indirectly influence the disease course (59,60).

1.1.6 NK cells in viral infections.

Following viral infections, the increased levels of inflammatory cytokines, including interleukin (IL)-8, IL-12, and IL-15, can activate cellular innate immune

responses (54,56,57). Innate immune cells are the first line of defence against viral infections, which contribute to the containment of viral replication and determine the level of immune activation and subsequent disease outcomes (61). Natural killer (NK) cells represent a key cellular component of innate immunity and contribute to the early control of viral replication, modulating the pathogenesis of different viral infections. NK cells were originally described almost 50 years ago as innate cytotoxic lymphocytes and a type of innate lymphoid cell (ILC) (62). Their fundamental roles in recognition of target cells, mediating cytotoxic killing of virus-infected cells, and controlling viral replication, as well as their ability to regulate activation and maturation of other immune subsets, have put NK cells as a key focus for research and a promising target for novel immunotherapeutic approaches.

NK cells occupy a unique niche in the immune system, bridging innate and adaptive immune responses (63). The anatomical site for NK cell development is the bone marrow, in which the interaction with other immune cells, growth factors, and soluble mediators drives NK cell development (64). NK cell activation is tightly regulated by integrating signals from an array of germline-encoded inhibitory and activating receptors (65). This dynamic balance ensures self-tolerance whilst permitting robust responses against virally infected cells that have downregulated major histocompatibility complex class I (MHC I) molecules that ligate NK-expressed inhibitory receptors, such as killer immunoglobulin-like receptors (KIRs) and CD94/NKG2A, and/or upregulated stress ligands or viral associated molecules recognised by activating receptors, such as NKG2D or

natural cytotoxicity receptors (NCRs) (66,67). During NK cell development, the interaction between inhibitory receptors and self-MHC molecules is critical for promoting their education and fine-tuning their level of responsiveness (68,69).

1.1.6.1 NK cell-mediated recognition of viral infections.

In viral infections, NK cells sense the inflammatory signals and viral ligands through multiple mechanisms **(Figure. 1.3)**. During the early phase of infection, there is a substantial upregulation of NK cell cytokine receptors which sense inflammatory cytokines, including IFN-α, IL-15, IL-18, and IL-12, through ligand-receptor interactions (70). The majority of NK cell subsets express multiple cytokine receptors, indicative of a universal role for the cytokine–cytokine receptor axis in the NK cell-mediated recognition of viral infections (70). In addition to NK cell activation, pro-inflammatory cytokines, particularly IL-12, IL-18, and IL-15, provide crucial signals for NK cell proliferation, differentiation and effector functions, including IFN-γ production, which represents a key stimulus for the subsequent activation/maturation of other immune cells (70). The expression of the low-affinity immunoglobulin G receptor FcγRIII (CD16) mediates NK cell activation in response to the antibody-coated target cells, a process known as “antibody-dependent cellular cytotoxicity” (ADCC) (62,70). The downregulation of self-antigens such as MHC-I molecules on the surface of infected or stressed cells and/or upregulation of stress ligands or viral-associated molecules can lead to NK cell activation through interaction with activating or inhibitory receptors (66,67).

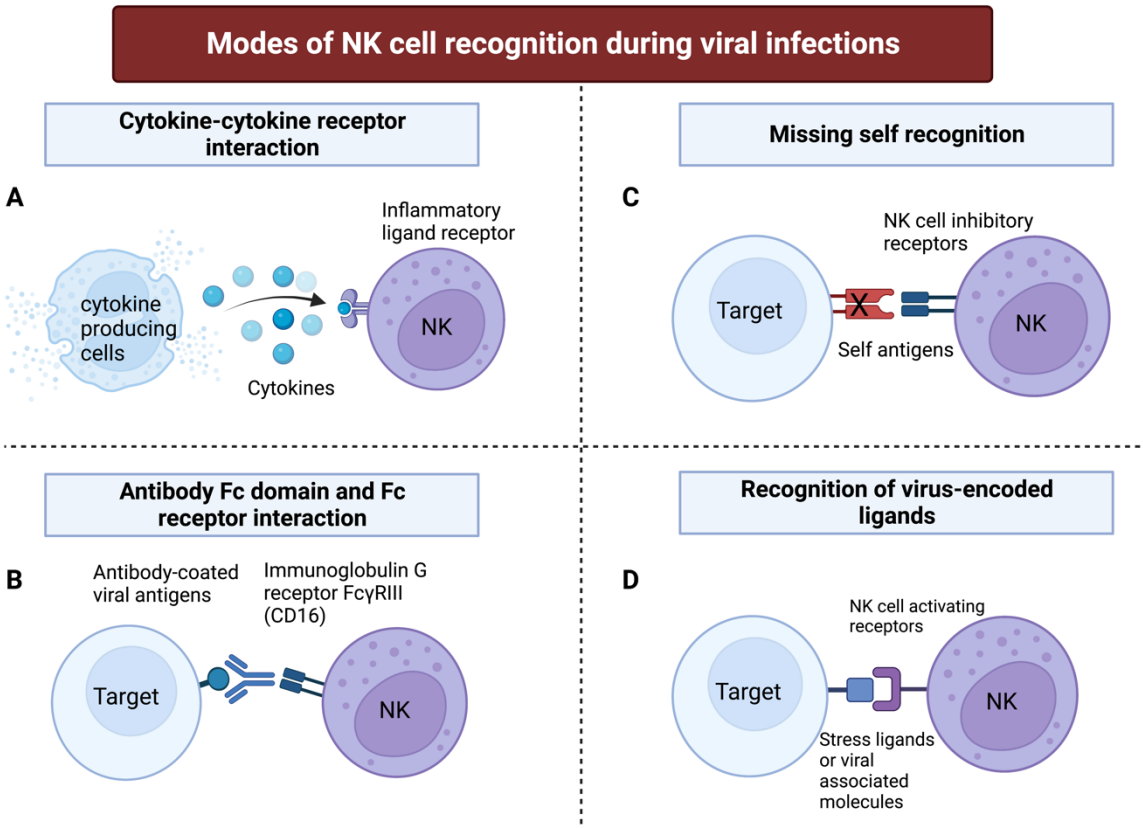


Figure 1.3. Mechanisms of NK cell recognition in viral infections.

A. NK cells can be activated by cytokines, such as IFN-I, IL-15, IL-12 or IL-18, secreted by other immune cells. **B.** NK cells can be activated by antibody-coated target cells that cross-link the CD16 receptor expressed on the surface of NK cells. **C.** Missing or downregulating self-antigens such as MHC-I on stressed cells can lead to NK cell activation. **D.** Recognising stressed infected cells expressing virus-encoded ligands that engage NK cell activating receptors, such as NKG2D, can activate NK cell functions.

1.1.6.2 Roles of NK cells in immunity to viral infections.

1.1.6.2.1 Direct antiviral response.

Upon stimulation and recruitment to the site of the infection, NK cells exert cytotoxicity via exocytosis of cytolytic granules or perforin-mediated mechanisms or pathways involving the engagement of extracellular death receptors (e.g. Fas,

TRAIL-Rs) on target cells (71,72), or indirectly through ADCC (63). During viral infections, the Fab domain of antigen-specific antibodies binds to viral antigens expressed on the surface of infected cells, while the Fc domain of antibodies cross-links NK cell CD16 Fc receptors, triggering the secretion of cytolytic granules, cytokines and chemokines (73). These cytotoxic granules, particularly perforin and granzyme B, cause cell permeabilisation, cell cycle disruption, and DNA damage, mediating the killing of target cells (74). In viral infections, NK cell-mediated cytotoxicity is particularly crucial for controlling viral replication and has been associated with viral control in the context of different viral infections.

1.1.6.2.2 Immunoregulatory capacity of NK cells.

In addition to eliminating target cells, increasing evidence has highlighted the functions of NK cells in the activation and regulation of adaptive immune responses **(Figure. 1.4).** NK cells promote the survival, function and maturation of antigen-presenting cells (APC) through the secretion of cytokines and chemokines, including IFN-γ and TNF-a, or via direct cell-cell contact. Along these lines, NK cells facilitate noncanonical interactions with dendritic cells (DCs) through a process called “DC editing” (75). NK cells selectively target immature DCs while sparing and supporting the differentiation of mature DCs for more efficient antigen presentation (76). Additionally, NK cells produce cytokines and chemokines that can mediate immunosuppression or immunomodulation of antigen presentation (77). Whereas NK cell-mediated regulation of APCs can indirectly shape adaptive immune responses, NK cells can have a direct impact on the development of adaptive immunity, either positively or negatively **(Figure.**

1.4). NK cell-derived IFN-γ primes $CD4^+$ T-cell polarisation and the induction of T helper cell type 1 (T_H1) responses (78,79). IFN-γ production by NK cells promotes IL-12 secretion by DCs, which induces long-lived memory $CD8^+$ T-cell responses (80,81). Engagement of NK cell activating receptors, such as NKG2D, with their ligands expressed on the surface of activated $CD8^+$ T cells leads to the elimination of activated T cells. Notably, the early depletion of NK cells in acute murine cytomegalovirus (CMV) infection results in a larger pool of $CD8^+$ T cells with IL-7 receptor alpha (IL-7Rα) expressing memory precursor effector cells capable of generating long-lived memory responses (82). This phenomenon has also been observed in lymph nodes, in which triggering NK cell trafficking to T-cell-rich areas via CXCR3-CXCL10 interactions limits virus-specific T-cell responses (83). In humans, previous studies have shown how NK cells can limit hepatitis B virus (HBV)-specific T cells and modulate the induction of broadly neutralising antibodies in HIV-1 infection (72,84). NK cell regulation of $CD4^+$ T cells can influence T-cell-dependent humoral responses, including germinal centre (GC) responses (75). NK cells suppress B cell maturation, IgG class switching and the production of neutralising antibodies by impairing the development of $CD4^+$ follicular helper T (T_{FH}) cells, likely through perforin-dependent elimination (75,84,85).

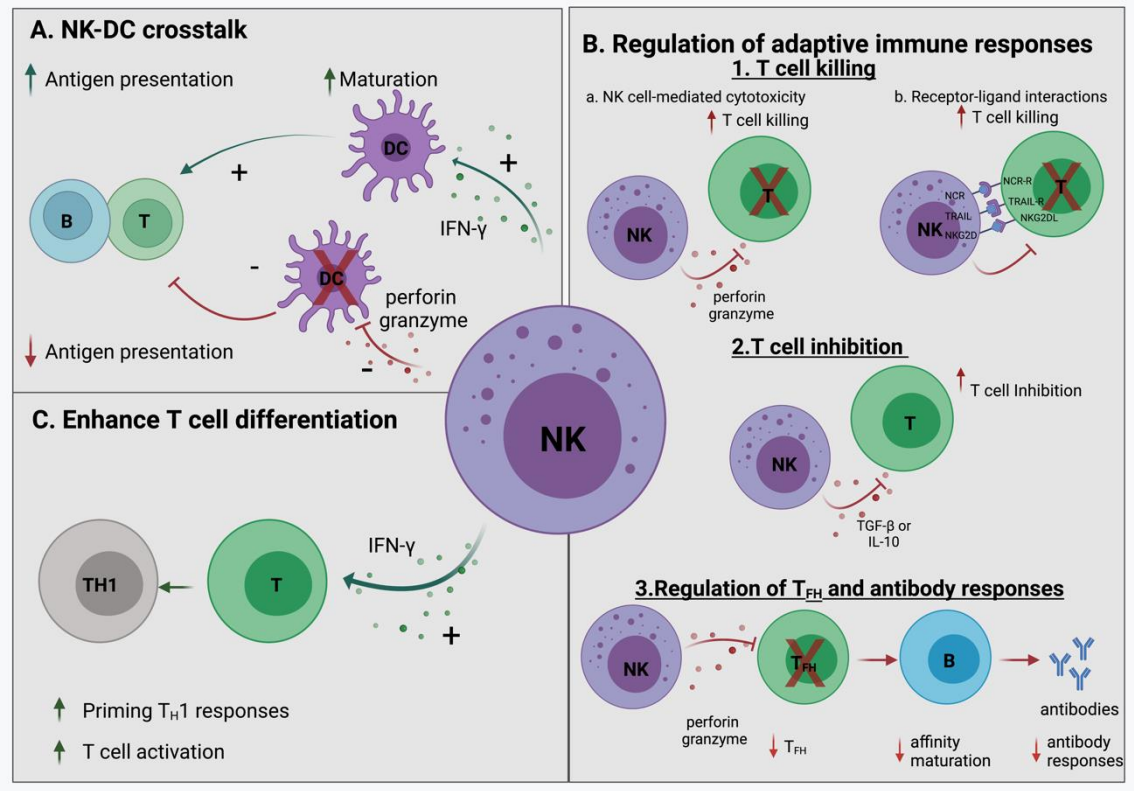


Figure 1.4. NK cell immunoregulatory functions.

A. NK cells can directly interact with, and positively or negatively modulate dendritic cells. Crosstalk between NK cells and dendritic cells augments dendritic cell maturation and enhances their antigen-presenting capacity, which in turn promotes adaptive immune responses. **B.** NK cells can also interact directly or indirectly with $CD4^+$ and $CD8^+$ T cells and modulate the magnitude of T and B cell responses through different mechanisms depicted. **C.** NK cell-derived cytokines, such as IFN-γ, promote T-cell differentiation and enhance T-cell responses.

1.1.6.2.3 Adaptive/memory NK cells in viral infections.

The recognition that NK cells can expand and form long-lasting pools of memory-like cells in response to viral infection resembling the responsiveness previously regarded as a unique feature of adaptive T and B cells represents a major advance in the field of NK cell research. Several types of adaptive NK cells have

been described in humans, including in response to cytokines, antibody-mediated stimulation, vaccination and CMV-derived peptides **(Figure. 1.5)** (86–88).

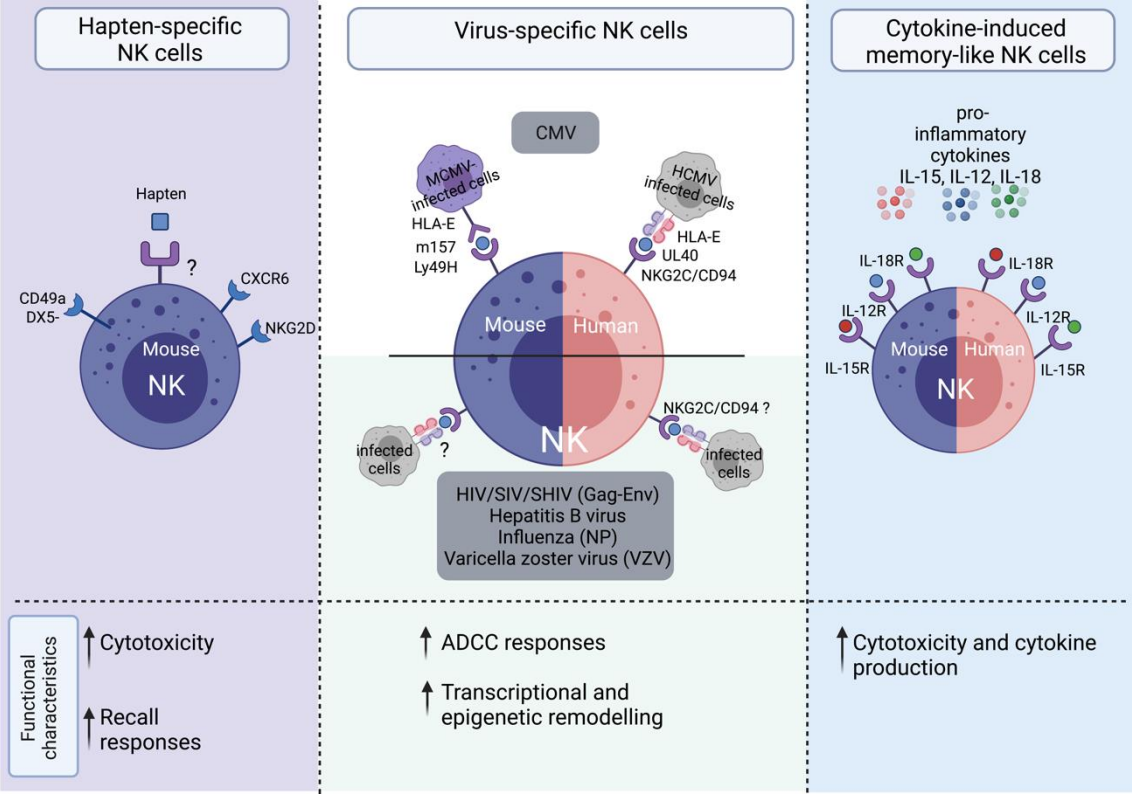


Figure 1.5. Summary of different adaptive/memory NK cell subsets.

A. NK cell immunological memory has been described to haptens in mice, in a subset of NK cells residing in the liver. **B.** Antigen-specific NK cell responses have been described in mice and humans/non-human primates. During MCMV infection, the viral m157 protein is recognised by Ly49H-expressing NK cells, which leads to the expansion of CMV-specific NK cells. In humans, NK cells expressing NKG2C/CD94 recognise HLA-E bound HCMV peptides (UL40). Virus-specific NK cell responses have also been identified in other viral infections, including HIV-1 and SIV. **C.** Cytokine-induced memory-like NK cells in mice and humans can be generated by stimulation with IL-12/15/18.

The best characterised adaptive NK cell subset in humans, expressing high levels of the activating receptor NKG2C, the activating counterpart of NKG2A, that binds to HLA-E, is driven by human CMV (HCMV) infection (89–91).

Recently, highly specific recognition of certain HCMV-encoded HLA-E presented peptides was demonstrated to promote adaptive NK cell expansions (92,93). In addition, a rare HCMV-derived UL40 peptide that is identical to the HLA-E-binding peptide in the HLA-G signal sequence was reported to trigger optimal NK stimulation and enhance NK cell ADCC responses (92,93). These CMV-reactive adaptive NK cells are delineated by a distinct epigenetic signature, similar to memory $CD8^+$ T cells, and changes in receptor expression, key transcription factors and signalling adaptor proteins (94–96). They are characterised by the downregulation of key adaptor molecules such as FcεRI gamma chain (FcεRγ), EWS-activated transcript 2 (EAT-2), and the transcription factor promyelocytic leukaemia zinc finger (PLZF) (97–99). They have a skewed receptor repertoire towards differentiated $CD57^+$ NK cells with a preferential oligoclonal pattern of KIRs for self-HLA-C (87,92,100). They are functionally specialised with a more selective recognition repertoire and a reduced ability to respond to bystander activation/engagement of multiple activating receptors (96,101,102). Instead, they favour strong Fc receptor-dependent effector functions, especially IFN-γ production (96,103–106). Adaptive NK cell expansions have been observed in different viral infections, including hantavirus, chikungunya virus, HBV, and HIV-1 infections (62). Notably, these adaptive NK cell responses were associated with HCMV co-infection, suggesting that HCMV infection/reactivation could be one mechanism underlying the observed adaptive NK cell expansion (62).

In addition to the influence of HCMV co-infection, the expansion of memory-like NK cells was also observed following cytokine stimulation. Human NK cells

preactivated with various combinations of cytokines, including IL-12, IL-2, IL-15 and IL-18, showed enhanced IFN-γ production after restimulation with cytokines or tumour target cells (107). Cytokine-induced memory-like NK cells (CIML) showed an enhanced proliferation capacity and maintenance of their increased responsiveness even after multiple rounds of cell divisions (107). CIML NK cells are phenotypically distinct; they are characterised by increased expression of CD94, NKp46, and CD69, and reduced expression of KIR (108). More recently, the pro-inflammatory milieu associated with viral infections, such as HCMV and HIV-1, was shown to drive the expansion of a defined NK subset with memory-like properties, characterised by $CD94^{+}CD56^{hi}$ and high expression of the transcription factor TCF7 (109). A combination of IL-12 and IL-15 induced the generation of $CD94^{+}CD56^{hi}$ NK cells from $CD94^{-}CD56^{+}$ NK cells from healthy individuals (109). These $CD94^{+}CD56^{hi}$ NK cells exhibited features in keeping with adaptive NK cells, including higher NKG2C expression, increased cytotoxicity and a more pronounced degranulation against virally-infected $CD4^{+}$ T cells (110). The presence of $NKG2C^{+}TFC7^{+}CD56^{hi}$ NK cells correlated with inflammatory cytokines and altered homeostasis of the gut resident and circulating innate lymphoid cells (ILCs) (109). CIML NK cells are currently used as a safe and highly effective treatment in cancer immunotherapy, with the first Acute myeloid leukaemia (AML) patient treated with CIML NK cells (110), and their properties are also being tested in antiviral treatments.

1.1.7 NK cells in AHI.

1.1.7.1 NK cells in HIV-1 infection.

In the setting of HIV-1 infection, accumulating evidence supports the central role of NK cells in the control of HIV-1 viraemia (63). As a component of the early response to virus infection, NK cells eliminate HIV-1 infected target cells and produce IFN-γ and TNFa, influencing antiviral responses and controlling viral spread (62). NK cells also secrete the β-chemokines, CCL3, CCL4 and CCL5, which serve as ligands for CCR5, limiting HIV-1 infectivity of CCR5-expressing target cells (111). Both epidemiological and mechanistic studies have linked NK cell activity and HLA-mediated immune control of HIV-1 (112,113). Here, I discuss the different roles of NK cells in HIV-1 infection, covering the role of adaptive NK cell expansions, as well as the progressive NK cell dysregulation in the course of acute and chronic infection.

1.1.7.2 NK cell-mediated control of HIV-1 replication during early infection and progressive dysregulation.

Previous work has demonstrated that following viral transmission, the absolute number of NK cells increases during hyperacute infection preceding adaptive responses **(Figure. 1.6)** (114). This expansion of NK cells at the earliest window of AHI is dominated by an increase in $CD56^{dim}$, cytotoxic NK cells, and a depletion of $CD56^{bright}$ NK cells (115). Increased NK cell activity on the basis of induction of IFN-γ and CD107a against MHC class I devoid target cells has been detected during the hyperacute phase (114,115). The levels of NK cell degranulation associated with HIV-1 replication were found to correlate inversely with the

magnitude of HIV-specific $CD8^+$ T cells, in keeping with the distinct trajectories of NK cell and T-cell effector functions during AHI (114,116). More recently, the dynamics of immune cell responses following HIV-1 exposure and during the first month of infection were described in the FRESH cohort (58). The levels of genes associated with NK cell cytotoxicity (*PRF1, GZMB*) and chemokine signalling pathway (*CCL3, CCL4*) were upregulated before or during peak viraemia (58). While these two pathways were linked during the earliest stage of infection, the correlation strength declined over time, suggesting maximal NK cell plasticity near the time of peak viraemia (58). Notably, the presence of proliferative and cytotoxic NK cells at the earliest stage, one week following HIV-1 infection, correlated with long-term viral control (58). Additionally, an early NK cell-mediated ADCC response has also been associated with a lower VL set-point (73) and a higher $CD4^+$ T-cell count (117). Overall, these findings suggest that NK cells are a key cytotoxic effector population at the initial phase of infection with a potentially important role in controlling peak viraemia.

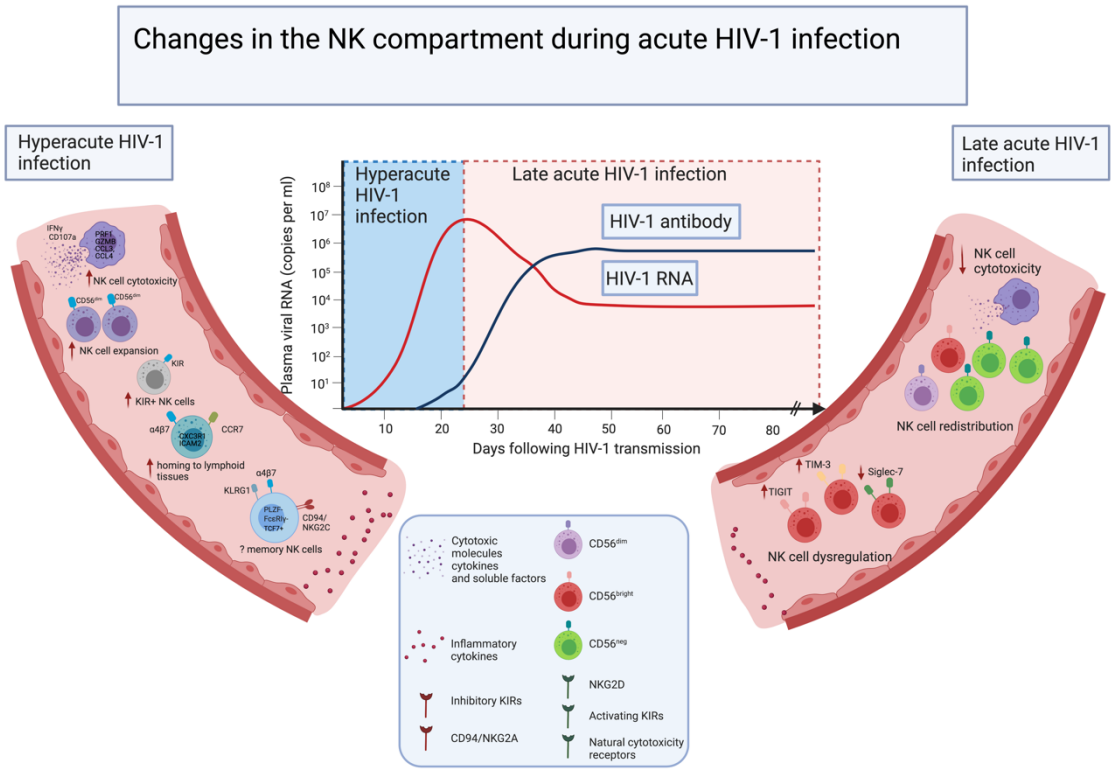


Figure 1.6. Changes in the NK cell compartment during acute and early HIV-1 infection.

Recent studies of the NK cell compartment during AHI have revealed different NK cell dynamics during the first months following infection, which can be divided into two stages; before seroconversion (hyperacute HIV-1 infection) and after seroconversion (late acute HIV-1 infection) based on the detection of HIV-1 specific antibodies in clinical diagnostic assays. During hyperacute HIV-1 infection, circulating NK cells are expanded with an increase in their antiviral responses and trafficking markers, followed by a moderate decline in the total NK cell number and pathological redistribution of NK cell subsets in late acute HIV-1 infection.

Findings from early studies indicate a progressive dysregulation of NK cell functional responses during primary HIV-1 infection, not solely attributed to the emergence of anergic $CD56^{-}CD16^{+}$ NK cells, suggesting wider defects of NK cell activation with progressive infection (115,116,118). Continuous activation and inflammation during early HIV-1 infection have been shown to result in altered expression of the immunoregulatory molecule T-cell immunoglobulin and mucin-domain containing-3 (TIM-3) (119) and appearance of $TIGIT^{+}$ (T-cell immunoreceptor with Ig and ITIM domains) NK cells with decreased NK cell functionality (120). Siglec-7, an inhibitory receptor highly expressed by NK cell subsets (121), has also been proposed as an early marker for NK cell dysregulation in early HIV-1 infection (122). NK cell subsets with decreased expression of Siglec-7 were expanded during AHI and were characterised by impairment of NK cell degranulation and cytokine production (122). The expansion of $Siglec\text{-}7^{-}$ NK cells in early infection is followed by NK cell subset redistribution and the emergence of dysfunctional $CD56^{-}CD16^{+}$ NK cells (122).

1.1.7.3 Adaptive/Memory NK cell responses in AHI.

The adaptive reconfiguration of NK cells in HIV-1 infection, partially driven by HCMV co-infection, has been described during the early stages of HIV-1 infection (91,123). Such adaptive NK cell populations display retained responses to CD16 stimulation (106,124) and superior ADCC responses to overlapping HIV-1 peptides (98), which suggests that it may be possible to develop strategies that exploit these Fc-dependent functions. It is also conceivable that the downregulation of HLA-C by most primary HIV-1 clones (125) may also facilitate

'missing-self' recognition of HIV-1 infected cells by HCMV-primed adaptive NK cells.

Limited evidence from human studies demonstrated that the presence of NK cells with an adaptive-like phenotype ($CD57^{+}NKG2C^{+}$) during early HIV-1 infection is inversely correlated with HIV-1 viral load and associated with a lower VL set-point (126,127). Such data suggest that NK cells with adaptive features, despite the limited profile used for their identification, may constitute a readily armed population that confers better HIV-1 control, highlighting their potential value in early infection as a prognostic marker for monitoring PLWH and potentially leading to remission.

In addition to CMV-driven adaptive NK cells, durable antigen-specific NK cell responses have been reported in primates after SIV infection and vaccination (87). More recently, mechanistic evidence of human NK cell HIV-specific memory was reported and suggested as a potential correlate of HIV-1 control in a subgroup of PLWH, elite controllers, who maintain viral load suppression in the absence of ART (128). HIV-specific responses were dependent on the interaction between the activating NK cell NKG2C receptor and its ligand HLA-E bound to HIV-1 Gag or Env peptides (128). Comprehensive transcriptomic and phenotypic analysis of these antigen-specific NK cells showed an elevated expression level of KLRG1, which has also been reported to define NK cell subsets that mediate HBV-specific responses (129), and higher α4β7 expression, indicating mucosal homing potential (130,131). Terminally differentiated $NKG2A^{low}$ $CD16^{+}$ NK cells

with an adaptive gene expression profile (low expression of *ZAP70*, *FcεRγ*, and *SYK* and high expression of *GRAP2*), and HLA-E restricted cytotoxicity against SIV-infected cells has also been associated with strong viral control in the secondary lymphoid tissues of African green monkeys (132).

Antigen-specific memory could, however, develop independent of the NKG2C/HLA-E axis, and other pathways may be complementary or alternative to this pathway. The inflammatory milieu/higher levels of LPS in HIV-1 infection could further drive the expansion of NK cell subsets with cell-intrinsic memory properties (109,133). Recently the presence of a memory-like NK cell population, displaying higher cytotoxicity against HIV-infected $CD4^+$ T cells, has been linked with HIV-1 induced inflammation (109). *In vivo* studies showed a correlation between levels of CXCL10 (IP10) and expansions of adaptive NK cells during AHI (98). However, whether infection with different HIV-1 subtypes drives differential expansion of pre-existing populations of NK cells with adaptive features is currently unknown.

1.1.8 T cells in viral infections.

1.1.8.1 Roles of T cells in antiviral immunity.

The adaptive immune response is a major determinant of the clinical outcomes after viral infection and underpins vaccine efficacy (134). T-cell responses develop early in infection and correlate with protection and disease outcome (135). During the initial phase of a viral infection, there is a significant increase in T-cell activation and proliferation (134). By classical antigen presentation or

cross-presentational pathways, viral peptides can be presented on MHC class I or II molecules and thereby stimulate antiviral responses by both $CD8^+$ and $CD4^+$ T cells, respectively, leading to a broad cellular response to a viral infection. After infection, some of these activated T cells will develop into a memory pool, and upon second exposure, memory T cells can rapidly mature into effector cells and mediate protective responses to subsequent infection with the same virus (134,136).

Activated $CD8^+$ T cells can induce virally-infected cell apoptosis by producing TNF-α and IFN-γ and releasing cytotoxic granules, including perforin and granzymes (134). Perforins aid in delivering the contents of granules into the cytoplasm of the infected cells, and granzymes activate apoptosis of virally-infected T cells. IFN-γ is an important cytokine in the immune response to various viral infections since it plays a role in inducing an antiviral state in uninfected cells and enhancing cellular cytotoxicity. The magnitude of the initial viral load and the efficacy of the innate immune responses, including NK cells, seems to be critical in determining the extent of activation of T-cell responses and the subsequent clinical outcome (137,138).

A profound lymphocytopenia is seen in the blood of patients with different viral infections and is correlated with severe clinical outcomes (139,140). This leads to a pattern of “co-existing suppression and activation”, with peripheral loss of certain T-cell subsets (in HIV-1, $CD4^+$ T cells), concurrently with the proliferation of the $CD8^+$ T-cell pool (139,140). The mechanisms by which viral infection

induces the loss of T cells are unclear but could reflect impaired T-cell proliferation, apoptosis, or increased T-cell trafficking into infected tissues (138,140).

The functional capacity of the cellular response is essential for viral clearance and a key determinant of clinical outcome. Indeed, genetic and acquired factors have clearly demonstrated the importance of T-cell responses in viral infections. Several clinical outcomes are characterised by a slow decline in viral load and early and sustained T-cell responses (6,48,139). Early development of cytotoxic $CD8^+$ T cells, typically observed within a few weeks after infection, is correlated with effective viral clearance and reduced disease progression (134,139). Effective viral control is associated with a T_H1 $CD4^+$ T-cell phenotype and high expression levels of cytotoxic $CD8^+$ T-cell molecules (139,140). However, excessive activation of T cells might be detrimental, and although T-cell polyfunctionality is associated with viral control, excessively high levels of T-cell activation and T-cell-mediated inflammatory reactions are linked with persistent infection (6,139,140). Expression of markers of potential exhaustion, such as PD-1 and TIGIT, is also associated with a poorer outcome and rapid disease progression, although this may not necessarily reflect functional T-cell exhaustion but instead a hyperactivation state (141).

1.1.9 T cells in AHI.

1.1.9.1 CD8⁺ T cells in AHI.

In AHI, a high magnitude of CD8⁺ T-cell activation has been reported during the period of peak viraemia to VL set-point (142,143). Both the FRESH (AHI cohort based in South Africa) and RV254 (AHI cohort based in Bangkok, Thailand) studies have demonstrated an early expansion of CD8⁺ T cells and upregulation of cytotoxic effector molecules within the first month of infection (144–146), the extent of these responses have been associated with lower VL set-point and disease progression (145,147). The magnitude of the activated (HLA-DR⁺CD38⁺) CD8⁺ T cells negatively correlated with viral load and was linked to the delayed viraemia peak (145). Interestingly, the majority of these early-activated CD8⁺ T cells are HIV-1 specific, as inferred by their ability to respond when stimulated with infected CD4⁺ T cells (148). The preservation of these early cytotoxic T-cell (CTL) responses has been linked to the rate of disease progression and higher CD4⁺ T-cell count in untreated HIV-1 infection (149). However, under conditions of strong selection pressure, HIV-1 evolves, leading to the accumulation of viral escape mutations that enable the virus to escape from cytotoxic CD8⁺ T-cell recognition (150). Additionally, the continuous activation of CD8⁺ T cells leads to a progressive loss of their effector function coupled with sustained upregulation of inhibitory receptors and altered epigenetic, transcriptional and metabolic profiles (151,152).

1.1.9.2 CD4$^+$ T-cell responses in AHI.

The rapid loss of CD4$^+$ T cells in most tissue compartments is a hallmark of early HIV-1 infection, which is often accompanied by an exponential increase in the plasma viral load (150). Gut-homing CD4$^+$ T cells expressing α4β7 (153) are depleted in the GI mucosa very early (starting at the onset of plasma viraemia), but the peripheral blood CD4$^+$ T cells are not depleted until after peak viral load is achieved (6). Similar to CD8$^+$ T cells, CD4$^+$ T cells are activated, and these cells were shown to upregulate genes associated with differentiation and downstream production of pro-inflammatory cytokines IL-1β and TNF-α (58). The phenotype and roles of HIV-1-specific CD4$^+$ T cells are, however, diverse during AHI. Although the proliferation of CD4$^+$ T cells is limited during early infection, HIV-specific CD4$^+$ T cells produce a number of cytokines, including IL-17, IFN-γ, and IL-2, in responses to *ex vivo* stimulation with Gag, and the magnitude of these responses has been described to correlate with peak viral load (154). Moreover, cytolytic HIV-specific CD4$^+$ T cells (Granzyme A$^+$ and Granzyme B$^+$ CD4$^+$ T cells) have been identified during the hyperacute phase, and their frequencies also associate with pVL set-point (155). HIV-specific CD4$^+$ T cells have been shown to contribute to the maintenance of functional HIV-specific CD8$^+$ T-cell responses and control of viraemia during chronic HIV-1 infection. The preservation of HIV-specific CD4$^+$ T cells endowed with the ability to produce multiple cytokines in individuals also coincides with apparent protective responses against HIV-1. However, activation of memory CD4$^+$ T cells during AHI has also been shown to correlate positively with viral load, implying that the causative link between HIV-specific CD4$^+$ T-cell responses and viral control remains to be resolved (156).

Although both innate and adaptive immune responses are important in controlling viral replication in the initial stage, little is known about the interplay between these two arms and the contribution of innate immunity in developing protective adaptive immune responses.

1.2 Section 2: SARS-CoV-2 infection in people living with HIV-1.

1.2.1 COVID-19 outcomes in PLWH.

Following the HIV-1 pandemic in 1980s, SARS-CoV-2 emerged in late 2019 as a new pathogen and was responsible for over 6 million deaths, posing unprecedented healthcare challenges around the world (157). The clinical manifestations of SARS-CoV-2 vary, with some patients experiencing severe infections and developing fatal respiratory distress (158). The risk factors for severe infection are not completely understood, but emerging evidence demonstrates an association between the risk of severe outcomes and age, male sex, and the presence of underlying co-morbidities (159,160). PLWH, despite successful virological suppression on ART, experience an increased burden of co-morbid conditions associated with premature ageing (161,162). These multi-morbidities are partially driven by residual inflammation and ongoing immune dysregulation (163), and could accelerate COVID-19-associated inflammation and influence disease severity and the effectiveness of vaccination (164). Additionally, cellular immune deficiency and prior $CD4^+$ T-cell depletion may play an influential role in COVID-19 severity and have been described as potential risk factors for severe SARS-CoV-2 infection in PLWH, irrespective of HIV-1 virological suppression (165). PLWH may experience premature ageing due to chronic inflammation associated with HIV-1, which may also influence immune responses and disease outcomes (166). Consequently, the risk of hospitalisation for COVID-19 infection was higher among younger adults living with HIV-1 compared to the general population (167). In addition to cellular deficiency,

unsuppressed HIV-1 viraemia is linked to a higher risk of hospitalisation after COVID-19 infection (168). These data suggest that HIV-1 could be a risk factor for severe SARS-CoV-2 infection, although the conclusions regarding COVID-19 outcomes among PLWH are still a matter of debate.

1.2.2 Impact of HIV-1 infection on immune responses to SARS-CoV-2.

Despite virological suppression, PLWH are generally characterised by a dysregulated immune system. Chronic inflammation driven by HIV-mediated destruction of the gut mucosal barrier and dissemination of innate immune stimuli may influence the quality of innate immune responses, including IFN-I responses (169). This may result in defects in the process of antigen presentation and an altered innate immune environment, leading to a hyper-inflammatory response and increased tissue damage (170–172). In addition, progressive loss of $CD4^+$ T cells and persistent expansion of circulating $CD8^+$ T cells, resulting in an inversed $CD4^+/CD8^+$ ratio, can potentially impede clearance of SARS-CoV-2 through its effects on the generation of the antiviral T-cell response and antibody production (173,174). Reduction in T-cell proliferative capacity and progressive T-cell exhaustion can also lead to impaired responses to SARS-CoV-2 in PLWH (173,174). Potentially exhausted $CD8^+$ T cells with high expression of inhibitory molecules were found to be associated with severe outcomes (175,176). However, these activated $CD8^+$ T cells, characterised by elevated expression of inhibitory receptors, could nevertheless be functionally competent for IFN-γ production and may be beneficial for preventing hyperactivation leading to immunopathology (177,178). Although the “exhaustion “of T cells in SARS-CoV-

2 infection remains debated, exhausted T cells in chronic HIV-1 infection were found to be dysfunctional with impaired effector responses, which could potentially hamper viral clearance of SARS-CoV-2 when T cell-mediated immunity coordinates with humoral immunity (173) **(Figure. 1.7)**.

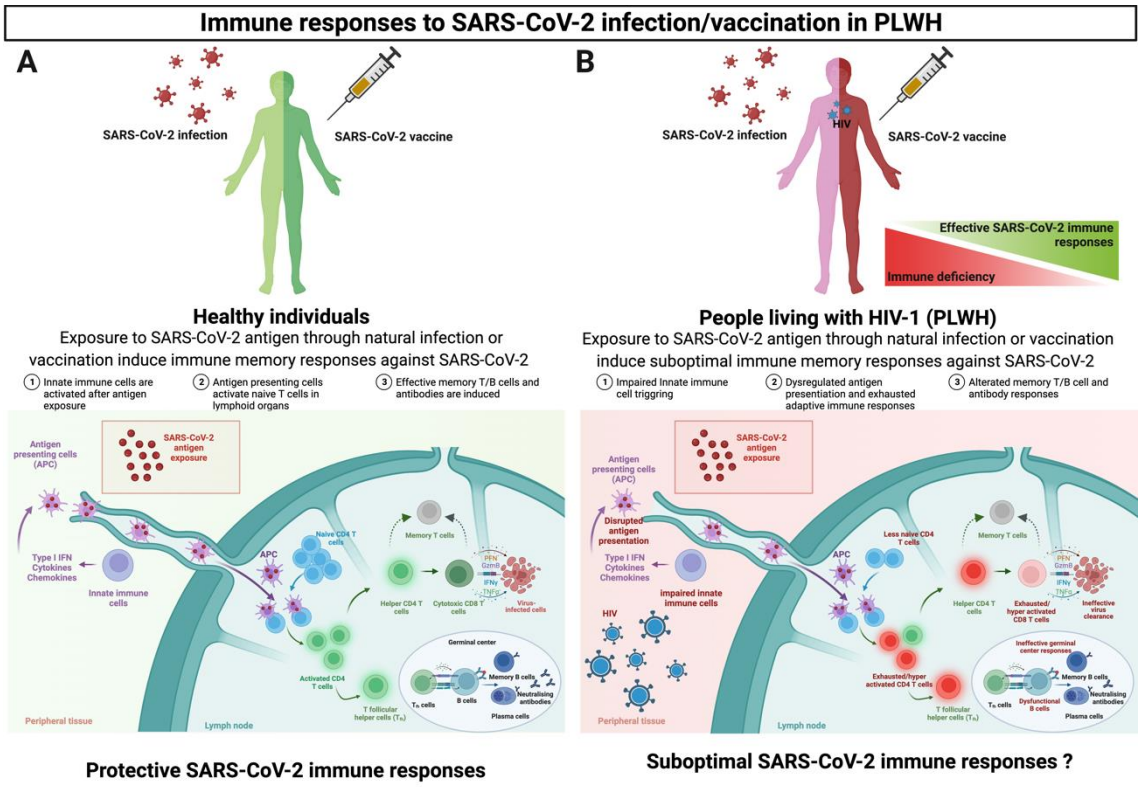


Figure 1.7. Immune responses to SARS-CoV-2 infection/vaccination in PLWH.

HIV-1 infection can lead to dysregulated innate immune responses, disrupted antigen presentation, and impaired adaptive immune cell responses. This can lead to suboptimal SARS-CoV-2-specific responses induced during natural infection/vaccination compared to those induced under normal conditions. HIV-1 may not only influence the development of effective antigen-specific responses but can also affect the durability of SARS-CoV-2 memory responses. Therefore, PLWH may have both dysregulation in generating primary immune responses to SARS-CoV-2 and alteration in the longevity of memory responses induced through SARS-CoV-2 infection/vaccination.

1.2.3 T-cell responses to SARS-CoV-2 in PLWH.

Insights from studies evaluating the quality and quantity of immune responses to SARS-CoV-2 can help inform the optimisation of vaccine strategies. Any pre-existing immune dysregulation (both innate and adaptive immune cells), in addition to uncontrolled viraemia and persistent inflammation in PLWH, could lead to poorly coordinated T-cell responses, affecting the trajectory of COVID-19 disease. Uncoordinated immune responses have been shown to attenuate protective immunity to SARS-CoV-2 in elderly individuals (179), which could be highly pertinent in PLWH with the dysregulated T-cell response and additional co-morbidities. While studies examining immune responses to SARS-CoV-2 have focused on antibodies, there are limited data on T cell-mediated immunity following SARS-CoV-2 infection in PLWH. A single report suggests a longer disease course and an increased rate of T-cell exhaustion driven by COVID-19 infection in PLWH (180). While overall antiviral T-cell responses to SARS-CoV-2 in PLWH were similar to those observed in the general population, HIV-1 patients with uncontrolled infection had a weakened T-cell response (180). These patients (HIV-1 patients with uncontrolled infection) exhibit higher IL-10 and TGFβ serum concentrations and lower $CD4^+/CD8^+$ and T_H1/T_H2 ratios with simultaneous exacerbation of COVID-19-related respiratory distress (180). These findings are in line with the recent observations in a South African cohort which demonstrated a link between unsuppressed HIV-1 infection and poor T-cell responses to SARS-CoV-2 (181). The presence of HIV-1 viraemia, low $CD4^+$ T-cell counts, and high levels of immune activation in PLWH were associated with diminished T-cell responses and poor cross-recognition of emerging SARS-CoV-2 variants (181).

These findings suggest that in addition to viraemic HIV-1 infection, inadequate reconstitution of the T-cell compartment after ART treatment and HIV-induced immune activation could negatively impact the potential to mount a robust T-cell response to SARS-CoV-2 infection (181).

Regarding COVID-19 vaccines in PLWH, to date, only a few observational studies have examined cellular responses to SARS-CoV-2. Similar to natural infection, PLWH with sustained HIV-1 suppression on ART showed a satisfactory T-cell response following the primary vaccination cycle (i.e. two doses of vaccine) with mRNA vaccines (182). A third dose of mRNA vaccine was also able to elicit strong T-cell responses in PLWH, and the magnitude of these responses was comparable between PLWH and HIV-negative individuals (183). However, the T-cell response induced by the third dose was similar to that observed after the primary vaccine cycle (two doses), suggesting that T-cell immunisation was fully achieved after the first two doses of vaccine in PLWH (183). Similar to the mRNA vaccines, T-cell responses following prime-boost dosing of the chimpanzee adenovirus-vectored ChAdOx1-nCoV-19 vaccine was robust in PLWH on stable ART and with $CD4^+$ T-cell counts > 350 cells/mm^3 (184,185). However, more pronounced immunodeficiency, defined as a current $CD4^+$ T-cell count <350/mm^3, was associated with poorer cellular responses following vaccination, suggesting that immune deficiency in ART-treated patients may affect T-cell immunity to SARS-CoV2 vaccination (186). However, to date, an in-depth characterisation of SARS-CoV-2 infection or vaccine-induced T-cell responses and their resistance to emerging viral variants in PLWH is currently limited.

1.2.4 NK cell responses in SARS-CoV-2 infection.

1.2.4.1 The early NK cell response to SARS-CoV-2 infection.

Emerging evidence supports the important role of NK cells in the control of SARS-CoV-2 infection, including their association with SARS-CoV-2 immunopathogenesis (187,188). In acute SARS-CoV-2 infection, NK cells are robustly activated, highly proliferative, express high levels of perforin and granzyme B, and display SARS-CoV-2 antiviral activity **(Figure. 1.7)** (187,189). Strong NK cell activation, assessed by expression of CD69 and HLA-DR, was noted in early SARS-CoV-2 infection (189). These activated NK cells display a less differentiated status, represented by lower expression of KIR and CD62L (62,189). Following infection, circulating NK cells are recruited to the site of the infection leading to a reduction in their numbers in the peripheral blood (189). The recruitment of NK cells to the lung could be mediated by chemokine-chemokine receptor interactions, as increased levels of CCL3, CCL4, CXCL9, and CXCL10 were reported in the lung of COVID-19 patients (190,191). It is, therefore, plausible that CXCR3 and CCR5 expressed on the surface of NK cells contribute to their trafficking to the lungs in acute SARS-CoV-2 infection (62). In the lungs of patients with COVID-19 disease, a gene module for activation and cytotoxic activity is induced in lung NK cells, characterised by high expression of *GZMB* (granzyme B), *PRF1* (perforin), and *CCL4* (MIP-1β) (190,191). Notably, patients with severe disease exhibited higher NK cell frequencies in the lung and higher representation of adaptive and cytotoxic $CD56^{bright}$ NK cells in the circulation,

suggesting severity-associated phenotypic and functional changes in the circulating and tissue-resident NK cells (175,189,192).

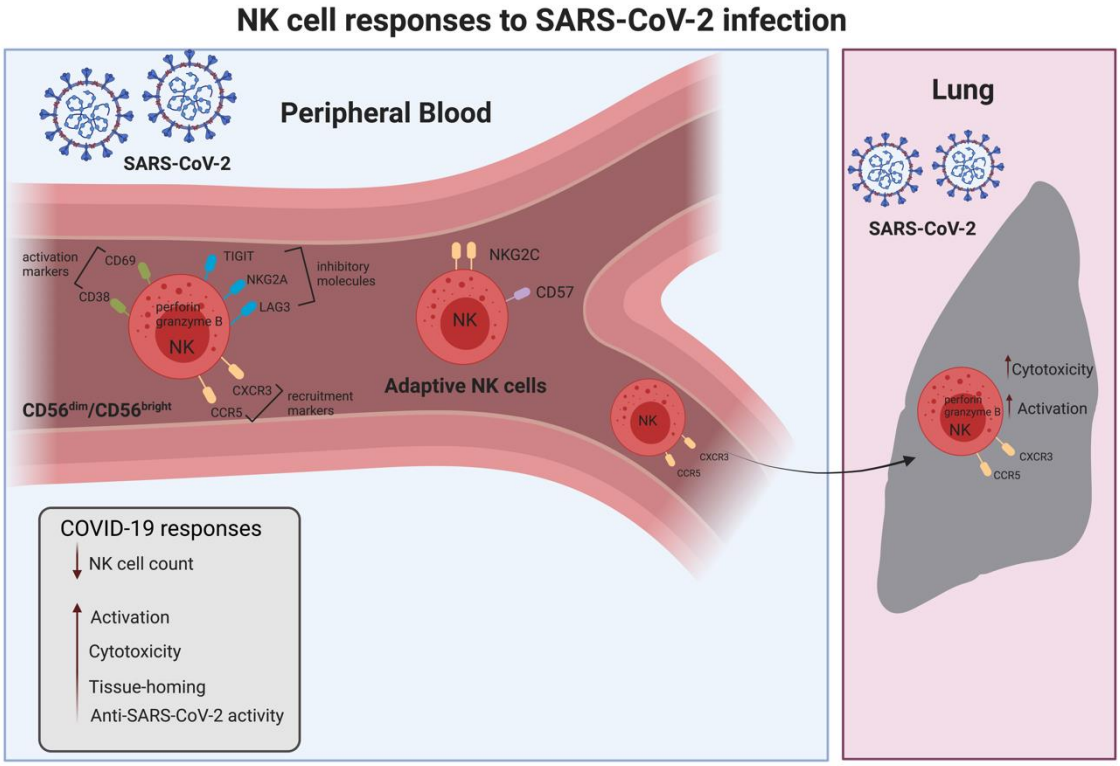


Figure 1.7. NK cell responses to SARS-CoV-2 infection.

Following SARS-CoV-2 infection, in peripheral blood, NK cells display an altered phenotype, including upregulation of activation molecules (CD38 and CD69), inhibitory checkpoint markers (TIGIT, LAG3, and NKG2A), and cytotoxic molecules (Granzyme B and perforin). An elevated expression of the tissue recruitment markers was also noted, suggesting the potential capacity of NK cells to migrate to the sites of infection, including lung tissue compartments. In the lung, NK cells display an activated and cytotoxic phenotype.

Studies examining the antiviral responses of NK cells have demonstrated a direct role of NK cells in viral suppression (193–195). In animal models, NK cell-mediated Fc-dependent responses correlated with protection against SARS-CoV-2 (196), and monoclonal antibody-mediated control of SARS-CoV-2 is

augmented by Fc-dependent functions (197–200). Similarly, in humans, NK cell-mediated ADCC responses contribute to viral suppression following SARS-CoV-2 infection, and S1 and S2 antibodies targeting SARS-CoV-2 spike protein can induce robust ADCC responses (201–205). In addition to Fc-mediated responses, NK cells are able to suppress viral replication through recognising viral peptides presented by HLA-E, which abrogates inhibition of NKG2A-expressing NK cells, resulting in missing-self recognition (194). More recently, SARS-CoV-2-specific NK cell responses have been identified in COVID-19 convalescent patients, and these responses were associated with enhanced IFN-γ production and were dominated by $NKG2C^{+}CD57^{+}$ NK cells (206). The importance of adaptive NK cell responses in SARS-CoV-2 was reflected by the significant association between the genetic deletion of NKG2C and severe disease (207). However, more studies are needed to fully characterise NK cell responses, including adaptive NK cell subsets, during SARS-CoV-2 and their contribution to the development of memory responses following primary infection and/or vaccination, especially in potentially vulnerable population such as PLWH.

1.3 Overall study aims

The overall aim of this thesis is to provide a detailed assessment of immune cell responses, with a particular emphasis on NK cells, and their association with viral control in HIV-1 and SARS-CoV-2 infections.

1.3.1 Specific aims.

Part I: NK cell responses during AHI.

Aim 1: To longitudinally characterise the phenotypic and functional aspects of NK cell subpopulations, incorporating detailed dissection of receptor patterns and adaptive features from the earliest time-point and up to three months post-infection. This will allow us to capture and correlate the evolution of NK cell responses and their functional capacity in relation to markers of disease progression (plasma viral load set-point, $CD4^+$ T-cell count, and viral load).

Aim 2: To assess the interplay between NK cell responses and adaptive immune subpopulations, including $CD8^+$ and $CD4^+$ T-cell subsets.

Part II: NK and T-cell responses in SARS-CoV-2 infection and vaccination in PLWH.

Aim 1: To dissect NK cell responses longitudinally following SARS-CoV-2 natural infection and/or vaccination in PLWH and their relationship with T-cell and antibody measures and breadth.

Aim 2: To characterise the phenotypic and functional aspects of T-cell responses, incorporating detailed dissection of receptor patterns and activation/exhaustion features from the convalescent phase of infection and after up to three doses of the COVID-19 vaccine.

Chapter 2: Methods.

Data disclaimer(s): Some data included in this thesis are part of collaborative projects and were kindly provided by study collaborators. Datasets that are not generated by me are listed below:

- **Chapter 3**: NK cell responses in acute HIV-1 infection.
  - Data for soluble innate immune markers were collected by Dr Amin S Hassan (KEMRI/Wellcome Trust Research Programme, Kilifi, Kenya and Department of Translational Medicine, Lund University, Sweden).
- **Chapter 5**: Adaptive immune cell responses in SARS-CoV2 infection.
  - Data for SARS-CoV-2-specific IgG binding titres and neutralising antibodies were provided by Emma Touizer (McCoy group, Division of Infection and Immunity, University College London).
  - Data for the global SARS-CoV-2 T-cell responses measured by IFN-γ-ELISpot (in the convalescent phase only) were collected by Dr Ester Gea-Mallorquí and Dr Jakub Kopycinski (Rowland-Jones and Dorrell groups, Nuffield Department of Medicine, University of Oxford).
- **Chapter 6**: NK cell responses in SARS-CoV-2 infection.
  - CMV-specific IgG ELISA data were provided by Bethany Charlton (Rowland-Jones group, Nuffield Department of Medicine, University of Oxford).
  - Soluble biomarkers data were provided by Dr Dan Hameiri-Bowen (Rowland-Jones group, Nuffield Department of Medicine, University of Oxford).
  - SARS-CoV-2-specific antibodies and B-cell responses were provided by Emma Touizer (McCoy group, Division of Infection and Immunity, University College London).

Chapter 2

2.1 General methods.

2.1.1 Peripheral blood mononuclear cells (PBMC) and plasma sample preparation.

Venous blood samples were collected in heparin tubes, and PBMCs were isolated using Ficoll gradient centrifugation. Whole blood was transferred to conical tubes and then centrifuged at 500 × g for 5 minutes. Plasma samples were then collected, and the remaining blood was diluted with RPMI (Corning, Manassas, VA, USA). Diluted blood was then layered over an appropriate volume of Histopaque (Histopaque-1077 Cell Separation Medium, Sigma Aldrich, St. Louis, MO, USA) and then centrifuged without brake for 20 min at 500 × g at room temperature. The PBMC layer was carefully removed, transferred to a fresh tube, and washed with RPMI. Cells were stained and counted using an Automated Cell Counter (BioRad, Hercules, California, USA). Isolated PBMCs were then cryopreserved in a freezing medium containing 10% dimethyl sulfoxide (DMSO) (MP Biomedicals, LLC, Irvine, CA, USA) and 90% heat-inactivated foetal bovine serum (FBS) and stored in liquid nitrogen tank (-150 to -180 °C) for further use.

2.1.2 Serum isolation.

For serum isolation, whole blood was collected in serum separator tubes and stored briefly at room temperature prior to sample processing. Serum tubes were centrifuged for 5 min at 500 × g, and then serum was collected, aliquoted and stored at −80 °C for further use.

2.1.3 Thawing PBMCs samples.

PBMC-containing cryotubes were retrieved from the liquid nitrogen tank and placed in dry Ice for transporting and then placed in a 37°C water bath for rapid thawing. The thawed PBMCs were then transferred to a 50ml conical tube containing a pre-warmed complete RPMI medium (RPMI supplemented with penicillin-streptomycin, l-Glutamine, N-2-hydroxyethyl piperazine-N-2-ethane sulfonic acid (HEPES), non-essential amino acids, 2-Mercaptoethanol, and 10% FBS) and Benzonase (Dilution 1 in 2500 µl). Cells were then centrifuged for 10 minutes at 350 × g at room temperature and resuspended in a fresh complete RPMI medium. Cells were stained and counted using an Automated Cell Counter (BioRad, Hercules, California, USA). Cells were then resuspended in an appropriate cell concentration for each assay.

2.1.4 NK and T-cell phenotypic flow cytometric analysis.

NK and T cell-focused panels were optimised and used in both studies presented in this thesis (acute HIV-1 infection and SARS-CoV-2 infection studies). Cryopreserved PBMCs were thawed and rested for 1 h at 37 °C in a complete RPMI medium (as described above). Cells were then washed and plated in a 96-well plate at 0.5-1x10^6 cells/well. Cells were then washed, resuspended in PBS, and surface stained at 4 °C for 20 min with different combinations of antibodies in the presence of fixable live/dead stain (Invitrogen). Cells were then fixed and permeabilised for the detection of intracellular (Cytofix/Cytoperm™, BD Biosciences) or intranuclear (The Foxp3 intranuclear staining buffer kit, eBioscience) antigens. Fixed cells were stained at room temperature for 30-45

min with different combinations of intranuclear and intranuclear antibodies. Samples were acquired on a BD Fortessa X20 using BD FACSDiva8.0 (BD Biosciences), and subsequent data analysis was performed using FlowJo 10 (TreeStar). The full list of fluorochrome-conjugated antibodies and dilutions for the three *ex vivo* panels are included in **Table 2.1** (NK cell panel), **Table 2.2** (T-cell panel), and **Table 2.3** (T_{FH} cell panel). The gating strategies used for flow cytometry experiments are provided in each figure in future chapters.

Table 2.1. NK cell phenotypic panel.

Laser	Filter	Antigen/mAb	Fluorochrome	Supplier	Identifier	Clone	Dilution
488 Blue	710/50	CD16	BB700	BD Biosciences	Cat # 746199	Clone # 3G8	0.25 in 50µl
	530/30	FcεRI	FITC	Milli-Mark	Cat # FCABS400F	Polyclonal	0.25 in 50µl
405 Violet	450/50	CD57	BV421	BD Biosciences	Cat # 563896	Clone # NK-1	0.25 in 50µl
	525/50	CD4	BV510	BioLegend	Cat # 300546	Clone # RPA-T4	0.25 in 50µl
		CD14	BV510	BioLegend	Cat # 301842	Clone # M5E2	0.25 in 50µl
		CD19	BV510	BioLegend	Cat # 302242	Clone # HIB19	0.25 in 50µl
		Live Dead stain	Aqua	Life technologies	Cat # L34957	N/A	1 in 800µl
	605/40	CD56	BV605	BD Biosciences	Cat # 562780	Clone # NCAM16.2	1 in 50µl
	677/20	CD3	BV650	BioLegend	Cat # 317324	Clone # OKT3	0.5 in 50µl
	710/50	CD2	BV711	BioLegend	Cat # 300231	Clone # RPA-2.10	0.5 in 50µl
	810/40	CD38	BV785	BioLegend	Cat # 303530	Clone # HIT2	1 in 50µl
637 Red	670/30	KIR2DL1/KIR2DS5	APC	R&D systems	Cat # FAB1844A-100	Clone # 143211	1 in 50µl
		KIR3DL2/ CD158K	APC	R&D systems	Cat # FAB2878A-100	Clone # 539304	1 in 50µl
		KIR3DL1/ CD158e	APC	Miltenyi Biotec	Cat # 130-092-474	Clone # DX9	1 in 50µl
		CD158b1/b2	APC	Beckman Coulter	Cat # A22333	Clone # GL183	1 in 50µl
	730/45	Granzyme B	Alexa Fluor®700	BD Biosciences	Cat # 560213	Clone # GB11	0.5 in 50µl
	7 80/60	Siglec-7	APC/Fire-750	BioLegend	Cat # 339207	Clone # 434	0.5 in 50µl
561 Yellow/ Green	586/15	NKG2C/ CD159c	PE	R&D systems	Cat # FAB138P-100	Clone # 134591	5 in 50µl
	660/20	NKG2A/ CD159a	PE-Cy-7	Beckman Coulter	Cat # B10246	Clone # Z199	0.5 in 50µl
	610/20	PLZF	PE-CF594	BD Biosciences	Cat # 565738	Clone # R17-809	0.5 in 50µl
	710/50	CD7	PE/Cyanine5	BioLegend	Cat # 343110	Clone # CD7-6B7	0.25 in 50µl

Table 2.2. T-cell phenotypic panel.

Laser	Filter	Antigen/mAb	Fluorochrome	Supplier	Identifier	Clone	Dilution
488 Blue	710/50	CD4	BB700	BD Biosciences	Cat # 566393	Clone # SK3	0.25 in 50µl
	530/30	TCF-1/TCF-7	FITC	Cell Signaling Technology	Cat # 6444S	Clone # C63D9	0.5 in 50µl
405 Violet	450/50	PD-1	BV421	BioLegend	Cat # 329920	Clone # EH12.2H7	0.5 in 50µl
	525/50	CD14	BV510	BioLegend	Cat # 301842	Clone # M5E2	0.25 in 50µl
		CD19	BV510	BioLegend	Cat # 302242	Clone # HIB19	0.25 in 50µl
		Live Dead stain	Aqua	Life technologies	Cat # L34957	N/A	1 in 800µl
	605/40	CD3	BV605	BD Biosciences	Cat # 317322	Clone # OKT3	0.5 in 50µl
	677/20	CD127	BV650	Cat # 351325	Cat # 351325	Clone # A019D5	0.5 in 50µl
	710/50	CD8	BV711	BioLegend	Cat # 301044	Clone # RPA-T8	0.5 in 50µl
	810/40	CD38	BV785	BioLegend	Cat # 303530	Clone # HIT2	1 in 50µl
637 Red	670/30	TOX	APC	Miltenyi Biotec	Cat # 130-118-474	Clone # REA473	0.5 in 50µl
	730/45	Granzyme B	Alexa Fluor®700	BD Biosciences	Cat # 560213	Clone # GB11	0.5 in 50µl
	7 80/60	CCR7	APC/Cy-7	BioLegend	Cat # 353212	Clone # G043H7	1 in 50µl
561 Yellow/ Green	586/15	TIGIT	PE	eBioscience	Cat # 12-9500-42	Clone # MBSA43	0.5 in 50µl
	660/20	CD45RA	PE-Cy-7	BioLegend	Cat # 304126	Clone # HI100	0.5 in 50µl
	710/50	HLA-DR	PE/Cyanine5	BD Biosciences	Cat # 562007	Clone # G46-6	0.25 in 50µl

Table 2.3. T_{FH} cell panel.

Laser	Filter	Antigen/mAb	Fluorochrome	Supplier	Identifier	Clone	Dilution	Staining
488 Blue	710/50	CD3	PerCP-eFluor™ 710	eBioscience	Cat # 46-0037-42	Clone # OKT3	0.5 in 50µl	Surface
	530/30	CXCR5	FITC	BD Biosciences	Cat # 564624	Clone # MAb11	1 in 50µl	Surface
405 Violet	450/50	PD-1	BV421	BioLegend	Cat # 329920	Clone # EH12.2H7	0.5 in 50µl	Surface
	525/50	CD14	BV510	BioLegend	Cat # 301842	Clone # M5E2	0.25 in 50µl	Surface
		Live Dead stain	Aqua	Life technologies			1 in 800µl	Surface
	605/40	CD56	BV605	BD Biosciences	Cat # 562780	Clone # NCAM16.2	1 in 50µl	Surface
	677/20	CD127	BV650	BioLegend	Cat # 351325	Clone # A019D5	1 in 50µl	Surface
	710/50	CD8	BV711	BioLegend	Cat # 301044	Clone # RPA-T8	0.5 in 50µl	Surface
	810/40	CD38	BV785	BioLegend	Cat # 303530	Clone # HIT2	1 in 50µl	Surface
637 Red	670/30	CD19	APC	BioLegend	Cat # 302211	Clone # HIB19	1 in 50µl	Surface
	730/45	CD45RA	Alexa Fluor®700	BioLegend	Cat # 304120	Clone # HI100	1 in 50µl	Surface
	7 80/60	CCR7	APC/Cy-7	BioLegend	Cat # 353212	Clone # G043H7	1 in 50µl	Surface
561 Yellow/ Green	660/20	CD25	PE-Cy-7	BD Biosciences	Cat # 335824	Clone # 2A3	1 in 50µl	Surface
	610/20	CD4	PE/Dazzle 594	BioLegend	Cat # 300548	Clone # RPA-T4	0.5 in 50µl	Surface
	710/50	CXCR3	PE/Cyanine5	BD Biosciences	Cat # 551128	Clone # 1C6/CXCR3	2 in 50µl	Surface

2.1.5 Statistical analyses.

Prism 8 (GraphPad Software) was used for statistical analysis as follows: the Mann–Whitney U test was used for single comparisons of independent groups; the Wilcoxon-test paired t-test was used to compare two paired groups. For multiple groups, statistical significance was assessed using a two-way analysis of variance (ANOVA) with multiple comparisons. The non-parametric Spearman test was used for correlation analysis. The statistical significances are indicated in the figures (*$p < 0.05$, **$p < 0.01$, ***$p < 0.001$, and ****$p < 0.0001$), and all tests were two-tailed. Polyfunctionality tests were performed in SPICE version 6.0. The exact statistical test used in each analysis is reported in figure legends.

2.1.6 High-dimensional data analysis.

To evaluate the co-expression of the markers at a single cell level and to identify various cell clusters with similar phenotypic profiles, unsupervised multidimensional analysis was performed using different algorithms in Cytobank (https://www.cytobank.org). Concatenated files were used to evaluate the overall immune cell landscape in different groups. Cells were manually gated for lymphocytes, singlets, live cells, and $CD3^+CD8^+$, $CD3^+CD4^+$, or $CD3^-CD7^+CD56^+/CD16^{+/-}$ (for total $CD8^+$ T cells, $CD4^+$ T cells, or NK cells, respectively) and then subjected to viSNE analysis. Equal event sampling was selected across all samples. The FlowSOM algorithm uses Self-Organising Maps (SOMs) to define different clusters based on selected markers and reveal related phenotypic clusters (208). The samples were subjected to viSNE analysis before running FlowSOM with equal event sampling. The number of metaclusters was set to 7-10, the number of the clusters was set to 100, and the size of clusters was set to relative with 15 pixels as Max relative size (Cytobank default).

2.1.7 Correlation analysis and heatmap visualisations.

The Correlograms plots were created with the corrplot package (version 0.84) in Rstudio (version 1.2.5042). The plots show the Spearman rank correlation coefficient (*r*) and *p* values between all paired parameters. Clustering of parameters was performed using the 'hclust' option. Parameters with incomplete information (i.e. missing information for some participants) were removed prior to graphing. Spearman rank *p* values (two-tailed) were calculated using corr.test

and graphed based on $*p < 0.05$, $**p < 0.01$, $***p < 0.001$. The code used in this analysis was extracted from (179,209) and detailed below:

```
M = cor(DataFrame, method = "spearman", use = "pairwise.complete.obs")
MP = cor.mtest(DataFrame, method = "spearman", use = "pairwise.complete.obs", conf.level = 0.95, exact = FALSE)
corrplot(M, p.mat = MP$p, method = 'square', tl.col = "black", tl.cex = 0.7, tl.srt = 45, cl.align = "l", type = 'lower', sig.level = c(0.001, 0.01, 0.05), pch.cex = 0.7, insig = 'label_sig', pch.col = 'white')
```

The “DataFrame” is the data from each correlation matrix shown in each figure. Correlogram parameter labels were shortened in the figure text for clarity.

2.1.8 Figure visualisations.

The majority of the figures were generated using Adobe Illustrator; however, the following figures were created with BioRender.com (subscription: Student Plan, agreement number: TT253MFSRH)

- Chapter 1: Figures 1.1-1.7.
- Chapter 2: Figures 2.1-2.4.
- Chapter 3: Figure 3.1.
- All graphical abstracts (Chapters 3-6).

2.2 Methods for acute HIV-1 infection study (Chapters 3 and 4)

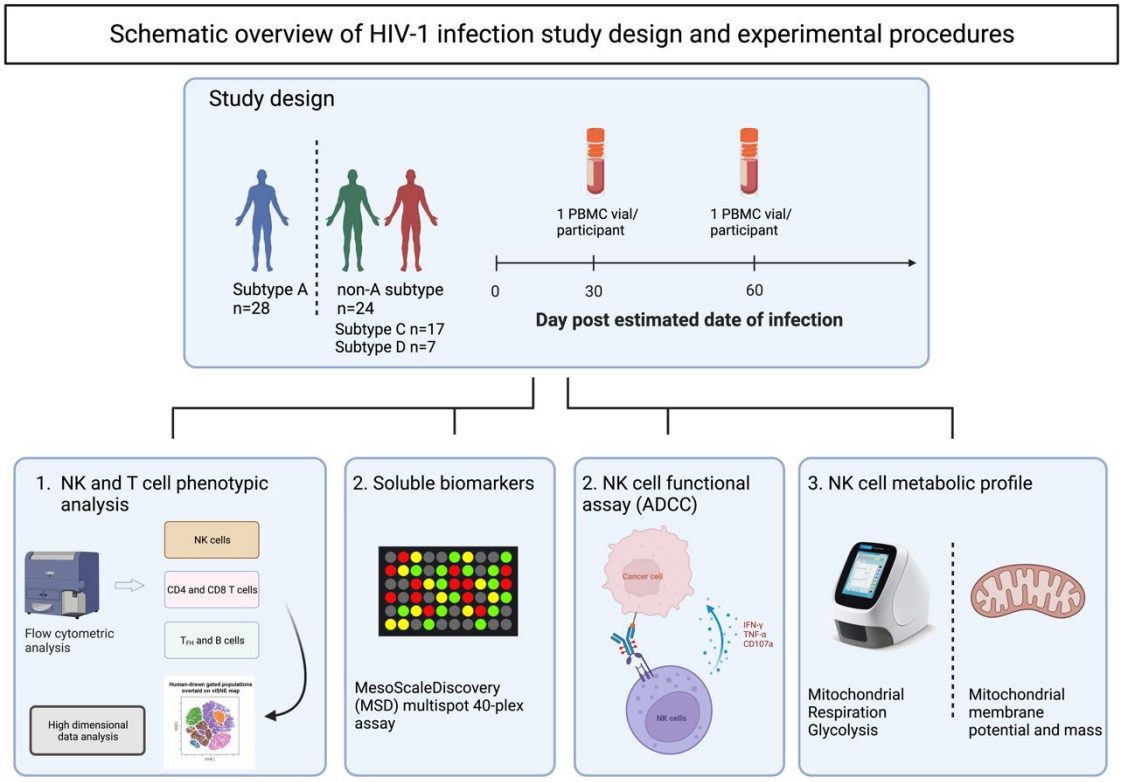


Figure 2.1. Schematic overview of AHI study.

A total of 56 participants with AHI were sampled longitudinally at two time-points (1 month and 3 months post estimated date of infection (EDI)) under "IAVI Protocol C" (n=28 subtype A, n=17 subtype C, n=7 subtype D). Multiparameter flow cytometry was used for phenotypic characterisation. NK cell ADCC responses were determined against antibody-coated Raji cells. The metabolic profile was assessed by Seahorse technology. Plasma soluble markers were measured using multiplexed assays.

2.2.1 Chapters 3 and 4 ethics statement.

Prior to enrolment, all volunteers in the IAVI Protocol C study provided informed consent. Ethical approvals were obtained from respective country-specific ethics review boards (the Kenya Medical Research Institute Ethical Review Committee, the Kenyatta National Hospital Ethical Review Committee of the University of

Nairobi, the Rwanda National Ethics Committee, the Uganda Virus Research Institute Science and Ethics Committee, the Uganda National Council of Science and Technology, the University of Cape Town Health Science Research and Ethics Committee, the University of Zambia Research Ethics Committee, and the Bio-Medical Research Ethics Committee at the University of KwaZulu Natal) (4,210).

2.2.3 Chapters 3 and 4 study subjects.

The IAVI Protocol C study included screening adults (18-49 years old) for risk behaviour associated with an increased risk of HIV-1 acquisition at nine clinical sites in Kenya, Rwanda, Uganda, and Zambia between 2006-2011 (4,210). Volunteers identified with incident HIV-1 infection by PCR were invited to enrol in the study very soon after acquiring HIV-1. After enrolment, visits were scheduled monthly for the first three months, quarterly for the first two years, and every six months thereafter (4). The estimated date of infection (EDI) was defined as either i) the midpoint between the last negative and first HIV-antibody positive test, ii) 10 days prior to the first positive HIV-1 PCR test, iii) 14 days prior to the first positive p24 antigen test, or iv) the date of a self-reported high-risk exposure HIV-1 incident (4). HIV-1 viral load levels, $CD4^+$ and $CD8^+$ T-cell counts were recorded from each participant at the enrolment and in each subsequent visit. All of the participants included in this study were ART-naïve as the ART programmes in Eastern and Southern Africa were in their infancy at the time of enrolment. Demographic data, including date of birth, sex, ethnicity, date of HIV-1 diagnosis, and transmission risk group, were obtained from a centralised and curated

repository for the IAVI Protocol C study. HIV-1 subtypes were determined through sequencing of the *pol* region of the genome, as previously described (211), and confirmed by *env* sequences in all of the participants included in this study (5). Further details in the IAVI Protocol C cohort, including enrolment criteria and epidemiological information, have been published elsewhere (4,210).

PBMC samples from IAVI Protocol C participants collected longitudinally at approximately 1 month (the earliest time-point) and 3 months post-EDI were used in the study presented in Chapters 3 and 4. One vial of PBMCs from each participant was requested, and the samples were transported from the storage site at IAVI-HIL (The IAVI-Human Immunology Laboratory (HIL), Imperial College, London) to Oxford in 2019. The clinical characteristics of participants are summarised in Chapter 3, Table 1. Further details of the exact number of subjects utilised for each assay are indicated in the figure legends and "Results" section for both Chapters 3 and 4.

2.2.4 NK cell functional assay.

Purified PBMCs were thawed and rested for 1 h at 37 °C and 5% carbon dioxide in a complete RPMI medium. Raji cells (target cells, the Burkitt lymphoma cell line Raji) were resuspended in complete RPMI at $5x10^5$/ml and incubated with 2.5 µg/ml of anti-human CD20 antibody (InvivoGen, France) or PBS as a negative control for 30 minutes at 37 °C. After 30 minutes, Raji cells were washed and resuspended to the desired concentration in complete RPMI. PBMCs from each participant were co-cultured with Raji cells at 1:5 ratio for 6 hrs at 37°C, in the

presence of CD107a APC-H7 antibody (BD Biosciences, dilution 1 in 200 µl). After 1 h, GolgiStop (containing Monensin, 2 µmol/ml) and GolgiPlug (containing brefeldin A, 10 µg/ml) (BD Biosciences) were added to inhibit protein transport. After stimulation, cells were washed and surface stained at 4 °C for 20 min in the presence of fixable live/dead stain (Invitrogen). Cells were then fixed and permeabilised (CytoFix/CytoPerm; BD Biosciences), followed by intracellular cytokine staining with IFN-γ BV421 (BioLegend, dilution 1 in 100) and TNF-α BV711 (BioLegend, dilution 1 in 50). Samples were acquired on a BD Fortessa X20 using BD FACSDiva8.0 (BD Biosciences), and data were analysed using FlowJo 10 (TreeStar). A full list of antibodies used in the NK cell functional assay is listed in **Table 2.3**.

Table 2.3. NK cell functional assay panel.

Laser	Filter	Antigen/mAb	Fluorochrome	Supplier	Identifier	Clone	Dilution
488 Blue	710/50	CD16	BB700	BD Biosciences	Cat # 746199	Clone # 3G8	0.25 in 50µl
	530/30	FcεRI	FITC	Milli-Mark	Cat # FCABS400F	Polyclonal	0.25 in 50µl
405 Violet	450/50	IFN-γ	BV421	BD Biosciences	Cat # 562988	Clone # B27	1 in 50µl
	525/50	CD4	BV510	BioLegend	Cat # 300546	Clone # RPA-T4	0.25 in 50µl
		CD14	BV510	BioLegend	Cat # 301842	Clone # M5E2	0.25 in 50µl
		CD19	BV510	BioLegend	Cat # 302242	Clone # HIB19	0.25 in 50µl
		Live Dead stain	Aqua	Life technologies	Cat # L34957	N/A	1 in 300µl
	605/40	CD56	BV605	BD Biosciences	Cat # 562780	Clone # NCAM16.2	1 in 50µl
	677/20	CD3	BV650	BioLegend	Cat # 317324	Clone # OKT3	0.5 in 50µl
	710/50	TNF-α	BV711	BioLegend	Cat # 502940	Clone # MAb11	1 in 50µl
	810/40	CD38	BV785	BioLegend	Cat # 303530	Clone # HIT2	1 in 50µl
637 Red	670/30	KIR2DL1/KIR2DS5	APC	R&D systems	Cat # FAB1844A-100	Clone # 143211	1 in 50µl
		KIR3DL2/ CD158K	APC	R&D systems	Cat # FAB2878A-100	Clone # 539304	1 in 50µl
		KIR3DL1/ CD158e	APC	Miltenyi Biotec	Cat # 130-092-474	Clone # DX9	1 in 50µl
		CD158b1/b2	APC	Beckman Coulter	Cat # A22333	Clone # GL183	1 in 50µl
	730/45	Granzyme B	Alexa Fluor®700	BD Biosciences	Cat # 560213	Clone # GB11	0.5 in 50µl
	7 80/60	CD107a	APC/H-7	BD Biosciences	Cat # 561343	Clone # H4A3	1 in 200µl
561 Yellow/ Green	586/15	NKG2C/ CD159c	PE	R&D systems	Cat # FAB138P-100	Clone # 134591	5 in 50µl
	660/20	NKG2A/ CD159a	PE-Cy-7	Beckman Coulter	Cat # B10246	Clone # Z199	0.5 in 50µl
	610/20	CD57	PE/Dazzle 594	BioLegend	Cat # 359620	Clone # HNK-1	0.25 in 50µl

2.2.5 Measurement of soluble biomarkers.

Cryopreserved plasma samples collected from whole blood treated with ethylenediaminetetraacetic acid (EDTA) were used (5). Multiplexed analysis was performed in duplicates and measured by electrochemiluminescence using the MesoScaleDiscovery (MSD) multisport 40-plex assay (MesoScaleDiagnostics, LLC) according to the manufacturer's instructions. The values for analyte concentration, including respective lower (LLOQ) and upper (ULOQ) limits of quantification, were calculated from standard curves. A full list of biomarkers measured is listed in **Table 2.4.**

Table 2.4. List of biomarkers measured in acute HIV-1 study.

Panel	Abbreviation	Full name
Cytokine	GM-CSF	Granulocyte-macrophage colony-stimulating factor
Cytokine	IL-1α	Interleukin-1 alpha
Cytokine	IL-5	Interleukin-5
Cytokine	IL-7	Interleukin-7
Cytokine	IL-12	Interleukin-12
Cytokine	IL-15	Interleukin-15
Cytokine	IL-16	Interleukin-16
Cytokine	IL-17A	Interleukin-17 alpha
Cytokine	TNF-β	Tumor necrosis factor-beta
Cytokine	VEGF	Vascular endothelial growth factors
Chemokine	MIP-1β	Macrophage Inflammatory Proteins (MIP)-beta
Chemokine	Eotaxin-3/ CCL-26	Chemokine (C-C motif) ligand 26
Chemokine	TARC	Thymus and activation-regulated chemokine
Chemokine	IP-10	Interferon gamma inducible protein-10
Chemokine	MIP-1α	Macrophage Inflammatory Proteins (MIP)-alpha
Chemokine	IL-8	Interleukin-8
Chemokine	MCP-1	Monocyte Chemoattractant Protein-1
Chemokine	MDC	Serum Macrophage-derived Chemokine
Chemokine	MCP-4	Monocyte Chemoattractant Protein-1
Angiogenesis	VEGF	Vascular Endothelial Growth Factor
Angiogenesis	VEGF-C	Vascular Endothelial Growth Factor-C
Angiogenesis	VEGF-D	Vascular Endothelial Growth Factor-D
Angiogenesis	Tie-2	The tyrosine kinase receptor TIE-2
Angiogenesis	Flt-1	FMS-Like Tyrosine kinase 1
Angiogenesis	sFlt-1/PIGF	Soluble Fms-Like Tyrosine kinase 1
Angiogenesis	bFGF	Basic Fibroblast Growth Factor
Proinflammatory	IFN-γ	Interferon-gamma
Proinflammatory	IL-1β	Interleukin-1-beta
Proinflammatory	IL-2	Interleukin-2
Proinflammatory	IL-4	Interleukin-4
Proinflammatory	IL-6	Interleukin-6
Proinflammatory	IL-8	Interleukin-8
Proinflammatory	IL-10	Interleukin-10
Proinflammatory	IL-12p70	Interleukin-12p70
Proinflammatory	IL-13	Interleukin-13
Proinflammatory	TNF-α	Tumor Necrosis Factor-alpha
Vascular inflammation	SAA	Human Serum Amyloid A
Vascular inflammation	C-reactive protein	Tumor Necrosis Factor-alpha
Vascular inflammation	VCAM-1	Vascular Cell Adhesion Molecule-1
Vascular inflammation	ICAM-1	Intercellular Adhesion Molecule-1

2.2.6 Extracellular flux assays.

Oxygen consumption rate (OCR) and extracellular acidification rate (ECAR) were measured using an XFp Analyser following the manufacturer's instructions (Seahorse XF Technology, Agilent). NK cells were enriched from PBMCs using a negative-selection magnetic bead kit (Miltenyi Biotec) as per the manufacturer's instructions (>85% purity and viability). Purified NK cells were seeded at $3x10^5$ cells per well in Seahorse cell plates pre-coated with Cell-Tak (Corning) in duplicate. Purified NK cells were then incubated for 45 min in a CO_2-free incubator at 37 °C before loading the plate in the Seahorse analyser. The cells were seeded in an XF RPMI medium supplemented with 10 mM glucose, 1 mM pyruvate and 2 mM glutamine. The OCR and ECAR were measured at baseline and following injection of different compounds: oligomycin (1 μM), carbonyl cyanide-4 (trifluoromethoxy) phenylhydrazone (FCCP; 1.5 μM), rotenone/antimycin A (0.5 μM) and 2-deoxy-glucose (2-DG; 50 mM) (Agilent technologies). Maximum respiration was calculated as average OCR values post-FCCP injection. The spare respiratory capacity (SRC) was calculated as average OCR values post-FCCP injection minus basal OCR. Glycolysis was calculated as the basal ECAR values minus post-2-DG injection values. Glycolytic reserve was calculated as post-rotenone/antimycin A injection ECAR values minus basal ECAR values.

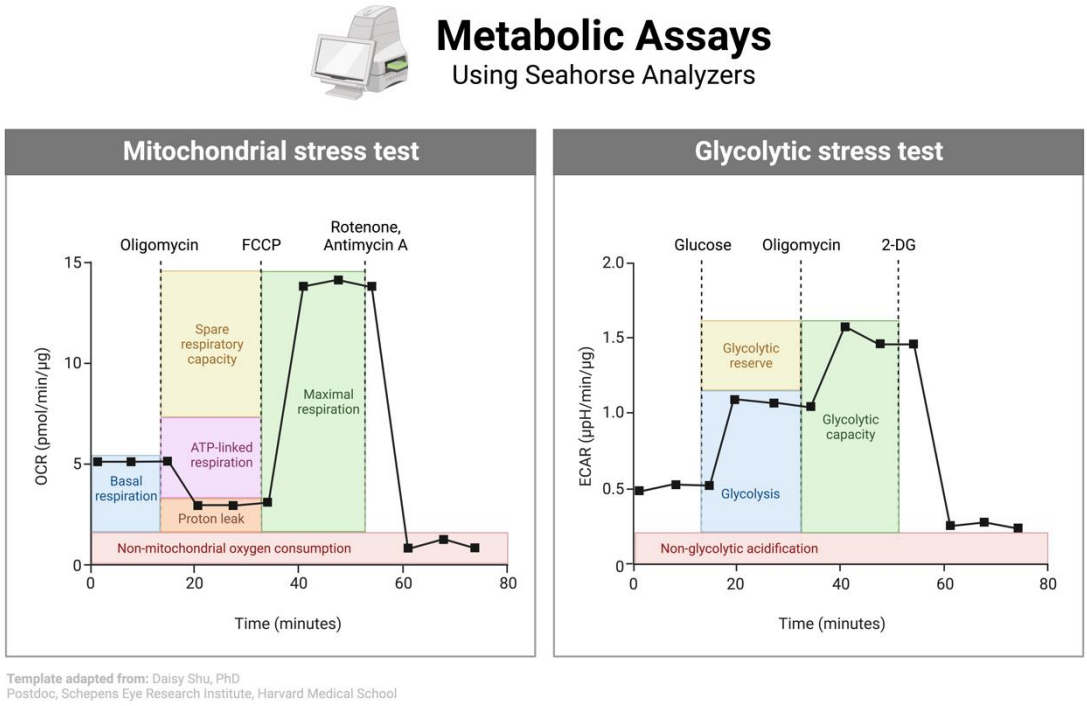


Figure 2.2. Principle of mitochondrial and glycolytic stress assays.

(Source: Agilent Seahorse XF Cell Mito Stress (6)).

2.2.7 Mitochondrial membrane potential measurement.

Assessment of mitochondrial mass and mitochondrial membrane potential was performed by incubation with Mito-Tracker Green (100 nM) (Invitrogen) or potentiometric dye tetramethyl rhodamine methyl ester (TMRM 25 nM; Sigma Aldrich), respectively, according to manufacturer's instructions before surface staining. After a 30-minute incubation, cells were washed with PBS and subjected to surface staining as described in the phenotypic Flow cytometric analysis section.

2.3 Methods for SARS-CoV-2 infection study (Chapters 5 and 6).

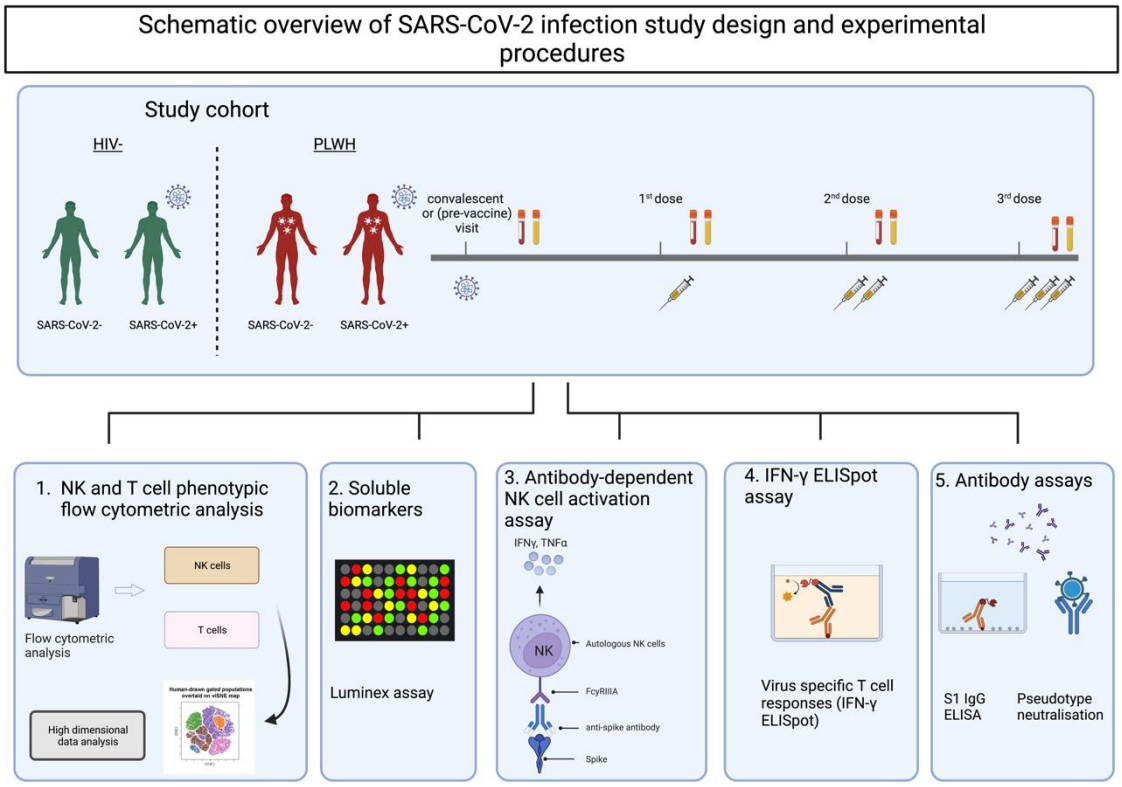


Figure 2.3. Schematic overview of SARS-CoV-2 infection study.

HIV-1 negative controls and PLWH, with or without prior SARS-CoV-2 infection, were sampled during the convalescent phase and after one, two, or three doses of COVID-19 vaccine. Multiparameter flow cytometry was used for phenotypic characterisation or for ICS functional assays. Plasma soluble markers were measured using Luminex assays. Antibody-dependent NK cell activation was measured using a plate-bound spike glycoprotein (GP) in the presence of autologous serum. SARS-CoV-2 specific T-cell responses were measured by IFN-γ ELISpot or ICS functional assays. Antibodies were measured by anti-spike IgG and neutralisation assays.

2.3.1 Chapters 5 and 6 ethics statement.

The protocols for the human study were approved by the local NHS Research Ethics Committee —Berkshire (REC 16/SC/0265). The study complied with all relevant ethical regulations for work with human participants and conformed to

the Helsinki declaration principles and Good Clinical Practice (GCP) guidelines, and all subjects enrolled on the study provided written informed consent.

2.3.2 Chapters 5 and 6 study subjects.

HIV-seronegative adults (>18 years of age, comprising hospital-based healthcare workers) and chronically HIV-infected patients, on ART, were recruited after recovering from SARS-CoV-2 infection and/or vaccination. Participants with prior confirmed or suspected COVID-19 disease were sampled during the convalescent phase of SARS-CoV-2 infection. Confirmed SARS-CoV-2 infection by SARS-CoV-2 PCR and/or Roche antibody tests was declared by participants, who were asked to provide details on the timing and nature of their symptoms. Additional demographic information and underlying medical conditions were captured on a health questionnaire. European Centre for Disease Prevention (ECDP) criteria were used for the case definition of COVID-19 disease. The severity of COVID-19 disease was defined according to the WHO criteria. A total of $n = 47$ PLWH and $n = 35$ HIV-negative subjects with recovered confirmed and/or suspected COVID-19 disease were included. Sixteen demographically age-, sex-matched HIV-1 seropositive individuals were included for comparison, from whom samples were collected between February 2017 and November 2019 (pre-pandemic). This is a cross-sectional analysis of baseline samples collected during the convalescent phase of SARS-CoV-2 infection as part of a prospective, observational longitudinal cohort study.

For the vaccine study, a total of n=46 PLWH and n=35 HIV-negative donors were recruited after the first dose (median of 20 days, range 6-85), second dose (median 32 days, range 5-218), and third dose (median 64 days, range 5-199) of the vaccine. Participants received a mix of available SARS-CoV-2 vaccination (Pfizer-BioNTech's BNT162b2; Moderna's mRNA-1273 or AstraZeneca AZD1222) according to Joint Committee on Vaccination and Immunisation, UK, guidelines. At each visit, participants were asked to report any history of SARS-CoV-2 infection, and, between vaccinations, four SARS-CoV-2 naïve participants reported a breakthrough infection; thus, any subsequent time-points were moved into the 'prior SARS-CoV-2 infection' group for analysis. This is a longitudinal analysis of baseline samples collected during the convalescent phase of SARS-CoV-2 infection (or prior to vaccination) and vaccine samples collected after each dose of vaccine. However, baseline samples were not available for all participants, and similarly, not all participants were sampled after each dose of vaccine. All participants were recruited at the Mortimer Market Centre for Sexual Health and HIV Research and the Ian Charleson Day Centre at the Royal Free Hospital (London, UK) following written informed consent as part of a study approved by the local ethics board committee. Further details on the exact number of subjects included in the cohort for each study are provided in the "Study cohort" section (Chapter 5: **section 5.2.1.1** and **5.2.2.1**, Chapter 6; **6.2.1**). Additional information about demographic and sampling can be found in the "Cohort Demographics and Clinical Characteristics" tables in future chapters (Chapter 5: **Table 5.1** and **5.2**, Chapter 6; **Table 6.1**).

2.3.3 IgG purification.

For individuals on ART, to avoid off-target neutralisation due to the HIV-1 pseudovirus backbone, IgG was purified from serum using Mini Bio-Spin Chromatography Columns (BioRad) by incubating sera with a resin of protein G Sepharose beads (GE Healthcare) for 2 h, eluting with 0.1 M Glycine (pH 2.2) into 2 M Tris-base, concentrating the IgG-containing fraction in a 50 kDa concentrator (Amicon, Merck) and quantifying the amount of IgG by Nanodrop. The purified IgG was serially diluted from 200µg/ml in neutralisation assays, and the resulting ID50 was calculated using the total IgG concentration of each serum sample prior to purification.

2.3.4 Semiquantitative S1 ELISA.

Anti-spike IgG titres were measured using an ELISA assay, as previously described (212). Briefly, nine columns of a 96-half-well Maxisorp plate (Nalgene, NUNC International, Hereford, UK) were coated with 25µl of SARS-CoV-2 spike fraction S1 purified protein at 3 µg/ml in PBS overnight at 4 °C. Three columns were coated with 25µl goat anti-human F(ab)'2 (1:1000) in PBS to generate an internal standard curve. Plates were then washed with PBS-T (0.05% Tween in PBS) and blocked for 1 h with assay buffer (5% milk powder PBS-T) at room temperature. The patient serum was then added to the antigen-coated wells at 1:50−1:1000 dilution (25µl in assay buffer) and incubated for 2-h. Serial dilutions of known concentrations of IgG were added to the F(ab)'2 IgG-coated wells in triplicate. Following 2h incubation, wells were washed with PBS-T, and 25 µl alkaline phosphatase-conjugated goat anti-human IgG (Jackson

ImmunoResearch) was added at a 1:1000 dilution in assay buffer and incubated for 1 h at room temperature. Plates were then washed, and 25µl of alkaline phosphatase substrate (Sigma Aldrich) was added. Optical densities were measured using a MultiskanFC (ThermoFisher) plate reader at 405 nm and S1 & N-specific IgG titres interpolated from the IgG standard curve using 4PL regression curve-fitting on GraphPad Prism 8.

2.3.5 Pseudovirus production and neutralisation assays.

To produce HIV-1 particles pseudotyped with SARS-CoV-2 spike, $3x10^6$ HEK-293T cells were seeded in 10ml of complete DMEM Dulbecco's Modified Eagle's Medium (Gibco) supplemented with 10% FBS and 50µg/ml penicillin-streptomycin. Cells were then transfected with 9.1 µg of HIV-1 p8.91 packaging plasmid (213), 9.1 µg of HIV-1 luciferase reporter vector plasmid (214), 1.4 µg of wild type (Wuhan strain) SARS-CoV-2 spike plasmid and 60 µg of PEI-Max (Polysciences). After 48h of transfection, supernatants were harvested, filtered (0.45 µm filter), and either used directly in the assay or stored at −80 °C. Neutralisation assays were performed by incubating serial dilutions of patient serum with pseudovirus in 96-well plates for 1 h. Following 1 h incubation, HeLa ACE-2 cells (kindly gifted by James E. Voss, Scripps Institute) were added (10,000 cells per 100 µl/well). After 48/72 h, supernatants were removed, and the cells were lysed; Brightglo luciferase substrate (Promega) was added to the plates and read on a Glomax luminometer (Promega) as a proxy for infection. Measurements were performed in duplicate, and 50% inhibitory dilution (ID_{50}) values were then calculated using GraphPad Prism 8.

2.3.6 Standardised ELISA for measurement of CMV-specific IgG levels in plasma.

The levels of CMV-specific IgG were measured using the Abcam Anti-CMV IgG Human ELISA kit following the manufacturer's instructions. Assays were run in duplicate and mean values per participant were reported in International Units (IU) per ml.

2.3.7 Production and purification of recombinant Spike.

HEK-293F cells were seeded at $1x10^6$ cells/mL in Freestyle 293 Expression Medium (Gibco). The next day, a transfection mix was prepared (for 200 mL of cells) of 72 mg of Wuhan-hu1 Spike-Avi-His tag plasmid and 18 mg of BirA plasmid (Seow et al. 2020; Graham et al. 2021) into 11 ml of Opti-MEM, alongside 2ml of PEI-Max, and left to incubate at 37°C 5% CO_2 in a shaking incubator for 7 days before harvesting for purification. The supernatant was purified using 2 mM imidazole buffer (Sigma-Aldrich) buffer during binding to a His GraviTrap (Cytiva) column and 500 mM imidazole buffer for elution. The eluted protein was then concentrated with a 100KD Amicon Ultra concentrator (Millipore) and washed with PBS before quantification using a NanoDrop. Biotinylated protein was then further purified through size exclusion chromatography using an AKTA pure system with a Superdex 200 Increase 10/300 GL column (Sigma-Aldrich) to select for fractions containing trimeric Spike.

2.3.8 Antibody-dependent NK activation assay.

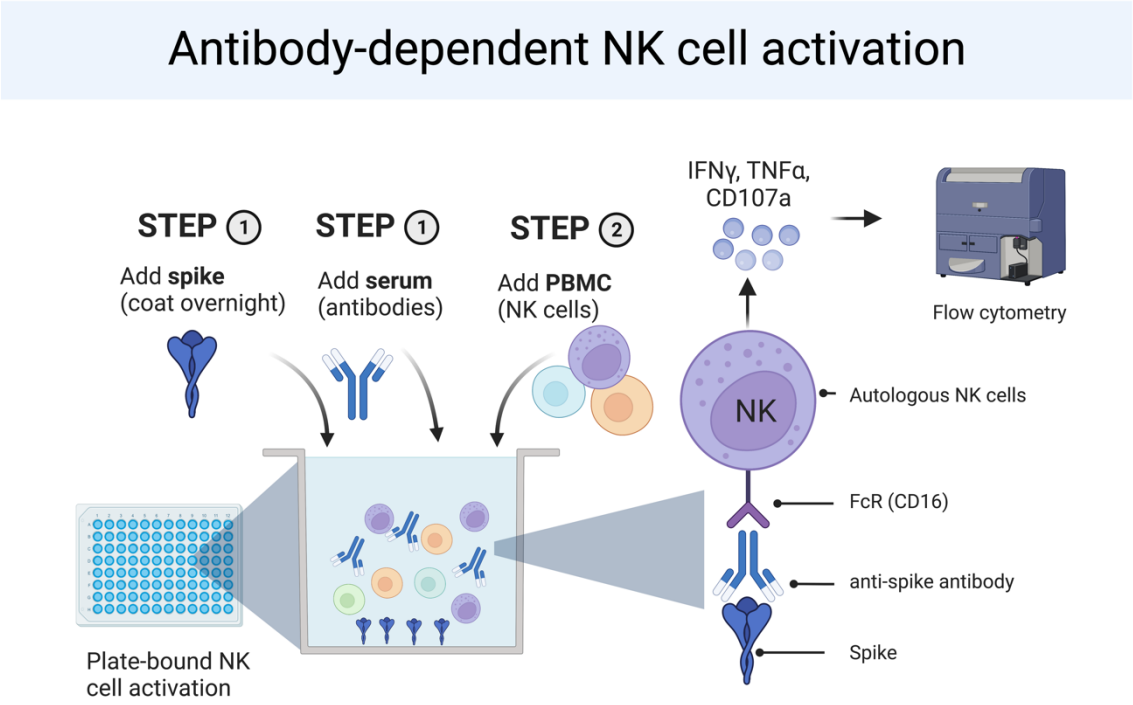


Figure 2.4. Schematic overview of antibody-dependent NK cell activation assay.

Cryopreserved PBMCs were thawed, resuspended in RPMI 1640 supplemented with 5% FBS, 100U/ml penicillin/streptomycin, and 20 mM L-glutamine (Gibco, ThermoFisher) and rested for 2 h at 37 °C. 5 µg/ml purified SARS-CoV-2 spike protein (Spike; Wuhan wild type variant, prepared in section 2.3.7) and an isotype-matched control antibody (mIgG1κ, BD Biosciences) were immobilised on 96-well flat bottom tissue culture plates overnight at 4 °C. Plates were then washed, blocked with 5% FBS (Gibco, ThermoFisher) in RPMI 1640 supplemented as above for 30 min. After a 30-min incubation, blocking medium was removed, and PBMCs from a single study donor or from an internal control

(non-study donor used to maintain variability between experimental batches) were added at a concentration of $0.5x10^6$ cells/well in RPMI 1640 supplemented as above. Heat-inactivated pre- or post-vaccination matched serum (autologous serum from the same study participant), pooled serum (post-vaccination serum from 6 SAR-CoV-2 infected donors), or pre-pandemic serum (serum samples collected before 2018) were added together with anti-CD107α APC-H7 antibody (BD Biosciences, Catalog # 561343, dilution 1 in 200) and incubated for 6h at 37 °C. GolgiStop (containing Monensin, 2 µmol/l) and GolgiPlug (containing brefeldin A, 10 µg/ml) (BD Biosciences) were added for the final 5 h of culture. After stimulation, cells were surface stained with different combinations of surface antibodies in the presence of fixable live/dead stain (Invitrogen Catalog # L34957, dilution 1 in 300). Cells were then fixed and permeabilised (CytoFix/CytoPerm; BD Biosciences), followed by intracellular cytokine staining with IFN-γ BV421 (BD Biosciences, Catalog # 562988, dilution 1 in 50) and TNF-α BV711 (BioLegend, Catalog # 554512, dilution 1 in 50). Samples were acquired on a BD Fortessa X20 using BD FACSDiva8.0 (BD Biosciences), and data were analysed using FlowJo 10 (TreeStar). A full list of antibodies used in the NK cell activation assay is listed in **Table 2.3.**

2.3.9 *Ex vivo* IFN-γ ELISpot assay.

IFN-γ ELISpot assays to measure spike-specific T-cell responses were measured using IFN-γ ELISpot assay (11). ELISPOT plates (S5EJ044I10; Merck Millipore, Darmstadt, Germany) were pre-wetted with 30 µl of 70% ethanol for a maximum of 2 min, washed with sterile PBS and coated overnight at 4 °C with anti-IFN-γ

antibody (10 µg/ml in PBS; clone 1-D1K; Mabtech, Nacka Strand, Sweden). Following overnight incubation, plates were washed with PBS and blocked with R10 (RPMI supplemented with penicillin-streptomycin, L-Glutamine, and 10% FBS) for a minimum of 2 h at 37 °C. The cells were then plated at 2×10^5 cells/well and cultured with overlapping peptide pools (15 to 18-mers overlapping by 10 amino acid residues) at 2 µg/ml or PHA (Sigma Aldrich, St Louis, MO) at 10 µg/ml as a positive control for 16−18 h at 37 °C. Plates were then washed four times with 0.05% Tween/PBS (Sigma Aldrich) followed by two washes with PBS and then incubated for 2 h at room temperature with biotinylated anti-IFN-γ (1 µg/ml; clone mAb-7B6-1; Mabtech). Plates were then washed and incubated with alkaline phosphatase-conjugated streptavidin (Mabtech) at 1:1000 dilution for 1 h. After six further washes, plates were developed using VECTASTAIN® Elite ABC-HRP according to the manufacturer's instructions (Mabtech). All assays were performed in duplicate. Spots were counted using an automated ELISpot Reader System (Autoimmun Diagnostika GmbH).

Overlapping Peptide pools:

For the detection of virus-specific T-cell responses, PBMCs were stimulated with the following peptide pools:

1. Wild-type SARS-CoV-2 spike: a total of 15 to18-mers overlapping by 10 amino acid residues for Spike (S) synthesised using two-dimensional peptide Matrix pools, divided into 16 "mini pools" P1−P16 and grouped into pools S1 (P1−8) and S2 (P9−16) (kindly provided by Prof. Tao Dong's laboratory, University of Oxford).

2. Wild-type SARS-CoV-2 structural and accessory proteins: 15-mer peptides overlapping by 10 amino acid residues for Membrane protein (M) (Miltenyi Biotec), Nucleoprotein (N) (Miltenyi Biotec), Envelope (Env) protein and open reading frame (ORF) 3, 6, 7, 8 (kindly provided by Prof. Tao Dong's laboratory, University of Oxford)

3. Variant of concerns (VOC) spike-specific peptide pools; the WuhanHu-1 and variant pools containing peptides from the Wuhan Hu-1, Alpha (B.1.1.7), Beta (B.1.351), Delta (B.1.617.2) and Omicron (BA.1/B.1.1.529.1) sequences (9, 19, 32 and 83 peptides, respectively) were used to define T-cell responses to mutated sequences in SARS-CoV-2 variants. Alpha and Beta peptide pools were synthesised by GL Biochem Shanghai Ltd, China and previously used in (215). The corresponding controls to Alpha and Beta pools with Wuhan Hu-1amino acid sequences were compared in parallel within the same donor. Delta and Omicron pools were obtained from Miltenyi Biotec.

4. Non-SARS-CoV-2 antigens: Peptide pools of the pp65 protein of HCMV (Miltenyi Biotec, and NIH AIDS Reagent Repository), or HIVconsv peptide pools (NIH AIDS Reagent Repository).

2.3.10 Intracellular cytokine stimulation (ICS) functional assay.

Purified PBMCs were thawed and rested overnight at 37 °C and 5% carbon dioxide in complete RPMI medium (RPMI supplemented with penicillin-streptomycin, L-Glutamine, HEPES, non-essential amino acids, 2-Mercaptoethanol, and 10% FBS). After overnight rest, PBMCs were stimulated for 6 h with 2 µg/ml of SARS-CoV-2 peptide pools, HIV-1 Gag or cytomegalovirus (CMV)-pp65 peptide pools, or with 0.005% DMSO as a negative control in the presence of αCD28/αCD49d co-Stim antibodies (1 µg/ml) GolgiStop (containing Monensin, 2 µmol/l), GolgiPlug (containing brefeldin A, 10 µg/ml) (BD Biosciences) and anti-CD107α BV421 antibody (BD Biosciences, Catalog # 562623, dilution 1 in 200). After stimulation, cells were washed and stained with anti-CCR7 (BioLegend, Catalog # 353212, dilution 1 in 50) for 30 min at 37 °C and then surface stained at 4 °C for 20 min with different combinations of surface antibodies in the presence of fixable live/dead stain (Invitrogen Catalog # L34957, dilution 1 in 300). Cells were then fixed and permeabilised (CytoFix/CytoPerm; BD Biosciences), followed by intracellular cytokine staining with IFN-γ APC (BioLegend, Catalog # 506510, dilution 1 in 100), CD154 PE-Cy7 (BioLegend Catalog # 310832, dilution 1 in 200), TNF-α FITC (BD Biosciences, Catalog # 554512, dilution 1 in 400) and PerCP-eFluor 710 IL-2 (eBioscience, Catalog # 46-7029-42, dilution 1 in 50). Samples were acquired on a BD Fortessa X20 using BD FACSDiva8.0 (BD Biosciences), and data were analysed using FlowJo 10 (TreeStar). The gates applied for the identification of virus-specific $CD4^+$ and $CD8^+$ T cells were based on the double-positive populations for interferon-γ (IFN-γ), tumour necrosis factor (TNF-α), interleukin-2 (IL-2), and CD40 ligand (CD154)

(See Chapter 5, Figure 5.4. and 5.5.). The total population of SARS-CoV-2 $CD4^+$ T cells was calculated by summing the magnitude of $CD154^+IFN\text{-}\gamma^+$, $CD154^+IL\text{-}2^+$, and $CD154^+$ $TNF\text{-}\alpha^+$ responses; SARS-CoV-2 $CD8^+$ T cells were defined as ($IFN\text{-}\gamma^+TNF\text{-}\alpha^+$, $IFN\text{-}\gamma^+IL\text{-}2^+$). A complete list of antibodies used in the ICS assay is listed in **Table 2.5.**

Table 2.5. ICS functional assay panel.

Laser	Filter	Antigen/mAb	Fluorochrome	Supplier	Identifier	Clone	Dilution	Staining
488 Blue	710/50	IL-2	PerCP-eFluor™ 710	eBioscience	Cat # 46-7029-42	Clone # MQ1-17H12	1 in 50µl	Intracellular
	530/30	TNF-α	FITC	BD Biosciences	Cat # 554512	Clone # MAb11	0.125 in 50µl	Intracellular
405 Violet	450/50	CD107a	BV421	BD Biosciences	Cat # 562623	Clone # H4A3	0.25 in 50µl	During stimulation
	525/50	CD14	BV510	BioLegend	Cat # 301842	Clone # M5E2	0.25 in 50µl	Surface
		CD19	BV510	BioLegend	Cat # 302242	Clone # HIB19	0.25 in 50µl	Surface
		Live Dead stain	Aqua	Life technologies			1 in 300µl	Surface
	605/40	CD56	BV605	BD Biosciences	Cat # 562780	Clone # NCAM16.2	1 in 50µl	Surface
	677/20	CD3	BV650	BioLegend	Cat # 317324	Clone # OKT3	0.5 in 50µl	Surface
	710/50	PD-1	BV711	BioLegend	Cat # 329928	Clone # EH12.2H7	1 in 50µl	Surface
	810/40	CD8	BV785	BioLegend	Cat # 301046	Clone # RPA-T8	1 in 50µl	Surface
637 Red	670/30	IFN-γ	APC	BioLegend	Cat # 506510	Clone # B27	1 in 50µl	Intracellular
	730/45	CD45RA	Alexa Fluor®700	BioLegend	Cat # 304120	Clone # HI100	1 in 50µl	Surface
	7 80/60	CCR7	APC/Cy-7	BioLegend	Cat # 353212	Clone # G043H7	1 in 50µl	Surface
561 Yellow/ Green	660/20	CD154	PE-Cy-7	BioLegend	Cat # 310832	Clone # 24-31	0.25 in 50µl	Intracellular
	610/20	CD4	PE/Dazzle 594	BioLegend	Cat # 300548	Clone # RPA-T4	0.5 in 50µl	Surface

2.3.11 Cytokine bead assays.

Biomarkers were measured from cryopreserved plasma stored at -80 ºC. The full list of biomarkers measured is listed in **Table 2.6.** The levels of all plasma soluble biomarkers were measured using the Luminex multiplex bead assay on a BioPlex-100 instrument according to the manufacturer's protocol and dilutions (Luminex technology, Hertogenbosch, Netherlands). Biomarker levels were calculated from a standard curve using standards of known concentration. All plasma samples were measured on the same machine, used on their first thaw and measured in duplicate, with a mean value taken from the two measurements.

Table 2.6: List of biomarkers measured in SARS-CoV-2 study.

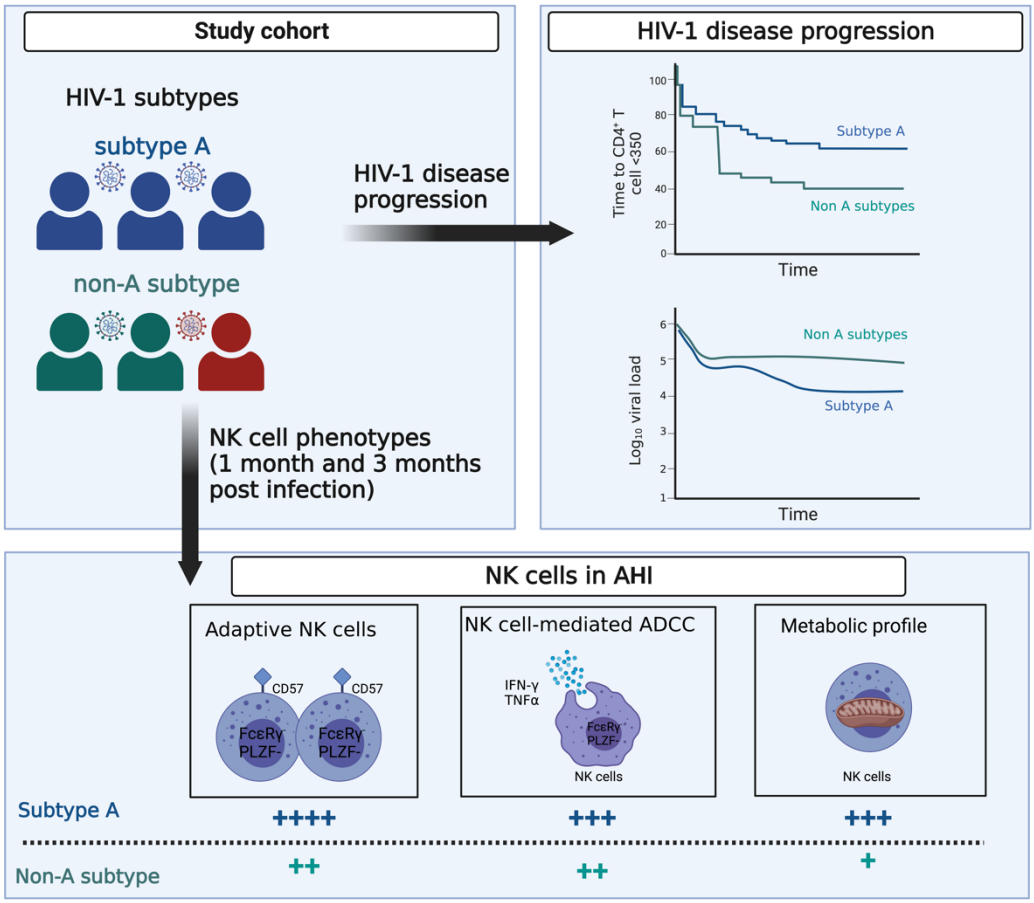
Biomarker	Bead Region	Dilution	Standard curve (pg/mL)
VEGF	26	1:2	0.89-217
IL-6	13	1:2	0.49-118
sCD14	29	1:200	21-5103
CRP	62	1:200	10.37-2520
sCCL5/RANTES	36	1:50	2.25-547
D-Dimer	43	1:4000	0.03-7.6
Angiopoietin-1	65	1:2	12.63-3069
sCCL2	25	1:2	3.41-828
sCD25	47	1:2	2.7-657
sCD40-L	74	1:2	74.6-18129
CXCL8/IL-8	18	1:2	0.47-114
Fas	73	1:2	14.58-3544
IL-12p70	43	1:2	3.5-851
TNF-R1	66	1:2	22.15-5382
Angiopoietin-2	26	1:2	25.77-6263
sCD163	28	1:2	519.56-126252
sCD27	67	1:2	17.06-4146
IP-10	21	1:2	0.28-69
Fas-L	39	1:2	1.78-433
IFN-y	29	1:2	4.93-1197
IL-10	22	1:2	0.37-89

Chapter 3: The NK cell landscape during acute HIV-1 infection with different subtypes.

Publication.

Alrubayyi A et al. Adaptive NK cells during acute HIV-1 infection with different subtypes. CROI2022. 2022 Feb 16; Abstract no.306.

Chapter 3 graphical abstract.



Chapter 3 written abstract.

Understanding the early immune response to HIV-1 infection represents a unique opportunity to identify novel targets for prophylactic/therapeutic approaches. NK cells are an important component of innate immunity that can modulate the pathogenesis of AHI. However, the role of NK cells in mediating early host defence against infection with different HIV-1 subtypes and clinical outcomes remains poorly understood. In this chapter, I studied the early imprinting effects of different HIV-1 subtypes and the pro-inflammatory environment on the NK cell compartment in a subset of the IAVI Protocol C cohort. Participants were sampled longitudinally at 1 month and 3 months post-EDI in four different sub-Saharan African sites (n=28 subtype A, n=17 subtype C, n=7 subtype D)). Subtype A infection was associated with a lower rate of $CD4^+$ T-cell decline to <350 cells/mm^3 and a trend towards a lower median HIV-1 viral load over a period of three years in the absence of ART. Participants with subtype A infection had higher frequencies of NK cell subsets with adaptive/memory features compared to non-A subtype infection. This adaptive NK cell signature was delineated by lower expression of the signalling molecule FcεRγ and transcription factor PLZF and was further enriched by higher expression of the activating receptor NKG2C. Increased frequencies of adaptive NK cells were associated with lower HIV-1 viral load and higher $CD4^+$ T-cell counts (>500 cells/mm^3). These phenotypic attributes were accompanied by enhanced NK cell ADCC capacity and higher IFN-γ and TNF-α production in subtype A versus non-A. The enhanced functionality of NK cells was reflected in their superior capacity for oxidative phosphorylation. These data suggest that specific NK cell subsets could confer better HIV-1 control, with implications for vaccine and immunotherapeutic development.

Chapter 3

3.1 Introduction.

Global trends in HIV-1 infection demonstrate an overall increase in HIV-1 prevalence and a substantial decline in the rate of HIV-1-related death, largely attributable to the survival benefits of ART (216). Access to ART treatment, however, remains a crucial issue for people with HIV-1 living in limited-resource countries such as sub-Saharan Africa (217). Sub-Saharan Africa carries a disproportionate burden of HIV-1, accounting for more than 70% of global HIV-1 infections (216,218). Developing effective and durable strategies that contribute to HIV-1 prevention in sub-Saharan Africa has the potential to impact the global burden of HIV-1 (216). A better understanding of important immune responses during the acute and early HIV-1 infection, defined here as the period between the estimated date of infection and up to 3 months post-infection in people with HIV-1 in Africa, could help in identifying future prophylactic and therapeutic targets. Early innate immune responses contribute to the containment of viral replication and are an important determinant of the level of adaptive immune activation and subsequent disease outcome (61).

NK cells precede adaptive immunity during the early stages of HIV-1 infection, where a rapid expansion of cytotoxic $CD56^{dim}$ NK cells is observed prior to $CD8^{+}$ T-cell expansion (219). Evidence from immunogenetic, antiviral functional, and viral evolution/immune evasion studies further implicate NK cells as important contributors to immune control of HIV-1, linking specific KIR/HLA combinations with disease outcome and protective KIRs with enhanced NK cell function *in vitro* (112,113,219,220). Further studies have indicated that the relative contribution of

NK cells in controlling virus replication is influenced by the degree of HIV-mediated changes to MHC class I expression and the strength of KIR/HLA interactions (221). Additionally, indirect NK cell-mediated ADCC is a potent means of control of HIV-1 infection, and has been associated with vaccine-induced protective immunity and implicated in phenotypes of virus control and slower disease progression (222–225). During hyperacute infection, NK cells have been described to constitute the highest proportion of proliferating cells in the first weeks of infection (within 0-1 weeks following infection), and their proliferative and cytotoxic capacities were associated with natural control of HIV-1 (58). In support of these observations, a recent study in Asian populations demonstrated that upregulation of genes related to NK cell degranulation, cytokine signalling, and inflammatory responses during AHI (at the VL set-point) was linked to reduced HIV-1 disease progression (226). Collectively, these findings suggest that NK cells are primed for increased responses at the initial phase of infection and that their early functions can potentially shape the course of disease.

The NK cell repertoire is not stable, and its diversity increases with exposure to HIV-induced inflammatory cytokines (109) and HCMV antigens (227), an almost universal co-infection in people with HIV-1 in Africa (228). HCMV infection drives the expansion of a specialised NK cell subset, adaptive NK cells (as described in Chapter 1, section 1.1.8.3). These long-lasting expansions were originally characterised by the upregulation of activating NKG2C receptor in NK cells from HCMV-seropositive individuals (96,99). However, HCMV-adaptive NK cells are

not confined to NKG2C-expressing cells alone; rather, they encompass heterogeneous subsets characterised by a number of phenotypic attributes (99). These adaptive NK cells are characterised by DNA methylation-dependent silencing of the transcription factor PLZF and stochastic loss of expression of key proximal signalling molecules such as FcεRI-γ (96,103,229). In AHI, adaptive NK cells ($CD57^{+}NKG2C^{+}$) correlated negatively with HIV-1 viral load and were associated with a lower VL set-point (126,127). Along these lines, adaptive NK cells were found to correlate with sustained post-treatment virus control in a patient who maintained an undetectable viral load for longer than 15 years without ART (230). Collectively, these data suggest that NK cells with adaptive features may constitute a readily armed population that may contribute to virus control.

In this chapter, I performed a comprehensive longitudinal phenotypic and functional analysis of NK cell subsets in subtype A, C, and D infection in individuals recruited within 1 month and 3 months following HIV-1 acquisition. The aim was to explore the early imprinting effects of different HIV-1 subtypes on the NK cell compartment and their association with long-term virus control following infection with different HIV-1 subtypes.

3.2 Results.

3.2.1 The study cohort

This study utilised archived PBMCs samples collected by a large multicentre study, IAVI Protocol C study (4,31). The IAVI Protocol C study recruited individuals with documented early HIV-1 infection between 2006 and 2011 through different research centres in Uganda, Kenya, Rwanda, and Zambia (4,31). Study participants were recruited from prospective incidence cohorts of HIV-negative individuals (HIV-serodiscordant couples, men who have sex with men (MSM), or female sex workers) who received HIV-1 prevention support and were tested monthly or quarterly (depending on the centre) for HIV-1 incidence (4). After HIV-1 diagnosis, participants were followed monthly for the first three months post-EDI, quarterly through two years, and semi-annually thereafter. Demographic and clinical information was recorded for each participant, including age, sex, risk factor, $CD4^+$ T-cell counts, and HIV-1 viral load. The HIV-1 virus subtype was determined by analysing the sequence of *pol* and *env* genes in the first specimen after HIV-1 detection.

In this study, a total of 56 individuals infected with different HIV-1 subtypes were included (**Table 1.1, Figure. 3.1A-C)**. Of these donors, 28 were infected with subtype A, and 24 were infected with non-A subtypes (n=7 subtype D and n=17 subtype C). The two study groups were sampled at a similar median number of days post-EDI (visit 1; subtype A = 32.5 days (range: 19-42), and non-A subtype = 34.5 days (range:17-42), visit 2; subtype A = 86 days (range: 66-110), and non-

A subtype = 91 days (range:75-117)). The majority of subtype A participants were recruited through research centres in Kenya (60%) and Rwanda (39%), and non-A subtype participants were predominantly recruited in Zambia (58.5%) or Uganda (29%). The median age of subtype A and non-A participants was 26 and 32 years, respectively, and they were predominantly males. The cohort included participants capturing a range of enrolment viral load (Log_{10} viral load (copies/ml): subtype A: median: 5.01, range: 2.78-7.29; non-A subtypes: median 5.10, range: 2.64-6.20). The enrolment visit plasma viral loads and $CD4^+$ T-cell counts did not differ significantly between subtype A and non-A subtypes **(Figure. 3.1B&C)**. All participants included in this study had not yet initiated ART treatment for the time-points analysed here. Further details on patients' characteristics are included in **Table 3.1.**

Table 3.1 Cohort Demographics and Clinical Characteristics

			Subtype A	Non-A subtypes
Group size		n (%)	28	24
HIV-1 subtypes	Viral subtypes	A	28(100%)	-
		C	-	17 (60.7)
		D	-	7 (25%)
Days post estimated date of infection (EDI)	Visit 1	Days post EDI [A], median (range)	32.5 (19-42)	34.5 (17-42)
	Visit 2	Days post EDI, median (range)	86 (66-110)	91 (75-117)
Recruitment clinical site	Research centre, country	Kigali, Rwanda, n (%)	11 (39.3%)	0 (0%)
		Kilifi, Kenya, n (%)	17 (60.7%)	5 (20%)
		Masaka, Uganda, n (%)	0 (0%)	6 (26%)
		Lusaka, Zambia, n (%)	0 (0%)	13 (54%)
Risk groups and demographics	Age	Age (years), median (range)	26.5 (19-52)	32.5 (20-51)
	Sex	Gender (n) female:male	5:23	4:20
	Risk group	Discordant couple (DC), n (%)	13 (46.5%)	18 (75%)
		men who have sex with men (MSM), n (%)	15 (53.5%)	6 (25%)
HIV-1 parameters	Visit 1	Log_{10} HIV-1 viral load, median (range)	5.01 (2.78-7.29)	5.10 (3.03-6.2)
		$CD4^+$ T cell count, median (range)	549 (189-1759)	485.5 (242-828)
	Visit 2	Log_{10} HIV-1 viral load, median (range)	4.87 (2.78-6.02)	4.82 (2.64-6.04)
		$CD4^+$ T cell count, median (range)	451 (267-1776)	503 (264- 1041)
	Set-point viral load	Log_{10} pVL set-point [B], median (range)	4.52 (1.66-5.69)	4.65 (3.3-5.77)
HLA-B variants	HLA-B*18 (B*18:01)	n (%)	0 (0)	2 (8.3)
	HLA-B*44 (B*44:03)	n (%)	0 (0)	1 (4.1)
	HLA-B*45 (B*45:01)	n (%)	4 (14)	0 (0)
	HLA-B*53 (B*53:01)	n (%)	1 (3.5)	0 (0)
	HLA-B*57 (B*57:03)	n (%)	1 (3.5)	1 (4.1)

[A] EDI was defined as the date of a high-risk exposure incident, midpoint between the last negative and the first HIV-antibody positive test, 10 days prior to the first positive PCR test, or 14 days prior to the first positive p24 antigen test.

[B] pVL set-point was defined according to the calculations for the Protocol C dataset. Data were missing for n=8 subtype A, and n=7 non-A subtype.

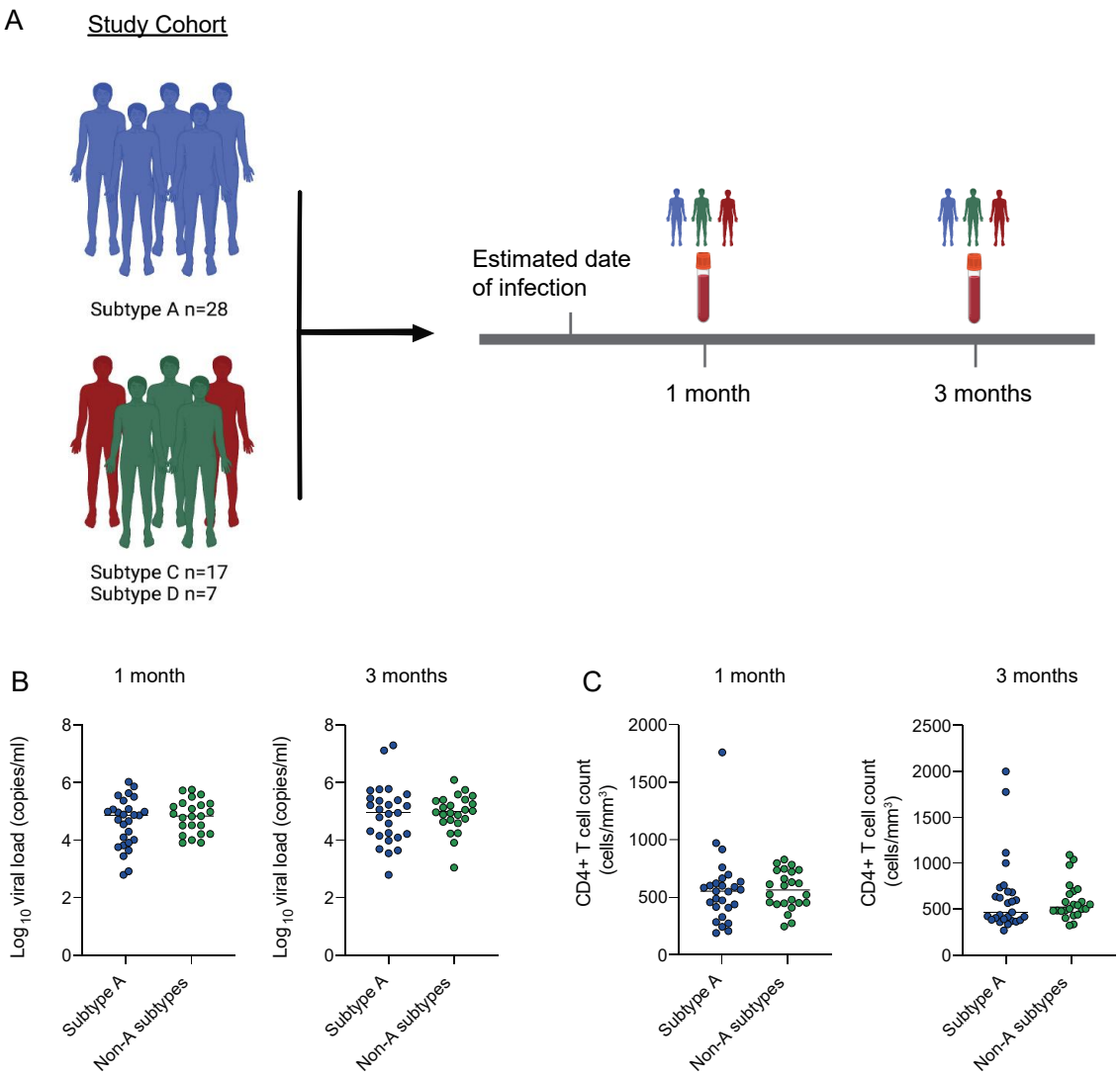


Figure 3.1. Schematic overview of patient cohorts.

(A) Overview of patient cohorts in this study, including subtype A (blue, n=28), subtype C (green, n=17), and subtype D (red, n=7) participants. This was a longitudinal study, with samples collected at each time-point (1 month and 3 months post-ED). **(B)** Plasma viral load and **(C)** $CD4^+$ T-cell counts after 1 month or 3 months post-EDI.

3.2.2 Subtype A is associated with slower disease progression in treatment-naïve participants.

Despite a comparable viral load at 1 month and 3 months post-infection in subtype A and non-A infections, subtype-specific differences in HIV-1 disease progression have been described in a number of studies using different endpoints (virological, immunological, and clinical outcomes) (27,29–31,231–233). To examine these associations in our cohort, I initially assessed the plasma viral load and $CD4^+$ T-cell counts from the first detection of viraemia and up to 3.5 years in subtype A and non-A subtype infected individuals **(Figure. 3.2A)**. The plasma viral load and $CD4^+$ T-cell counts were collected from the majority of participants after HIV-1 diagnosis, monthly for the first three months, quarterly through two years, and semi-annually thereafter **(Figure. 3.2A)**. Analysis of longitudinal VL data from the onset of detectable plasma viraemia and up to 3.5 years post-infection showed a trend towards a lower median HIV-1 viral load over time in participants with subtype A infection compared to non-A subtype infection in the absence of ART **(Figure. 3.2B-D),** consistent with previous observations in a larger cohort of the IAVI Protocol C participants (234). Similarly, the rate of $CD4^+$ T-cell decline to <350 cells/mm^3 was significantly slower among individuals infected with subtype A, compared to non-A subtype donors (without ART treatment) **(Figure. 3.3A-C)** (31). In a subset of untreated participants with available $CD4^+$ T-cell counts at 3.5 years post-EDI of infection, subtype A was also significantly associated with higher $CD4^+$ T-cell counts compared to non-A subtype participants **(Figure. 3.3D)**. Given the heterogeneous populations included in this cohort, HLA variants that were previously described to associate

with viral control and $CD4^+$ T-cell decline in the IAVI Protocol C cohort were analysed (234,235). These HLA-B variants (HLA-B*18, HLA-B*44, HLA-B*45, HLA-B*53, and HLA-B*57) were rarely detected in our cohort and were equally distributed between the two groups **(Table 3.1)**, suggesting that the influence of subtype A on disease progression was independent of host genetics. Collectively, these data reinforce previous observations in the IAVI Protocol C studies and suggest that subtype A infection is associated with a better long-term viral control compared to non-A subtype infection (subtypes C and D) (27,32,234).

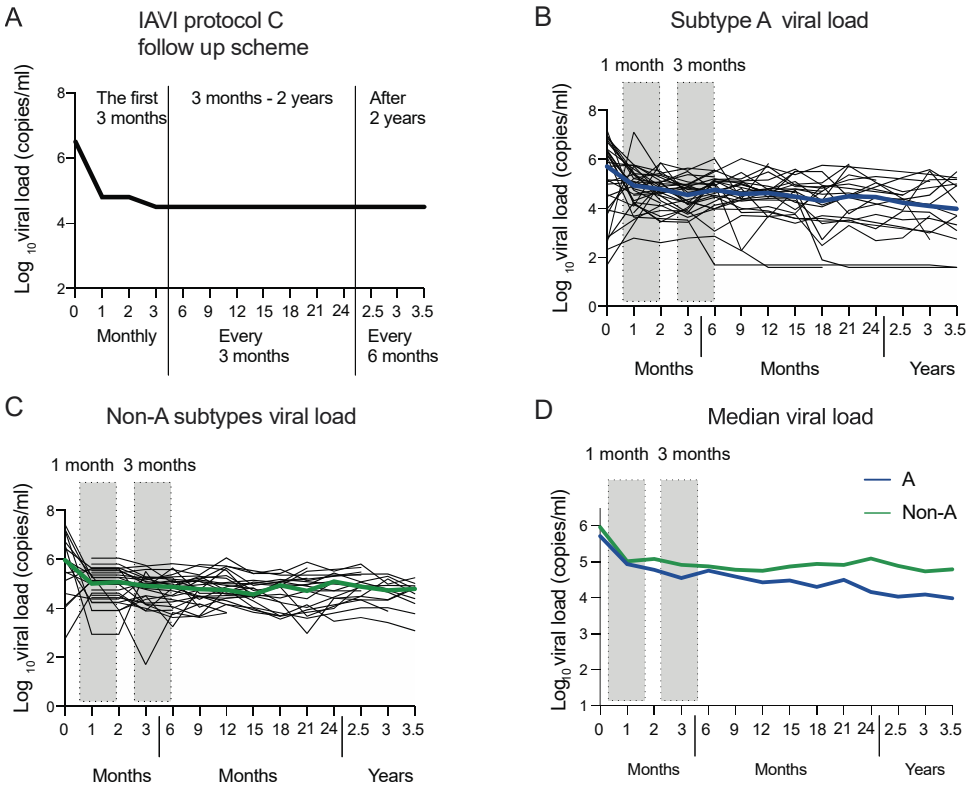


Figure 3.2. Longitudinal measurements of plasma viral load in the IAVI protocol C cohort.

(A) Depiction of the IAVI Protocol C follow-up scheme. Viral load (Log_{10}) for **(B)** subtype A and **(C)** non-A subtype participants following the onset of detectable plasma viraemia and up to 3.5 years. All measurements after the initiation of ART were excluded from the analysis. Thickened line represents the median viral load. The time-points sampled in this study are highlighted in the grey-shaded box (1st time-point = 1 month; 2nd time-point = 3 months). **(D)** Comparison of median viral load in ART treatment-naïve subtype and non-A participants.

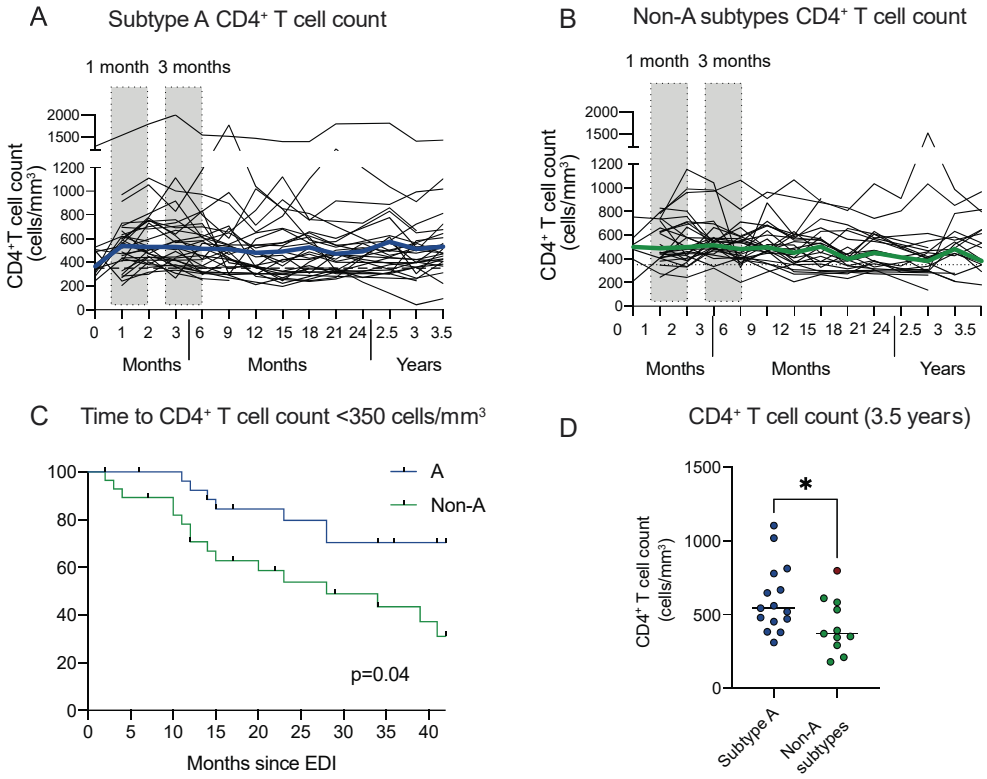


Figure 3.3. Lower rate of CD4⁺ T-cell count in subtype A infection.

CD4⁺ T-cell counts for **(A)** subtype A and **(B)** non-A subtype participants. (**C)** Kaplan-Meier survival curve representing time to CD4⁺ T-cell count ≤350 cells/mm^3 in the two study groups. (**D)** CD4⁺ T-cell counts at 3.5 years in subtype A and non-A subtype participants. Significance was determined by two-tailed Mann-Whitney U test, *p <0.05.

3.2.3 Distinct NK cell signatures in subtype A and non-A subtype infection during AHI

An association between NK cell responses during the early phase of infection and the subsequent disease course has been described in various patient cohorts (58,73,226,236). We, therefore, evaluated the changes in the NK cell subpopulations following infection with different subtypes and their association with HIV-1 viraemia. To this end, I utilised an NK-cell-focused flow cytometry panel that included markers of NK cell activation (CD38), maturation/differentiation (CD57) and features characteristic of adaptive NK cells (PLZF, FcεRIγ, NKG2C, NKG2A, and Siglec-7) **(Chapter 2; section 2.1.4, Table. 2.1)**. The frequencies of total NK cells, $CD56^{neg}$, $CD56^{dim}$, and $CD56^{bright}$ NK cell subsets were comparable between the two study groups at 1 month and 3 months post-EDI **(Figure. 3.4A&B)**. A decline in the total NK cell frequency was detected in participants with subtype A infection but not in non-A subtype infection **(Figure. 3.4B)**.

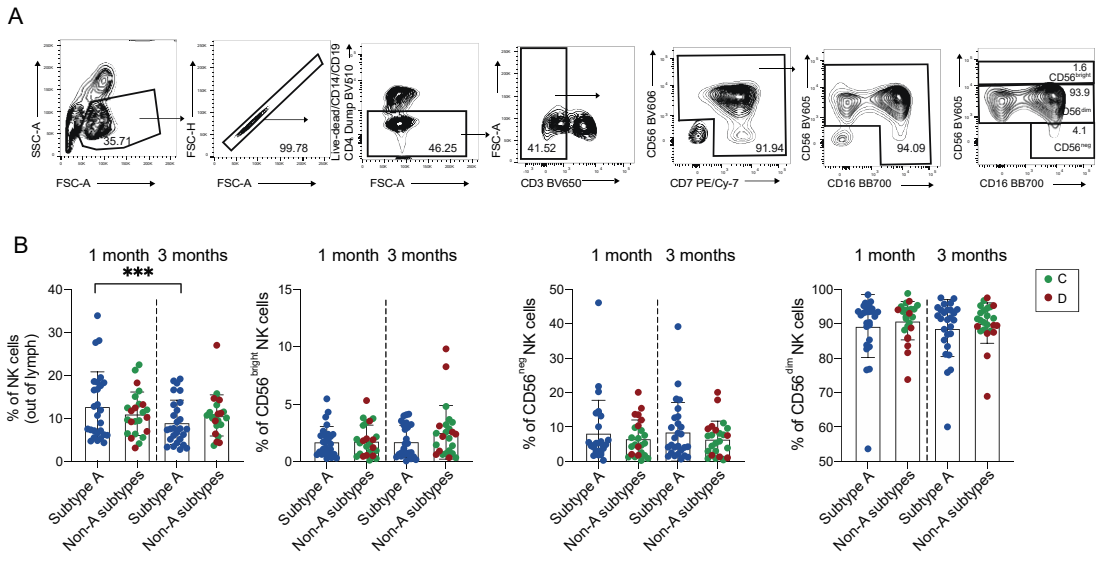


Figure 3.4. NK cell distribution in individuals infected with different subtypes.

(A) Example of gating strategy used to identify NK cell subsets. Cells were gated on a single lymphocyte population by side and forward side scatter, followed by live cells gating by excluding dead, $CD4^{+}$, $CD19^{+}$, and $CD14^{+}$ cells. Following gating on live $CD3^{-}$ T cells, cells were gated on $CD56^{+/-}$ and $CD7^{+/-}$. Total NK cells were then identified by gating in $CD16^{+/-}$ and $CD56^{+/-}$. **(B)** Summary analysis of the percentage of total NK cells, $CD56^{bright}$, $CD56^{dim}$, and $CD56^{neg}$ NK cells in subtype A and non-A subtype individuals at 1 and 3 months post-EDI. Plots show the geometric mean. In non-A subtypes, green dots denote subtype C and red dots subtype D participants. Significance determined by two-tailed Mann-Whitney U test or Wilcoxon matched-pairs signed rank test, ***p <0.001.

In order to identify a specific NK cell signature in the two study groups, I applied an unbiased approach and unsupervised high-dimensional analysis (t-SNE), followed by FlowSOM clustering **(Figure. 3.5A)**. Ten major NK cell subsets were identified using a combination of various markers, including PLZF, FcεRIγ, NKG2C, NKG2A, CD57, Siglec-7, CD38, and Granzyme B. A distinct NK cell

cluster representing adaptive NK cells ($PLZF^{-}FcεRIγ^{-}CD57^{+}$) was enriched in subtype A compared to non-A subtype individuals at both time-points (**Figure. 3.5B**); in contrast, NK cells from participants with non-A subtype infection were characterised by a higher abundance of non-adaptive NK cells ($PLZF^{+}FcεRIγ^{+}NKG2A^{+}$) (**Figure. 3.5B**). The higher proportion of adaptive NK cells in subtype A subjects was further confirmed by manual gating (**Figure. 3.5C**). Because of the heterogeneity of the cohort (different ethnicities and geographical locations), I performed an analysis looking only at the Kenyan participants. Although the number of non-A subtype individuals was low (n=5), it is worth noting that the frequency of $PLZF^{-}FcεRIγ^{-}CD57^{+}$ cells remained higher in subtype A compared to non-A individuals (**Figure. 3.5D**).

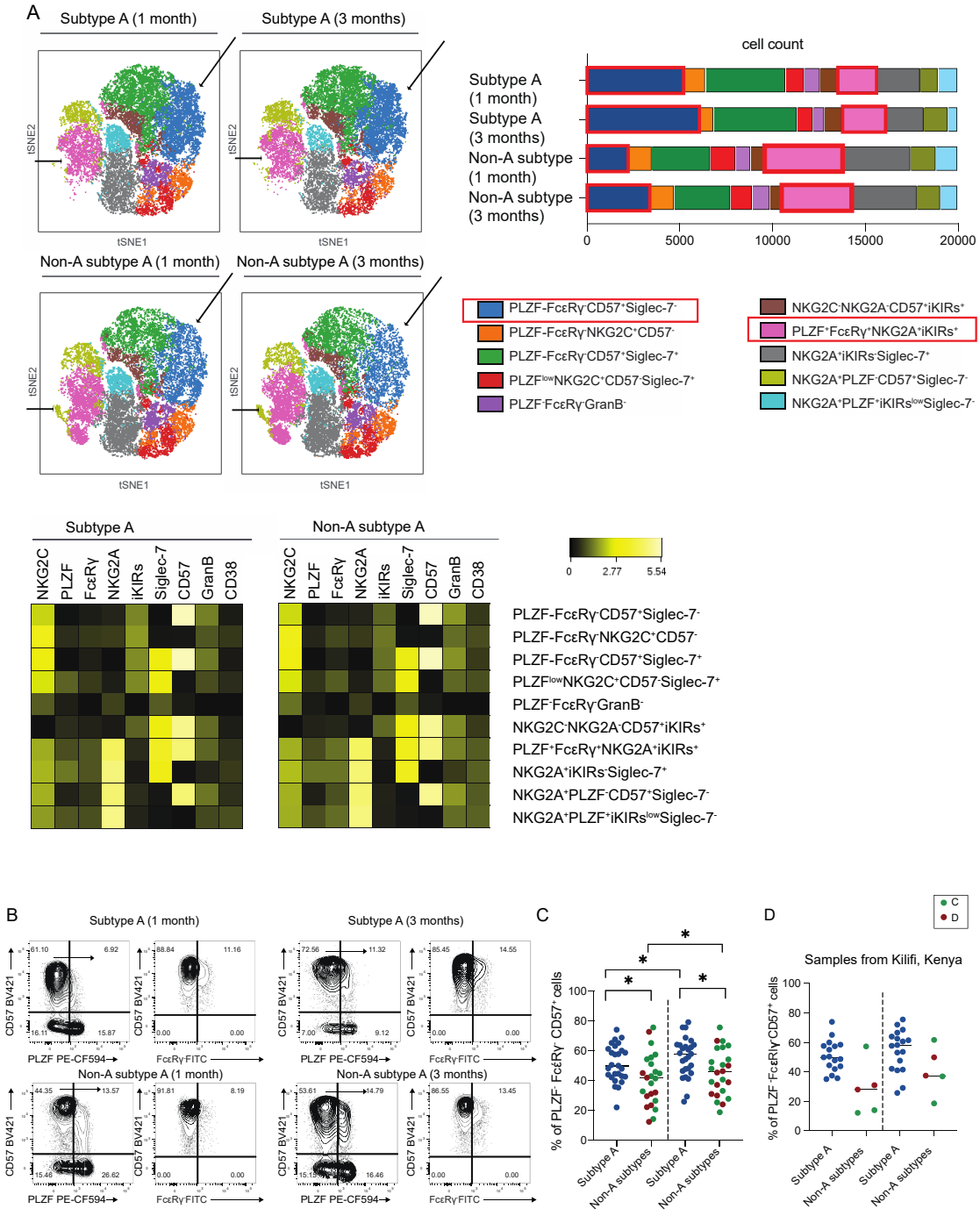


Figure 3.5. Subtype A infection is characterised by an expansion of adaptive NK cells.

(A) viSNE map of FlowSOM metaclusters of NK cells from subtype A and non-A subtype subjects at 1 month or 3 months post-EDI. Each point on the high-dimensional mapping represents an individual cell, and metaclusters are colour-coded. The bar chart represents the cell counts of

each FlowSOM metacluster out of the total NK cells in each group. (**B)** Representative flow plots and summary data of the percentage of PLZF$^-$FcεRγ$^-$CD57$^+$ NK cells in subtype A and non-A subtype donors. **(D)** Frequencies of PLZF$^-$FcεRγ$^-$CD57$^+$ NK cells in subtype A and non-A subtype participants from Kilifi, Kenya. Significance determined by two-tailed Mann-Whitney U test or Wilcoxon matched-pairs signed rank test, *p <0.05.

Next, I assessed in more detail what might be driving the higher frequencies of adaptive NK cells in subtype A infection. A recent report indicated an association between the presence of adaptive NK cells and inflammatory markers that are elevated during early infection (109). I, therefore, initially examined the correlation between the frequencies of PLZF$^-$FcεRγ$^-$CD57$^+$ adaptive NK cells and soluble markers measured at 1 month post-EDI. Forty soluble markers were measured in the plasma using multiplex assays by Hassan and Esbjörnsson *et al*. (5), collaborators and a co-supervisor in the study (**Chapter 2, Table 2.4).** A full analysis of pro-inflammatory markers and other soluble factors in Protocol C patients, including differences between subtypes, is reported elsewhere (5). Participants with subtype A and non-A subtype infections were classified into two groups: individuals with low (<44% of PLZF$^-$FcεRγ$^-$CD57$^+$) or high (>44% of PLZF$^-$FcεRγ$^-$CD57$^+$) proportion of adaptive NK cells (96), using the median frequencies of PLZF$^-$FcεRγ$^-$CD57$^+$ NK cells in the cohort as a threshold **(Figure. 3.6.A)**. No significant differences were detected in the level of measured analytes according to infecting subtype **(Table 3.2)**. Notably, plasma levels of IL-12 and IL-2 were significantly higher in individuals with a high percentage of adaptive NK cells (**Figure. 3.6B**). I next analysed the relationship between the frequency of adaptive NK cells and CD4$^+$ T-cell counts, or viral loads at 1 month post-infection

(**Figure. 3.6C&D**). A higher frequency of adaptive NK cells was associated with lower viral load and higher CD4⁺ T-cell counts (>500 cells/mm³) (**Figure. 3.6C&D**).

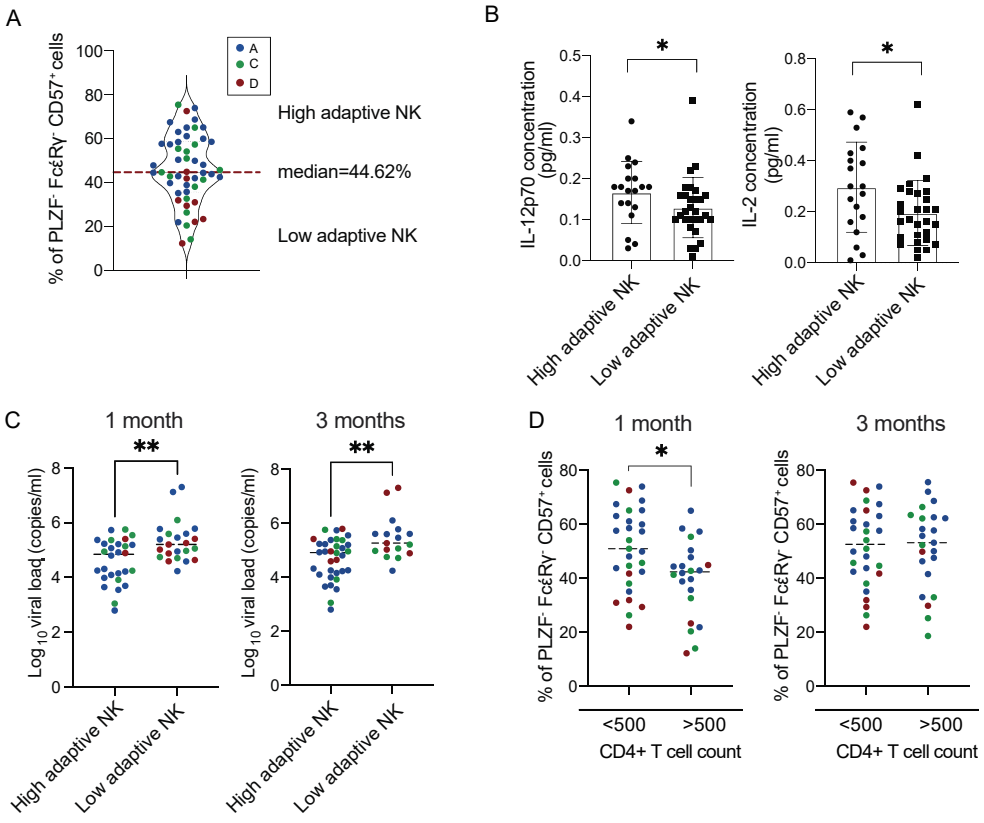


Figure 3.6. Associations between adaptive NK cells, viral load, and CD4⁺ T-cell count.

(**A)** The frequency of PLZF⁻FcεRγ⁻CD57⁺ NK cells in the cohort and threshold used to define the low and high frequency of adaptive NK cells. **(B)** IL-12p70 and IL-2 plasma levels in individuals with high or low frequencies of adaptive NK cells (High adaptive NK >44.62%; Low adaptive NK ≤44.62%). **(C)** Viral load (Log_{10}) in the indicated groups having a low or high proportion of adaptive NK cells at the two time-points. (**D)** The percentage of PLZF⁻FcεRγ⁻CD57⁺ NK cells in individuals with high CD4⁺ T-cell counts (>500 cells/mm³) or low CD4⁺ T-cell counts (≤500 cells/mm³). Significance determined by two-tailed Mann-Whitney U test. *p <0.05, **p <0.01.

Table 3.2. Comparison of plasma biomarker concentration between subtype and non-A subtype participants at 1 month visit.

Soluble factor	P value	Mean rank of Subtype A	Mean rank of Non-A subtypes	Mean rank diff.
GM-CSF	0.657	25.83	23.98	1.856
IL-1	0.613	25.94	23.84	2.104
IL-5	0.247	27.15	22.36	4.785
IL-7	0.439	26.44	23.23	3.217
IL-12	0.068	28.37	20.86	7.507
IL-15	0.315	23.13	27.3	-4.166
IL-16	0.430	23.52	26.82	-3.3
IL-17	0.513	23.78	26.5	-2.722
TNF-α	0.084	21.81	28.91	-7.094
VEGF	0.151	22.33	28.27	-5.939
MIP-1α	0.170	22.44	28.14	-5.692
IP-10	0.727	25.67	24.18	1.485
MIP-1β	0.530	23.81	26.45	-2.64
IL-8	0.791	24.5	25.61	-1.114
MCP-1	0.129	22.19	28.45	-6.269
MDC	0.433	23.54	26.8	-3.258
MCP-4	0.260	22.91	27.57	-4.661
VEGF	0.425	20.89	23.05	-2.157
Tie-2	0.089	28.15	21.14	7.012
Flt-1	0.115	27.93	21.41	6.517
PlGF	0.628	25.91	23.89	2.021
bFGF	0.679	24.22	25.95	-1.732
IL-1	0.263	23.02	27.43	-4.413
IL-2	0.075	21.72	29.02	-7.301
IL-4	0.476	23.7	26.59	-2.887
IL-6	0.156	22.37	28.23	-5.857
IL-8	0.196	22.59	27.95	-5.362
IL-10	0.377	23.35	27.02	-3.671
IL-12p70	0.964	24.91	25.11	-0.2062
IL-13	0.371	23.33	27.05	-3.712
TNF-α	0.119	22.11	28.55	-6.434
SAA	0.488	23.7	26.59	-2.887
CRP	0.672	24.2	25.98	-1.774
VCAM-1	0.881	25.3	24.64	0.6599
ICAM-1	0.430	26.48	23.18	3.3

3.2.4 The early antibody-dependent NK cell-mediated cytotoxicity response is associated with low viral load in AHI.

Next, NK cell ADCC capacity, which has been previously shown to be associated with the control of HIV-1 viraemia (237) and vaccine-induced protection (63), was measured in our cohort. The ADCC responses were measured via *in vitro* stimulation with antibody-coated Raji cells (Ab-coated Raji stimulation). The percentage of total NK cells from participants with subtype-A infection producing IFN-γ and TNF-α was significantly higher than those with non-A subtype infection, with a less marked effect being observed for CD107a production (**Figure. 3.7A-C)**. No significant differences were observed in NK cell degranulation, measured by CD107a expression, between the two study groups (**Figure. 3.7D**). In line with previous studies demonstrating an enhanced functional capacity of adaptive NK cells (86,87,92,100,238), a higher IFN-γ production mediated by FcεRIγ$^-$ compared to FcεRIγ$^+$ NK cells was observed in subtype A and non-A subtype infections at the two time-points (**Figure. 3.7E&F).** Notably, the frequency of IFN-γ$^+$ NK cells was negatively correlated with plasma viral load (r = 0.3432, p = 0.03018) (**Figure. 3.7G)**.

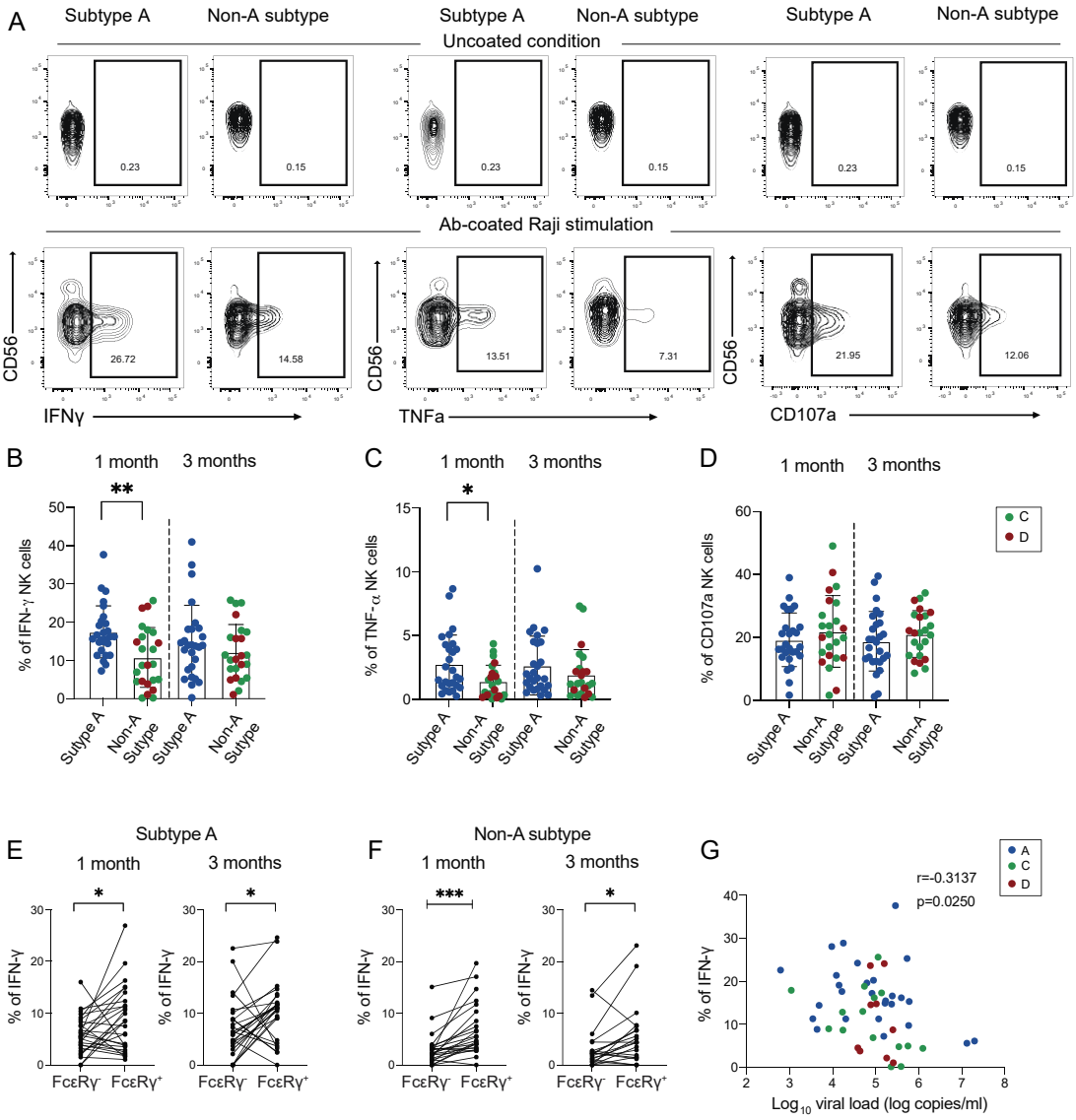


Figure 3.7. Enhanced NK cell-mediated ADCC capacity in subtype A infection.

(**A**) Representative flow plots and summary data for the frequency of (**B**) IFN-γ-, (**C**) TNFα-, or **(D)** CD107a producing NK cells following 6 hours stimulation with antibody-coated Raji cells in individuals with subtype A (n=28) and non-A (n=24) infections. The uncoated condition is the negative control of the assay. Paired analysis of IFN-γ responses in $Fc\varepsilon R\gamma^{+}CD57^{+}$ and $Fc\varepsilon R\gamma^{-}CD57^{+}$ NK cells in participants with (**E**) subtype A and (**F**) non-A subtype infections. **(G)** Correlation between the frequency of IFN-γ^{+} NK cells and viral load at 1 month post-EDI. The non-parametric Spearman test was used for correlation analysis. Significance determined by two-tailed Mann−Whitney U or Wilcoxon matched-pairs signed rank tests, *p <0.05, **p <0.01, ***p <0.001.

3.2.5 Enhanced mitochondrial oxidative phosphorylation is associated with ADCC capacity.

Recent studies demonstrated that NK cells have distinct metabolic requirements, which are critical for their effector function, during the acute (239) and chronic (240) stages of retroviral infection. This metabolic response involves the upregulation of energy flux through two main pathways: glycolysis and oxidative phosphorylation (OXPHOS), which allows energy production in the form of ATP and enhanced functional capacity (239). To investigate further the observed differences of higher NK cell functionality in subtype A infection, the metabolic profile of NK cells at 1 month post-EDI was evaluated by utilising a Seahorse XFp analyser. The glycolytic rate was measured in purified NK cells from the two study groups by assessment of the cellular extracellular acidification rate (ECAR), a measure of lactate production. Glycolysis was assessed at the basal level and after injection of rotenone and antimycin A, which target complex I and complex III of the electron transport chain (ETC), respectively, and 2-DG, a competitive inhibitor of glycolysis **(Figure. 3.8A).** The basal glycolytic activity of NK cells was comparable between subtype A and non-A subtype infections **(Figure. 3.8B).** Similarly, the maximal glycolysis and glycolytic reserve rate were similar between the two study groups **(Figure. 3.8C&D).** Next, the oxygen consumption rates (OCR), a measurement of mitochondrial OXPHOS and an important indicator of mitochondrial function (241), were evaluated. The OXPHOS was measured under basal conditions and following the addition of a stressor mix including oligomycin (an ATP synthesis inhibitor), FCCP (uncoupling synthesis of ATP from the ETC), and rotenone and antimycin A **(Figure. 3.8E)**. Despite the similarities

in the basal OCR between the two groups **(Figure. 3.8F)**, the maximal OCR and spare respiratory capacity (SRC), an essential indicator of the maintenance of the mitochondrial phenotype (242), were higher in participants with subtype A compared to non-A subtype infection **(Figure. 3.8G&H)**. To examine the relevance of the higher proportion of adaptive NK cells in subtype A as a contributor to the observed metabolic changes, the association between the percentage of $PLZF^{-}Fc\varepsilon R\gamma^{-}CD57^{+}$ NK cells and the SRC was investigated. Despite the low numbers, a positive correlation was observed **(Figure. 3.8I)**, suggestive of enhanced oxidative phosphorylation capacity in adaptive NK cells from individuals with subtype A infection (243).

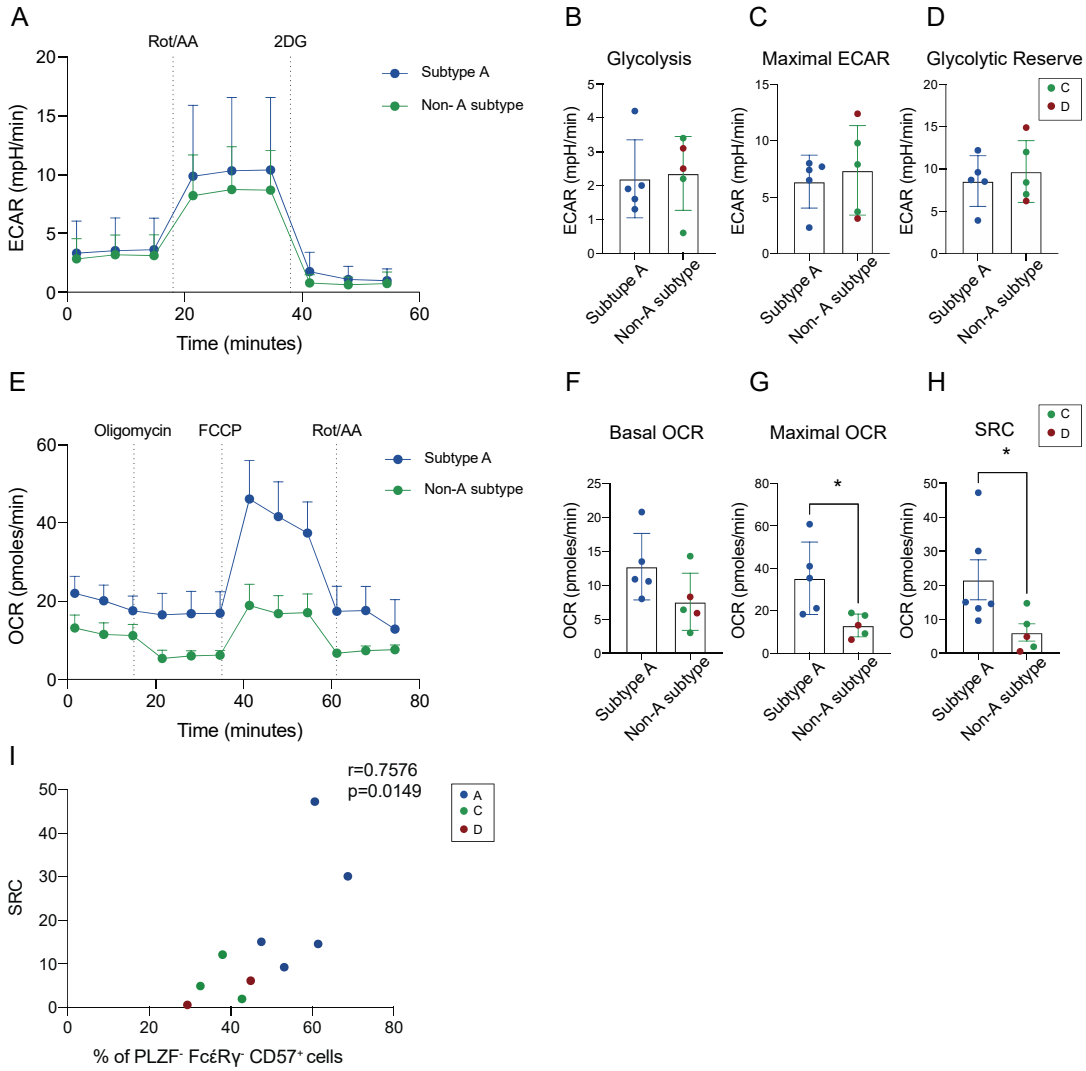


Figure 3.8. Improved mitochondrial oxidative phosphorylation in NK cells from subtype A infection.

(A) Cellular extracellular acidification rate (ECAR) of purified NK cells measured in real time *ex vivo* **(B)** Glycolysis, **(C)** Maximal ECAR, and **(D)** glycolytic reserve in isolated NK cells from subtype A and non-A subtype donors (n=5 in each group). **(E)** Oxygen consumption rate (OCR) of purified NK cells measured in real-time *ex vivo* **(F)** Basal OCR **(G)** Maximal OCR, and **(H)** Spare respiratory capacity (SRC) in purified NK cells from subtype A and non-A subtype subjects (n=5 in each group). **(I)** Correlation between percentage of PLZF^{-}FcεRγ^{-}CD57^{+} NK cells in subtype A and non-A subtype donors and SRC. The non-parametric Spearman test was used for correlation analysis. Significance determined by two-tailed Mann−Whitney U test, *p <0.05.

The increase in SRC in NK cells from participants with subtype A suggested an enhanced ability of these cells to maintain energy production in response to stimulation (242). Mitochondria maintain OXPHOS-mediated energy production by creating a membrane potential gradient which is generated from electron transport, driving the synthesis of ATP (244,245). To further evaluate whether the observed changes in the SRC are linked to the mitochondrial mass and/or mitochondrial membrane potential, I conducted further experiments to analyse the mitochondrial mass (MM) via staining cells with the mitochondrial-potential independent dye MitoTracker green. No significant differences were detected in the MM in total NK cells from the two study groups **(Figure. 3.9A**). Next, the mitochondrial membrane potential was assessed by utilising TMRM, a methyl ester which has been previously used to evaluate the presence of depolarised mitochondrial membranes (239). The membrane potential was significantly increased in NK cells from participants with subtype A compared to non-A subtype infection (**Figure. 3.9B&C)**. To assess the membrane potential in adaptive and canonical NK cells, the surface marker NKG2C was used to identify adaptive NK cell subsets (staining for PLZF or FcεRγ requires a cell permeabilisation step which could impact the TMRM staining (246)). TMRM MFI was higher in $NKG2C^+$ compared to $NKG2C^-$ NK cells **(Figure. 3.9D&E**), suggestive of enhanced mitochondrial activity in these subpopulations, as previously described (247). Interestingly, the membrane potential positively correlated with ADCC responses, measured by IFN-γ production (r = 3723, p = 0.0065) (**Figure. 3.9F)**, suggesting that enhanced NK cell effector responses in subtype A infection is associated with better mitochondrial fitness.

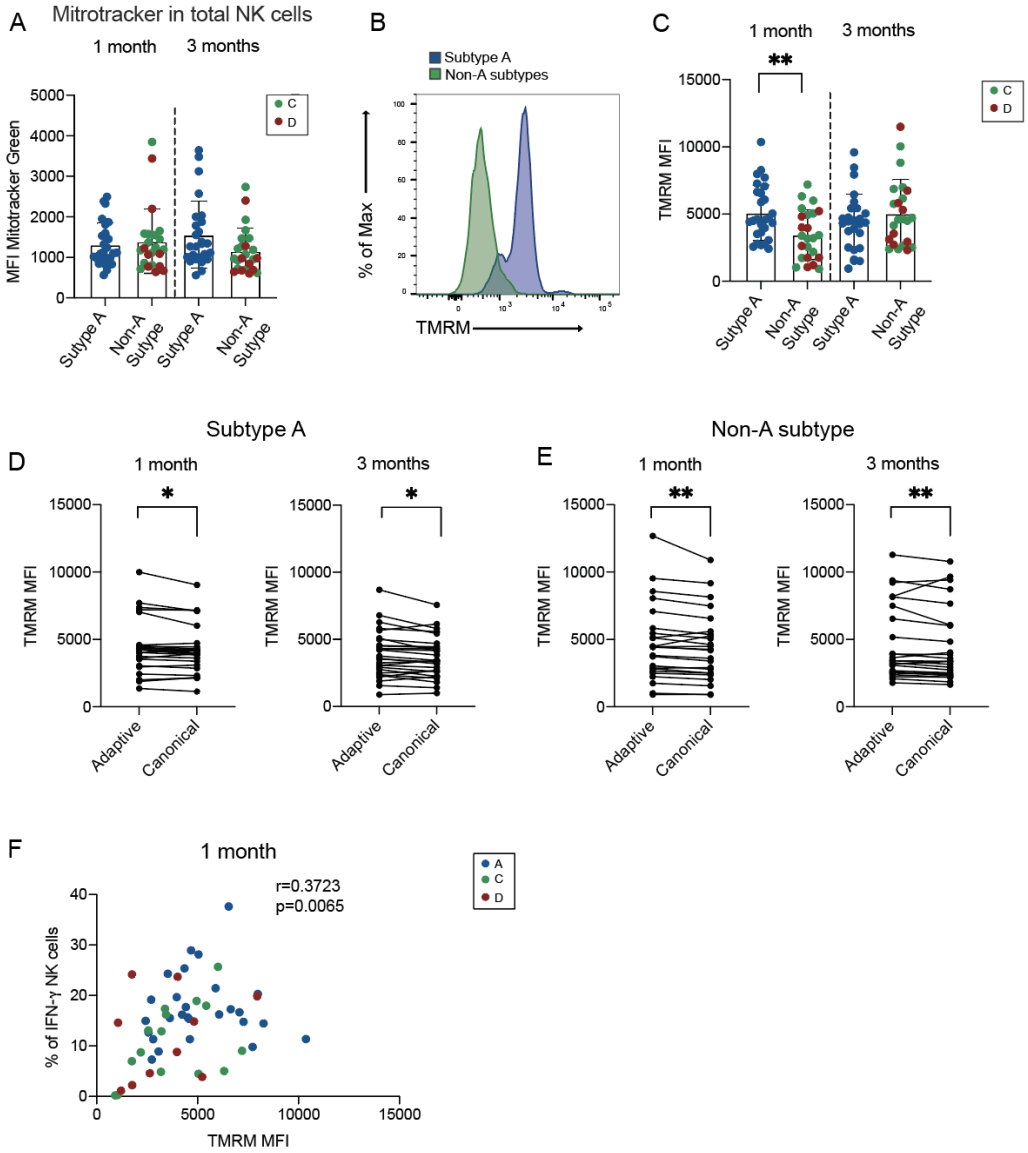


Figure 3.9. Enhanced mitochondrial membrane potential is associated with ADCC capacity.

(A) MFI of Mitotracker Green in NK cells from the two study groups. **(B)** Histogram and **(C)** summary data illustrating MFI of TMRM in NK cells. Paired analysis of TMRM MFI in NKG2C^{+}CD57^{+} and NKG2C^{-}CD57^{+} NK cells from participants with **(D)** subtype A and **(E)** non-A subtype infection. **(F)** Correlation between the frequency of IFN-γ^{+} NK cells and TMRM MFI in NK cells at 1 month post-EDI. The non-parametric Spearman test was used for correlation analysis. Significance determined by Mann-Whitney U or Wilcoxon matched-pairs signed rank tests, *p <0.05, **p <0.01.

3.2.6 Subtype A future controllers exhibit higher frequencies of $CD38^{+}NKG2A^{-}$ adaptive NK cells 1 month after EDI.

Our data suggested that subtype A infection was associated with distinct NK cell responses during AHI; however, whether these changes predict future control of HIV-1 viraemia is not known. Previous work in a larger cohort of IAVI Protocol C showed that 4.2% of participants had long-term viral control, and odds of viral control were increased in participants with subtype A infection (33). To examine the associations between NK cell responses and long-term viral control in our cohort, longitudinal viral loads were assessed in 18 untreated subtype-A participants with sufficient long-term viral load data (33). Out of these donors, six had a persistently undetectable or low viral load (<10,000 copies/ml) after 1.5 years and up to 6 years post-infection in the absence of ART (future controllers) (33,248) (**Figure. 3.10A)**. Longitudinal measurements of $CD4^{+}$ T-cell counts for future controllers showed that, in the majority of time-points analysed here, the counts remained above 350 cells/mm^3 (**Figure. 3.10A)**. Twelve age-, sex- and subtype-matched individuals, who did not initiate ART and had sufficient long-term viral load data, were included for comparison (non-controllers) **(Table 3.3).** Future viral controllers had a lower median viral load at 1 month (3.98 copies/ml) and 3 months (3.91 copies/ml) post-EDI compared to non-controllers (1 month: 5.46 copies/ml, 3 months: 4.82 copies/ml) **(Table 3.3)**. At 1 month, the median $CD4^{+}$ T-cell counts were comparable between future controllers and non-controllers (599 cells/mm^3 and 566 cells/mm^3, respectively), while at 3 months, the median $CD4^{+}$ T-cell count was slightly higher in future controllers (637 cells/mm^3) compared to non-controllers (466 cells/mm^3) **(Table 3.3)**. Next, I

applied a clustering analysis in circulating NK cells to evaluate NK cell subpopulations between the two groups. Notably, a PLZF^{-}FcεRIγ^{-}CD57^{+}CD38^{+} NKG2C^{-} adaptive NK cell cluster was significantly enriched in the future controller group (**Figure. 3.10B).** In contrast, NK cells from the non-controller group were characterised by an enrichment of NKG2A^{+}Siglec-7^{+}CD57^{+}CD38^{-} NK cells (**Figure. 3.10B).** Thus, our data show that the participants who maintain low HIV-1 viraemia (<10,000 copies/ml) up 3.5 years (in some individuals up to 6 years) post-infection without ART showed enrichment of activated adaptive NK cells during the early stage of HIV-1 infection.

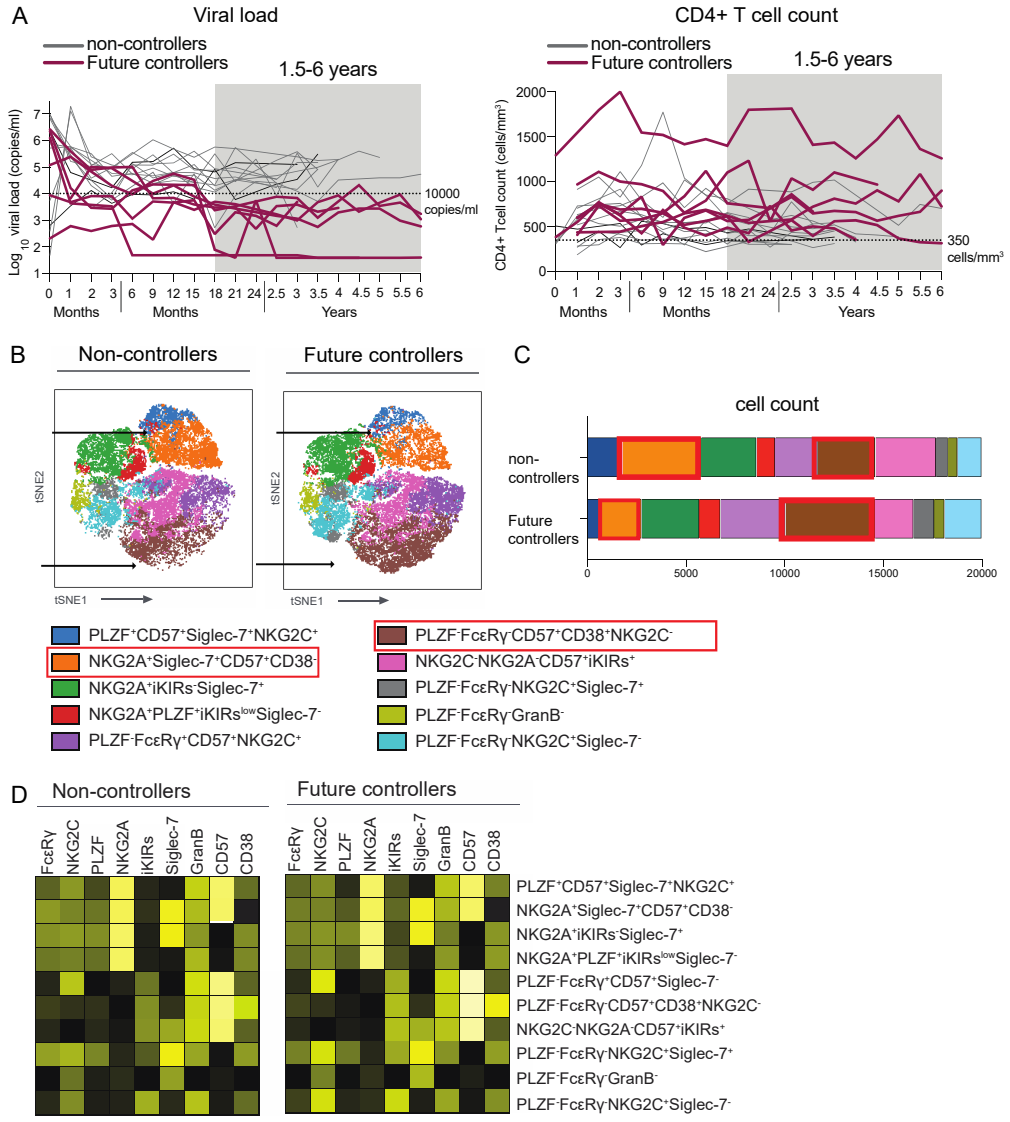


Figure 3.10. Phenotypic characterisation of NK cells in future viral controllers.

(A) Plasma viral loads (Log_{10}) and $CD4^+$ T-cell counts of future controllers and non-controllers. Time-points used in defining virus control are highlighted in the shaded grey box. Future controllers of HIV-1 maintain levels of plasma viraemia <10,000 copies/ml within 1.5-3.5 years (for four future controllers up to 6 years). **(B)** viSNE map of FlowSOM metaclusters of NK cells from future controllers and non-controllers at 1 month post-EDI. **(C)** Cell count of each FlowSOM metaclusters out of total NK cells (20,000 cells/group). **(D)** Surface expression intensity heatmap of the markers indicated for each FlowSOM metacluster.

Table 3.3. Clinical Characteristics of future controllers and non-controllers (Subtype A).

			Future controllers	Non-controllers
Group size		n (%)	6	12
HIV-1 subtype	Viral subtype		A	A
Days post estimated date of infection (EDI)	Visit 1	Days post EDI, median (range)	30.6 (28-41)	33 (25-42)
Recruitment clinical site	Research centre, country	Kigali, Rwanda, n (%)	3 (50%)	2 (16.7%)
		Kilifi, Kenya, n (%)	3 (50%)	9 (83.3%)
Risk factors and demographics	Age	Age (years), median (range)	24 (19-48)	29 (21-38)
	Sex	Gender (n) female:male	1:5	2:10
	Risk group	Discordant couple (DC), n (%)	3 (50%)	3 (25%)
		men who have sex with men (MSM), n (%)	3 (50%)	8 (66.7%)
		Other heterosexual, n (%)	-	1 (8.3%)
HIV parameters	Visit 1	Log_{10} HIV-1 viral load, median (range)	3.98 (2.79-5.60)	5.46 (3.54-7.30)
		CD4 count, median (range)	599 (409-1759)	566 (272-915)
	Visit 2	Log_{10} HIV-1 viral load, median (range)	3.91 (2.79-4.99)	4.82 (3.64-6.03)
		CD4 count, median (range)	637 (371-2000)	466 (267-1776)
	Set point viral load	Log_{10} pVL set-point [B] ,median (range)	3.76 (1.69-4.59)	4.66 (3.99-5.70)

3.3 Discussion.

HIV-1 subtypes are associated with different rates of disease progression, but the underlying biological mechanisms are unclear. In this chapter, we aimed to bridge the knowledge gap in our understanding of the role of NK cells in mediating early host responses against infection with different HIV-1 subtypes and their contribution to viraemia control in a well-defined cohort of subjects with incident infection in Africa enrolled within 1 month of their estimated date of infection. This integrative analysis demonstrated that participants with subtype A infection had a higher proportion of adaptive NK cells with enhanced ADCC functionality and superior capacity for mitochondrial oxidative phosphorylation. The increased frequencies of adaptive NK cells were associated with lower HIV-1 viral load and higher $CD4^+$ T-cell counts (>500 cells/mm^3) at 1 month post-infection.

Participants with subtype A infection had similar viral loads and $CD4^+$ T-cell counts compared to those with non-A subtype infection at 1 and 3 months post-EDI. Despite these similarities, a slower decline of $CD4^+$ T-cell count to less than 350 cells/mm^3 was observed among individuals with subtype A compared to non-A subtype infection, consistent with a previous observation in the larger cohort of IAVI Protocol C participants (31). These data are in line with previous studies suggesting that the infecting HIV-1 subtypes can exert an independent influence on disease outcomes (26,28,29,31,249). Aspects of the host-pathogen interaction, including the virus replicative capacity (38,250,250), co-receptor tropism (251–253), and host genetics (29) could partially explain differences in the disease progression observed between different HIV-1 subtypes.

NK cells have been identified as an important component of the early host defence against HIV-1 (1-2 weeks following infection), and their responses are associated with long-term control in the absence of ART treatment (226,254). In particular, adaptive NK cells have been found to respond rapidly during early infection, and their functional responses correlate with reduced HIV-1 viral load (126,127). In this study, a higher frequency of adaptive NK cells, characterised by PLZF^{-}FcεRIγ^{-}CD57^{+}, was detected in participants infected with subtype A compared to non-A subtypes. In both subtype A and non-A participants, the frequencies of adaptive NK cells were associated with elevated plasma levels of IL-2 and IL-12 at 1 month post-EDI. However, the overall plasma levels of IL-2 and IL-12 did not differ significantly between the two study groups, suggesting that the higher representation of adaptive NK cells in subtype A was independent of these two cytokines.

An important question to address in future studies is the underlying mechanism of the expansion of these PLZF^{-}FcεRIγ^{-}CD57^{+} subsets in subtype A infection. The increased abundance of these subsets in subtype A could result from slow homeostatic proliferation mediated by continuous activating receptor stimulation by antibodies, inflammatory mediators, or other ligands that are differentially induced between HIV-1 subtypes (255,256). These differences could also be attributed to the genetic variation within the *env* region (20-35% variation between different subtypes), which is one of the targets for cell-mediated immunity (257–260). Additionally, the differences in the magnitude or breadth of antibody

responses (due to genetic heterogeneity) may contribute to different degrees of activation and proliferation of NK cells (260–263). In this respect, subtype A infection has been shown to induce a broader antibody response compared to subtype C, leading to different levels of antibody-dependent NK cell responses (262). Another possibility is that the high frequencies observed in patients with subtype A infection were already high at the time of HIV-1 infection, as this study did not examine the proportion of adaptive NK cells before infection. Alternatively, reactivation of latent HCMV infection, which is one of the well-known drivers of adaptive NK cell expansion, may also contribute to the differences observed between HIV-1 subtypes (103,264). Although HCMV-seropositivity was not tested in this cohort (due to difficulties in accessing plasma samples), it is expected that a large proportion of the participants in both groups is HCMV-seropositive, given the high HCMV prevalence in PLWH, particularly in those living in African countries (265). It should be noted that differences between subtypes that circulate in distinct geographic regions could also reflect differences in the host populations, the mode of transmission, general health or other concomitant infections. The full impact of the HIV-1 subtype, in addition to other factors, including host genetics, the inflammatory environment and the presence of HCMV reactivation, on adaptive NK cell expansion needs to be addressed in future studies; however, such studies may not be feasible anymore as the current standard of treatment is ART initiation at the time of detection.

FcεRIγ-deficient NK cells are functionally distinct and exhibit superior responsiveness upon CD16 stimulation, particularly for cytokine production,

compared to canonical NK cells (96,103–106). In line with these observations and during early infection, adaptive NK cells (FcεRIγ^{-}CD57^{+}) exhibited a higher ADCC response, as shown by the expression of IFN-γ and TNF-α following antibody-coated target cell stimulation, compared to canonical NK cells in both A and non-A subtype participants. The lack of FcεRIγ expression and enhanced CD16 signalling through CD3ζ (signalling adaptor molecule associated with CD16 that can transmit biochemical signals through immunoreceptor tyrosine-based activation motifs (ITAMs)) may contribute to the superior ADCC response of these NK cell subsets (106,229,266). Interestingly, the production of IFN-γ by NK cells correlated inversely with HIV-1 viral load at 1 month post-EDI. These data reinforce recent observations demonstrating that ADCC responses may be significant for the control of HIV-1 during the early stages of infection (73,236).

Cellular metabolic alterations are crucial to fuel NK cell responses in viral diseases, including HIV-1, and dysfunctional mitochondria are linked to reduced NK cell function in chronic HIV-1 infection (239,240). Using a real-time analysis of ECAR and OCR of NK cells from subtype A and non-A participants, I show that NK cells derived from subtype A donors displayed a markedly enhanced metabolic profile. Although a defect in glucose uptake by NK cells cannot be formally excluded (267), no significant differences were detected in the basal glycolytic rate, maximal glycolysis, and glycolytic capacity in NK cells between the two study groups. Instead, an increased maximal oxidative phosphorylation and spare respiratory capacity, the amount of respiration that facilitates ATP production in response to increased stress (242), was observed in NK cells from

subtype A infected individuals, indicative of their enhanced mitochondrial respiration. We and others have shown that mitochondrial homeostasis and plasticity play a key role in immune cell fate (152,240). ATP production by mitochondria is established by an electrochemical proton motive force (Δp) across their inner and outer cell membranes, known as membrane potential (268–270). The mitochondrial membrane potential, measured by TMRM in this study, was higher in NK cells from subtype A participants, with TMRM level being higher in adaptive NK cell subsets (243). This mitochondrial pathway provides a potential mechanistic explanation for the functional advantage observed in NK cells in the subtype A infection (239).

In our cohort, there is a small group of subtype A participants (n=6) who were able to maintain low viraemia (<10,000 virus copies/ml) up to 3.5 years (and in 4 donors up to 6 years) post-infection in the absence of ART (33). Using an unsupervised high-dimensional analysis, I show a distinct NK cell signature associated with long-term virus control. A subset of activated adaptive NK cells ($PLZF^{-}Fc\varepsilon RI\gamma^{-}CD57^{+}CD38^{+}$) was found to be significantly enriched in circulating NK cells from future controllers. These cells may function alongside other immune cells, including cytotoxic $CD8^{+}$ T cells early in infection, mitigating T-cell exposure to high antigenic loads and subsequent exhaustion (58). These findings are consistent with observations in the FRESH cohort of hyperacute infection, where patients who maintain low viraemia at 2.75 years (two patients) exhibited a distinct NK cell subset (cytotoxic, proliferating NK cells) in early infection (58). However, a similar detailed analysis of NK cell phenotype, function and

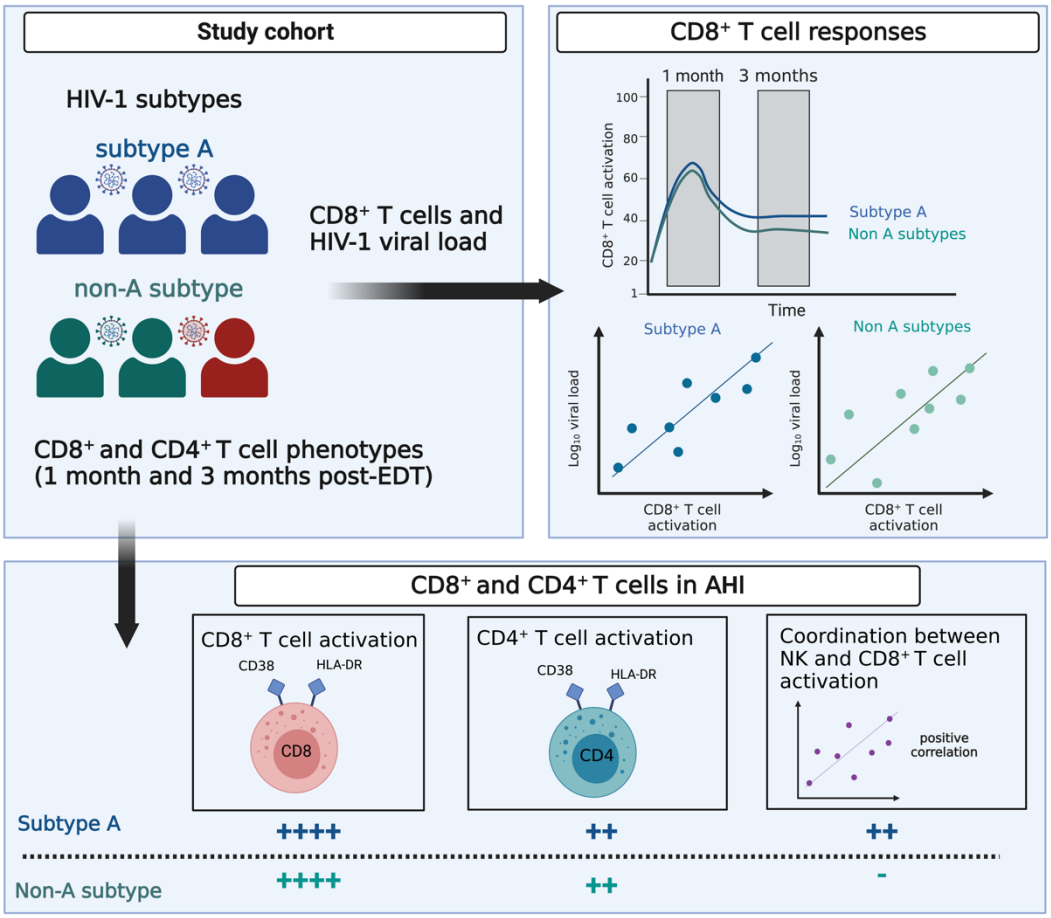
metabolism was not performed in the FRESH cohort study (58). These proliferating NK cells have been suggested to have adaptive features and respond to some previously encountered antigens (e.g. HCMV) (58). In addition to the FRESH cohort, a more recent report indicated an association between the presence of activated NK cells and delayed HIV-1 disease progression in an Asian cohort (226). Together, this analysis suggests that the presence of adaptive NK cells in early infection could be beneficial for long-term control.

There are limitations to this study. This study was not powered to characterise NK cell responses in individual non-A subtypes (i.e. subtype C vs D) due to the limited number of participants with subtype D infection in our cohort. The multi-regional nature of the cohort may have biased our analysis, as participants included in the study were from different populations and represented different risk groups. However, different HIV-1 subtypes typically dominate in regional pandemics (subtype A in Eastern Africa and subtype C in Southern Africa) and don't usually co-circulate at high frequencies with each other (19); thus, there are limited opportunities to compare NK cell responses and generate meaningful data related to different HIV-1 subtypes in a single country or ethnic group.

In conclusion, this study provides new insights into the NK cell responses during AHI with different subtypes and highlights the potential role of adaptive NK cells as a prognostic marker and as a new target for the development of novel immunotherapeutic strategies.

Chapter 4: The evolution of T-cell responses during acute HIV-1 infection.

Chapter 4 graphical abstract.



Chapter 4 written abstract.

CD8$^+$ and CD4$^+$ T cells are important components of antiviral immunity and contribute to the control of HIV-1 infection. Early T-cell responses, in particular CD8$^+$ T cells, play an important role in subsequent viral control, but whether initial T-cell responses differ in individuals infected with different HIV-1 subtypes and whether these responses are regulated by NK cells has not been determined. In this chapter, I sought to define the magnitude and evolution of CD4$^+$ and CD8$^+$ T-cell responses and their relation to viral load dynamics and NK cell responses during AHI in individuals infected with different HIV-1 subtypes. This study included samples from the same participants involved in the study presented in Chapter 3 (a subset of the IAVI Protocol C cohort). CD8$^+$ T cells are robustly activated during the first month of infection in both subtype A and non-subtype A infections. By three months after infection, a decline in CD8$^+$ T-cell activation was observed in both study groups. The levels of CD8$^+$ and CD4$^+$ T-cell activation correlated positively with HIV-1 viral load at one and three months post-infection. A positive association was observed between CD8$^+$ T-cell and NK cell activation in subtype A infection but not in non-A subtype infection. The results from this chapter suggest that AHI induced strong T-cell activation during infection with different subtypes, and subtype A infection is characterised by better coordination between NK and T-cell activation.

Chapter 4

4.1 Introduction.

Effective control of HIV-1 is likely to require both innate and adaptive immune responses, with $CD4^+$ and cytotoxic $CD8^+$ T-cell responses being key components of the immune-mediated control of HIV-1 replication (6,271,272). $CD8^+$ T cells play a central role in controlling HIV-1 viraemia, and the magnitude of early $CD8^+$ T-cell responses is associated with delayed disease progression (272). The emergence of cytotoxic $CD8^+$ T-cell responses is correlated with the resolution of peak viraemia (6,148,273) and the experimental depletion of $CD8^+$ T cells in rhesus macaques prior to infection with SIV delays the resolution of acute viraemia (274). $CD8^+$ T cells exert immunological pressure on HIV-1, as evidenced by the accumulation of CTL escape mutations throughout the various phases of infection (272). Further evidence of the role of $CD8^+$ T cells in HIV-1 control is demonstrated by the association between certain MHC class I alleles and viral suppression in elite controllers and long-term non-progressors (275). AHI induces robust $CD8^+$ T-cell activation (142,148,276), and the magnitude of activation, measured by the expression of HLA-DR and CD38, has been associated with VL set-point (148) and has been shown to be highly predictive of long-term disease outcome (277).

Although AHI results in a remarkable depletion of $CD4^+$ T cells, growing evidence supports the important role of $CD4^+$ T cells in controlling HIV-1 infection, including long-term HIV-1 suppression in two independent cohorts of HIV-1 controllers (155,278). In particular, the results of the RV144 phase III vaccine trial, which shows that the vaccine-induced not only non-neutralising antibody responses but

also robust $CD4^+$ T-cell responses, demonstrated the importance of these cells in the initial control of HIV-1 viraemia (155,279). The induction of $CD4^+$ T-cell responses during AHI is associated with improved viral control (155,280). These protective benefits of $CD4^+$ T cells could be mediated by providing helper signals for B cells or $CD8^+$ T-cell functions (281). However, the ability of $CD4^+$ T cells to degranulate and release cytotoxic molecules, including granzyme B, may also have a special significance for HIV-1 pathogenesis and could provide a second route of cytolytic pressure on HIV-1 (155). This cytolytic activity of $CD4^+$ T cells can arise early in infection and has been shown to mediate some degree of protection against CMV (282), influenza (282), and HIV-1 (155).

More recently, the importance of NK cells in shaping T-cell antiviral function and their contribution to the orchestration of a complex network of innate and adaptive immune cells has emerged as an important aspect of immunotherapeutics/vaccination aimed at promoting efficient adaptive immune responses; however, this remains under-investigated in HIV-1 infection, especially during the early phase of infection. NK cells can promote T-cell activation by stimulating antigen-presenting cells and producing cytokines, including IFN-γ, which enhance T-cell expansion (283,284). In addition to cytokines, NK cells can indirectly regulate T-cell activation by controlling the viral load in early infection, thereby reducing the level of antigen exposure that may cause T-cell inhibition (114). On the other hand, NK cells can exert a negative effect on T-cell responses by inhibiting antigen presentation (285), producing immunosuppressive factors (286), or through the elimination of activated T cells

during early infection (83,287). NK cells can eliminate activated $CD4^+$ T cells, either limiting immunopathology induced by a viral infection or contributing to exhaustion and inefficient $CD8^+$ T-cell control (288,289). NK cells have also been described to shape the induction of germinal centre formation; cytotoxic elimination of T_{FH} cells in the lymph node by NK cells in acute infection has been shown to disrupt germinal centre formation, limiting immune memory development (290). This is particularly pertinent for acute HIV-1 infection, as T_{FH} cells are likely to be the dominant subsets supporting the virus production (291) and one of the main contributors to the HIV-1 reservoir (292). Thus, by eliminating T_{FH} cells, NK cells may also influence the size of the latent reservoir that is established early during the acute phase of infection. This phenomenon has been described in non-pathogenic SIV infection (293) and, more recently, in human HIV-1 infection (294), in which NK cells have been shown to play a role in controlling the viral reservoir by homing into lymph node follicles. Thus, NK cells can act as rheostats, regulating adaptive immune cells that control viral pathogenesis and persistence.

However, this interplay between NK and T-cell responses has not been studied in detail during the initial stage of HIV-1 infection. In this chapter, I characterised $CD4^+$ and $CD8^+$ T-cell activation and their relationship with viral load dynamics and NK cell responses in individuals infected with different HIV-1 subtypes.

4.2 Results.

4.2.1 The magnitude of CD8$^+$ T-cell activation correlated with HIV-1 viraemia during the first month of infection.

To assess CD8$^+$ T-cell activation during AHI and its association with HIV-1 viraemia, I used PBMC samples from the same participants included in the study presented in Chapter 3. CD8$^+$ T-cell activation was defined by using co-expression of HLA-DR and CD38, the two activation markers that have previously been used to characterise activated CD8$^+$ T cells during hyperacute HIV-1 infection (148), as well as in chronic infection (295). We and others have previously reported that both markers exhibit low cell surface expression in HIV-1 uninfected patients or ART-treated HIV-1 patients (148,212), allowing for the unequivocal identification of the activated T cells induced by AHI. Within one month following infection, extensive CD8$^+$ T-cell activation was detected, with more than 30% of total CD8$^+$ T cells expressing CD38$^+$HLA-DR$^+$ **(Figure. 4.1.A&B).** The percentage of activated CD8$^+$ T cells declined at 3 months post-infection, with the median percentage of CD38$^+$HLA-DR$^+$CD8$^+$ T cells reaching approximately 20% of total CD8$^+$ T cells in both study groups **(Figure. 4.1.B).** The magnitude of CD8$^+$ T-cell activation was comparable between subtype A and non-A subtype infection **(Figure. 4.1.B).**

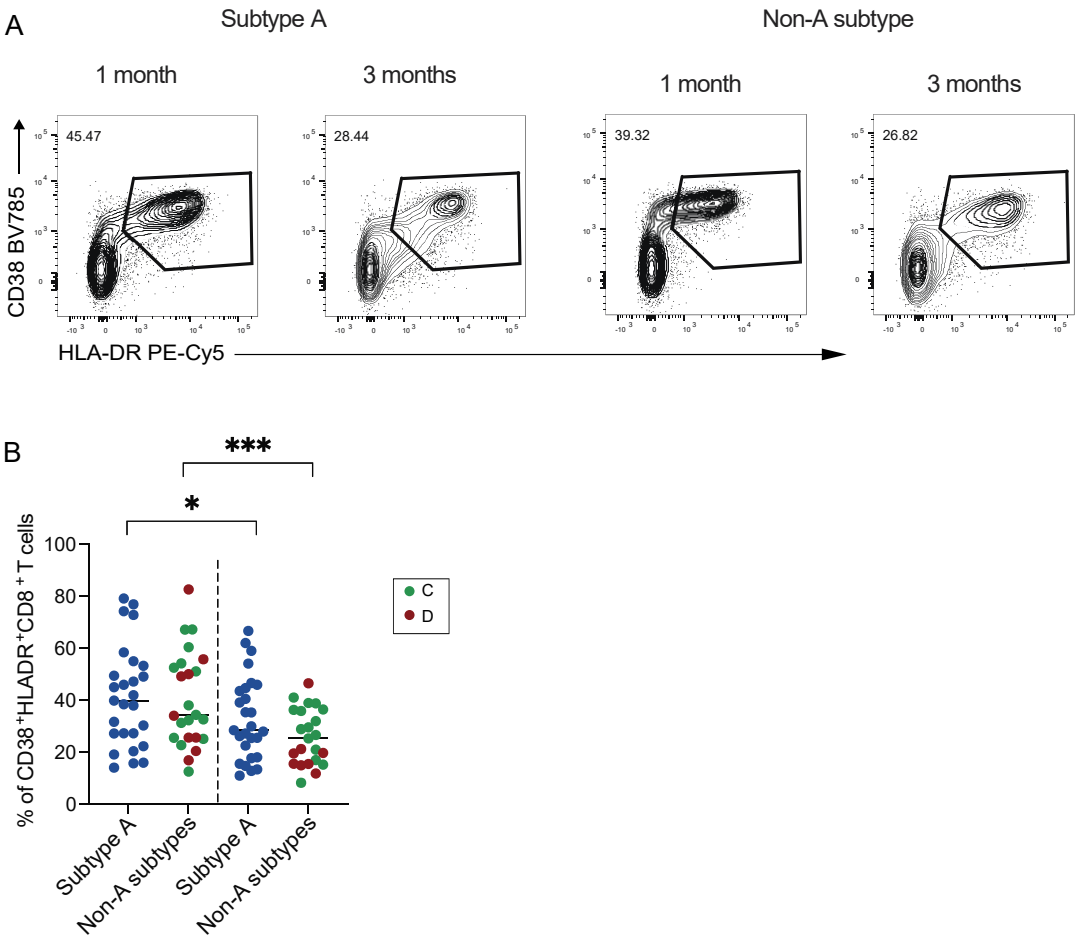


Figure 4.1. CD8⁺ T-cell activation during early HIV-1 infection.

(A) Representative flow cytometric plots and **(B)** summary data representing the frequency of $CD38^+HLA\text{-}DR^+CD8^+$ T cells in subtype A and non-A subtype individuals at 1 and 3 months post EDI. Significance determined by two-tailed Mann−Whitney U test or Wilcoxon matched-pairs signed rank test, $*p < 0.05$, $***p < 0.001$.

Given the considerable inter-individual variability in the magnitude of CD8⁺ T-cell activation, these responses were related to HIV-1 viral load, one of the known drivers of CD8⁺ T-cell activation in AHI (148). In line with previous studies, a positive correlation was observed between the percentage of CD38⁺HLA-DR⁺ CD8⁺ T cells and viral load in both study groups (114,148) **(Figure. 4.2.A&B).** These data suggest that the magnitude of HIV-induced CD8⁺ T-cell activation in early infection might be partly driven by the high level of HIV-1 viraemia.

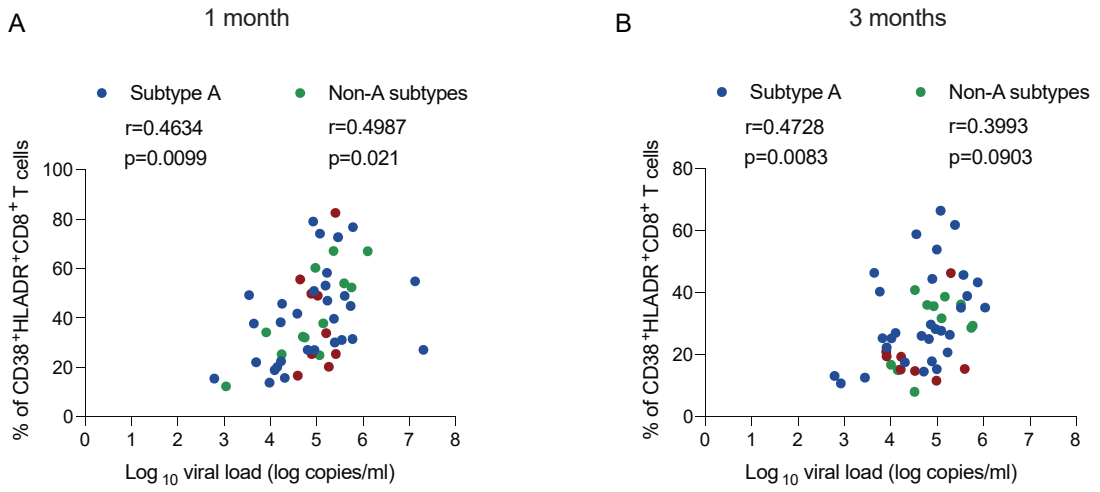


Figure. 4.2. CD8⁺ T-cell activation correlates with HIV-1 viral load.

Correlation between the percentage of CD38⁺HLA-DR⁺ CD8⁺ T cells and viral load at **(A)** 1 month and **(B)** 3 months post-infection. The non-parametric Spearman test was used for correlation analysis.

4.2.2 CD4⁺ T-cell activation correlated with CD4⁺ T-cell count.

The emergence of activated CD4⁺ T cells during the early stage of infection has been associated with the levels of HIV-1 viraemia and the rate of CD4⁺ T-cell decline (155,296,297). Given the observed differences in the rate of CD4⁺ T-cell decline in subtype A compared to non-A subtype individuals, I analysed CD4⁺ T-cell activation in both groups, using the expression of CD38 and HLA-DR. Consistent with previous studies (297), CD4⁺ T-cell activation was detected at 1 month and 3 months post-infection but at lower levels compared to CD8⁺ T cells **(Figure. 4.3.A&B).** Unlike CD8⁺ T cells, no significant changes were detected in the percentage of CD38⁺HLA-DR⁺CD4⁺ T cells across the two time-points in subtype A and non-A subtype participants **(Figure. 4.3.B).**

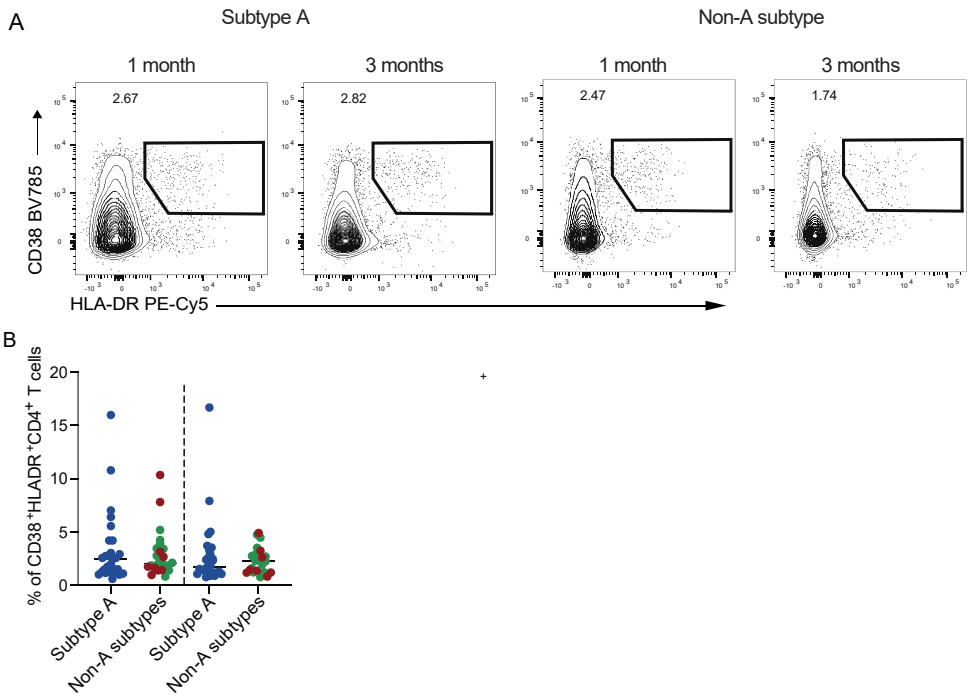


Figure 4.3. CD4⁺ T-cell activation during early HIV-1 infection.

A) Representative flow plots and **(B)** summary data showing the frequency of CD38⁺HLA-DR⁺CD4⁺ T cells in subtype A and non-A subtype individuals.

Consistent with previous studies (297), during the first month of infection, the percentages of CD38⁺HLA-DR⁺CD4⁺ T cells positively correlated with viral load and negatively correlated with CD4⁺ T-cell count (**Figure. 4.4.A&B).** These data suggest that the level of CD4⁺ T-cell activation during early infection could influence the level of viral replication and the rate of CD4⁺ T-cell decline.

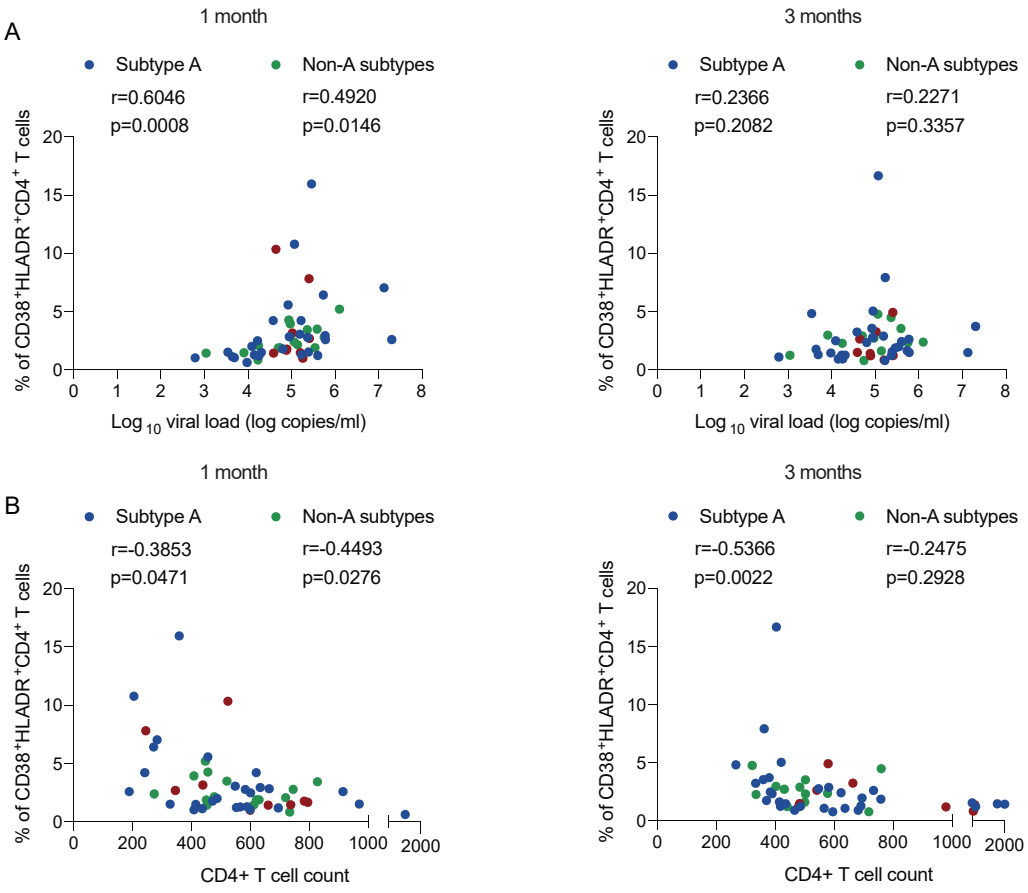


Figure 4.4. CD4⁺ T-cell activation correlates with HIV-1 viral load.

Correlation between the percentage of CD38⁺HLA-DR⁺CD4⁺ T cells and **(A)** viral load or **(B)** CD4⁺ T cells count at 1 month and 3 months post-infection. The non-parametric Spearman test was used for correlation analysis.

4.2.3 Future viral controllers demonstrated an expansion of CD127$^+$TCF-1$^+$CCR7$^+$CD45RA$^+$ CD8$^+$ T cells.

T-cell responses contribute to the control of HIV-1 viraemia and can influence the long-term disease outcome. Their responses during the initial stage of the infection have been described to associate with long-term viral control (148). To further evaluate the relationship between T-cell responses during AHI and future viral control in our cohort, I applied an unsupervised analysis to the circulating T-cell compartment in future controllers (as described in Chapter 3; individuals who maintain a low level of HIV-1 viraemia (<10,000 viral copies/ml) between 1.5-6 years post-infection in the absence of ART treatment (33)) and non-controllers. Notably, a cluster of naïve and effector memory CD8$^+$ T cells, expressing CD127 and TCF-1, was more abundant in future viral controllers compared to non-controllers (**Figure. 4.5A-C).** The increased frequencies of CD127$^+$TCF-1$^+$EM and naïve CD8$^+$ T cells were further confirmed by manual gating (**Figure. 4.5D).**

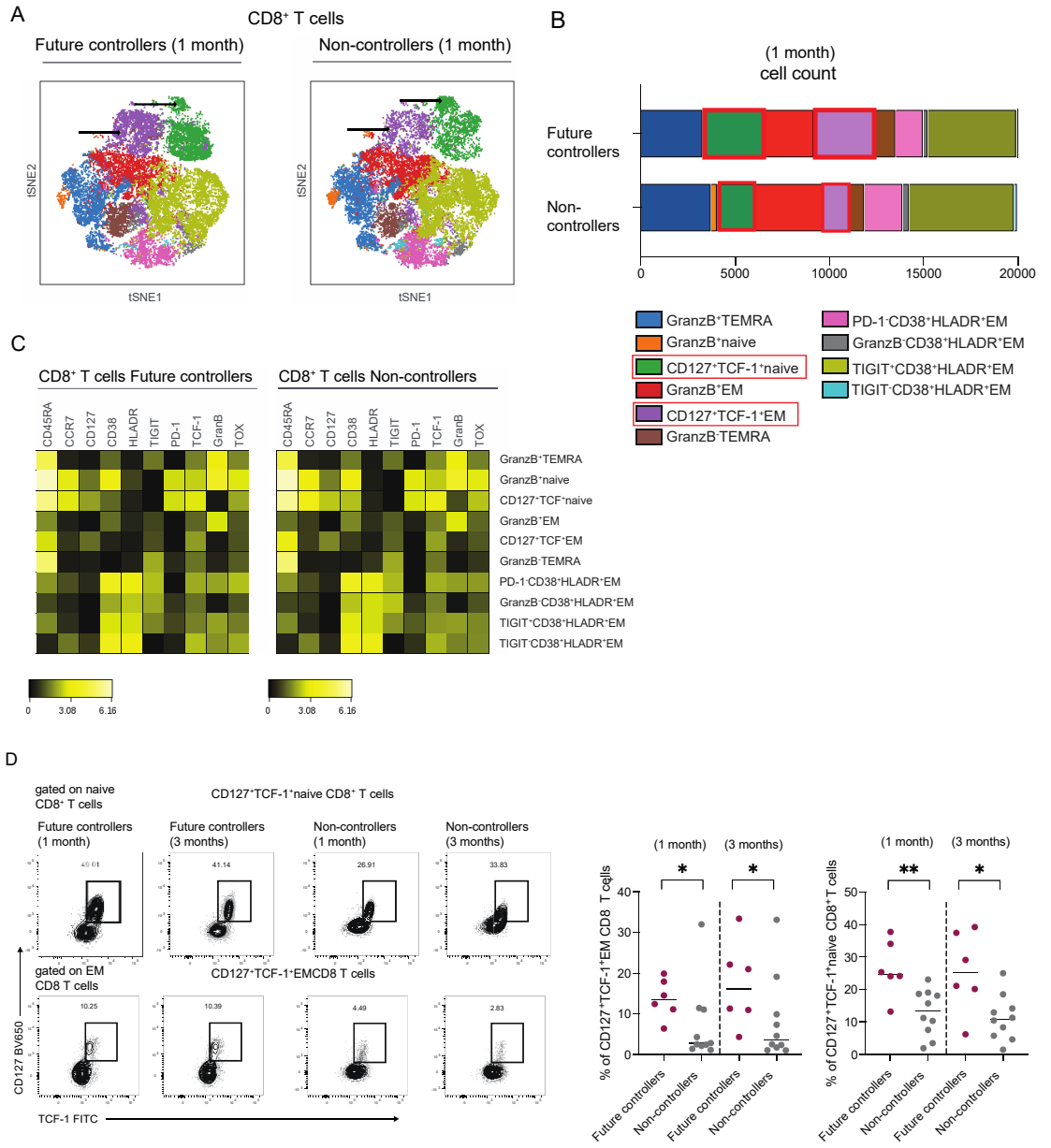


Figure 4.5. Phenotypic characterisation of CD8⁺ T cells in future viral controllers.

(A) viSNE map of CD8⁺ T cells from future controllers and non-controllers. **(B)** Cell count of each metaclusters out of total CD8⁺ T cells. **(C)** Surface expression intensity heatmap of the markers indicated for each meta-cluster of CD8⁺ T cells. **(D)** Example flow plots and summary data showing the percentage of CD127⁺TCF-1⁺naive or EM CD8⁺ T cells in future controllers and non-controllers. Significance determined by two-tailed Mann−Whitney U test. *p < 0.05, ** p < 0.01.

Examining the total $CD4^+$ T-cell landscape in future controllers and non-controllers revealed an enrichment of a cytotoxic effector memory $CD4^+$ T-cell cluster ($GranzB^+$EM $CD4^+$) in future controllers compared to non-controllers at 1 month post-EDI (**Figure. 4.6A-C).** The higher abundance of $GranzB^+$EM $CD4^+$ T cells in future controllers was also confirmed by manual gating **(Figure. 4.6D).** Thus, this analysis identified subpopulations of $CD8^+$ and $CD4^+$ T cells that were enriched early in infection in individuals who subsequently maintained a low level of viraemia in the absence of ART treatment.

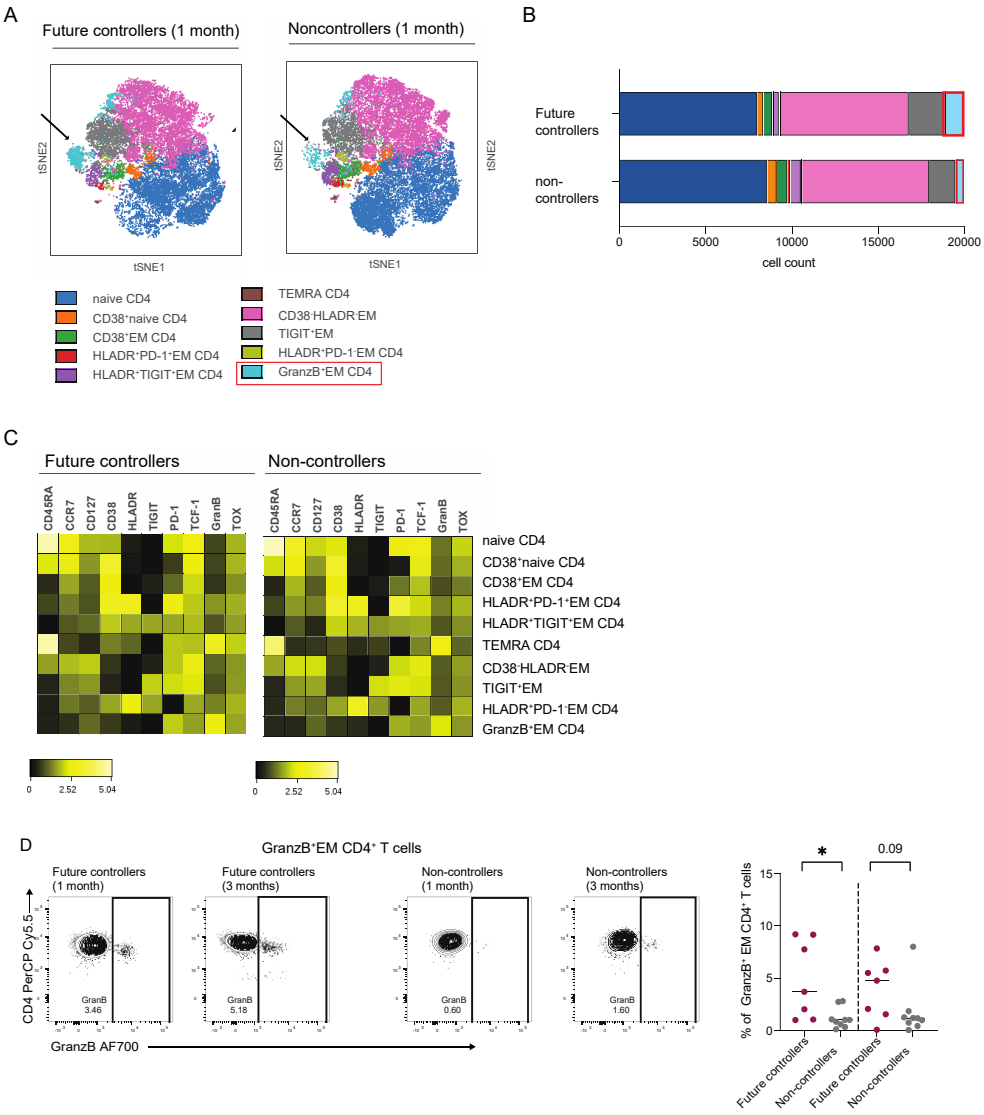


Figure 4.6. Unsupervised clustering analysis of CD4⁺ T-cell subpopulations in future viral controllers.

(A) viSNE map of FlowSOM metaclusters of CD4⁺ T cells from future controllers and non-controllers. **(B)** Cell count of each FlowSOM metaclusters out of total CD8⁺ T cells (20,000 cells/group). **(C)** Representative flow cytometric plots and summary data showing the percentage of GranzB⁺ CD4⁺ T cells in future controllers and non-controllers. Significance determined by two-tailed Mann−Whitney U test. *p < 0.05.

4.2.4 Distinct NK and T-cell relationships between subtype A and non-A subtype infections during early HIV-1 infection.

NK cells have been shown to cooperate with T cells in controlling HIV-1 viraemia during early infection (114,254). I, therefore, assessed the potential associations between NK and T-cell responses using a multiparametric correlation analysis, comparing subtype A and non-A subtype infection. The correlation analysis indicated a distinct relationship between NK and T cells in both subtype A and non-A subtype individuals, with NK and $CD8^+$ T-cell associations being more prominent (black outlined cluster labelled "NK and $CD8^+$ T cells") (**Figure. 4.7A&B).** While the magnitude of $CD8^+$ T-cell activation ($CD38^+HLA\text{-}DR^+CD8^+$) correlated positively with NK cell activation ($CD38^+$ NK cells) in subtype A, this relationship is lost in non-A subtype infection **(Figure. 4.7.C-E, Figure. 4.8.A).** Instead, in non-A subtype infection, $CD8^+$ T-cell activation correlated positively with the proportion of anergic $CD56^{neg}$ NK cells and negatively with cytotoxic $CD56^{dim}$ NK cells **(Figure. 4.8.B&C).** These data demonstrated a distinct pattern of coordination between NK and $CD8^+$ T-cell responses that is observed between participants with either subtype A or non-A subtype infection.

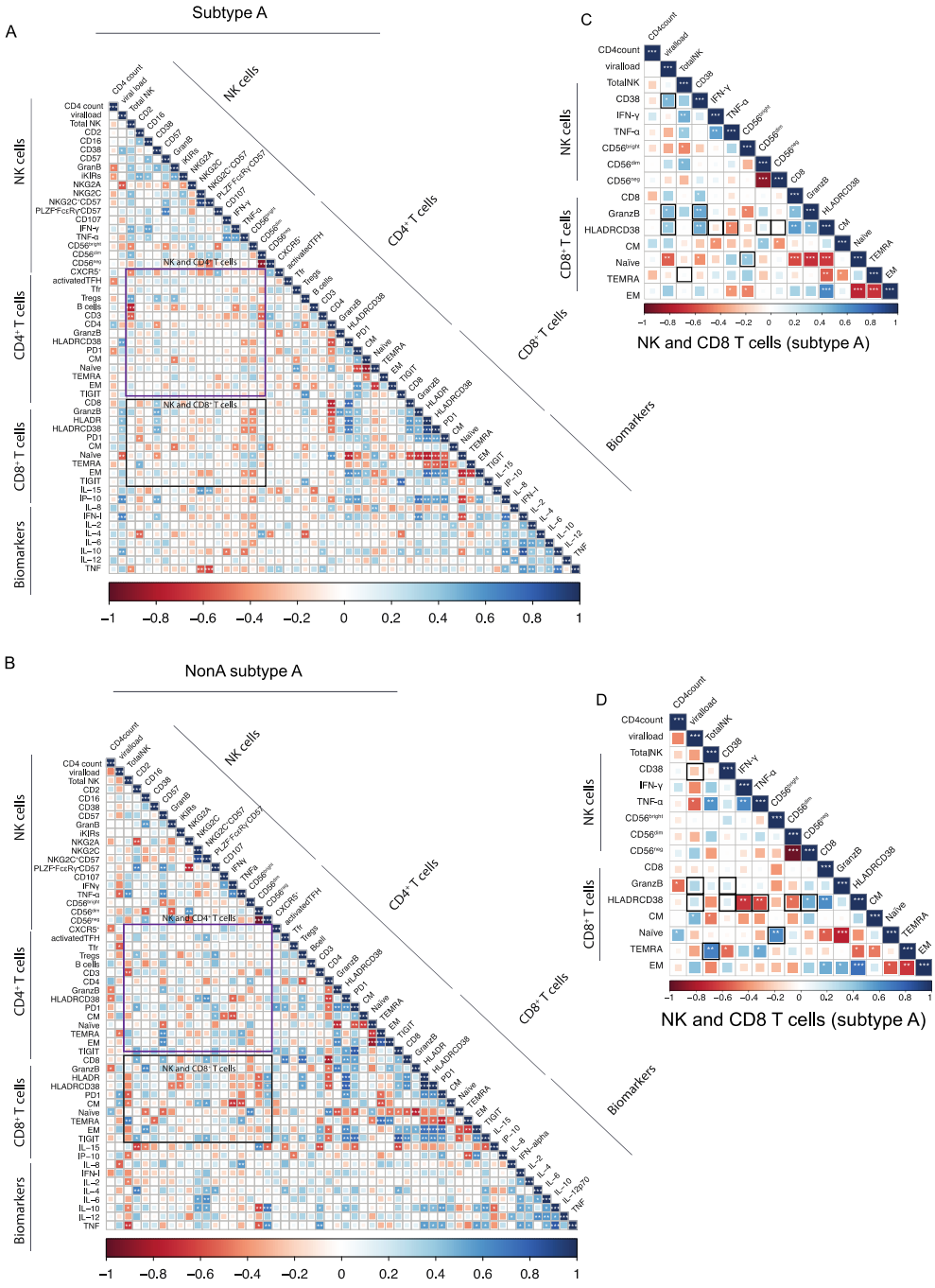


Figure 4.7. Multiparameter correlation analysis of innate and adaptive immune responses at one-month post-infection.

Correlograms of **(A)** subtype A and **(B)** non-A subtype infection, including NK, CD4⁺, and CD8⁺ T-cell subsets and inflammatory cytokines (1 month post-infection). Correlation matrix of CD8⁺ and NK cell subsets in **(C)** subtype A and **(D)** non-A subtype infection.

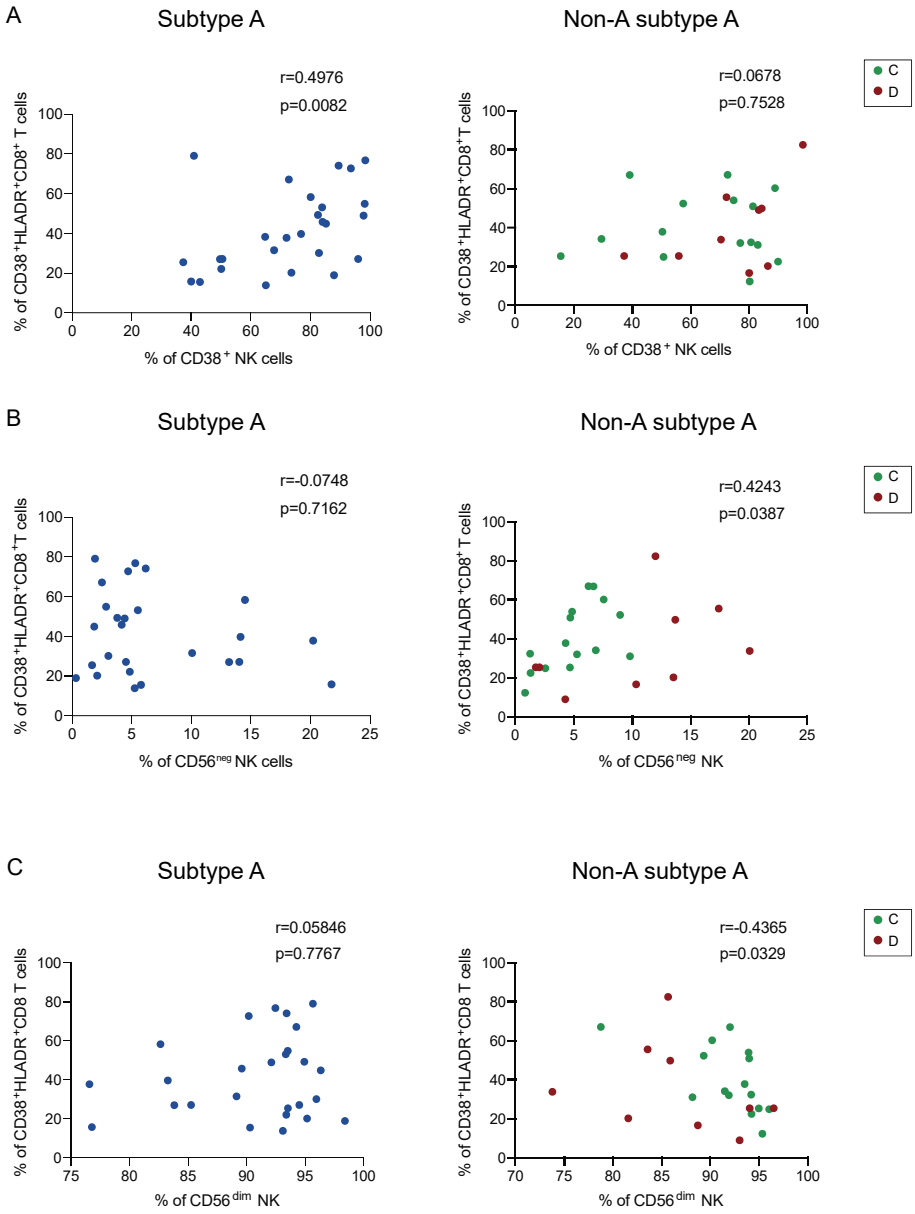


Figure. 4.8. Correlation analysis between NK and T-cell immune responses.

(A) Correlation between the percentage of $CD38^{+}HLA\text{-}DR^{+}$ $CD8^{+}$ T cells and $CD38^{+}$NK cells. **(B)** Correlation between the proportion of $CD38^{+}HLA\text{-}DR^{+}$ $CD8^{+}$ T cells and $CD56^{neg}$ NK cells. **(C)** Correlation between the frequency of $CD38^{+}HLA\text{-}DR^{+}$ $CD8^{+}$ T cells and $CD56^{dim}$ NK cells. The non-parametric Spearman test was used for correlation analysis.

4.3 Discussion.

The relationship between NK and T-cell responses during the earliest stage of infection and their association with HIV-1 viraemia has not been well established. In this chapter, I sought to define the characteristics of $CD4^+$ and $CD8^+$ T-cell responses and their relationship to viral load and NK cell responses at one month and three months post-infection in individuals infected with different subtypes. This represents a unique opportunity to identify potential targets for therapeutic and preventative applications. This analysis demonstrated robust $CD8^+$ T-cell activation during the first month of infection, with a modest decline in the magnitude of activation at three months post-infection in both study groups (subtype A and non-A subtype infection). The initial $CD8^+$ and $CD4^+$ T-cell activation correlated positively with HIV-1 viral load, suggesting that the magnitude of T-cell activation might be partly driven by the high viral load in the acute phase of infection, although future studies will be needed to confirm this hypothesis. A multiparameter correlation analysis showed a distinct relationship between T and NK cell responses in individuals with subtype A and non-A infection. A positive relationship was observed between the activation of NK cells and T cells in subtype A infection, while NK cells were found to be negatively associated with T-cell activation in non-A subtype infection. The results from this chapter demonstrate that AHI induced strong T-cell activation in different subtypes, and subtype A infection is characterised by better coordination between NK and T-cell activation.

Several lines of evidence have suggested an important role of $CD8^+$ T cells in the control of HIV-1 viraemia, including the temporal correlation between the induction of $CD8^+$ T-cell activation and the reduction in acute HIV-1 viraemia (273,298). During AHI, activated $CD8^+$ T cells have been described to influence HIV-1 replication, and the majority of these cells, defined by co-expression of HLA-DR and CD38, are HIV-specific $CD8^+$ T cells (148). Using the same activation markers, a robust $CD8^+$ T-cell activation was detected in individuals infected with both subtype A and non-A subtype infections at one month post-infection, with a similar magnitude of T-cell activation observed in both study groups. The magnitude of $CD8^+$ T-cell activation correlated positively with the viral load, suggesting that HIV-1 replication during the first month of infection could be the driver of T-cell activation, as has been shown in previous studies (114,148). At three months post-infection, a decline in $CD8^+$ T-cell activation was observed in both study groups, indicating that the peak of activation was achieved during the first month of infection (148). This decline of activated $CD8^+$ T cells could be driven by apoptosis or cell trafficking to infected tissues, as previously described (142,148). Similar to $CD8^+$ T cells, the magnitude of $CD4^+$ T-cell activation was comparable between subtype A and non-A subtype infection, and it correlated positively with viral load, suggesting that HIV-1 viraemia may contribute to $CD4^+$ T-cell activation (154) and/or activated $CD4^+$ T cells are the target cell for HIV-1 that can support viral replication (296). In addition to the viral load, there was an association between $CD4^+$ T-cell activation and $CD4^+$ T-cell count during the first month of infection, suggesting that these cells could play a role in $CD4^+$ T-cell decline during the initial stage of infection (297).

I next identified a distinct T-cell signature, arising early in the infection, that may contribute to subsequent viral control. Individuals who maintain a low level of HIV-1 viraemia (<10,000 viral copies/ml) between 1.5-3.5 years post-infection in the absence of ART treatment (33) (future controllers) exhibited an expansion of $CD127^{+}TCF\text{-}1^{+}CCDR7^{+}CD45RA^{+}$ $CD8^{+}$ T cells. This population has been shown to retain proliferative capacity, regenerate, and produce effector $CD8^{+}$ T cells (299,300). They also have been described to play a role in sustaining the T-cell response during chronic infection and were important for the re-expansion of antigen-specific $CD8^{+}$ T cells (299), suggesting that the expansion of these cells during early infection could play a role in mediating viral control in chronic infection (300). In addition to $CD8^{+}$ T cells, an expansion of cytolytic $CD4^{+}$ T cells was detected in future controllers. $CD4^{+}$ T cells from future viral controllers are characterised by an over-representation of $GranzB^{+}CD4^{+}$ T cells at one- and three months post-infection. These cells have been previously shown to emerge during AHI and follow the trajectory of acute viraemia (301). In chronic infection, they exhibit similar killing activity relative to $CD8^{+}$ T cells and work cooperatively in the elimination of HIV-1 infected cells (155,301). Overall, these data demonstrate specific $CD4^{+}$ and $CD8^{+}$ T-cell features that could predict long-term viral control.

NK cells have an immunoregulatory capacity and have been described to exert either a positive or a negative effect on T-cell responses (302,303). NK cells can produce cytokines which promote antigen presentation and $CD8^{+}$ T-cell

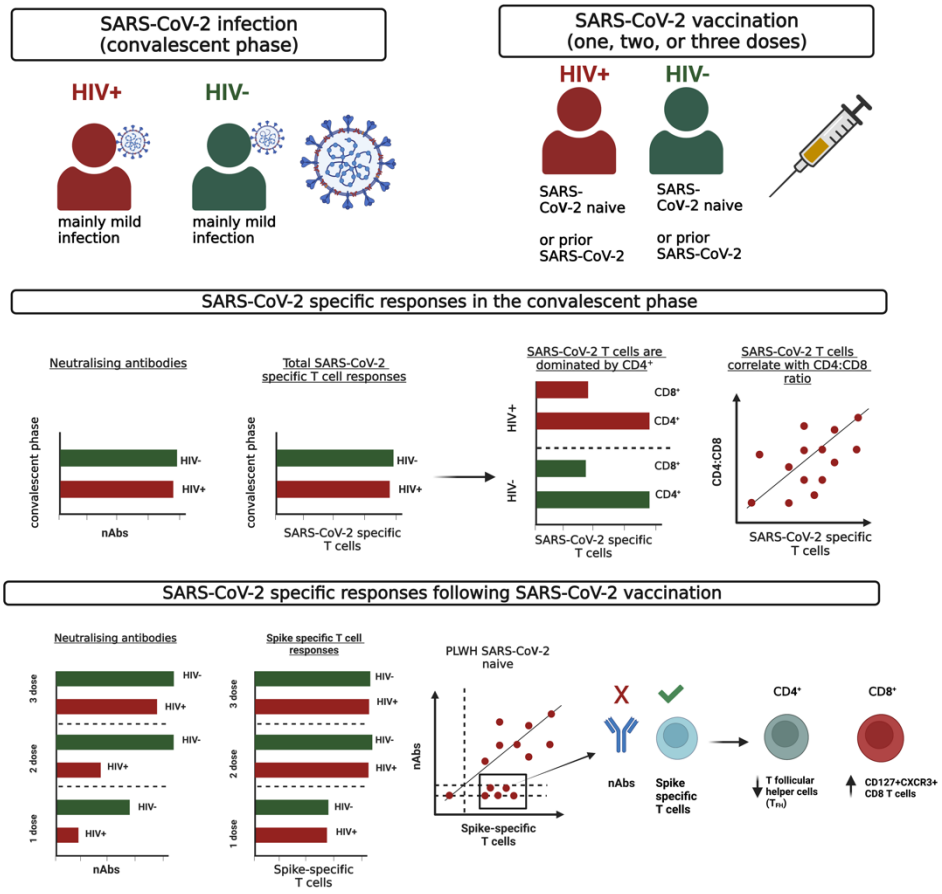
activation, but they can also mediate cytotoxic killing of activated $CD8^+$ T cells, limiting their ability to control infection (302,303). Here, a distinct relationship was observed between NK cell and T-cell responses in subtype A and non-A subtype infection. In subtype A infection, a positive association was observed between NK and $CD8^+$ T-cell activation, suggesting potential synergy between the two immune responses (114). NK cells in subtype A infected individuals are characterised by increased IFN-γ production (described in Chapter 3), which has been described to contribute to the $CD8^+$ T-cell activation (304). On the other hand, in non-A subtype infection, a negative association was observed between the proportion of activated $CD8^+$ T cells and the magnitude of the cytotoxic NK cell subset ($CD56^{dim}$), whereas a positive correlation was observed between the $CD56^{neg}CD16^+$NK cell subset and activated $CD8^+$ T cells, suggestive of a more prominent immunoregulatory role of NK cells in non-A subtype infection. The cytotoxic NK cell subset ($CD56^{dim}$) expresses activating receptors that mediate the recognition and elimination of target cells, including activated T cells, through direct or indirect mechanisms (305). $CD56^{neg}$ NK cells have alterations in the expression of activating and inhibitory receptors that may diminish their activation in response to target cells (306). The exact mechanisms by which different HIV-1 subtypes modulate the cooperation between innate and adaptive immunity and the involvement of HCMV co-infection, and the levels of immune activation in these associations will need to be addressed in future studies.

Chapter 5: Characterisation of T-cell responses in PLWH following SARS-CoV-2 infection and vaccination.

Publication.

1. Alrubayyi A, et al. Characterization of humoral and SARS-CoV-2 specific T cell responses in people living with HIV. Nat Commun. 2021 Oct 5.
    - Figures were reproduced under license (a Creative Commons Attribution 4.0 International License)
2. Touizer E*, Alrubayyi A*, et al. Attenuated humoral responses in HIV after SARS-CoV-2 vaccination linked to B cell defects and altered immune profiles. iScience. 2023 Jan 20.
   * Shared co-first authorship
    - Figures were reproduced under license (a Creative Commons CC-BY License)

Chapter 5 graphical abstract.



Chapter 5 written abstract.

Susceptibility to severe SARS-CoV-2 infection and the risk of mortality increases in PLWH, especially in the context of advanced immunodeficiency and/or unsuppressed HIV-1 viraemia. T-cell responses are a key component of immunity to SARS-CoV-2 and likely contribute to the attenuated clinical severity. In this chapter, I examined the magnitude and phenotype of T-cell responses, including their reactivity to SARS-CoV-2 variants, following SARS-CoV-2 infection (convalescent phase) and vaccination in PLWH and HIV-negative individuals, in relation to induction of humoral responses. This analysis shows that the majority of PLWH with ART-suppressed HIV-1 viral load mount a detectable T-cell response to SARS-CoV-2 following primary infection or vaccination. In contrast, humoral responses elicited by SARS-CoV-2 vaccination were lower in PLWH relative to HIV-negative controls. Given the complementary roles of cellular and humoral responses, evaluating T-cell immunity is critical to better understand the correlates of protection and vaccine efficacy in PLWH.

Chapter 5

5.1 Introduction.

The SARS-CoV-2 pandemic has led to more than 6 million deaths worldwide (157), posing unprecedented social, economic and health system disruptions globally. Given the profound sequelae associated with the COVID-19 pandemic, vaccines were rapidly developed and licenced, with more than 13 million doses administrated worldwide, and have proved to be highly effective in reducing disease burden (157). However, only a small number of PLWH were included in the initial vaccine trials (307). As a result, the magnitude and quality of the immune response to SARS-CoV-2 primary infection or vaccination are not well defined in these potentially more vulnerable patients who may be at a higher risk of COVID-19-associated morbidity and mortality (308). Such knowledge is crucial for clinical decision-making and public health policy for PLWH.

PLWH, despite efficient virological suppression on ART, experience persistent immune dysregulation, residual inflammation, and ongoing immune activation leading to immune cell dysfunction and progressive immune exhaustion that could influence COVID-19 disease severity and responsiveness to vaccination (reviewed in (174)). Although with discrepancies between studies, PLWH appear to be at higher risk of severe SARS-CoV-2 infection with some evidence for increased hospitalisation and mortality rates among PLWH (168,309,310) that might be due to low socioeconomic status, occupational risk, or HIV-1-related co-morbidities (165,311). These multi-morbidities are driven by residual inflammation on ART and ongoing immune dysregulation (163) that can exacerbate SARS-CoV-2-induced inflammation and influence COVID-19 disease

severity (312). More recently, cellular immune deficiency and a lower $CD4^+$ T-cell count/low $CD4^+$ T-cell nadir have been identified as risk factors for severe outcomes in PLWH, irrespective of virological suppression (165). Emerging evidence supports the role of $CD4^+$ T cells in the effective control and resolution of SARS-CoV-2 infection (139). Therefore, any pre-existing $CD4^+$ T-cell depletion in PLWH, especially in those with advanced immunodeficiency, could be a potential driver of dysregulated SARS-CoV-2 immunity, hampering antiviral responses and influencing disease progression (183,313).

Although the correlates of immune protection against SARS-CoV-2 have not been well defined, emerging evidence supports the potential role of T cells in both preventing initial productive infection and, more importantly, limiting the extent of disease severity (139). The majority of people infected with SARS-CoV-2 in the absence of HIV-1 develop durable T-cell responses, including $CD4^+$ and $CD8^+$ T-cell responses (179,314). $CD4^+$ T cells have been shown to play a central role in the development of neutralising antibodies (139,315,316), in addition to providing $CD8^+$ T-cell and B-cell help for long-term immunity (314,317–319). Early development of $CD8^+$ T-cell responses has also been associated with effective viral clearance (139), and high expression of cytotoxic molecules of $CD8^+$ T cells has been linked to a better disease outcome (179,320,321). Further evidence of the importance of T-cell responses comes from studies in people with inherited or acquired impairment of antibody responses (322), with T-cell responses being associated with protection in patients with haematological malignancies on B cell–depleting agents (323). However, excessive T-cell activation and

progressive exhaustion may also be detrimental, and high levels of T-cell activation have been associated with poor clinical outcomes (324). This is particularly pertinent in PLWH, in whom residual T-cell activation/abnormalities persist despite years of effective ART (174). Additionally, co-morbid conditions, premature ageing/ immunosenescence, and pre-existing $CD4^+$ T-cell depletion, which have all been shown to be risk factors for poor disease outcomes, could have important consequences for developing T-cell responses to a new pathogen or vaccination (174,313,325). While most studies on SARS-CoV-2 infection or vaccination in PLWH have mostly focused on evaluating humoral responses, data on functional SARS-CoV-2 specific T-cell responses remain limited.

To date, only two studies reported T-cell responses in the first wave of pandemic in PLWH with or without suppressed viraemia (both in South Africa) (180,181). These studies showed that SARS-CoV-2 infection with wild-type Wuhan strain induced a detectable T-cell response in PLWH, particularly in those with efficient immune recovery after suppressive therapy (180,181); such responses were, however, significantly poorer in PLWH with unsuppressed viraemia and/or advanced immunodeficiency (180,181). Following SARS-CoV-2 vaccination, one randomised, phase 2/3 trial in the UK examined T-cell responses to prime-boost dosing with the chimpanzee adenovirus-vectored ChAdOx1-nCoV-19 vaccine in PLWH on stable ART (184) and their durability after six months (185). These data showed that two doses of vaccine induced a robust T-cell response in PLWH, and although a decline in responses was observed after 6 months, the magnitude of the T-cell response didn't differ significantly between PLWH and HIV-negative

controls (185). These data are consistent with observations following vaccination with mRNA vaccines in PLWH with $CD4^+$ T-cell counts above 200 cells/$mm^{3,}$ demonstrating a functional T-cell response induced by two doses of vaccine (182,313). However, an in-depth characterisation of T-cell responses following natural infection or vaccination, including responses to an additional third dose and their resistance to emerging variants in PLWH, is currently limited. To bridge this knowledge gap, I examined the magnitude and phenotype of T-cell responses in the convalescent phase of COVID-19 disease and following vaccination in PLWH and HIV-negative individuals, in relation to the induction of humoral responses.

5.2 Results.

5.2.1 Section 1: Adaptive immune responses in convalescent SARS-CoV-2 infection.

5.2.1.1 Study cohort.

To study the impact of HIV-1 on immune responses to primary SARS-CoV-2 infection, forty-seven individuals with HIV-1 infection, well-controlled on ART, were recruited to this study between July 2020 and November 2020. Of these donors, twenty-four had laboratory-confirmed SARS-CoV-2 diagnosis (RT-PCR and/or Roche antibody tests) with a median days post-symptom onset (DPSO) of 148; twenty-three were probable/possible cases (had COVID-19-related symptoms but never tested) with a higher median DPSO of 181 days. The majority had mild COVID-19 disease, not requiring hospitalisation (score 1−2 on WHO criteria). Eight subjects out of the laboratory-confirmed cases had moderate disease requiring hospitalisation (score 4−5 on WHO criteria). The ages of the subjects ranged from 30 to 73 years and were predominately White Caucasian males. The cohort included donors capturing a range of $CD4^+$ T-cell counts (22−1360 cells/mm^3) and CD4:CD8 ratios (0.13−3.05), reflective of the different lengths of HIV-1 infection/$CD4^+$ T-cell nadir and variable levels of immune reconstitution post-treatment. As a comparator group, HIV-seronegative individuals were included in the study, thirty-one with laboratory-confirmed SARS-CoV-2 diagnosis and four suspected/household contacts of a confirmed case. The majority of HIV-negative individuals had a mild infection, and four donors had moderate disease (score 4−5 on WHO criteria) and were sampled at

a similar median DPSO (median 144 cells/mm^3; range 101-220 cells/mm^3). HIV-negative subjects were younger (range 26−65 years) with an equal female:male distribution. Inter-experimental variability was minimised by running matched cryopreserved samples in batches with inter-assay quality controls. Further details on patients' characteristics and co-morbidities are included in **Table. 5.1**.

Table. 5.1. Cohort Demographics and Clinical Characteristics for Convalescent Infection.

		HIV+		HIV-	
		Confirmed	Suspected	Confirmed	Suspected
Group size	Primary infection, n	24	23	31	4
COVID-19 severity [B]	Asymptomatic (score 1), n (%)	2 (8.3)	0 (0.0)	4 (12.9)	1 (25.0)
	Non-hospitalised (score 2), n (%)	14 (58.3)	22 (95.7)	23 (74.2)	3 (75.0)
	Hospitalised (score 4-5), n (%)	8 (33.3)	1 (4.3)	4 (12.9)	0 (0.0)
	Days post-symptom onset (DPSO), median (range)	148 (46-232)	181 (34-241)	144 (101-220)	200 (125-203)
Risk factors	Age, median (range)	51 (30-73)	53 (30-67)	42 (26-65)	35.5 (30-41)
	Sex, n female:male:other	4:19:1	2:21:0	16:15:0	2:2:0
Ethnicity	White, n (%)	16 (66.7)	17 (73.9)	19 (61.3)	1 (25.0)
	BAME, n (%)	8 (33.3)	6 (26.1)	12 (38.7)	3 (75.0)
HIV-1 parameters	HIV-1 viral load	<50	<50	-	-
	CD4, median (range)	571 (133-1110)	586 (310-1360)	-	-
	CD4:CD8, median (range)	0.84 (0.17-2.54)	0.97 (0.37-2.15)	-	-
Pre-existing conditions	None, n (%)	10 (41.7)	8 (34.8)	15 (48.4)	4 (100.0)
	Diabetes, n (%)	6 (25.0)	1 (4.3)	1 (3.2)	0 (0.0)
	Hypertension/CVD, n (%)	7 (29.2)	2 (8.7)	3 (9.7)	0 (0.0)
	Renal disease, n (%)	2 (8.3)	2 (8.7)	0 (0.0)	0 (0.0)
	Respiratory disease (asthma and COPD), n (%)	2 (8.3)	4 (17.4)	1 (3.2)	0 (0.0)
	Liver disease, n (%)	1 (4.2)	2 (8.7)	0 (0.0)	0 (0.0)
	Weakened immune system [C]	-	-	-	-
	Other	ITP, psoriasis, pituitary gland failure	Osteoporosis, Peripheral, neuropathy, hypothyroidism	RA, iron deficiency, psoriasis, gout, SLE, hypothyroidism	

[A] Confirmed, possible and probable cases specified by the case definition for COVID-19, as of 29 May 2020, European Centre for Disease Prevention and Control [https://www.ecdc.europa.eu/en/covid-19/surveillance/case- definition].

[B] Severity of COVID-19 was classified according to the WHO (World Health Organisation) clinical progression scale.

[C] Participants who had organ transplantation, including renal or liver transplantation.

5.2.1.2 Levels of SARS-CoV-2 antibodies during the convalescent phase.

Initial screening to confirm prior infection (i.e. SARS-CoV-2 seropositivity) was performed by ELISA to detect antibodies against the external spike antigen, using immobilised recombinant spike S11−530 subunit protein (S1) and against immobilised full-length internal nucleoprotein (N) antigen, as previously described (326–328). A sample absorbance >4-fold above the average background of the assay was regarded as positive, using a threshold established with pre-pandemic samples **(Figure. 5.1.A-C)** and as previously described (328). The screening assay, followed by titre quantification, demonstrated that 95.8% (23/24) of PLWH with prior laboratory-confirmed COVID-19 and 30.43% (7/23) with suspected disease, during the first wave of the pandemic, had measurable titres for SARS-CoV-2 S1 and N **(Figure. 5.1.D)**. Similarly, in the HIV-negative group with laboratory-confirmed COVID-19 disease, 93.5% (29/31) had detectable SARS-CoV-2 antibodies to S1 and N, whereas none of the suspected/household contacts in this group (0/4) had quantifiable titres **(Figure. 5.1.D)**. S1 and N titres were comparable between PLWH and HIV-negative donors **(Figure. 5.1.E&F)**. To determine whether the SARS-CoV-2 antibodies generated can inhibit SARS-CoV-2 infection, a serum neutralisation assay with pseudotyped SARS-CoV-2 was performed to calculate the 50% inhibitory serum dilution (ID_{50}) (214). Overall, similar neutralisation levels and similar profiles were observed across the two study groups in terms of the number of individuals with high potency, low potency or no neutralising activity (ID_{50}<50) **(Figure. 5.1.G)**. Taken together, these data show no significant differences in the IgG-specific antibody response to SARS-

CoV-2 and neutralisation capacity according to HIV-1 status after recovery from COVID-19 disease.

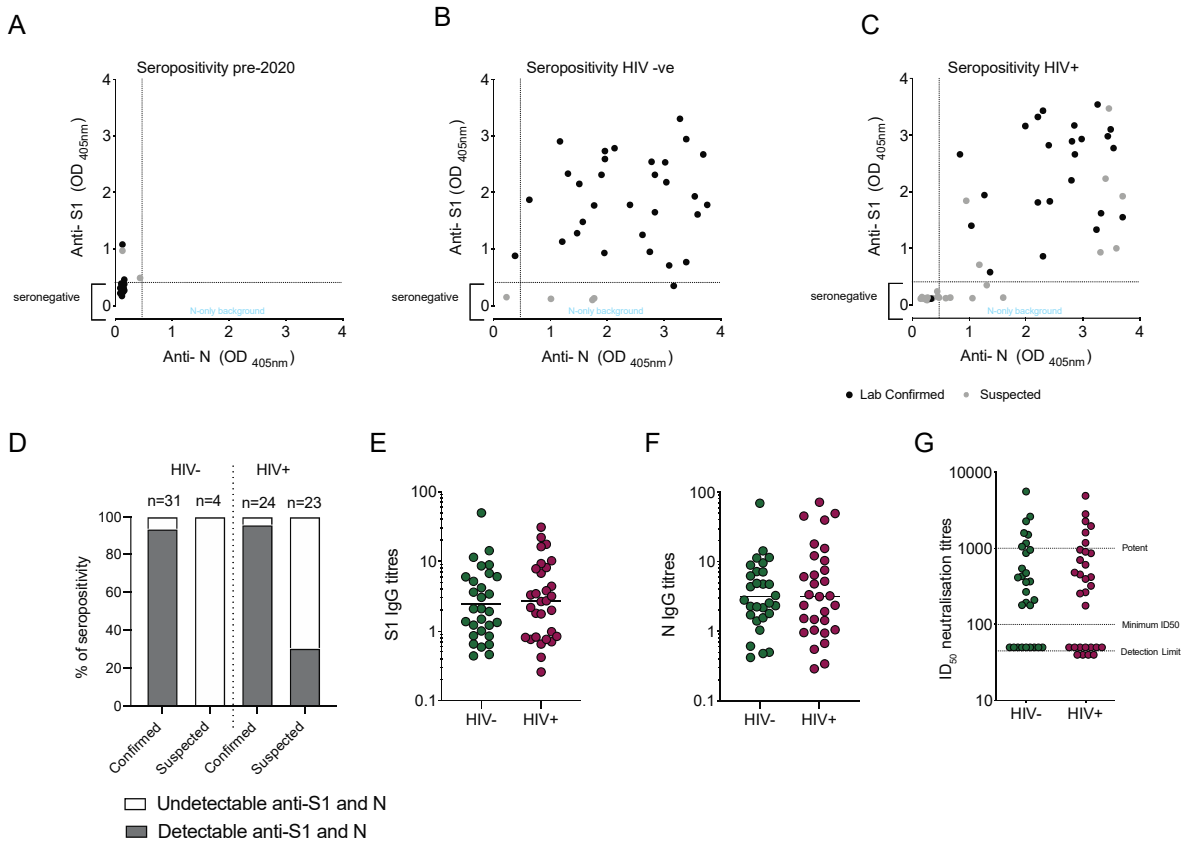


Figure 5.1. Antibody response in PLWH and HIV-negative donors recovered from COVID-19 disease.

Seropositivity screen for antibodies against the external spike and internal nucleoprotein (N) antigens to confirm prior infection in **(A)** pre-pandemic samples (samples collected before 2020) **(B)** HIV-negative donors, and **(C)** PLWH. A sample absorbance >4-fold above the average background of the assay was regarded as positive. Black dots denote laboratory-confirmed cases, and grey dots suspected/household contacts. **(D)** Percentage of seropositivity in HIV-negative donors and PLWH with confirmed or suspected SARS-CoV-2 infection. Comparison of S1 IgG **(E)** and N IgG **(F)** antibody titres in HIV-negative donors (n = 29) and PLWH (n = 30). **(G)** Neutralisation titres in HIV-negative and -positive donors. The dotted lines indicate the detection limit, minimum ID_{50} and potent levels. Two-tailed Mann–Whitney U test was used.

5.2.1.3 The magnitude of SARS-CoV-2-specific T-cell responses in the convalescent infection.

Cellular immune responses have been shown to have a potential role in controlling viral replication and, more importantly, determining disease outcome (139,329–331). We, therefore, assessed SARS-CoV-2 specific T-cell frequencies by IFN-γ-ELISpot using overlapping peptide (OLP) pools to detect T-cell responses and cumulative frequencies directed against defined immunogenic regions, including spike, nucleoprotein (N), membrane (M), envelope (Env), and open reading frame (ORF)3a, ORF6, ORF7 and ORF8**.** Out of the 30 PLWH and 30 HIV-negative individuals (including previously laboratory-confirmed cases and additional subjects found to be SARS-CoV-2 seropositive on screening), the majority of donors in each group (>90%) had a demonstrable cellular response directed predominately against spike and N/M **(Figure. 5.2.A&B).** The overall magnitude of responses against spike, M and N, and total SARS-CoV-2 responses did not differ significantly between the two study groups **(Figure. 5.2.B)**. T-cell responses to SARS-CoV-2 were predominantly directed against spike and N/M **(Figure. 5.2.C)**. Responses to accessory peptide pools (ORFs) and the structural protein Env were less frequent and significantly lower to other antigens, irrespective of HIV-1 status **(Figure. 5.2.C)**. Given the considerable heterogeneity in the magnitude of the observed responses in both groups, these responses were related to HIV-1 parameters (both $CD4^+$ T-cell count and CD4:CD8 ratio). Notably, a positive correlation was observed between the CD4:CD8 ratio (but not $CD4^+$ T-cell count) and summed total responses to OLP pools against SARS-CoV-2 in PLWH (r = 0.3820, p = 0.037) **(Figure. 5.2.D&E)**;

this relationship was similar for N (r = 0.4282, p = 0.018) and stronger for responses against M (r = 0.4855, p = 0.0065). These data suggest that, despite effective ART, incomplete immune reconstitution may potentially impact the magnitude of T-cell responses to SARS-CoV-2. Previous observations have demonstrated an association between SARS-CoV-2-specific T cells, age and gender, with T-cell immunity to spike increasing with age and male gender in some studies (332). Despite an older age and male predominance in this cohort, no significant association was detected between ELISpot responses to spike and donor age (data not shown). Similarly, there was no correlation between DPSO and T-cell responses (data not shown). Overall, these data suggest that PLWH who recovered from mild infection could mount T-cell responses against SARS-CoV-2 at a comparable level to HIV-negative controls. These findings should be considered in the context of this cohort in which the majority of cases were mild and, therefore, may not reflect the full burden of disease associated with SARS-CoV-2 infection.

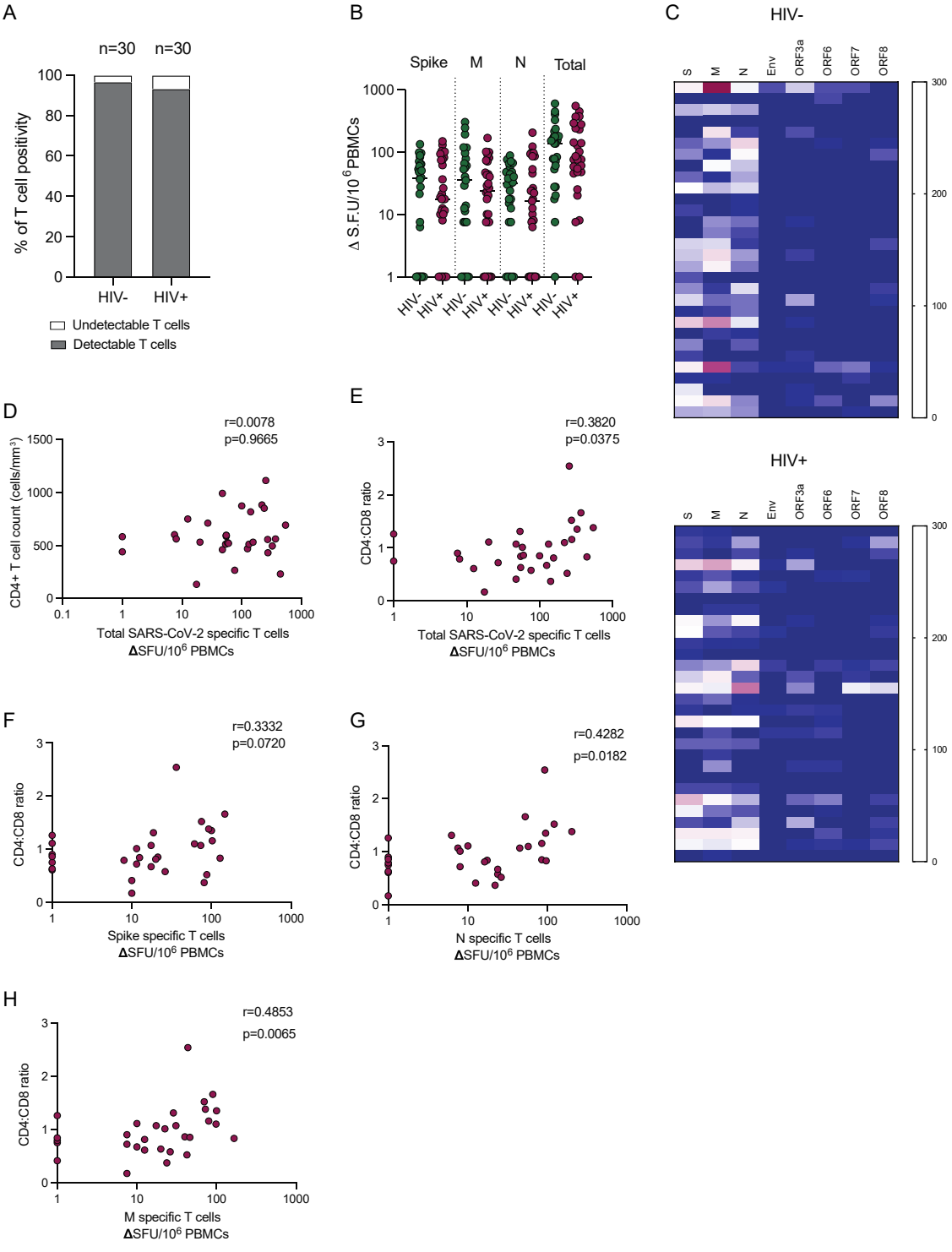

A
n=30
n=30
% of T cell positivity
HIV-
HIV+
Undetectable T cells
Detectable T cells
B
Spike
M
N
Total
Δ S.F.U/10^6 PBMCs
C
HIV-
HIV+
S
M
N
Env
ORF3a
ORF6
ORF7
ORF8
D
r=0.0078
p=0.9665
CD4+ T cell count (cells/mm³)
Total SARS-CoV-2 specific T cells
ΔSFU/10^6 PBMCs
E
r=0.3820
p=0.0375
CD4:CD8 ratio
Total SARS-CoV-2 specific T cells
ΔSFU/10^6 PBMCs
F
r=0.3332
p=0.0720
CD4:CD8 ratio
Spike specific T cells
ΔSFU/10^6 PBMCs
G
r=0.4282
p=0.0182
CD4:CD8 ratio
N specific T cells
ΔSFU/10^6 PBMCs
H
r=0.4853
p=0.0065
CD4:CD8 ratio
M specific T cells
ΔSFU/10^6 PBMCs

Figure 5.2. Similar SARS-CoV-2-specific T-cell responses by IFN-γ-ELISpot in convalescent PLWH and HIV-negative donors.

(A) Percentage of HIV-negative and -positive individuals with confirmed SARS-CoV-2 infection and detectable (grey) or undetectable (white) T-cell response (n = 30 in each group). **(B)** The magnitude of the IFN-γ-ELISpot responses. IFN-γ SFU/10^6 PBMCs are shown for SARS-CoV-2 spike (S), membrane (M), nucleocapsid (N), or cumulative (total) responses between HIV-negative (green) and PLWH (red). **(C)** Heatmap depicting the magnitude of the IFN-γ-ELISpot responses to the different SARS-CoV-2 peptide pools (S, M, N, ORF3a, ORF6, ORF7, ORF8 and Env) in HIV-negative individuals and PLWH (n = 30 in each group). **(D)** Correlation between $CD4^+$ T-cell counts in PLWH with their total SARS-CoV-2 responses. Correlation between CD4:CD8 ratio and **(E)** total SARS-CoV-2 responses, **(F)** spike-specific responses, **(G)** nucleocapsid-specific responses, or **(H)** membrane-specific responses in PLWH. The non-parametric Spearman test was used for correlation analysis. For multiple groups, significance was assessed by two-way ANOVA with multiple comparisons.

5.2.1.4 T-cell and antibody response complementarity in the convalescent infection.

Next, T-cell responses, antibody levels and antibody responses were compared in individual donors to better understand any complementarity between humoral and cellular responses detected by IFN-γ-ELISpot. Spike-specific T cells correlated positively with respective S1 IgG titres in HIV-negative and PLWH (HIV- $r = 0.4039$, $p = 0.0339$: HIV+ $r = 0.5720$, $p = 0.0022$) (**Figure. 5.3.A**). A similar association was observed between N-specific T-cell responses and N IgG titres in PLWH but not in HIV-negative donors (HIV- $r = 0.3099$, $p = 0.1157$: HIV+ $r = 0.4381$, $p = 0.0252$) (**Figure. 5.3.B**). When total T-cell responses were compared to both S1 and N IgG levels, the magnitude of the cellular immune

responses correlated weakly with N IgG binding titres but not with S1 IgG binding titres in PLWH (**Figure. 5.3.C&D**). In HIV-1 negative donors, a weak correlation was observed between total T-cell responses and S1 and N IgG binding titres (**Figure. 5.3.C&D**). Next, spike-specific T-cell responses and cumulative responses were examined in relation to neutralisation ID_{50} values for individual donors. In HIV-negative donors, a correlation was observed only between T-cell responses to spike protein and ID_{50} ($r = 0.4002$, $p = 0.0315$) (**Figure. 5.3.E**). In PLWH, no correlation was detected between neutralisation capacity and cellular responses (both spike-specific and pooled T-cell responses) (**Figure. 5.3.E&F**). These data suggest that memory T-cell and antibody responses were sometimes discordant in PLWH who recovered from a mild infection, as previously described in the general population (332).

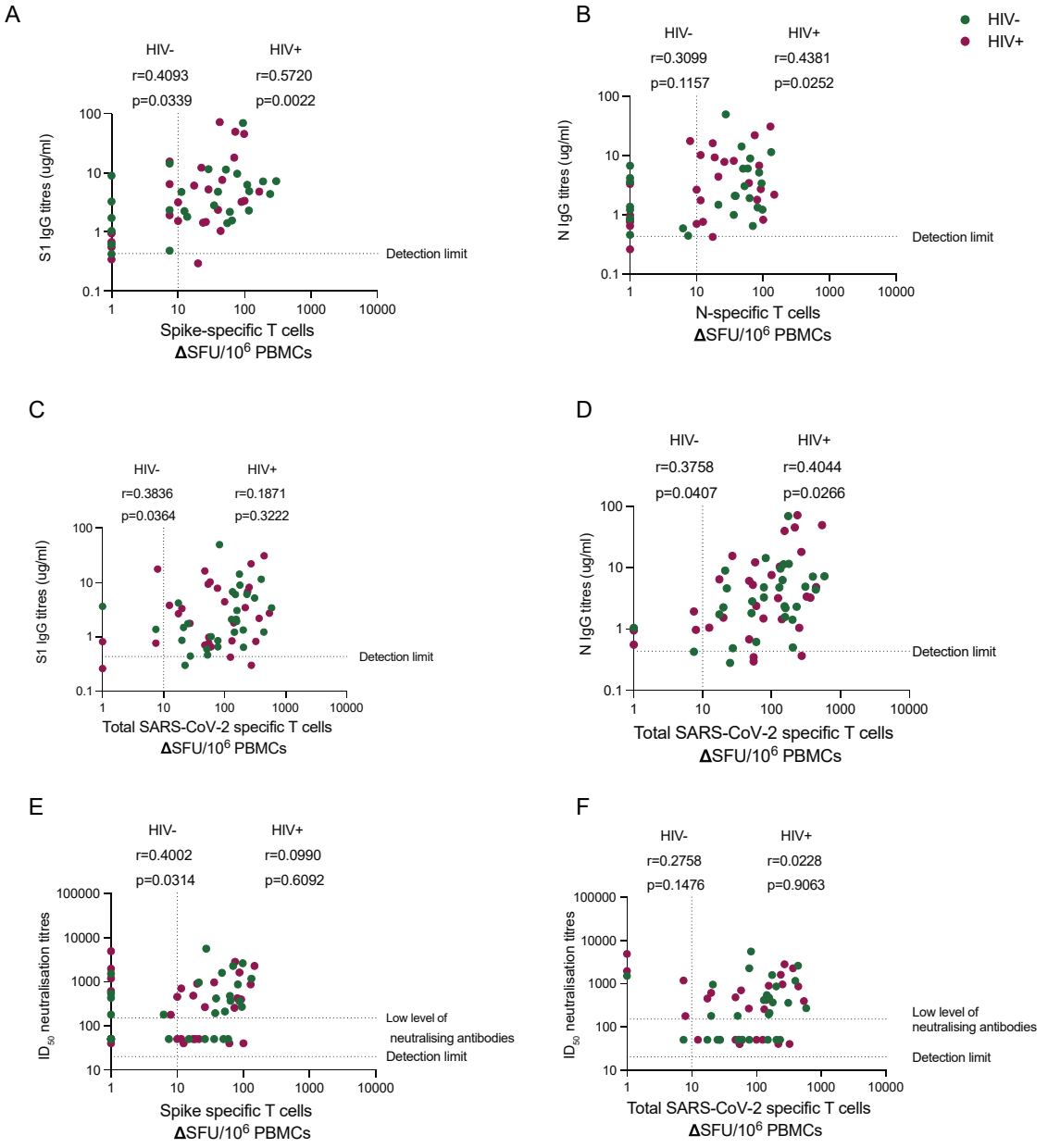


Figure 5.3. Interrelations between T-cell and antibody responses in convalescent PLWH and HIV-negative donors.

(A) Correlation between spike-specific T cells with S1 IgG titres in HIV-negative donors (green) and PLWH (red). **(B)** Correlation between N-specific T cells with N IgG titres. Correlation of total SARS-CoV-2 responses with **(C)** S1 IgG or **(D)** N IgG titres. Correlation of neutralisation titres against spike protein with **(E)** spike-specific or **(F)** total SARS-CoV-2 T cells in HIV-negative donors and PLWH. The non-parametric Spearman test was used for correlation analysis.

5.2.1.5 SARS-CoV-2-specific T-cell responses are dominated by CD4⁺ T cells in convalescent individuals.

Following the broad initial screening of the antiviral responses to SARS-CoV-2, intracellular cytokine staining (ICS) was used to assess the composition and polyfunctionality of T-cell responses in donors with available PBMC and detectable responses by IFN-γ-ELISpot. To determine the functional capacity of SARS-CoV-2-specific $CD4^+$ and $CD8^+$ T cells, PBMCs were stimulated with overlapping spike, M and N (non-spike) peptide pools. Expression of the activation marker CD154 and production of IFN-γ, IL-2 and TNF-α were measured as functional readouts. SARS-CoV-2-specific $CD4^+$ T cells directed against spike and non-spike (M/N) predominantly expressed CD154 alone or in combination with IL-2, TNF-α and IFN-γ, consistent with a T_H1 profile, and these aggregated responses were comparable between the groups (**Figure. 5.4.A,B**). SARS-CoV-2-specific $CD4^+$ T cells exhibited polyfunctional responses, with T cells expressing up to three cytokines (**Figure. 5.4.C**). There were no significant differences in $CD4^+$ T-cell responses, according to cytokine profile, to individual pools directed against spike, M, and N in the two groups (**Figure. 5.4.C**).

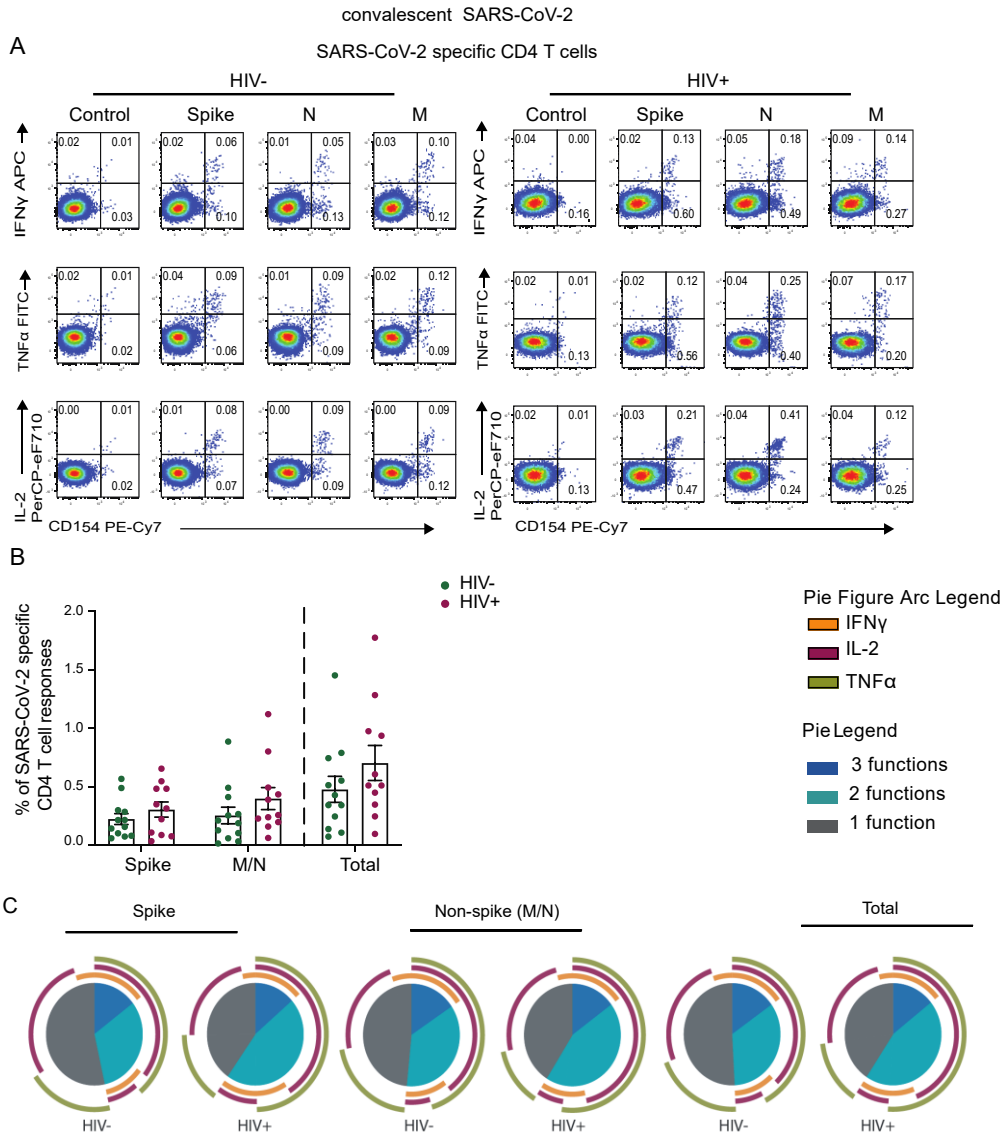


Figure 5.4. Polyfunctional SARS-CoV-2-specific CD4⁺ T cells in convalescent and vaccinated HIV-negative individuals and PLWH.

(A) Representative plots showing antigen-specific CD4⁺ T cells based on double expression (CD154⁺IFN-γ⁺, CD154⁺IL-2⁺, and CD154⁺TNF-α⁺) following 6-h stimulation with media alone (control) or overlapping SARS-CoV-2 peptides against spike (spike), nucleoprotein (N), and membrane protein (M), (HIV−, n = 12) and PLWH (HIV+, n = 11). **(B)** Frequency of aggregated CD4⁺ T-cell responses against spike, M/N or combined (spike and M/N) peptide pools. **(C)** Pie charts representing the relative proportions of CD4⁺ T-cell responses for one (grey), two (green) or three (dark blue) cytokines. SPICE was used for polyfunctional analysis.

Next, $CD8^+$ T-cell responses were examined in convalescent PLWH and HIV-negative individuals. SARS-CoV-2-specific $CD8^+$ T cells broadly expressed IFN-γ alone or in combination with TNF-α, exhibiting a different cytokine profile to $CD4^+$ T cells. A trend toward lower mean aggregated $CD8^+$ T-cell responses and polyfunctionality against spike relative to non-spike was observed in HIV-negative individuals (**Figure. 5.5.A-C)**. The magnitude of SARS-CoV-2-specific $CD8^+$ T-cell responses against non-spike protein was lower in convalescent PLWH, but the overall SARS-CoV-2-specific $CD8^+$ T-cell responses did not differ significantly between the two groups (**Figure. 5.5.B)**. Notably, SARS-CoV-2-specific $CD8^+$ T cells were less frequent, with $CD4^+$ T cells similarly outnumbering $CD8^+$ T cells regardless of HIV-1 status (**Figure. 5.6.A)**. These data indicate that $CD4^+$ T cells are the dominant population responding to SARS-CoV-2 in PLWH.

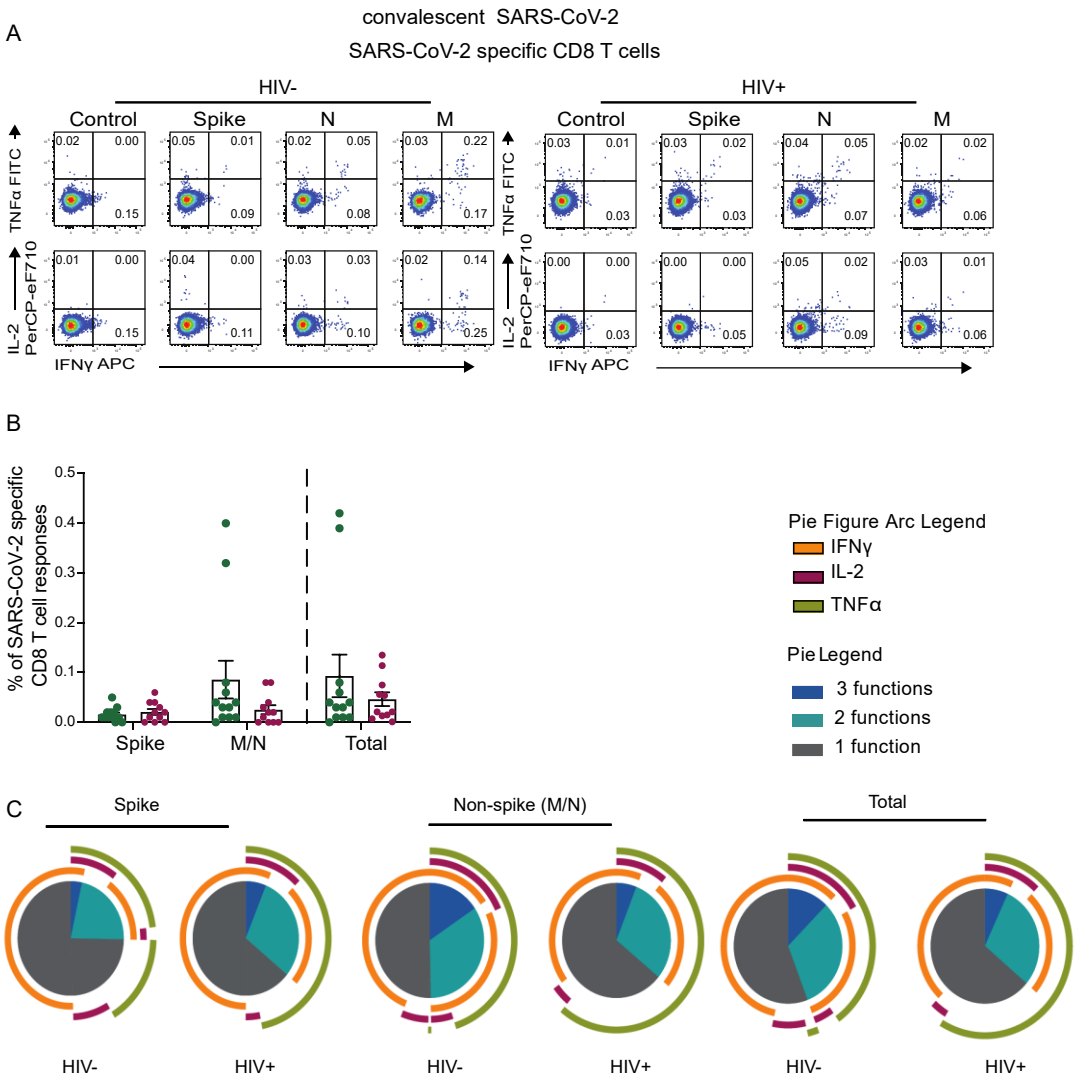


Figure 5.5. Polyfunctional SARS-CoV-2-specific CD8+T cells in convalescent and vaccinated PLWH and HIV-negative donors.

(A) Representative plots for the identification of antigen-specific $CD8^+$ T cells based on the expression of ($IFN\text{-}\gamma^+$, $TNF\text{-}\alpha^+$, and $IL\text{-}2^+$) against the specified peptide pools or media alone (control). **(B)** The proportion of aggregated $CD8^+$ T-cell responses. **(C)** Pie charts representing the relative proportions of spike, M/N and combined $CD8^+$ T-cell responses for one (grey), two (green) or three (dark blue) cytokines, and pie arcs showing IFN-γ, TNF-α and IL-2. Significance determined by two-tailed Mann−Whitney U test. SPICE was used for polyfunctional analysis.

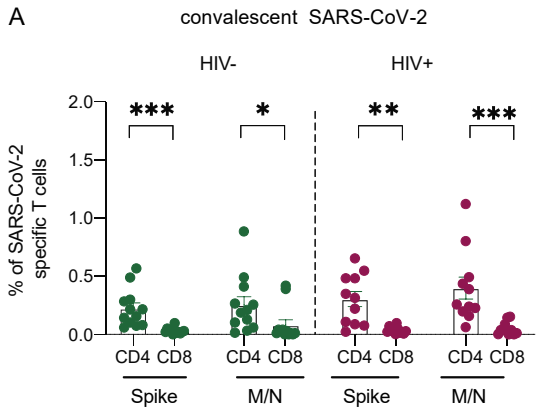


Figure. 5.6. Composition of SARS-CoV-2-specific T cells in convalescent and vaccinated PLWH and HIV-negative individuals.

(A) Comparison of the frequencies of summed SARS-CoV-2-specific $CD4^+$ and $CD8^+$ T-cell responses against Spike and M/N proteins in convalescent HIV-negative and -positive donors. Significance determined by two-tailed Wilcoxon matched-pairs signed rank test, $*p < 0.05$, $**p < 0.01$, $***p < 0.001$.

5.2.1.6 Immune profile relationships between convalescent PLWH and HIV-negative individuals.

During acute COVID-19 disease, excessive activation of T cells can lead to lymphopenia, including altered subset distribution and function, and these alterations can persist into convalescence phase (318,324,333). This prompted us to evaluate further changes in the T-cell compartment and the relationship between antigen-specific T cells and antibodies with individual T-cell parameters and immunological metrics in our cohort. To this end, a broad immunophenotyping flow cytometry panel was used to capture major cell types (**Chapter 2, section 2.1.4, Table. 2.2**). t-SNE high-dimensional analysis demonstrated significant alterations in the T-cell compartment between HIV-

negative individuals and PLWH recovered from COVID-19 disease (**Figure. 5.7.A)**. Lower proportions of circulating $CD4^+$ T cells and higher proportions of $CD8^+$ T cells were confirmed by traditional gating in convalescent PLWH compared to HIV-negative individuals (**Figure. 5.7.B)**. Consistent with alterations described in HIV-1 infection (334–336), naïve T-cell frequency was reduced in SARS-CoV-2 convalescent PLWH compared to HIV-negative subjects. This was accompanied by higher proportions of terminally differentiated effector memory (TEMRA: $CD45RA^+CCR7^-$) within the total $CD8^+$ T-cell population in PLWH, contributing to an altered representation of naïve/memory T cells (**Figure. 5.7.C)**. Notably, the percentage of naïve $CD4^+$ T cells correlated with the CD4:CD8 ratio ($r = 0.6789$, $p = 0.0014$) and SARS-CoV-2-specific T-cell responses in PLWH ($r = 0.5518$, $p = 0.0143$) (**Figure. 5.7.D&E)**, suggesting that the scarce availability of naïve $CD4^+$ T cells could influence the extent/magnitude of the T-cell response to SARS-CoV-2 infection (179).

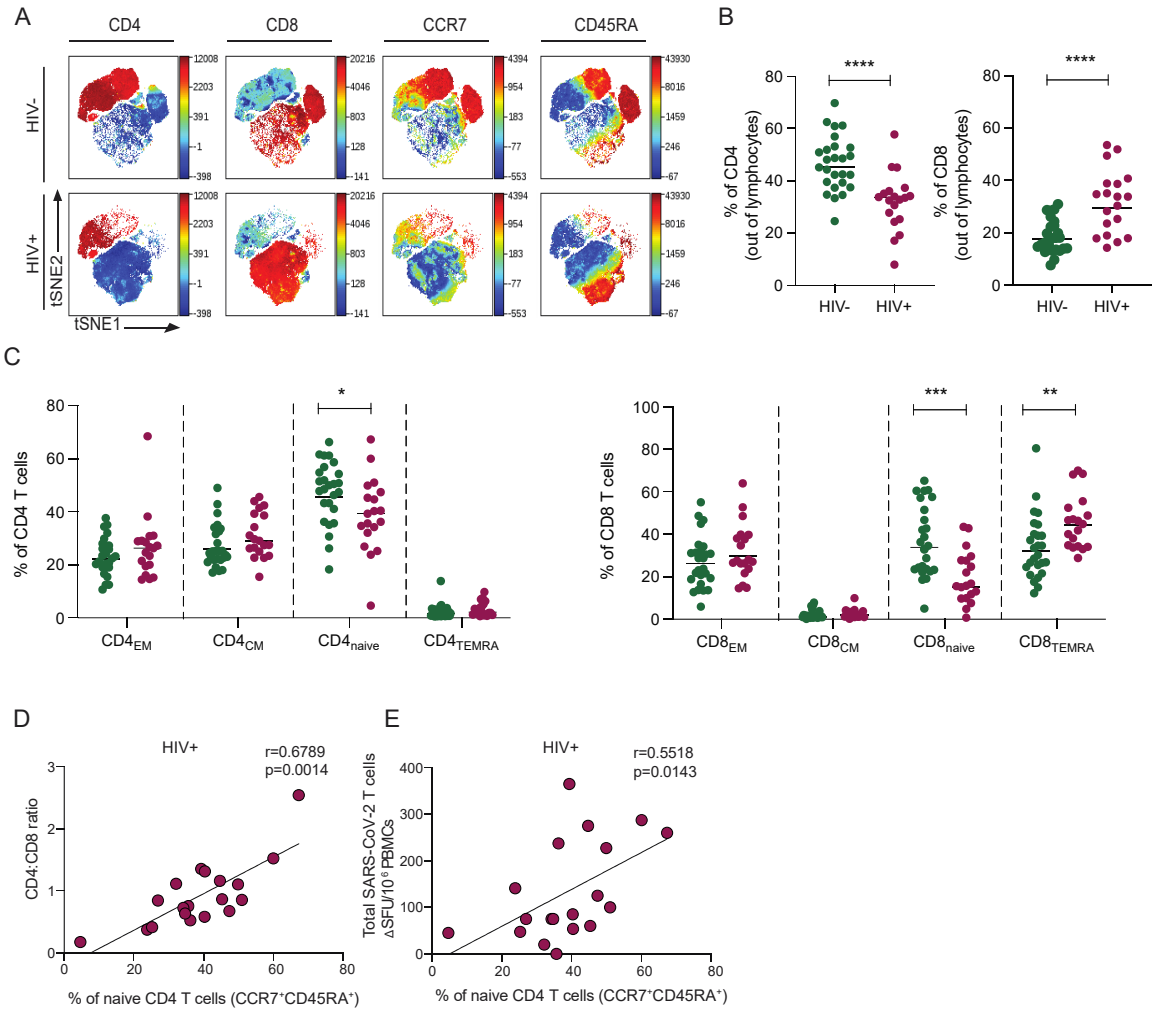


Figure 5.7. Immune profile relationships between convalescent PLWH and HIV-negative individuals.

(A) viSNE analysis of CD3 T cells in HIV-negative donors (top panel) and PLWH (lower panel). **(B)** Frequency of $CD4^+$ and $CD8^+$ T cells out of total lymphocytes in SARS-CoV-2 convalescent HIV-negative donors (HIV−, n = 26) and PLWH (HIV+, n = 19). **(C)** Summary data of the proportion of $CD45RA^-/CCR7^+$ central memory (CM), $CD45RA^+/CCR7^+$ naïve, $CD45RA^+/CCR7^-$ terminally differentiated effector memory (TEMRA) and $CD45RA^-/CCR7^-$ effector memory (EM) $CD4^+$ and $CD8^+$ T-cell subsets. **(D)** Correlation between CD4:CD8 ratio and naïve $CD4^+$ T cells in PLWH. **(E)** Correlation between naïve $CD4^+$ T cells and total SARS-CoV-2 T cells in PLWH. Significance determined by two-tailed Mann−Whitney U test, *p < 0.05, **p < 0.01, ***p < 0.001, ****p < 0.0001. The non-parametric Spearman test was used for correlation analysis (two-tailed).

5.2.2 Section 2: Adaptive immune responses in SARS-CoV-2 vaccination.

5.2.2.1 Study cohort.

In a subgroup of convalescent patients and newly recruited patients, vaccine-induced immune responses were studied in PLWH and HIV-negative controls. Forty-six PLWH (n=24 donors included in the convalescent study and n=22 individuals newly recruited), virally suppressed on ART, were sampled between January 2021 and April 2022 after SARS-CoV-2 vaccination. Of these donors, fifteen had previous SARS-CoV-2 infection, and thirty-one had no history of SARS-CoV-2 exposure before vaccination. Participants were sampled after SARS-CoV-2 immunisation with a primary course (i.e. two doses) of Oxford/AstraZeneca (ChAdOx1-S) or mRNA Pfizer/Moderna (BNT162b2) and a third dose of mRNA vaccine (BNT162b2 or mRNA-1273), according to the Joint Committee on Vaccination and Immunisation (JCVI) recommendations. PLWH with $CD4^+$ T-cell counts < 200/mm^3 or/and additional co-morbidities at the time of their first vaccine dose (n=5) were included in the priority group 4 and received their third dose of vaccine earlier than the general population. All participants were screened for prior exposure using ELISA to detect the presence of SARS-CoV-2 IgG against spike and nucleoprotein. PLWH were stratified according to their history of prior SARS-CoV-2 infection as prior SARS-CoV-2 (including infection before or after vaccination) or as SARS-CoV-2 naïve. The subjects' ages ranged from 35 to 65 years and were predominately White Caucasian males. The cohort included virally suppressed donors with $CD4^+$ T-cell counts (22−1360 cells/mm^3) and CD4:CD8 ratios (0.13−2.55). As a comparator group,

forty-five HIV-negative individuals were included in the study following SARS-CoV-2 vaccination, twenty-seven had prior SARS-CoV-2 infection, and eighteen had no history of SARS-CoV-2 exposure before immunisation. These donors were sampled at similar median days post each dose of vaccine (14 and 19 days post-first dose, 29 and 26 days post-second dose, and 35 and 43 days post-third dose, for SARS-CoV-2-naïve and SARS-CoV-2-exposed donors, respectively). Further details on patients' characteristics and co-morbidities are included in **Table. 5.2**.

Table. 5.2. Cohort Demographics and Clinical Characteristics for SARS-CoV-2 vaccination.

		HIV-		HIV+	
		SARSCoV-2-	SARSCoV-2+	SARSCoV-2-	SARSCoV-2+
Group size	1st dose, n	9	23	15	12
	2nd dose, n	18	27	29	13
	3rd dose, n	14	20	31	15
Vaccine type (AZ : Pfizer: Moderna)	1st dose, n	3:6:0	1:22:0	5:10:1	5:7:0
	2nd dose, n	3:11:4	2:25:0	17:12:0	4:9:0
	3rd dose, n	0:11:3	0:19:1	0:29:2	0:14:1
Days post-vaccination	1st dose, median (range)	14 (12-74)	19 (12-60)	20 (12-102)	22 (13-82)
	2nd dose, median (range)	29 (23-67)	26 (15-68)	20 (7-48)	21 (9-52)
	3rd dose, median (range)	35 (13-43)	43 (9-129)	40 (9-149)	65 (7-140)
Risk factors	Age, median (range)	38 (33-65)	42 (29-58)	46 (35-65)	50 (38-63)
	Sex, n female:male:other	6:3	9:14	0:15	1:11
Ethnicity	White, n (%)	2 (22.3)	15 (65.2)	9 (60.0)	7 (58.3)
	BAME, n (%)	7 (77.7)	8 (34.8)	6 (40.0)	5 (41.6)
HIV-1 parameters	HIV-1 viral load	-	-	<50	<50
	CD4, median (range)	-	-	610 (22-1360)	590 (200-1229)
	CD4:CD8, median (range)	-	-	0.93 (0.13-3.05)	1.19 (0.37-2.55)
Pre-existing conditions	None, n (%)	18	27	25	9
	Diabetes, n (%)	-	1	5	3
	Hypertension/CVD, n (%)	-	3	3	6
	Renal disease, n (%)	-		2	1
	Respiratory disease (asthma and COPD), n (%)	-	1	3	1
	Liver disease, n (%)	-		2	2
	Weakened immune system [A]	-	-	8	1
	Other	-		Splenectomy Sarcoidosis; HBV-co-infection	Splenectomy

[A] Participants who had organ transplantation, including renal or liver transplantation.

5.2.2.2 Levels of SARS-CoV-2 antibodies after SARS-CoV-2 immunisation.

SARS-CoV-2 infection has been reported to enhance both the potency and breadth of immune responses after vaccination, compared to vaccination alone (326–328). We, therefore, measured the humoral responses to vaccination in PLWH with or without prior SARS-CoV-2 infection. The screening assay for seropositivity showed that 80% of PLWH with no prior history of SARS-CoV-2 and 100% of PLWH with prior SARS-CoV-2 infection, had detectable IgG titres against S1 after one dose of vaccine **(Figure. 5.8A).** Consistent with previous findings in the healthy population (184,337), S1 titres were found to be higher in individuals with prior SARS-CoV-2 infection compared to SARS-CoV-2 naïve donors across all time-points, irrespective of HIV-1 status **(Figure. 5.8A)**. However, while PLWH with prior SARS-CoV-2 showed comparable S1 IgG titres compared to HIV-negative controls, SARS-CoV-2 naïve individuals had significantly lower responses, especially after the first dose **(Figure. 5.8A).** Similarly, the percentage of SARS-CoV-2 naive PLWH who had a detectable neutralising response after one vaccine dose was significantly lower (only 19%) compared to HIV-negative controls (100%) **(Figure. 5.8B).** Neutralising antibody responses were enhanced after an additional vaccine dose, with 75% and 87% of PLWH demonstrating a response after two or three doses of vaccine, respectively **(Figure. 5.8B).** When the levels of neutralising antibodies (nAbs) were compared according to HIV-1 status, responses were found to be significantly lower in PLWH at all time-points, regardless of the history of SARS-CoV-2 exposure **(Figure. 5.8C)**. Overall, these data suggest that neutralising antibody responses to COVID-19 vaccination are reduced in PLWH, particularly

in those who have not previously been exposed to SARS-CoV-2 prior to their vaccination (SARS-CoV-2 naïve).

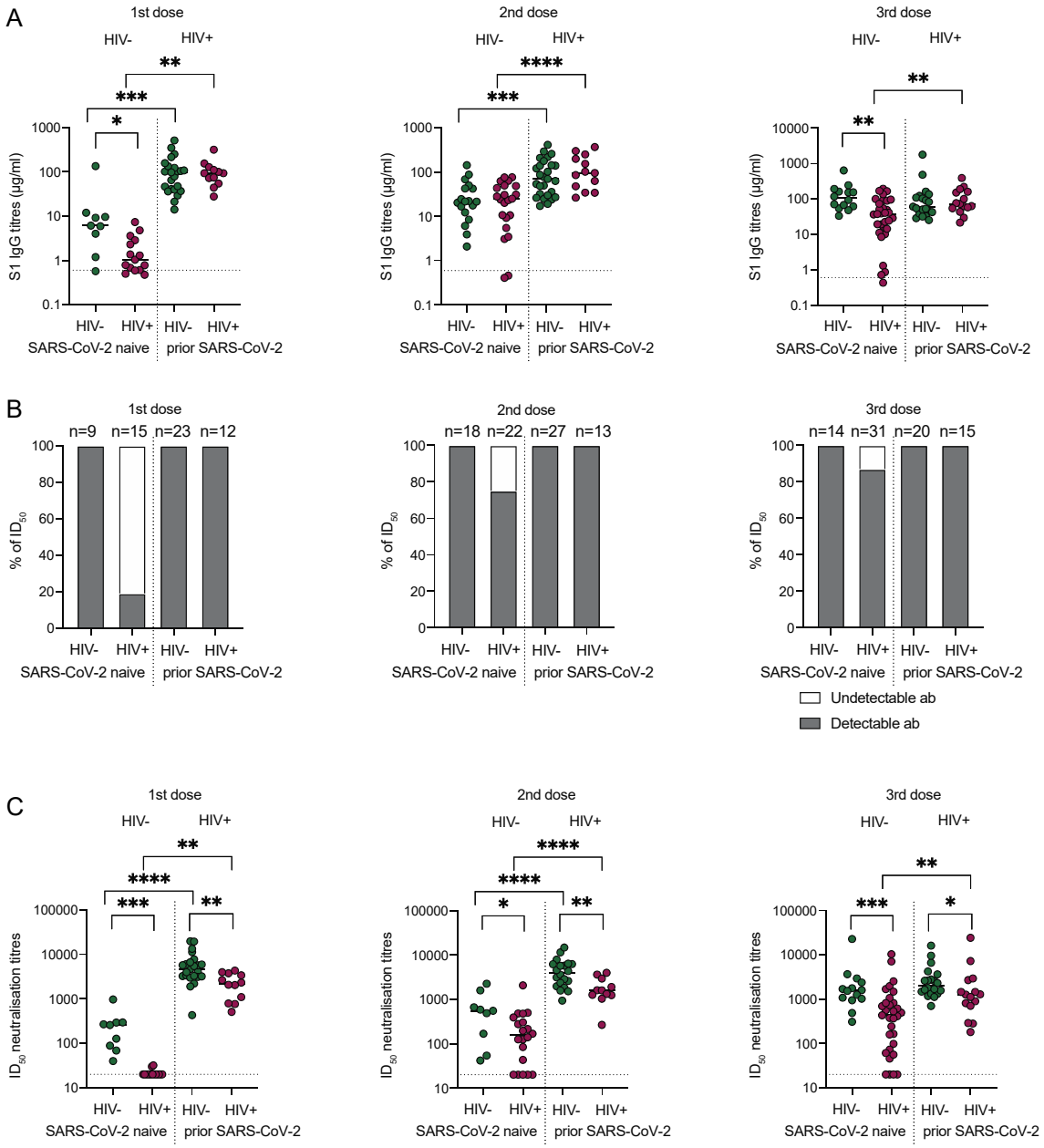


Figure 5.8. Antibody responses in PLWH and HIV-negative donors following SARS-CoV-2 vaccination.

(A) Comparison of S1 IgG antibody titres in HIV-negative donors and PLWH, with or without prior SARS-CoV-2 infection, after 1, 2, or 3 doses of vaccine. The dotted line represents the assay's lower limit (0.6µg/ml). (1 dose: SARS-CoV-2 naïve (n=9 HIV, n=15 HIV+), prior SARS-CoV-2 (n=23 HIV-, n=12 HIV+), 2 doses: SARS-CoV-2 naïve (n=18 HIV, n=29 HIV+), prior SARS-CoV-2 (n=22 HIV-, n=13 HIV+), 3 doses: SARS-CoV-2 naïve (n=14 HIV, n=31 HIV+), prior SARS-CoV-2 (n=20 HIV-, n=15 HIV+)). **(B)** Percentage of individuals with detectable (grey) or undetectable (white) neutralising antibody response at each time-point. **(C)** Pseudovirus neutralisation reciprocal 50% inhibitory titres (ID_{50}) in PLWH and HIV-negative donors with or without prior SARS-CoV-2 infection. The dotted line represents the lower limit of the assay (ID_{50}=1:20). Each data point represents the mean of n=2 biological repeats, each measured in duplicates. Two-tailed Mann–Whitney U test was used for group comparisons. *p < 0.05, **p < 0.01, ****p < 0.0001.

Given the reduced neutralising titres in PLWH, these responses were related to $CD4^+$ T-cell count. No associations were found between neutralising antibody titres and $CD4^+$ T-cell counts **(Figure. 5.9.A-C).**

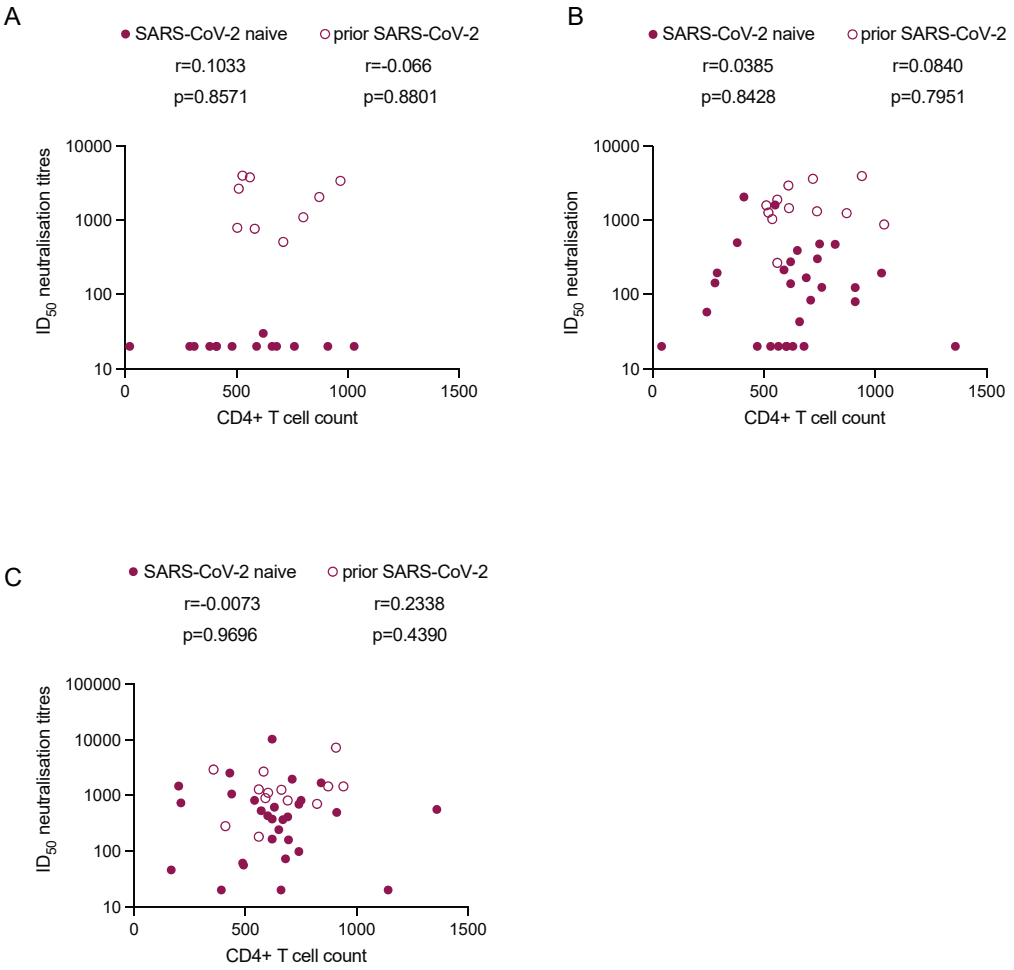


Figure 5.9. Correlation between CD4⁺ T-cell count and nAbs following SARS-CoV-2 vaccination.

Correlation between the CD4⁺ T-cell count and neutralisation levels after **(A)** first dose, **(B)** second dose, and **(C)** third dose. The non-parametric Spearman test was used for correlation analysis.

5.2.2.3 The magnitude of SARS-CoV-2-specific T-cell responses after SARS-CoV-2 vaccination.

To increase our understanding of the effects of vaccination on T-cell responses in PLWH, spike-specific T-cell responses were measured in convalescent individuals following vaccination (prior SARS-CoV-2) and in SARS-CoV-2 naïve

PLWH and HIV-negative controls. Similar to convalescent infection, the majority of PLWH (over 80% in SARS-CoV-2 naïve and 100% in the prior SARS-Cov-2 group) had a measurable cellular response **(Figure. 5.10.A).** There were no detectable T-cell responses in a small number of PLWH with no prior exposure to SARS-CoV-2 across all time-points. These participants had incomplete immune reconstitution on ART and/or additional co-morbidities, such as transplant recipients on immunosuppressive therapy. All HIV-negative individuals (both with or without SARS-CoV-2 infection) had a detectable T-cell response across all time-points **(Figure. 5.10.A).** Overall, the levels of SARS-CoV-2-specific T-cell responses were found to be comparable between PLWH and HIV-negative individuals following each vaccine dose (**Figure. 5.10.B)**. In line with previous observations in the general population (215,321,338), a greater magnitude of spike-specific T cells was observed in individuals with prior SARS-CoV-2 infection compared to SARS-CoV-2 naïve group, irrespective of HIV-1 status (**Figure. 5.10.B**). Given that this observational cohort includes a mixture of SARS-CoV-2 vaccine types, the magnitude of T-cell responses was evaluated in a subgroup of PLWH and HIV-negative donors who had received the same vaccine (mRNA vaccine). This analysis showed comparable T-cell responses between PLWH and HIV-negative controls who had received an mRNA vaccine across all time-points (**Figure. 5.10.C**). A similar analysis for viral vector-based vaccines was not feasible due to insufficient numbers in the HIV-negative control group.

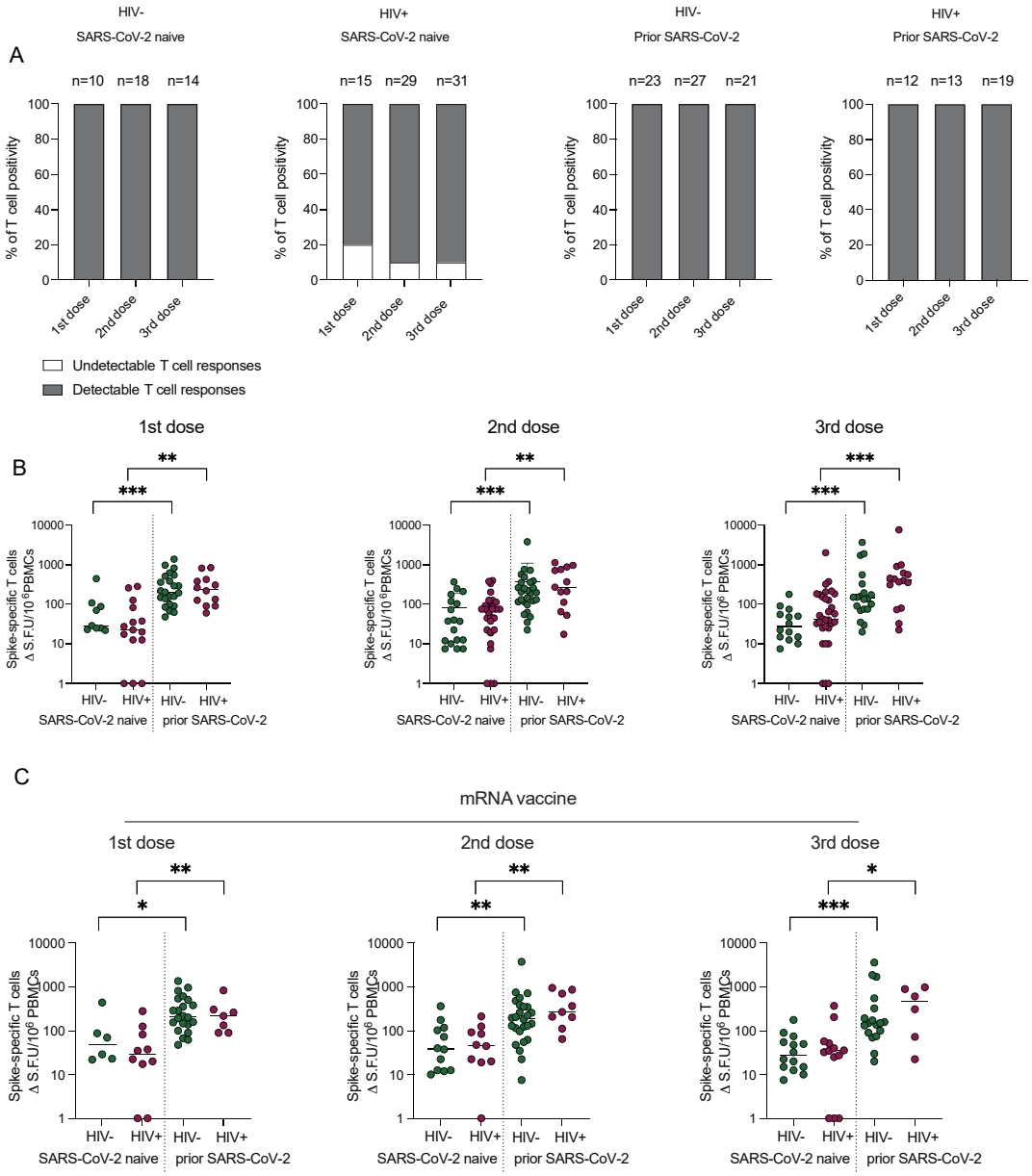


Figure 5.10. Comparable magnitude of spike-specific T-cell responses following SARS-CoV-2 vaccination in PLWH and HIV-negative individuals.

(A) Percentage of individuals with detectable (grey) or undetectable (white) T-cell response after 1, 2, or 3 doses of vaccine. N numbers for each group are indicated above each column. **(B)** The magnitude of spike-specific T cells in HIV-negative donors (green) and PLWH (red), with or without prior SARS-CoV-2 infection, at each time-point. **(C)** Spike-specific T cells in individuals who received an mRNA vaccine for their primary course (i.e. first and second dose) and for their booster dose. Significance determined by two-tailed Mann−Whitney U test, *p < 0.05, **p < 0.01, ***p < 0.001.

Next, the evolution of T-cell responses was examined longitudinally in a subgroup of donors with available PBMC samples. While spike-specific T-cell responses were mostly undetectable at baseline in PLWH with no prior SARS-CoV-2, these responses significantly increased following the first vaccine dose, peaked after the second dose and were maintained after the third vaccine dose (**Figure. 5.11.A)**. The detectable T-cell responses observed in a small proportion of SARS-CoV-2 naïve individuals at baseline (n=5) could represent cross-reactive T-cell responses to other coronaviruses (185,339–343). However, due to the small number of participants with pre-existing T-cell responses at baseline, this study was not powered to detect any association between the presence of cross-reactive T cells and the magnitude of vaccine-induced T-cell responses. In donors with prior SARS-CoV-2 infection, there was a boosting effect in spike-specific T cells only after the first vaccine dose in both study groups (**Figure. 5.11.A**). In one HIV-positive, SARS-CoV-2-naïve donor with advanced immunosuppression and persistently low $CD4^+$ T-cell count of 100 cells/mm^3 on ART, a third dose (mRNA vaccine) was able to elicit a T-cell response despite no evidence of neutralisation (**Figure. 5.11.A**). Overall, these results demonstrate a robust induction of T-cell responses to SARS-CoV-2 vaccination in PLWH despite attenuated antibody responses.

A

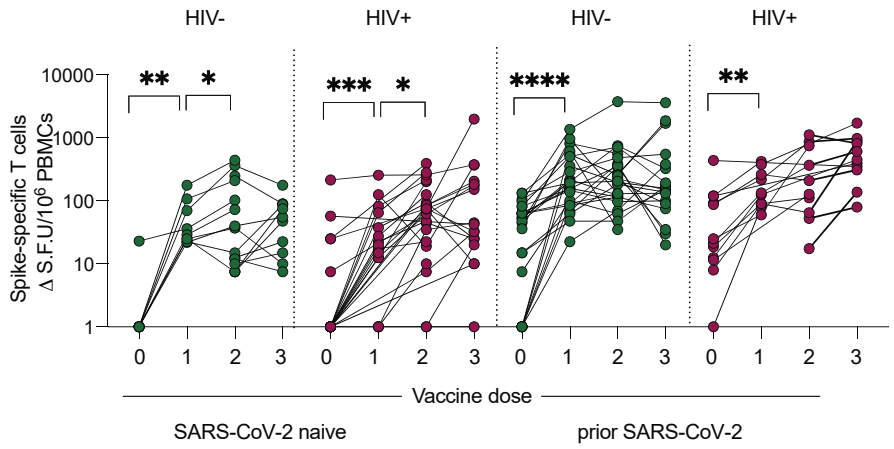


Figure 5.11. Longitudinal analysis of spike-specific T-cell responses following SARS-CoV-2 vaccination in PLWH and HIV-negative individuals.

(A) Longitudinal analysis of the spike-specific T-cell responses in the study groups. Significance determined by Wilcoxon matched-pairs signed rank test, *p < 0.05, **p < 0.01, ***p < 0.001.

Previous work has demonstrated that T-cell responses are largely retained against VOCs, including the highly transmissible BA.1 Omicron variant. To determine T-cell reactivity to VOCs, T-cell responses to the mutated regions described in SARS-CoV-2 variants, including Omicron, were assessed. Notably, the magnitude of T-cell responses against BA.1 Omicron was comparable between PLWH and HIV-negative donors regardless of prior SARS-CoV-2 infection **(Figure. 5.12.A)**. These responses were further enhanced by a third vaccine dose in all donors, irrespective of prior SARS-CoV-2 infection or HIV-1 status **(Figure. 5.12.A)**. T-cell reactivity to Omicron and other VOCs, including Alpha, Beta and Delta, was comparable between PLWH and HIV-negative donors, with or without prior SARS-CoV-2 infection, after three vaccine doses, and these responses were maintained against the ancestral Wuhan Hu-1 spike

peptide pool, reinforcing the relative resilience of T-cell responses to spike variation **(Figure. 5.12.B&C)**. It should be noted that three HIV-negative and five PLWH, regardless of prior SARS-CoV-2 infection, had no detectable T-cell responses to the Wuhan Hu-1 peptide pool, covering only the mutated regions of the spike. This could be partly due to the VOC mutations occurring in regions poorly targeted by T-cell responses in some individuals (321). Together these observations suggest that SARS-CoV-2 vaccination induces a robust T-cell response that can cross recognise VOCs, including Omicron, in PLWH.

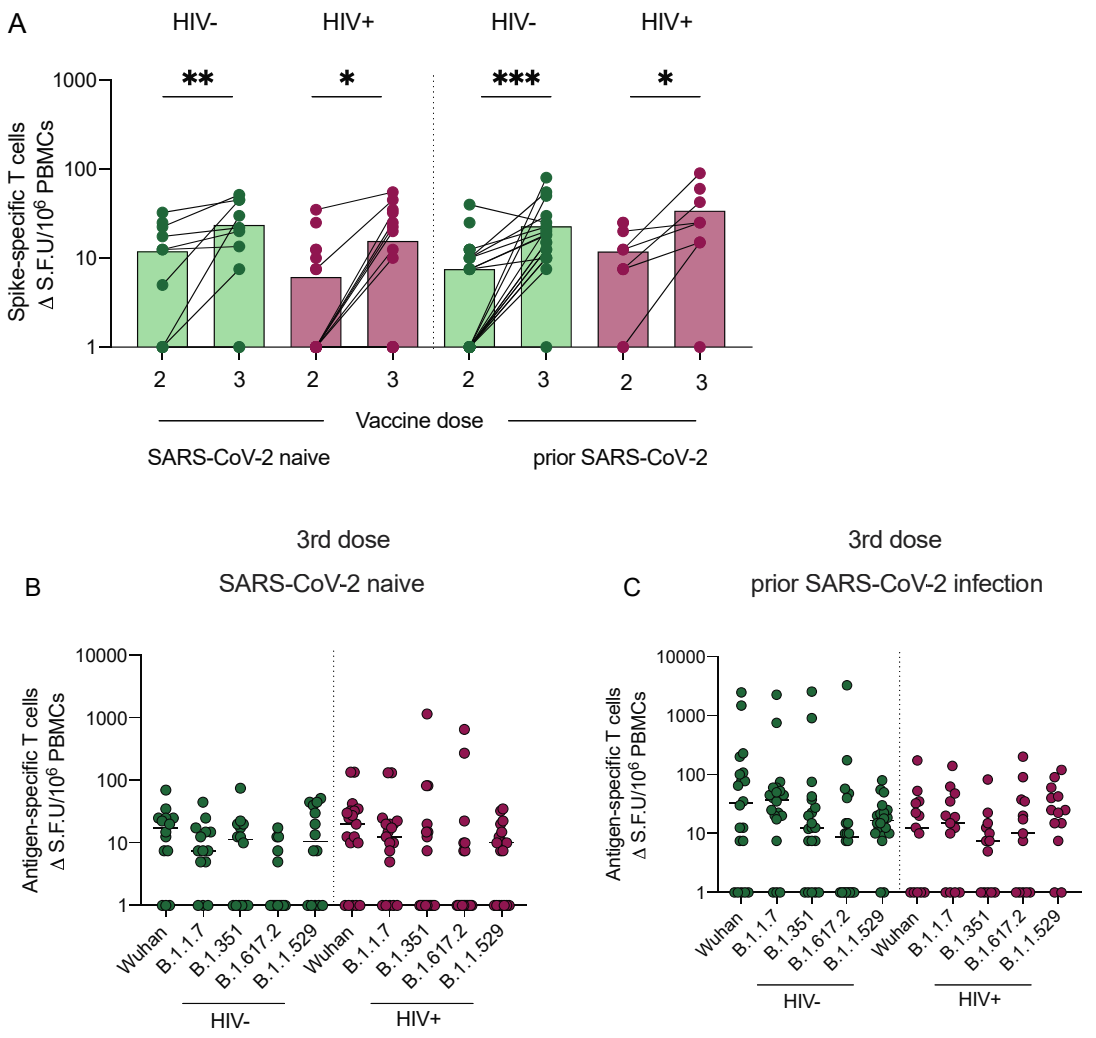


Figure 5.12. T-cell responses induced by SARS-CoV-2 vaccination are preserved against VOCs.

(A) Longitudinal and cross-sectional analysis of the magnitude of T-cell responses to Omicron after two or three vaccine doses (n=11 HIV-SARS-CoV-2-, n=20 HIV+SARS-CoV-2-, n=22 HIV-SARS-CoV-2+, n=10 HIV+SARS-CoV-2+). The magnitude of T-cell responses to Wuhan, Alpha, Beta, and Delta after three vaccine doses in HIV-negative donors and PLWH with **(B)** no prior SARS-CoV-2 infection and **(C)** with prior SARS-CoV-2 exposure.

Given the variation in the magnitude of spike-specific T-cell responses and to better understand the factors underlying this heterogeneity, T-cell responses were considered in relation to HIV-1 parameters. In contrast to findings in convalescent infection, no correlation was observed between the CD4:CD8 ratio and spike-specific T-cell responses following each dose of vaccine (**Figure. 5.13.A).** However, a positive correlation was detected between the $CD4^+$ T-cell count and spike-specific T-cell responses after the first vaccine dose ($r = 0.5153$, $p = 0.0239$) in SARS-CoV-2 naïve PLWH (**Figure. 5.13.B**). This association was weaker after the second vaccine dose ($r = 0.4596$, $p = 0.0121$) and not significant after the third dose (**Figure. 5.13.B**). Together these observations suggest that an effective $CD4^+$ T-cell response could drive the induction of cellular immunity following vaccination, especially in individuals who lacked memory responses (i.e. SARS-CoV-2 naïve).

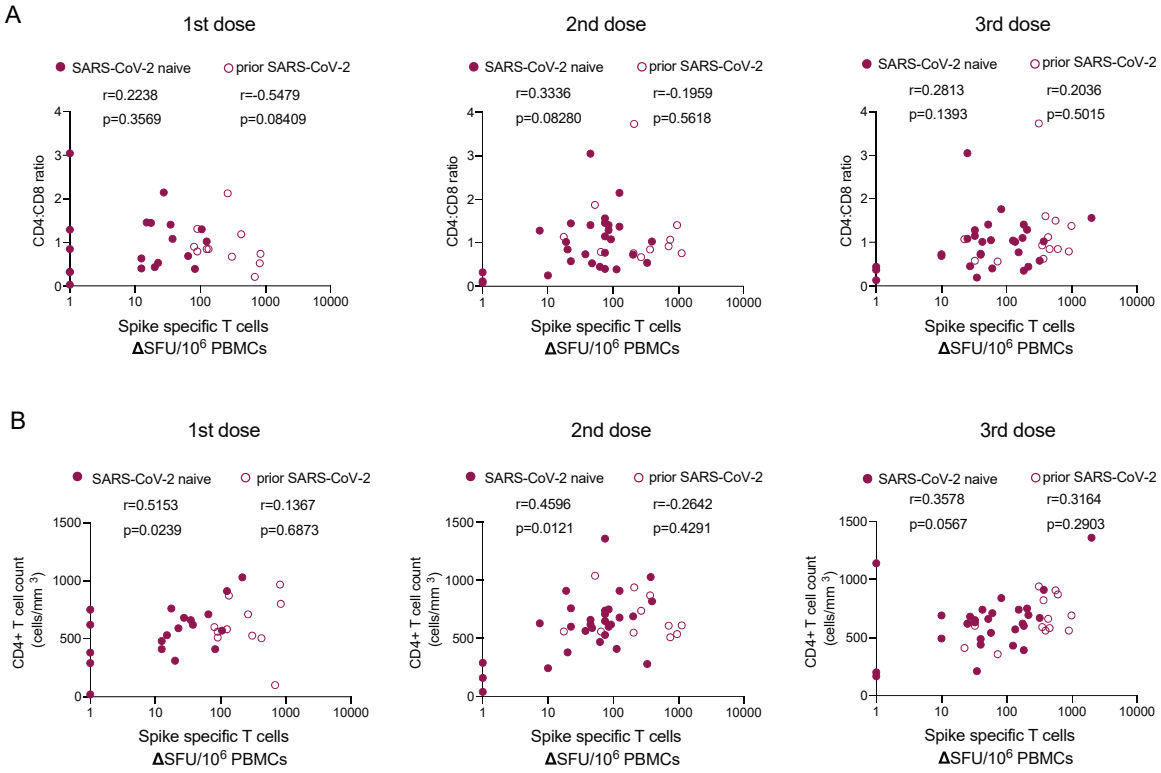


Figure 5.13. Correlation between CD4⁺ T-cell count, CD4:CD8 ratio, and spike-specific T-cell response following SARS-CoV-2 vaccination.

(A) Correlation between CD4:CD8 ratio in PLWH and the magnitude of spike-specific T-cell responses after the first, second, and third dose. **(B)** Correlation between the CD4⁺ T-cell count and magnitude of spike-specific T-cell responses. The non-parametric Spearman test was used for correlation analysis.

5.2.2.4 T-cell responses are induced in a proportion of PLWH who had low or absent nAbs (ID_{50} <150) following vaccination.

Next, T-cell responses, antibody levels, and nAb responses in individual donors were compared to better understand any complementarity between humoral and cellular responses in PLWH following vaccination. Overall, T-cell responses correlated positively with both S1 IgG and neutralising antibody titres after the first dose (S1 IgG $r = 5672$, $p = 0.002$, ID_{50} $r = 6755$ $p = 0.0001$) and second dose of vaccine (S1 IgG $r = 5675$ $p = 0.0003$, ID_{50} $r = 6262$ $p = 0.0001$) (**Figure. 5.14.A-E**). Similar associations were observed in HIV-negative controls (**Figure. 5.14.A-E**). However, these associations were weaker after the third dose of vaccine in both study groups (**Figure. 5.14.C&F**). One HIV-positive SARS-CoV-2 naïve donor with a low $CD4^+$ T-cell count of 40 cells/mm^3 on ART, and one individual with relapsed lymphoma, had no detectable humoral and cellular responses after 2 or 3 doses of mRNA vaccine. Interestingly a proportion of SARS-CoV-2 naïve PLWH with low (ID_{50}< 150) or absent nAbs (ID_{50}< 50 “detection limit”) (n=9 out of 10) had measurable cellular responses to the spike protein after two vaccine doses (**Figure. 5.14.E**). These donors were all controlled on ART with a median $CD4^+$ T-cell count of 680 cells/ mm^3 and no significant underlying co-morbidities **(Table. 5.3).** These data suggest that T-cell responses were induced in a small proportion of PLWH, despite attenuated serological responses, and these cellular responses may play a compensatory role.

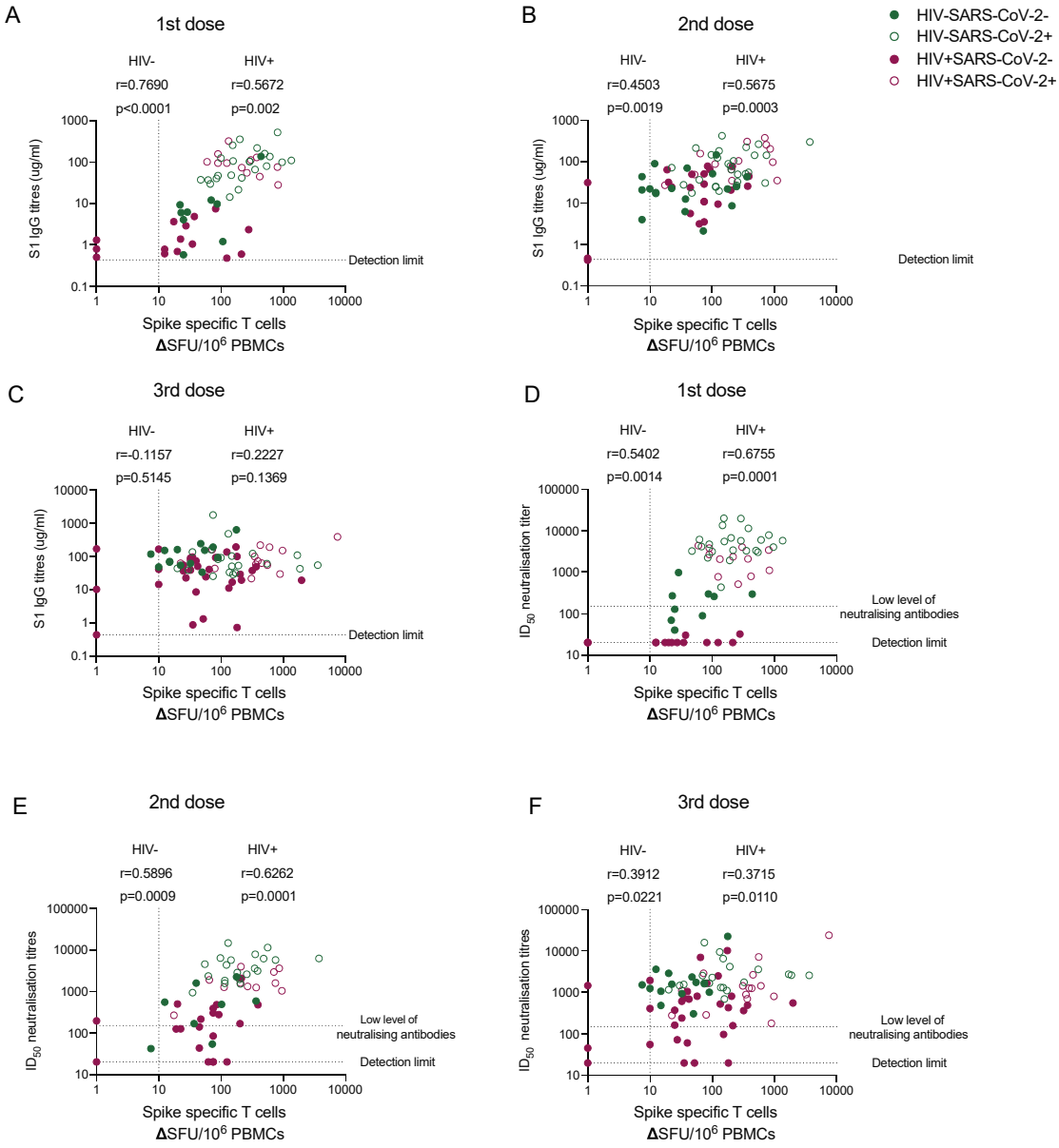


Figure 5.14. Interrelations between T-cell and antibody responses following SARS-CoV-2 vaccination.

Correlation of spike-specific T cells with S1 IgG titres after **(A)** first dose **(B)** second dose, and **(C)** third vaccine dose in HIV-negative donors and PLWH, with or without prior SARS-CoV-2 infection (limit of detection = 0.6μg/ml). Correlation of spike-specific T cells with neutralisation titres after **(D)** first dose **(E)** second dose, and **(F)** third vaccine dose (limit of detection ID_{50}=1:20, low level of neutralisation antibodies ID_{50} 1:150). The non-parametric Spearman test was used for correlation analysis.

5.2.2.5 PLWH with suboptimal antibody responses demonstrate an expansion of CXCR3^{+}CD127^{+} CD8^{+} T cells after two doses of SARS-CoV-2 vaccination.

The presence of detectable T-cell responses in a subgroup of SARS-CoV-2 naïve PLWH with low or absent nAbs after two vaccine doses prompted us to evaluate the phenotype of the T-cell compartment further. To this end, I compared T-cell immune signatures in SARS-CoV-2 naïve PLWH with high neutralisation titres (>1:150) and functional T-cell responses (PLWH SARS-CoV-2 naive nAb^{high}T^{+}, n=9) with SARS-CoV-2 naïve PLWH with low/absent neutralising antibody responses and functional T-cell responses (PLWH SARS-CoV-2- nAb$^{-/low}$T^{+}, n=9). Both groups were age- and sex-matched, well-controlled on ART and with a similar median CD4^{+} T-cell count **(Table. 5.3).** An unbiased approach was used by applying clustering analysis, (viSNE) followed by FlowSOM, in circulating T-cell populations in the two groups. Ten major CD4^{+} and CD8^{+} T-cell subsets were examined using a combination of various activation and differentiation markers, including CD45RA, CCR7, CD127, CD25, CXCR3, CXCR5, PD-1, and CD38 **(Figure. 5.15.A&B).** Among CD4^{+} T cells, there was a reduction in circulating CXCR3^{+}CXCR5^{+} T_{FH} cells observed in PLWH nAb$^{-/low}$ compared to nAb^{+} donors **(Figure. 5.15.A-C).** The reduced abundance of CXCR3^{+}CXCR5^{+} T_{FH} in nAb$^{-/low}$ subjects was further confirmed by manual gating **(Figure. 5.15.D&E)**. The frequency of CXCR3^{+}CXCR5^{+} T_{FH} cells correlated with SARS-CoV-2 neutralisation levels in SARS-CoV-2 naïve PLWH (r = 0.5294 p = 0.0238) **(Figure. 5.15.F),** suggesting that reduced availability of T_{FH} cells could influence the magnitude of vaccine-induced SARS-CoV-2 antibody responses.

Table 5.3. Cohort Demographics and Clinical Characteristics for SARS-CoV-2 naïve PLWH ($nAb^{-}/lowT^{+}$ or $nAb^{+}T^{+}$).

		SARS-CoV-2 naïve PLWH $nAbs^{low/-}$, T-cell responses^{+}	SARS-CoV-2 naïve PLWH $nAbs^{high}$, T-cell responses^{+}
Group size	n	9	9
COVID-19 vaccine	mRNA-based vaccine (BNT162b2/Pfizer or Moderna), n (%)	3 (33.3%)	5 (55.6%)
	ChAdOx1/ AstraZeneca, n (%)	6 (66.7%)	4 (44.4%)
	Day post 2nd dose, median (range)	16 (12-32)	19 (7-41)
Demographics	Age, median (range)	52 (35-63)	57 (29-62)
	Sex, n female:male	1:8	0:9
	Ethnicity, White: BAME	7:2	7:2
HIV-1 parameters	cART	9 (100%)	9 (100%)
	HIV-1 viral load	<50	<50
	$CD4^{+}$ T-cell count, median (range)	680 (470-1360)	650 (380-820)
	CD4:CD8, median (range)	1 (0.4-3.05)	1 (0.39-1.29)
Pre-existing conditions	None, n (%)	7 (77.8%)	6 (66.7%)
	Respiratory disease (asthma and COPD), n (%)	-	1 (11.1%)
	Liver disease, n (%)	1 (11.1%)	-
	Renal disease or Osteoporosis, n (%)	1 (11.1%)	3 (33.3%)

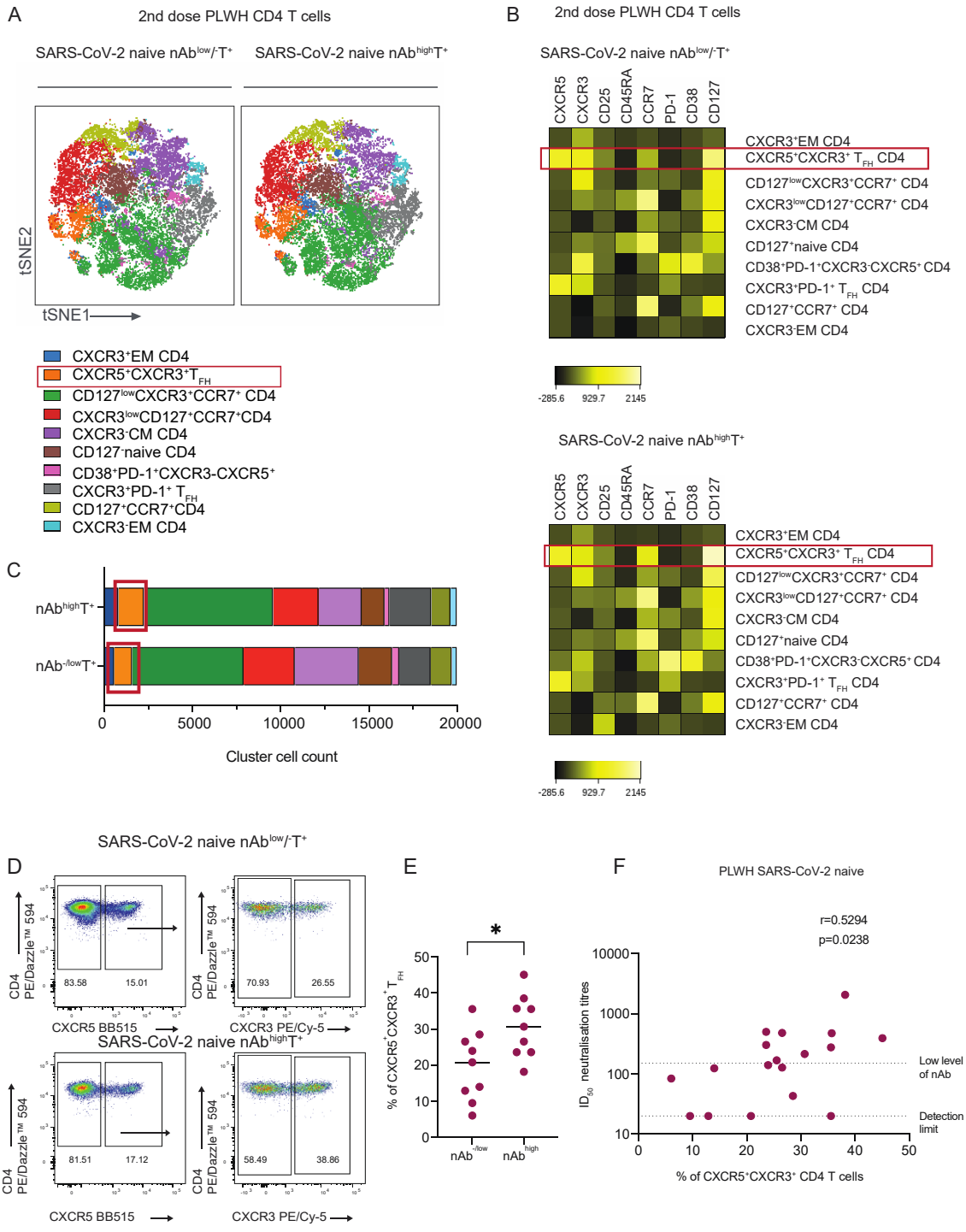

A
2nd dose PLWH CD4 T cells
SARS-CoV-2 naive nAb^low/-T+
SARS-CoV-2 naive nAb^highT+
tSNE2
tSNE1
CXCR3+EM CD4
CXCR5+CXCR3+ TFH
CD127lowCXCR3+CCR7+ CD4
CXCR3lowCD127+CCR7+CD4
CXCR3-CM CD4
CD127-naive CD4
CD38+PD-1+CXCR3-CXCR5+
CXCR3+PD-1+ TFH
CD127+CCR7+CD4
CXCR3-EM CD4
B
2nd dose PLWH CD4 T cells
SARS-CoV-2 naive nAb^low/-T+
CXCR5
CXCR3
CD25
CD45RA
CCR7
PD-1
CD38
CD127
CXCR3+EM CD4
CXCR5+CXCR3+ TFH CD4
CD127lowCXCR3+CCR7+ CD4
CXCR3lowCD127+CCR7+ CD4
CXCR3-CM CD4
CD127+naive CD4
CD38+PD-1+CXCR3-CXCR5+ CD4
CXCR3+PD-1+ TFH CD4
CD127+CCR7+ CD4
CXCR3-EM CD4
-285.6
929.7
2145
SARS-CoV-2 naive nAb^highT+
C
nAb^highT+
nAb^-/lowT+
0
5000
10000
15000
20000
Cluster cell count
D
SARS-CoV-2 naive nAb^low/-T+
CD4 PE/Dazzle™ 594
83.58
15.01
70.93
26.55
CXCR5 BB515
CXCR3 PE/Cy-5
SARS-CoV-2 naive nAb^highT+
81.51
17.12
58.49
38.86
E
% of CXCR5+CXCR3+ TFH
nAb-/low
nAb high
F
PLWH SARS-CoV-2 naive
r=0.5294
p=0.0238
ID50 neutralisation titres
Low level of nAb
Detection limit
% of CXCR5+CXCR3+ CD4 T cells

Figure 5.15. Phenotypic characterisation of CD4+ T cells from SARS-CoV-2 naïve PLWH according to their neutralisation levels.

(A) viSNE map of FlowSOM metaclusters of $CD4^+$ T cells from SARS-CoV-2 naïve PLWH after two vaccine doses ($nAb^{-/low}$= no neutralisation or low level of neutralisation, nAb^{high}=high neutralisation level; n=9 in each group). Each point on the high-dimensional mapping represents an individual cell, and metaclusters are colour-coded. **(B)** Surface expression intensity heatmap of the markers indicated for each FlowSOM meta-cluster of $CD4^+$ T cells. (colour scale: row z-score expression for each individual marker). **(C)** Cell count of each FlowSOM metaclusters out of total $CD4^+$ T cells (20,000 cells/group). **(D)** Representative flow plots from a $nAb^{-/low}$ and nAb^{high} SARS-CoV-2 naïve PLWH showing expression of CXCR5 and CXCR3 within $CD4^+$ T cells. **(E)** Summary analysis of the percentage of $CXCR5^+CXCR3^+CD4^+$ T cells (n=9 for each group). **(F)** Correlation between frequency of $CXCR5^+CXCR3^+CD4^+$ T cells and ID_{50} neutralisation level in $nAb^{-/low}$ and nAb^{high} SARS-CoV-2 naïve PLWH after two vaccine doses. The non-parametric Spearman test was used for correlation analysis. Significance determined by two-tailed Mann−Whitney U test, *$p < 0.05$.

Next, the $CD8^+$ T-cell compartment was examined in the two groups. Notably, a prominent cluster delineated by the expression of $CXCR3^+CD127^+CD38^+CCR7^+CD45RA^+$ was significantly enriched in PLWH SARS-CoV-2-naive $nAb^{-/low}T^+$ (**Figure. 5.16.A-C).** The higher abundance of $CXCR3^+CD127^+CD38^+CCR7^+CD45RA^+$ cells in PLWH SARS-CoV-2-naive $nAb^{-/low}T^+$ was further confirmed by manual gating (**Figure. 5.16.D&E).** Correlation analysis of these $CD8^+$ T-cell populations showed a positive association between their frequencies and SARS-CoV-2-specific T-cell responses following two vaccine doses in PLWH with $nAb^{-/low}$ (r = 0.6740 p = 0.0035) (**Figure. 5.16.F)**, supporting the notion that these subsets could contribute to the observed

induction of T-cell responses in PLWH who lacked or generated low nAb responses. These data are consistent with recent findings showing that $CXCR3^+$ $CD8^+$ T cells are induced in SARS-CoV-2 infected patients, and their presence was associated with survival in COVID-19 patients with critical infection (344).

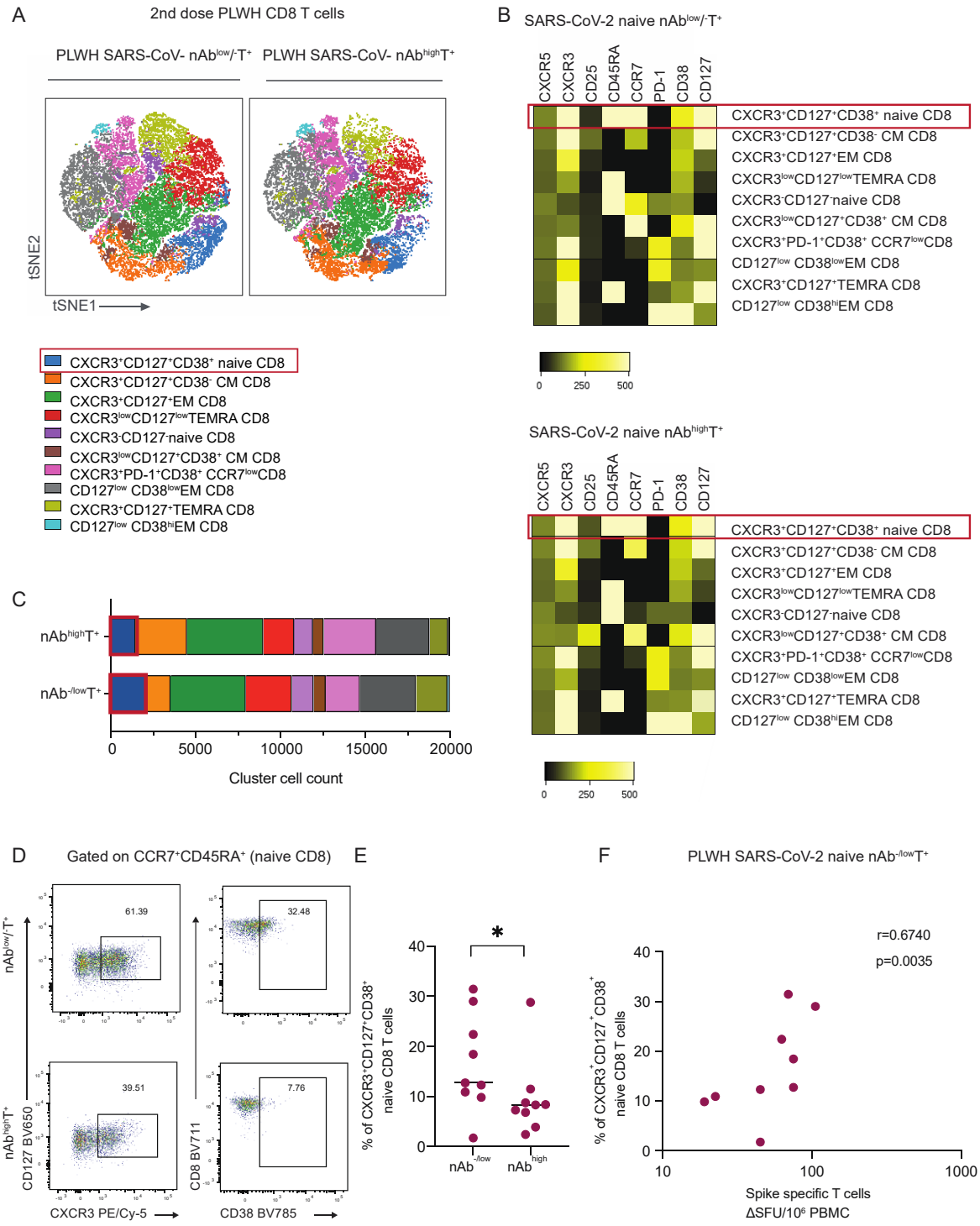

A
2nd dose PLWH CD8 T cells
PLWH SARS-CoV- nAb^low/-T+
PLWH SARS-CoV- nAb^highT+
tSNE2
tSNE1
CXCR3+CD127+CD38+ naive CD8
CXCR3+CD127+CD38- CM CD8
CXCR3+CD127+EM CD8
CXCR3lowCD127lowTEMRA CD8
CXCR3-CD127-naive CD8
CXCR3lowCD127+CD38+ CM CD8
CXCR3+PD-1+CD38+ CCR7lowCD8
CD127low CD38lowEM CD8
CXCR3+CD127+TEMRA CD8
CD127low CD38hiEM CD8
B
SARS-CoV-2 naive nAb^low/-T+
CXCR5
CXCR3
CD25
CD45RA
CCR7
PD-1
CD38
CD127
0
250
500
SARS-CoV-2 naive nAb^highT+
C
nAb^highT+
nAb^-/lowT+
0
5000
10000
15000
20000
Cluster cell count
D
Gated on CCR7+CD45RA+ (naive CD8)
61.39
32.48
39.51
7.76
nAb^low/-T+
nAb^highT+
CXCR3 PE/Cy-5
CD38 BV785
CD127 BV650
CD8 BV711
E
% of CXCR3+CD127+CD38+ naive CD8 T cells
nAb^-/low
nAb^high
F
PLWH SARS-CoV-2 naive nAb^-/lowT+
r=0.6740
p=0.0035
% of CXCR3+CD127+CD38+ naive CD8 T cells
Spike specific T cells
ΔSFU/10^6 PBMC

Figure 5.16. Phenotypic characterisation of CD8+ T cells from SARS-CoV-2 PLWH according to their neutralisation levels.

(A) viSNE map of FlowSOM metaclusters of $CD8^+$ T cells from SARS-CoV-2 naïve PLWH after two vaccine doses ($nAb^{-/low}$= no neutralisation or low level of neutralisation, nAb^{high}=high neutralisation level; n=9 in each group). Each point on the high-dimensional mapping represents an individual cell, and metaclusters are colour-coded. **(B)** Surface expression intensity heatmap of the markers indicated for each FlowSOM meta-cluster of $CD8^+$ T cells. **(C)** Cell count of each FlowSOM metaclusters out of total $CD8^+$ T cells (20,000 cells/group). **(D)** Representative flow plots from a $nAb^{-/low}$ and nAb^{high} SARS-CoV-2 naïve HIV-positive donor showing expression CXCR3, CD127, and CD38 within naïve $CD8^+$ T cells. **(E)** Summary analysis of the percentage of $CD127^+CXCR3^+CD38^+$naive $CD8^+$ T cells (n=9 for each group). **(F)** Correlation between frequency of $CD127^+CXCR3^+CD38^+$naive $CD8^+$ T cells and SARS-CoV-2 specific T-cell responses in $nAb^{-/low}$ SARS-CoV-2 naïve PLWH after two vaccine doses. The non-parametric Spearman test was used for correlation analysis. Significance determined by two-tailed Mann−Whitney U test, *$p < 0.05$.

5.3 Discussion.

Accumulating evidence suggests that a broad and well-coordinated immune response elicited by SARS-CoV-2 infection or vaccination is required for protection against severe COVID-19 disease, and a third vaccine dose is necessary to maintain adequate protection against severe disease, especially in vulnerable sub-populations such as PLWH (183,345,346). The emergence of VOCs with an increased ability to evade humoral response has reinforced the need for a more comprehensive assessment of adaptive immunity, including T-cell responses, which have been shown to contribute to the attenuated clinical severity observed upon infection with VOCs (139). In this chapter, we aimed to bridge the knowledge gaps in our understanding of the specificity, magnitude and duration of adaptive immunity to SARS-CoV-2 infection or vaccination in this patient group. This analysis showed that while primary infection induced comparable S1/N IgG titres and neutralising antibodies between PLWH and HIV-negative controls, these responses were significantly reduced in PLWH following SARS-CoV-2 vaccination. In contrast, both SARS-CoV-2 infection and vaccination induced robust T-cell responses that cross-recognise VOCs in PLWH. Given the potential role of T cells in providing long-term protection and their complementary to humoral response, evaluating T-cell immunity is critical to better understand the correlates of protection and vaccine efficacy in PLWH.

The majority of PLWH developed anti-SARS-CoV-2 IgG and neutralising antibody responses similar to HIV-negative donors in our study, and these responses were durable for at least five months after primary infection, similar to

observations reported in the general population (214,332,347). Circulating SARS-CoV-2 neutralising antibody titres were, however, low in a proportion of recovered COVID-19 cases (214,314,348,349), indicating that either the IgG binding/neutralising antibody potency was suboptimal or, more likely, that an earlier response could have waned by the time of sampling at DPSO as previously observed (214). Some samples in both groups showed strong neutralisation despite low anti-S1 binding titres, suggesting the possibility of the presence of neutralising antibodies directed against other viral epitopes and/or greater production of non-neutralising antibodies or the role of different isotypes in neutralising responses. It should be noted that our data reflect those who recovered from mostly mild COVID-19 disease, limiting our conclusions about disease associations. Whether seroconversion rates and kinetics of antibody responses differ according to HIV-1 status need to be addressed in longitudinal studies from acute infection into convalescence. Notably, a seroprevalence study combined with SARS-CoV-2 PCR testing suggested lower binding/neutralisation titres in PLWH (350). However, in contrast to our study, this cohort included a greater proportion of people with a detectable HIV-1 viral load.

While natural infection induced satisfactory responses, humoral responses to SARS-CoV-2 vaccination were weaker in PLWH compared to HIV-negative controls after each dose of vaccine. Although the third dose increased the neutralisation titres and largely narrowed the gap between PLWH and controls, a small subset of SARS-CoV-2 naïve PLWH still had no nAbs after three vaccine doses. These participants had incomplete immune reconstitution on ART and/or

additional co-morbidities, such as transplant recipients on immunosuppressive therapy. However, the overall defects in humoral responses in PLWH persisted even if the responses were stratified for co-morbidities. These defects could be due to germinal centre structural alterations in chronic HIV-1 infection impacting T and B cell homeostasis, and thus preventing the development of efficient humoral immunity post-vaccination (351,352). In our cohort, the reduced ability to produce neutralising response was linked to a reduced frequency of spike-specific memory B cells and the persistent alterations in the global memory B cell phenotype in PLWH on ART (data reported elsewhere (353)). These data are consistent with the observation that HIV-1 infection induces a poor serological response induced following vaccination against other viral agents, including influenza (354) and HBV (355). The observed differences in natural infection versus vaccine-induced antibody responses might be due to the different study cohorts, as a larger proportion of newly recruited patients had additional co-morbidities and/or had an advanced HIV-1 infection, including patients with $CD4^+$ T-cell counts of less than 200 cells/mm^3 (see Table. 5.1 and Table. 5.2). The fact that these defects persisted after stratification for co-morbidities and $CD4^+$ T-cell counts suggests that other factors may be involved in the reduced humoral responses to vaccination. These differences could be attributed to distinct SARS-CoV-2 antibody reactivity patterns elicited by natural infection (356). Exposure to other immunogenic viral antigens (non-spike proteins) has been shown to induce a broader antibody response with a potent neutralising capacity (356,357). It is also possible that these observed differences resulted from a broader immune activation elicited by other SARS-CoV-2 proteins (non-spike) that emerge after

infection, enhancing B cell maturation and production of humoral responses (358–361).

Although neutralising antibodies against SARS-CoV-2 are likely to be important in protection against SARS-CoV-2, the precise correlates of protection are incompletely defined, and recent observations highlighted the role of T cells in modulating disease outcomes (362–364). In line with published literature (318,329,340), SARS-CoV-2 infection elicited comparable T-cell responses between PLWH and HIV-negative controls, and these responses were variable in magnitude and predominately targeted spike, nucleocapsid (N) and membrane (M). Given that T-cell responses specific to any viral protein can be relevant for protective immunity, non-spike proteins could also represent valuable components for future vaccine strategies. In particular, the structural nucleocapsid protein and non-structural ORF1 proteins (including NSP7 and NSP13), which have been shown to be targeted for cross-reactive T responses and have been suggested to play a role in protection against COVID-19 disease in SARS-CoV-2 exposed seronegative individuals (reviewed in (365). In this respect, in our cohort, a higher proportion of PLWH without prior SARS-CoV-2 infection showed detectable T-cell responses at baseline (pre-vaccine) compared to HIV-negative controls, which could represent the presence of cross-reactive responses to other pathogens, probably to related coronaviruses (339–342,366). However, due to the small number of participants with T-cell responses at baseline, this study was not powered to detect any association between the presence of cross-reactive T cells and the magnitude of vaccine-induced T-cell

responses. Future studies are required to evaluate the extent to which pre-existing T-cell immunity influences the efficacy and immunogenicity of SARS-CoV-2 vaccine in PLWH.

Similar to natural infection, SARS-CoV-2 vaccination induced a robust T-cell response in PLWH, despite poor humoral responses. These data suggest that vaccinating PLWH is still likely to provide some measure of immunity to SARS-CoV-2, given that T-cell responses may be preserved against VOCs that have escaped antibody neutralisation (367,368). Both the primary vaccination course (i.e. two doses) and the third dose were able to elicit spike-specific T-cell responses. In contrast to humoral responses, the magnitude of T-cell responses elicited by the third dose of vaccine was similar to the second dose in SARS-CoV-2 naïve individuals and to the first dose in SARS-CoV-2 exposed, suggesting that optimal T-cell responses are achieved after one or two doses of vaccine in PLWH, similarly to HIV-1 negative controls (369). However, unlike responses to the wild-type spike protein, T-cell responses to B.1.1.529 Omicron variant–specific mutations were further enhanced by an additional third dose in PLWH, suggesting the beneficial effect of booster vaccination in T-cell cross-recognition (370). These findings are in agreement with previously published literature showing a robust T-cell response to SARS-CoV-2 in PLWH after a full course of vaccination (183,371,372). However, one recent study showed that despite the detection of a significant T-cell response to a third dose mRNA vaccine in PLWH with an mRNA primary course, the magnitude of responses was lower compared to the general population (183). These results contrast our

findings and could be attributed to the different study designs/vaccine platforms. While our cohort represents patients with suppressed viraemia (all patients had an undetectable HIV-1 viral load), a study by Vergori et al. included a fraction of HIV-1 patients with unsuppressed viraemia (16% of PLWH had HIV-1 viral load >50 copies/ml). This study also included a larger proportion of immunodeficient patients with $CD4^+$ T-cell count <200 cells/mm^3 (20% vs 8% in our cohort) (183). Given that both unsuppressed viraemia and/or low $CD4^+$ T-cell counts have been reported to impact T-cell responses to SARS-CoV-2 (165,184,313,337,373), it is possible that these factors, in addition to the fact that T-cell responses were measured using whole blood assay stimulation and IFN-γ quantification via ELISA, could explain the differences. Although T-cell responses are a promising indicator of immunity in PLWH, future clinical studies examining the rate of SARS-CoV-2 infection, vulnerability to VOCs, and COVID-19 outcomes in PLWH will be necessary to fully interrogate the degree of clinical protection in these patients.

Notably, the magnitude of T-cell responses, especially against the nucleocapsid (N) and membrane (M), induced by natural infection correlated positively with the CD4:CD8 ratio in PLWH. A positive association was also observed between $CD4^+$ T-cell count and vaccine-induced spike-specific responses after one or two vaccine doses, particularly in PLWH who lacked memory responses generated by natural infection (i.e. SARS-CoV-2 naïve). This suggests that some PLWH with incomplete immune recovery after suppressive therapy reflected by a low $CD4^+$ T-cell count and/or low CD4:CD8 ratio may generate suboptimal T-cell memory responses to SARS-CoV-2 infection or vaccination. A more pronounced

immunodeficiency, defined as a current $CD4^+$ T-cell count <200 cells/mm^3, has been associated with a higher risk for severe disease (183,313) and a poor response to a primary course of SARS-CoV-2 vaccination; as a result, an earlier administration of a third dose was recommended for these patients to complete a full course of vaccination (183,374). The loss of this association after three doses of vaccine may imply that a third dose of vaccine can restore a good T-cell response, even in patients with low $CD4^+$ T-cell count (183), highlighting the benefits of additional booster vaccination in this group of patients. These data have implications for people who might benefit from closer monitoring and may be a target population for novel interventions or optimised vaccine strategies. However, the full impact of HIV-related immunosuppression, in addition to other factors, including age, sex and presence of co-morbidities, in dampening effective and long-lived memory responses needs to be addressed in future larger prospective studies.

Discordant memory T-cell and antibody responses were noted in some patients who lacked nAbs but had detectable T-cell responses. This could reflect different rates of persistence between antibody and T-cell memory responses as our cohort of convalescent infection comprised individuals sampled 5-7 months after infection. While a rapid waning of nAb responses has been observed in mild infection, memory T-cell responses have been suggested to be long-lived (314,332,375). The overall magnitude of T-cell responses induced by vaccination correlated with humoral responses, although these associations were less marked in some PLWH; a small group of SARS-CoV-2 naïve patients with low or

absent neutralisation had detectable functional T-cell responses, implying that T-cell mediated immunity can be induced despite the lack of optimal antibody responses. PLWH who lacked or had low levels of neutralisation after vaccination had a selective reduction in T_{FH} populations, highlighting the importance of T_{FH} responses in the induction of effective humoral responses. Notably, a distinct subset of $CD8^+$ T cells ($CXCR3^+CD127^+$cells) was enriched in PLWH with low or absent neutralisation, and these cells correlated positively with the magnitude of spike-specific T-cell responses. Upregulation of CXCR3 in vaccine-induced T cells with the potential to home to lung mucosa in tuberculosis (376) suggests that these $CD8^+$ T cells described herein could play a role in the protection against severe respiratory diseases such as SARS-CoV-2. An important question to address in future studies is the underlying mechanism of the overrepresentation of these $CD8^+$ T-cell subsets. One possibility is that in the absence of functional antibody responses, the increased abundance of viral antigens could drive $CXCR3^+$ $CD8^+$ T-cell proliferation, as these cells have been shown to have an enhanced proliferative capacity (377) and improved effector differentiation (378,379). These $CXCR3^+$ $CD8^+$ T cells could confer a degree of protection by localisation to infected tissue compartments (377,380), providing site-specific responses, which are known to be important in protection against respiratory disease (381). $CD8^+$ T cells have also been shown to expand following vaccination in patients receiving B cell-depleting therapies (382) and to contribute to vaccine-mediated protection against SARS-CoV-2 in rhesus macaques (383). However, studies in larger cohorts with breakthrough infections are necessary to

evaluate the contribution of these $CD8^+$ T-cell populations in vaccine-mediated protection.

There are several limitations to this study. First, our cohorts for both convalescent and vaccine studies are heterogeneous, with differences in sex, age and levels of immunosuppression that may contribute to the variability in the magnitude of memory responses. Further work is required to determine the role of gender, racial and ethnicity effects, especially in areas of high HIV-1 burden and additional co-morbidities, to help identify individuals who are particularly vulnerable to the impact of SARS-CoV-2 infection. Second, PLWH recovered from mostly mild COVID-19 disease in our study, and thus, any association between disease severity and immune responses will need to be addressed in future studies. Another caveat is that adaptive immune responses were evaluated 5-7 months into convalescence cross-sectionally, and we did not capture peak responses occurring during the acute phase of disease nor the rate of decline over a period of time.

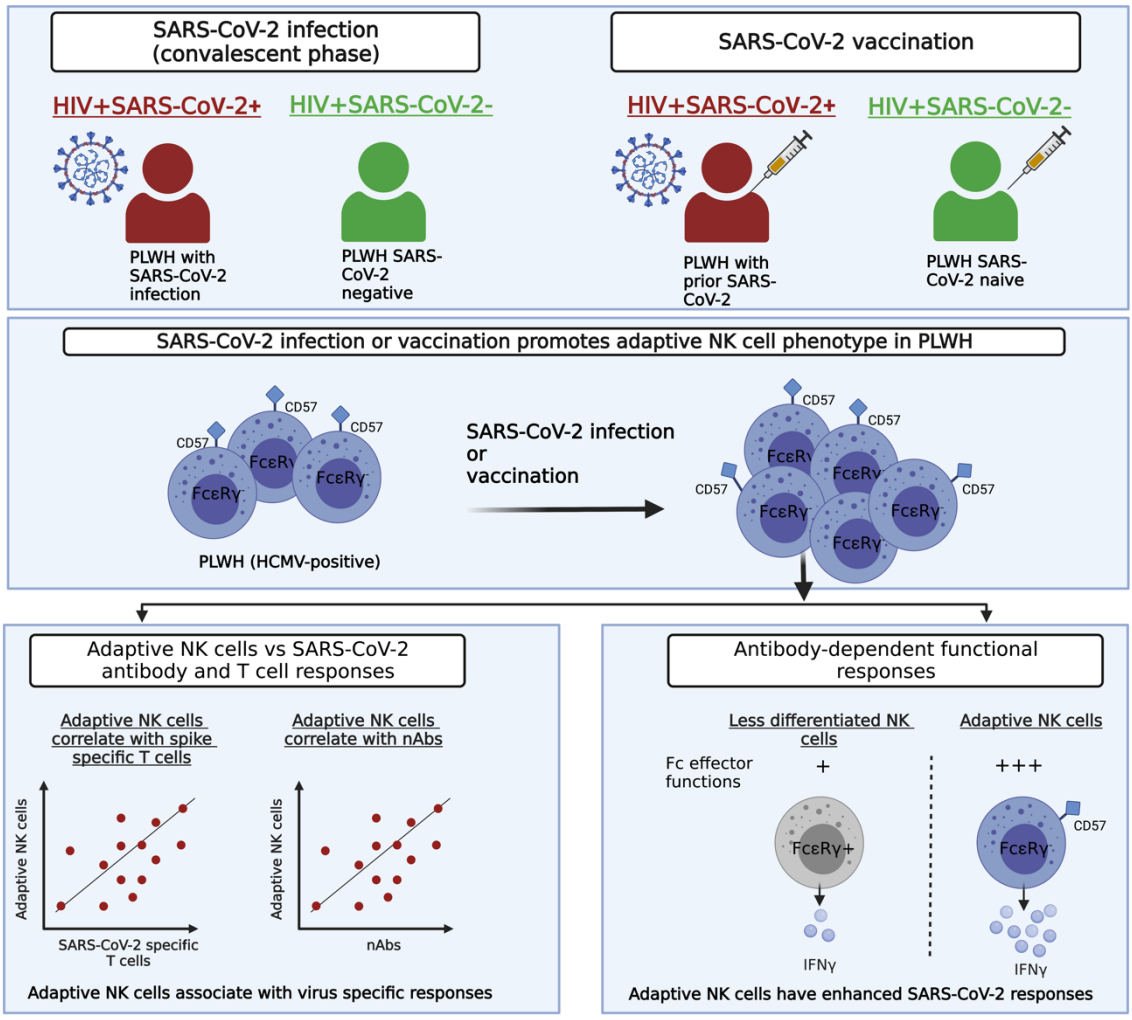
The main limitation of our vaccine study is that our cohort comprised individuals with a mixture of SARS-CoV-2 vaccine types, and due to limited numbers, our analysis couldn't fully dissect responses according to a specific vaccine platform. Nonetheless, in a small number of patients who received mRNA vaccines, a comparable response was observed between PLWH and HIV-negative controls. Similarly, equivalent T-cell responses were detected following ChAdOx1 nCoV-19 vaccine in PLWH and HIV-negative individuals (184). In regard to responses

to different vaccine platforms, previous work has shown that the adenovirus-based platforms induce a higher T-cell response (compared to mRNA) (209,384,385), and the use of heterologous boosting strategies has been shown to expand the quantity and breadth of T-cell immunity and improve the serological response in PLWH (384,386–388). Therefore, it is possible that different vaccine platforms and/or heterologous vs homogenous combinations could lead to different magnitude T-cell responses in our cohort. However, the lack of adequate data makes it challenging to recommend the best vaccine approach to induce a more effective, resilient, and durable response in PLWH. Another limitation is that the current analysis provides an overview of responses after up to three vaccine doses, and therefore further work is required to assess the durability and persistence of these responses against subvariants and additional vaccine doses. Additionally, given the limited number of participants with breakthrough infections in our cohort, any associations between the magnitude of responses and breakthrough infections are limited. Future studies in larger cohorts are necessary to evaluate the contribution of T-cell responses in vaccine-mediated protection/breakthrough infection in PLWH. Such knowledge will help identify PLWH who may be more vulnerable to circulating virus with implications for prioritisation for additional boosters.

Collectively, these results provide benchmark data into the facets of adaptive immunity against SARS-CoV-2 infection and/or vaccination in the setting of treated HIV-1 infection, showing induction of robust T-cell responses against SARS-CoV-2.

Chapter 6: NK cell responses during SARS-CoV-2 infection and vaccination in PLWH.

Chapter 6 graphical abstract.



Chapter 6 written abstract.

The reduced neutralisation capacity observed in PLWH following SARS-CoV-2 vaccination highlighted the need to better understand other compenent of SARS-CoV-2 immunity in this patient group. NK cell subsets with adaptive properties are emerging as regulators of vaccine-induced T- and B-cell responses and are specialised towards antibody-dependent functions contributing to SARS-CoV-2 control. However, the impact of SARS-CoV-2 infection and/or vaccination shaping NK cell function and repertoire in PLWH has remained unexplored. In this chapter, I performed a detailed assessment of NK cells, including their phenotypic changes and functional capacity in PLWH following SARS-CoV-2 infection or vaccination. This analysis is discussed in relation to T-cell and antibody responses. These data show that SARS-CoV-2 infection skews NK cells towards a more differentiated/adaptive $CD57^{+}FcεRIγ^{-}$ phenotype in PLWH. A similar NK cell subset was induced following vaccination in PLWH SARS-CoV-2 naïve. Assessment of antibody-mediated NK cell function demonstrated robust and durable NK cell responses to spike glycoprotein elicited by primary infection or vaccination in PLWH. These responses were enriched in adaptive NK cell subsets. The presence of adaptive NK cells was associated with a higher magnitude of cellular and humoral responses, suggesting that features of adaptive NK cells can be effectively engaged after SARS-CoV-2 infection or vaccination in PLWH.

Chapter 6

6.1 Introduction.

As shown in Chapter 5, some PLWH, despite effective ART, generate a poorer neutralising antibody response to vaccination compared to HIV-negative controls (183,325,353,389). While T cell-mediated immunity may provide some degree of protection, evaluating other components of immune responses that can be activated to generate broad and durable responses in PLWH could be beneficial for future vaccine strategies.

NK cells provide early host defence against SARS-CoV-2 infection (187–189,193,194,206). They can directly eliminate virus-infected cells and produce cytokines and chemokines that can mediate antiviral effects and stimulate robust adaptive responses, facilitating viral control (62). In COVID-19 disease, some studies have shown an association between specific NK cell pro-inflammatory phenotypes and disease severity (187–189,195,390–392). Notably, the depletion of NK cells and the impaired NK cell function during acute SARS-CoV-2 infection have been associated with worse disease outcomes, indicating that SARS-CoV-2 infection can affect NK cell redistribution and effector function (188,189,390). The contribution of NK cells to SARS-CoV-2 immunity is supported by studies showing that NK cell-mediated Fc-dependent functions and ADCC responses can provide functional antiviral activity and suppress viral replication (187,194,195,393–395). Anti-SARS-CoV-2 antibodies, not restricted to those binding to the spike protein, have been shown to induce NK cell-mediated ADCC responses following natural infection (394,395). Similarly, SARS-CoV-2 vaccination mediated strong NK cell activation in HIV-negative recipients

(393,396). Polyfunctional antibody responses with the capacity to mediate strong ADCC responses have been linked to favourable COVID-19 disease outcomes (201,397) and vaccine protection in non-human primates (196,347,398). These ADCC responses decay slowly after natural infection or vaccination, persisting beyond neutralising responses and, therefore, may be important for long-term immunity (202,203,396,397).

Adaptive NK cells are expanded in HIV-1 infection and have been shown to have preserved ADCC capacity (98,106,124,264); however, the additional impact of SARS-CoV-2 infection/or vaccination in the adaptive NK cell compartment in PLWH is poorly defined. Given the unique immunological features of adaptive NK cells, including enhanced Fc-dependent effector functions and reduced ability for the immunoregulatory killing of autologous activated T cells (39,48,49), adaptive NK cells could augment humoral and T-cell responses to SARS-CoV-2 and/or provide a complementary layer of protection through antibodies that can mediate ADCC, especially in PLWH with suboptimal neutralising antibody responses. Adaptive/memory-like NK cells have been reported in patients with COVID-19 disease, suggesting that these NK cell subpopulations may arise in response to SARS-CoV-2 infection (189,256,400,401). Interestingly, genetic deletion of NKG2C is a risk factor for severe SARS-CoV-2 infection, underscoring the potential protective role of adaptive NK cells in SARS-CoV-2 infection (207).

Here I performed a comprehensive assessment of NK cell phenotypic changes, evaluated their relationship to T-cell and antibody measures and breadth, and

assessed their Fc-dependent responses to spike glycoprotein in PLWH in the convalescent phase of SARS-CoV-2 infection and post-vaccination.

6.2 Results.

6.2.1 Study cohort.

To assess NK cell responses following SARS-CoV-2 infection and post-vaccination, I used PBMC samples from a subset of participants included in the study presented in Chapter 5. Given the reduced antibody responses observed in PLWH and to avoid any confounders (e.g. HCMV co-infection, age and gender), this analysis was focused on PLWH. In this study, n=30 convalescent PLWH (prior SARS-CoV-2) and n=28 PLWH with no prior exposure (SARS-CoV-2 naïve) were included. SARS-CoV-2 naïve PLWH were screened for SARS-CoV-2 seropositivity and were found to be IgG seronegative for spike and nucleoprotein. The majority of PLWH in both groups were on ART (94% of prior SARS-CoV-2 and 89% of SARS-CoV-2 naïve) and had a similar median $CD4^+$ T-cell count (prior SARS-CoV-2: 560 cells/mm^3 and SARS-CoV-2 naïve: 573 cells/mm^3) and median CD4:CD8 ratio (prior SARS-CoV-2: 0.92 and SARS-CoV-2 naïve: 1.02). Two PLWH with prior SARS-CoV-2 and three PLWH SARS-CoV-2 naïve had detectable HIV-1 viraemia at the time of recruitment. A subset of these participants with prior SARS-CoV-2 infection (n=12) or SARS-CoV-2 naïve (n=19) were followed up longitudinally after one, two, or three doses of SARS-CoV-2 immunisation. All participants included in this analysis were HCMV-seropositive. Further details about the cohort of this study are included in **Table 6.1**.

Table 6.1. Cohort Demographics and Clinical Characteristics.

			SARS-CoV-2 infection		SARS-CoV-2 vaccination	
			SARS-CoV-2 negative	SARS-CoV-2 positive	SARS-CoV-2 negative	SARS-CoV-2 positive
Group size	Number of participants	n	28	30	19	12
	Vaccine dose	1st dose	-	-	18	11
		2nd dose	-	-	19	8
		3rd dose	-	-	14	10
HCMV co-infection		n (%)	28 (100%)	30 (100%)	19 (100%)	12 (100%)
Time interval	Days post infection, median (range)	Days post symptoms (DPSO),	-	148 (46-232)	-	-
	Days post-vaccination, median (range)	1st dose	-	-	20 (8-60)	23 (9-85)
		2nd dose	-	-	32 (7-218)	23 (5-193)
		3rd dose	-	-	55 (6-199)	64 (7-140)
Vaccine type	Vaccine, n (AZ | Moderna | Pfizer)	1st dose			7 | 1 |10	3 | 0 | 8
		2nd dose			8 | 0 |11	2 | 0 | 6
		3rd dose			0 | 1 |13	0 | 1 | 9
Risk factors and demographics	Age, median (range)	(years)	46 (30-65)	51 (31-72)	51 (35-65)	47 (33-72)
	Sex	Gender (n) female:male	2:26	5:25	1:18	1:11
	Ethnicity, n (%)	White	21 (75%)	21 (70%)	15 (79%)	5 (41%)
		BAME	7 (25%)	9 (30%)	4 (21%)	7 (59%)
HIV-1 parameters	On ART treatment	n (%)	25 (89%)	28 (94%)	18 (95%)	11 (92%)
	HIV-1 viral load (copies/ml)	Suppressed n (%)	25 (89%)	28 (94%)	16 (84%)	10 (83%)
		Viremic n (%)	3 (11%)	2 (6%)	3 (16%)	2 (17%)
		HIV-1 viral load; viremic patients only)	132-2.5x10^6	1549-2.5x10^6	437-0.8x10^6	257-0.1x10^5
	$CD4^+$ T-cell count median (range)	$CD4^+$ T-cell count	573 (20-1029)	560 (92-1110)	490 (20-1029)	591 (100-967)
		CD4:CD8 ratio	1.02 (0.03-2.26)	0.92 (0.12-2.54)	0.94 (0.03- 2.26)	0.82 (0.21-2.13)
Pre-existing conditions	n (%)	None	24 (85.5)	21 (70%)	15 (79%)	9 (76%)
		Diabetes	0 (0%)	4 (13%)	0 (0%)	2 (16%)
		Hypertension	1 (3.5%)	5 (16%)	0 (0%)	0 (0%)
		Respiratory disease	3 (11%)	2 (6%)	0 (0%)	0 (0%)
		Liver disease	0 (0%)	1 (3%)	0 (0%)	0 (0%)
		Weakened immune system[1]	0 (0%)	0 (0%)	4 (21%)	1 (8%)

[1] Participants who had organ transplantation, including renal or liver transplantation.

6.2.2 Increased frequencies of adaptive NK cells following SARS-CoV-2 infection in PLWH

NK cell depletion and/or subset redistribution have been previously reported during acute SARS-CoV-2 infection in the general population, but these changes largely recover in the convalescent phase (189,390,402,403). I, therefore, analysed the percentage of total NK cells and the main NK cell subsets ($CD56^{bright}$, $CD56^{dim}$, and $CD56^{neg}CD16^{+}$ NK cells) in the study groups. No significant changes were detected in the total NK cell frequencies or frequencies of main NK cell subsets ($CD56^{bright}$, $CD56^{dim}$, and $CD56^{neg}CD16^{+}$) in PLWH with or without prior SARS-CoV-2 infection **(Figure. 6.1A-E).** Similarly, the percentage of activated NK cells ($CD38^{+}$NK cells) or cytotoxic $CD56^{bright}$ NK cells ($CD56^{bright}GranzymeB^{+}$) were comparable between the study groups **(Figure. 6.1F&G).**

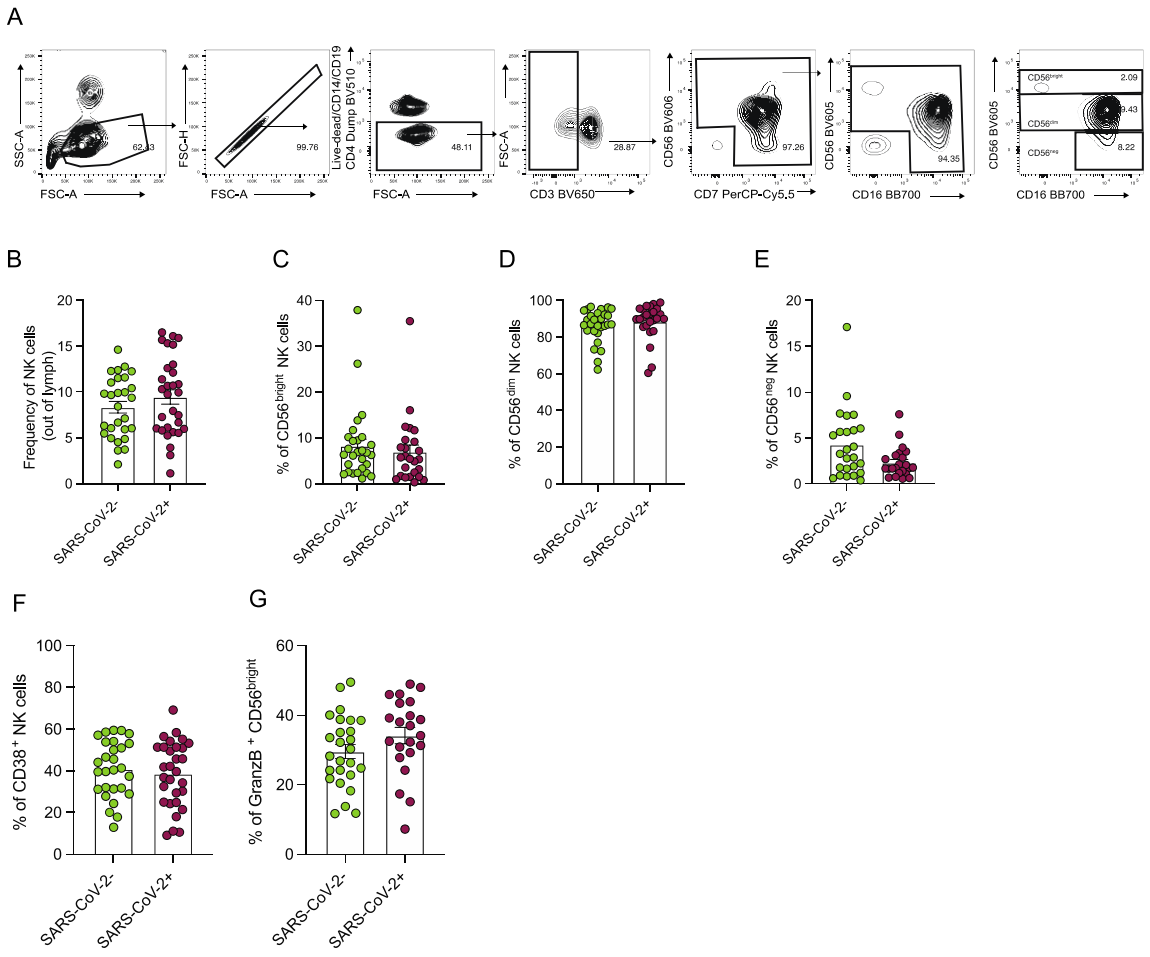


Figure 6.1. Phenotypic assessment of NK cells in convalescent SARS-CoV-2 infection in PLWH

(A) Representative flow cytometric plots showing the gating used to identify NK cell subsets. **(B)** Summary analysis of the frequency of total NK cells out of lymphocytes in SARS-CoV-2 negative (n=28, green) and SARS-CoV-2-positive (n=30, red) PLWH. Frequencies of **(C)** $CD56^{bright}$, **(D)** $CD56^{dim}$, and **(E)** $CD56^{neg}$ NK cells in the study groups. The percentage of **(F)** $CD38^{+}$ NK cells and **(G)** $GranzymB^{+}CD56^{bright}$ NK cells in both study groups. Significance determined by two-tailed Mann−Whitney U test.

The degree of NK cell differentiation was then assessed by evaluating the expression levels of CD57. A higher expression of CD57 (denoting maturation) was observed in PLWH with prior SARS-CoV-2 infection compared to SARS-CoV-2 naïve individuals **(Figure. 6.2A&B).** Further phenotypic characterisation of the $CD57^{+}$, compared to their $CD57^{-}$ NK cell counterparts, demonstrated enrichment of several adaptive NK cell markers within the same donors, including lower levels of PLZF and FcεRIγ, and higher expression of NKG2C and CD2 **(Figure. 6.2C).** Specifically, an increased frequency of $FcεRIγ^{-}CD57^{+}$NK cells, and a trend towards higher percentage of $NKG2C^{+}CD57^{+}$NK cells, were observed in PLWH SARS-CoV-2-positive compared to SARS-CoV-2 naïve donors (**Figure. 6.2D-F).** This indicated an increased frequency of adaptive NK cells, especially FcεRIγ-deficient subsets, which are often associated with HCMV infection and can expand upon exposure to antibody-coated targets and/or cross-linking CD16 receptor (106,256,404). In this respect, there was a non-significant trend towards lower CD16 expression, measured by CD16 MFI, in PLWH with prior SARS-CoV-2 infection compared to SARS-CoV-2 naïve individuals **(Figure. 6.2G)**.

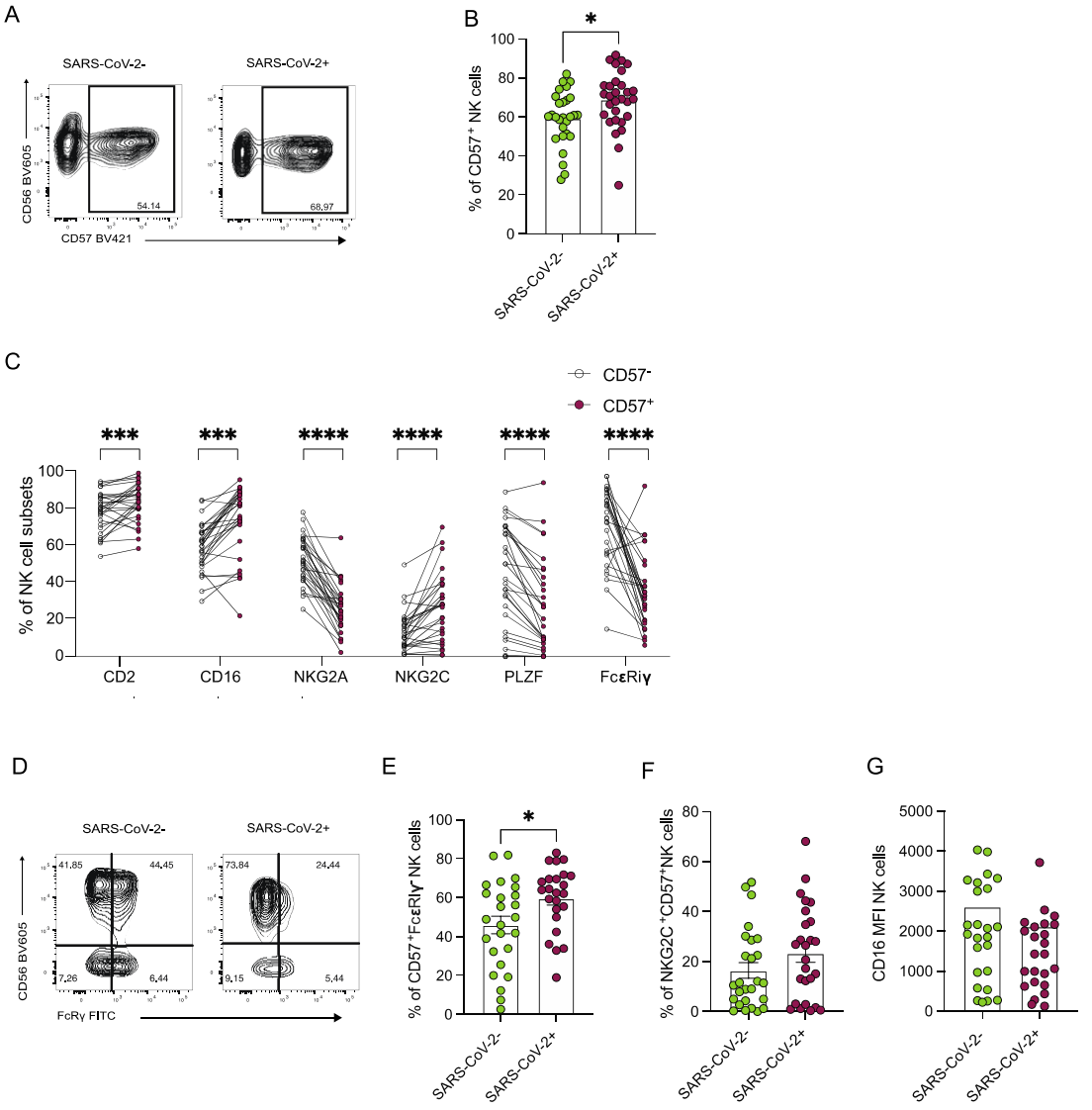


Figure 6.2. Increased frequencies of differentiated/adaptive NK cells in PLWH recovered from SARS-CoV-2 infection.

(A) Representative flow plots and (**B)** summary analysis of the percentage of CD57⁺ NK cells in SARS-CoV-2-positive and -negative individuals. (**C)** Paired analysis showing the expression of CD2, CD16, NKG2A, NKG2C, PLZF and FcεRIγ markers within CD57⁺ (red) and CD57⁻ (white) NK cells in SARS-CoV-2-positive PLWH. (**D)** Representative flow plots and **(E)** summary analysis of the percentage of FcεRIγ⁺CD57⁺ NK cells. (**F)** The percentage of NKG2C⁺ CD57⁺NK cells. (**G)** CD16 MFI in the total NK cells. Significance determined by two-tailed Mann−Whitney U test or Wilcoxon matched-pairs signed rank test, *p < 0.05, **p < 0.01, ***p < 0.001, ****p<0.0001.

The relationship between FcεRIγ^{-}CD57^{+}NK cells, antibody levels and circulating inflammatory markers was assessed in our cohort. The percentage of adaptive NK cells (FcεRIγ^{-}CD57^{+}NK cells) correlated positively with HCMV IgG titres (r = 0.5174, p = 0.0114) and levels of CXCL10 (IP-10) (r = 0.5648, p = 0.0383) in PLWH with prior SARS-CoV-2 infection but did not correlate with SARS-CoV-2 S or N IgG binding titres **(Figure. 6.3A-D)**; the relationship between HCMV IgG titres and FcεRIγ^{-}CD57^{+}NK cell frequencies were similar in SARS-CoV-2 naïve individuals but did not reach statistical significance **(Figure. 6.3E)**. Overall, no significant differences were observed in the levels of HCMV IgG titres and CXCL10 between the two groups **(Figure. 6.3F&G)**. These data suggest that SARS-CoV-2 exposure increases the frequency of adaptive NK cells (FcεRIγ^{-} CD57^{+}) in PLWH, as previously described in the general population (189,256,391,400), and this could be partly driven by HCMV co-infection/inflammation (189,256,391,400).

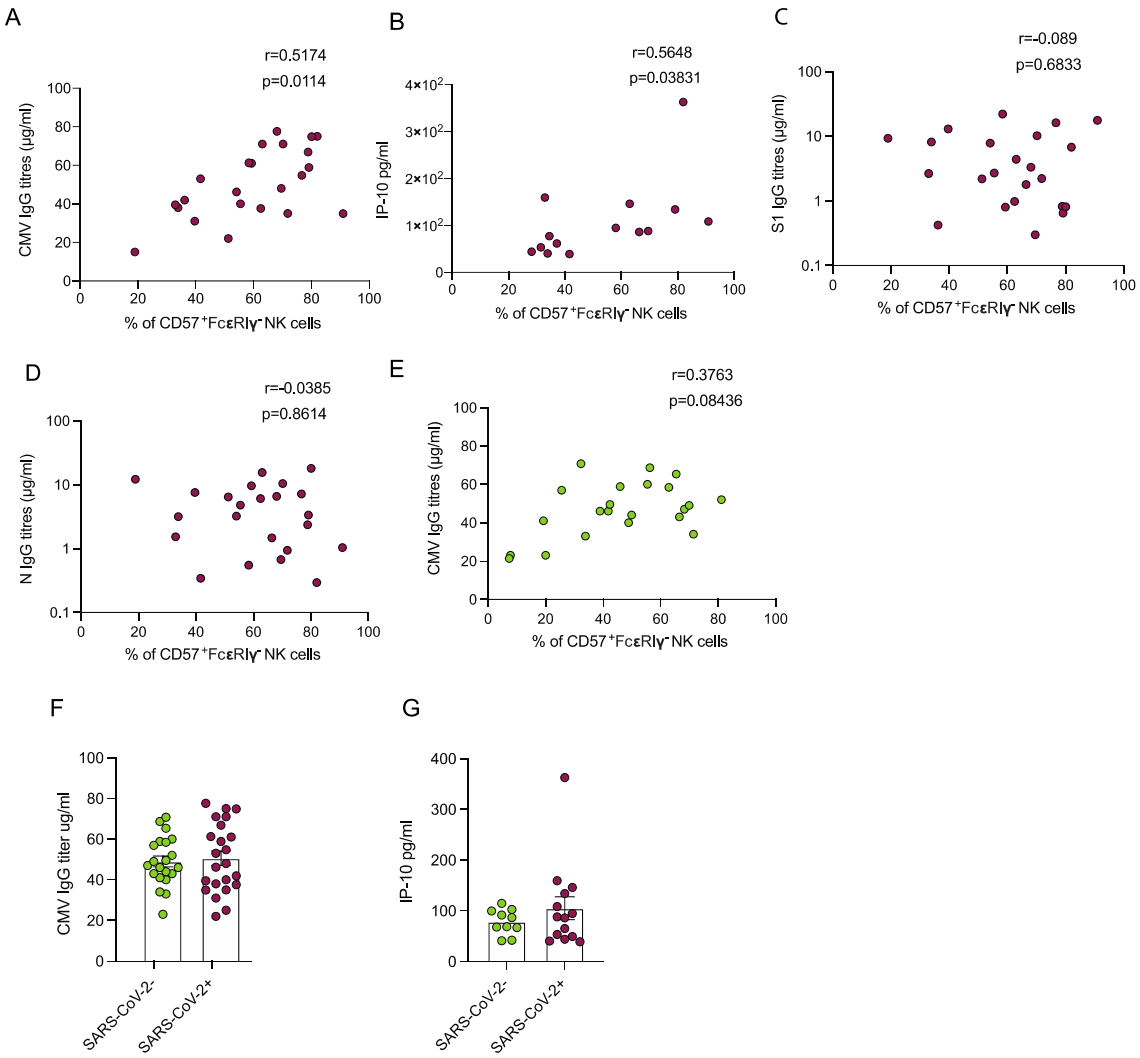


Figure 6.3. Increased frequencies of differentiated/adaptive NK cells in PLWH recovered from SARS-CoV-2 infection.

Correlation analysis between the frequency of FcεRIγ⁺CD57⁺ NK cells and (**A)** CMV IgG titres, (**B)** plasma level of IP10, (**C)** S1 IgG titres, and **(D)** N IgG titres in convalescent PLWH. **(E)** Correlation analysis between the frequency of FcεRIγ⁺CD57⁺ NK cells and CMV IgG titres in SARS-CoV-2 negative PLWH. Levels of (**F)** CMV IgG titres and (**G)** plasma IP10 in the study groups. Significance determined by two-tailed Mann−Whitney U test. The non-parametric Spearman test was used for correlation analysis (two-tailed).

Given the ability of NK cells to modulate T cells and antibody responses, the association between adaptive NK cell subsets and virus-specific responses was then evaluated (84,101). A positive correlation was observed between the percentage of FcεRIγ^{-}CD57^{+} NK cells and the magnitude of spike-specific T-cell responses, measured by IFN-γ ELISpot (r = 0.5519, p = 0.0286), and spike-specific CD4^{+} T cells, which I have previously shown to dominate SARS-CoV-2 specific T-cell responses in convalescent PLWH (see Chapter 5) (r = 0.6818, p = 0.0251) (**Figure. 6.4A&B)**. Notably, PLWH with higher frequencies of FcεRIγ^{-} CD57^{+} NK cells had more potent neutralisation levels (ID_{50}>1000) (**Figure. 6.4C)**. Taken together, these data suggest that SARS-CoV-2 infection leads to increased NK cell maturation and adaptiveness in convalescent PLWH, which associate with humoral and cellular SARS-CoV-2 specific responses.

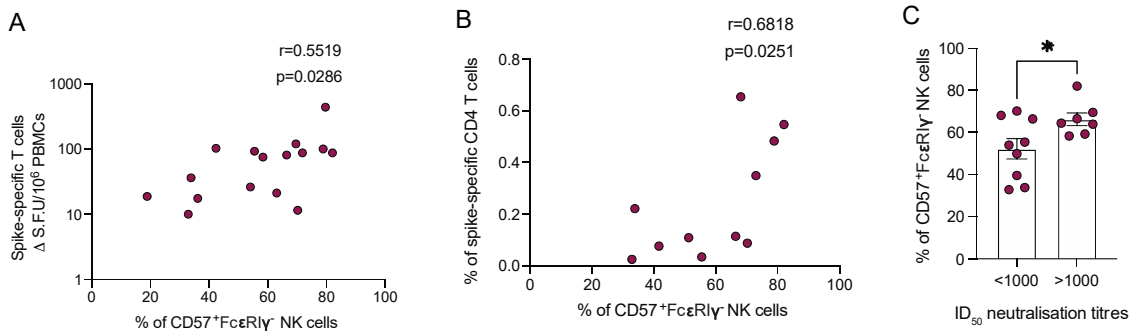
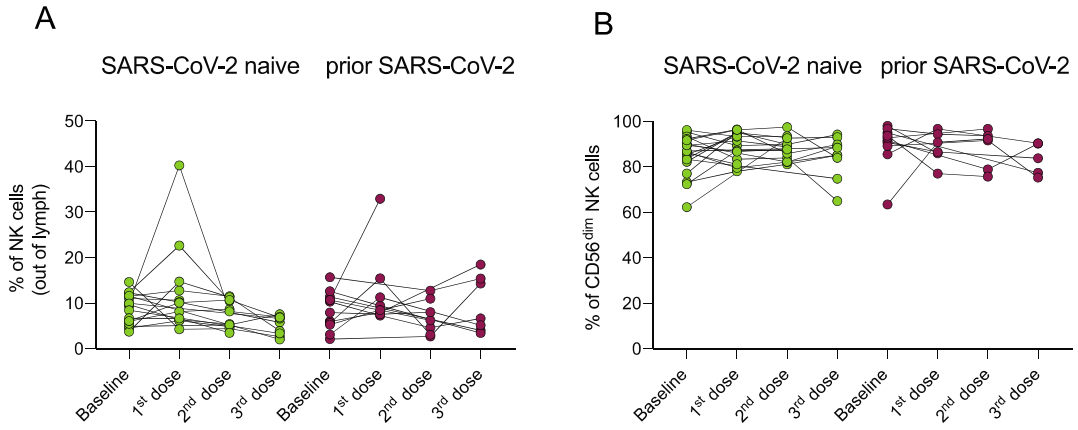


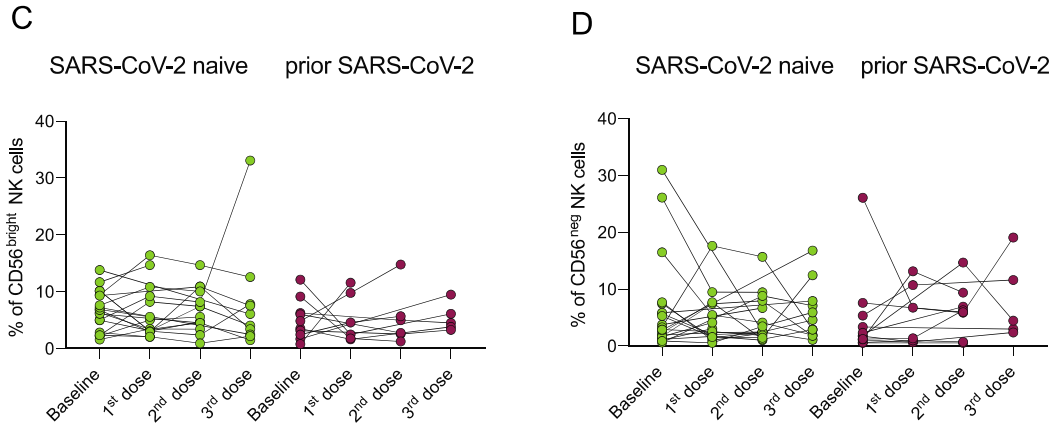
Figure 6.4. Correlation analysis between adaptive NK cells and SARS-CoV-2 specific responses in the convalescent phase.

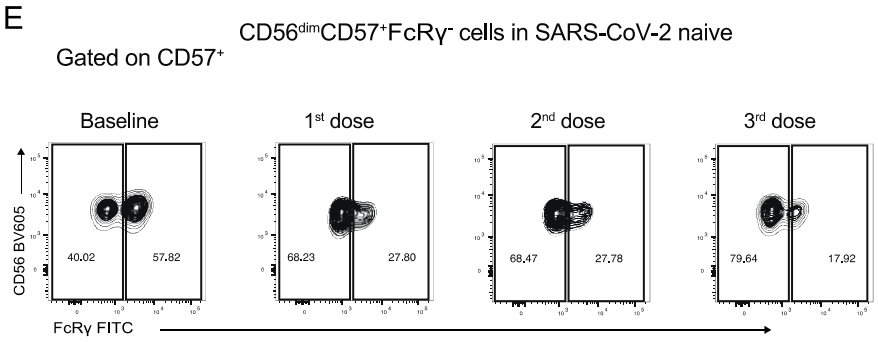
Correlation between the frequency of FcεRIγ^{+}CD57^{+} NK cells and **(A)** total spike-specific T cells or **(B)** spike-specific CD4^{+} T cells in convalescent PLWH. **(C)** The frequencies of FcεRIγ^{+}CD57^{+} NK cells in convalescent PLWH according to their neutralisation levels. Significance determined by two-tailed Mann−Whitney U test,* p<0.05.

6.2.3 Longitudinal assessment of NK cells in PLWH following SARS-CoV-2 vaccination.

The increased proportion of differentiated adaptive NK cells following natural SARS-CoV-2 infection prompted us to evaluate whether similar changes to the NK cell pool are observed following SARS-CoV-2 vaccination. A longitudinal analysis of the NK cell frequencies and phenotype was performed in a subset of PLWH with or without prior SARS-CoV-2 infection following vaccination. There was no significant difference in the frequency of total NK cells, or the percentage of $CD56^{bright}$, $CD56^{dim}$, and $CD56^{neg}CD16^{+}$ NK cell subsets, following SARS-CoV-2 vaccination (post- first, -second, and -third dose) in both study groups compared to baseline **(Figure. 6.5A-D).** Further phenotypic evaluation revealed a higher percentage of $Fc\varepsilon RI\gamma^{-}CD57^{+}$ $CD56^{dim}$ NK cells in SARS-CoV-2 naïve individuals following the first dose of vaccine, consistent with changes observed in the convalescent phase of SARS-CoV-2 infection in PLWH (**Figure. 6.5E&F)**.


A
SARS-CoV-2 naive
prior SARS-CoV-2
% of NK cells (out of lymph)
Baseline
1st dose
2nd dose
3rd dose
B
% of CD56dim NK cells


C
SARS-CoV-2 naive
prior SARS-CoV-2
% of CD56bright NK cells
D
% of CD56neg NK cells


E
CD56dimCD57+FcRγ- cells in SARS-CoV-2 naive
Gated on CD57+
Baseline
1st dose
2nd dose
3rd dose
CD56 BV605
FcRγ FITC
40.02
57.82
68.23
27.80
68.47
27.78
79.64
17.92

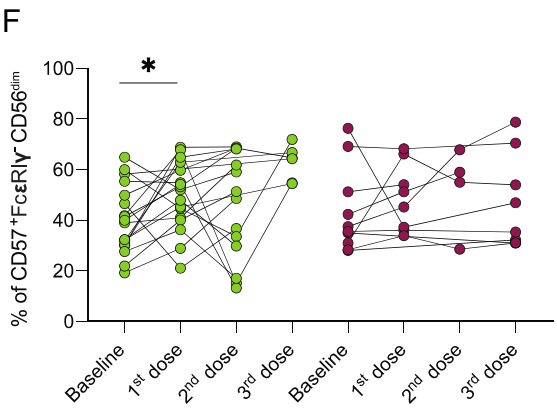

F
*
% of CD57+FcεRIγ- CD56dim

Figure 6.5. Longitudinal assessment of adaptive NK cells following SARS-CoV-2 vaccination in PLWH.

(A) Longitudinal analysis of the frequency of total NK cells in PLWH, with or without prior SARS-CoV-2 infection, at baseline (pre-vaccine) and following first, second, and third dose of vaccine. Longitudinal assessment of the frequencies of (**B)** $CD56^{bright}$, (**C)** $CD56^{dim}$, and (**D)** $CD56^{neg}$ NK cells in the study groups. (**E)** Representative flow plots and (**F)** summary analysis of the percentage $Fc\varepsilon RI\gamma^{+}CD57^{+}$ $CD56^{dim}$ NK cells. Significance determined by Wilcoxon matched-pairs signed rank t test. * $p<0.05$.

Given the potential role of NK cell subsets to modulate the induction of antibody responses (84) and observed associations in convalescent SARS-CoV-2 infection, the phenotypic findings were related to the magnitude of antibody responses. Consistent with previous observations in vaccinated HIV-negative individuals (401), the proportion of $Fc\varepsilon RI\gamma^{-}CD57^{+}$ NK cells correlated positively with vaccine-induced S1 IgG titres after one dose of vaccine in PLWH with prior infection but not in SARS-CoV-2 naïve group (due to the low antibody titres) (**Figure. 6.6A)**; however, after two doses of vaccine, a significant association was observed between $Fc\varepsilon RI\gamma^{-}CD57^{+}$ NK cells and S1 IgG titres in PLWH SARS-CoV-2 naïve (r = 0.6818, p = 0.0006) **(Figure. 6.6B)**. Similarly, a positive correlation was observed between $Fc\varepsilon RI\gamma^{-}CD57^{+}$ NK cells and neutralising antibody titres after two doses of vaccine in SARS-CoV-2 naïve PLWH (r = 0.6641, p = 0.0007) but not after the first dose **(Figure. 6.6C&D)**. Such association was not observed in PLWH with prior infection after one or two doses of vaccine (**Figure. 6.6C&D)**. With regards to cellular responses, spike-specific T-cell responses correlated positively with the proportion of $Fc\varepsilon RI\gamma^{-}CD57^{+}$ NK

cells after one dose of vaccine in PLWH with prior infection but not in SARS-CoV-2 naïve individuals; however, a trend towards a positive association was observed after two doses of vaccine in SARS-CoV-2 naïve subjects (**Figure. 6E&F)**. Interestingly, a positive correlation was observed between the percentage of FcεRIγ^{-}CD57^{+} NK cells and T_{FH} cell frequencies in PLWH SARS-CoV-2 naïve after two doses, suggesting that these cells may influence the development of nAbs through less negative regulation of T_{FH} cell responses supplying help to B cells (101,399) (**Figure. 6.6G)**. Supporting this notion, a higher proportion of FcεRIγ^{-}CD57^{+} NK cells was observed in PLWH with higher frequencies of spike-specific memory B cells (>0.5%) **(Figure. 6.6H)**. Collectively, these data suggest that one dose of SARS-CoV-2 vaccination induces expansion of adaptive FcεRIγ^{-}CD57^{+} NK cells in PLWH with no history of SARS-CoV-2 exposure, and the induction of these adaptive NK cell subsets is associated with a higher magnitude of humoral and cellular responses following two doses of vaccine.

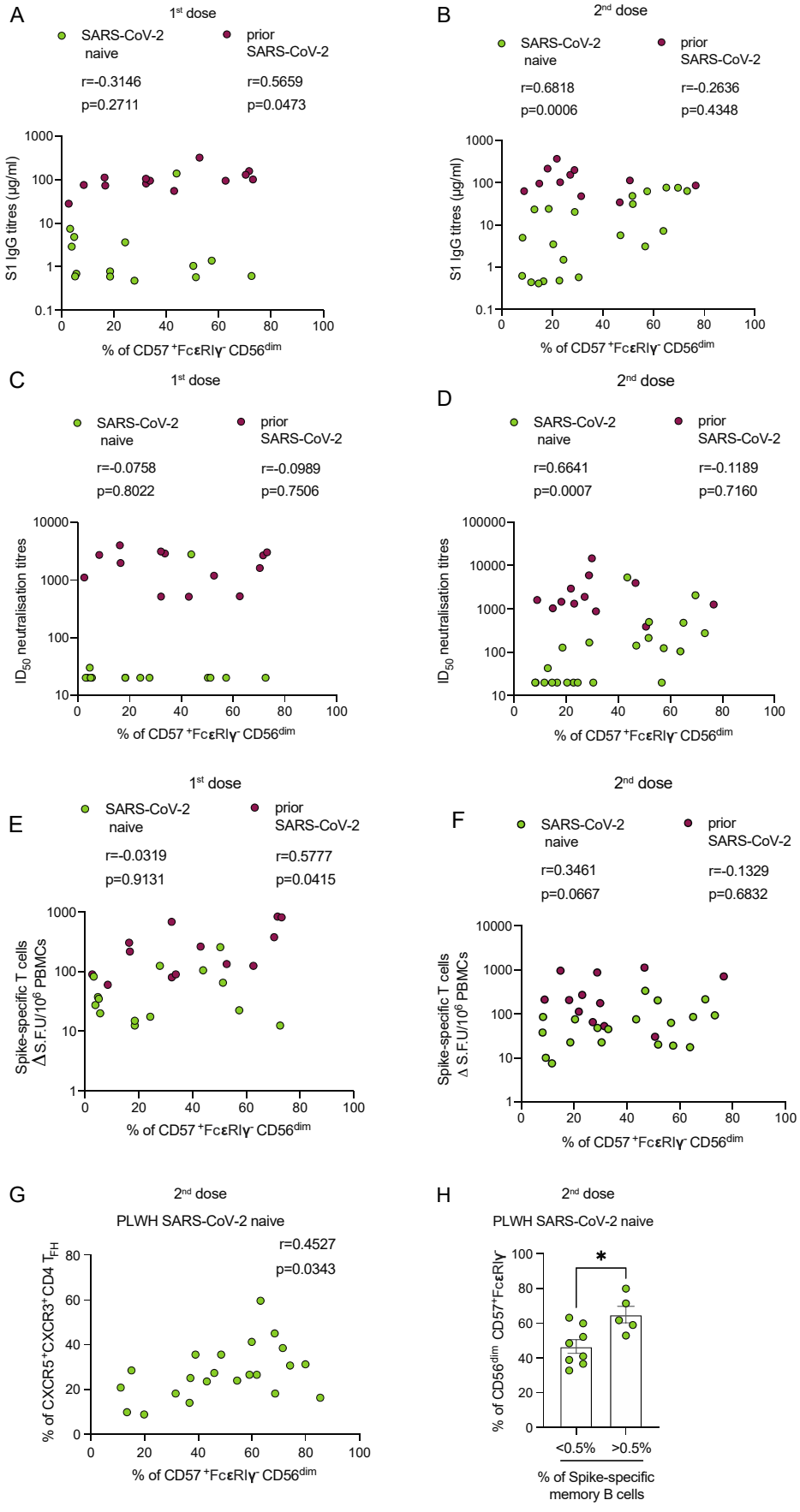

A
1st dose
SARS-CoV-2 naive
r=-0.3146
p=0.2711
prior SARS-CoV-2
r=0.5659
p=0.0473
S1 IgG titres (µg/ml)
% of CD57+FcεRIγ- CD56dim
B
2nd dose
SARS-CoV-2 naive
r=0.6818
p=0.0006
prior SARS-CoV-2
r=-0.2636
p=0.4348
S1 IgG titres (µg/ml)
% of CD57+FcεRIγ- CD56dim
C
1st dose
SARS-CoV-2 naive
r=-0.0758
p=0.8022
prior SARS-CoV-2
r=-0.0989
p=0.7506
ID50 neutralisation titres
% of CD57+FcεRIγ- CD56dim
D
2nd dose
SARS-CoV-2 naive
r=0.6641
p=0.0007
prior SARS-CoV-2
r=-0.1189
p=0.7160
ID50 neutralisation titres
% of CD57+FcεRIγ- CD56dim
E
1st dose
SARS-CoV-2 naive
r=-0.0319
p=0.9131
prior SARS-CoV-2
r=0.5777
p=0.0415
Spike-specific T cells Δ S.F.U/10^6 PBMCs
% of CD57+FcεRIγ- CD56dim
F
2nd dose
SARS-CoV-2 naive
r=0.3461
p=0.0667
prior SARS-CoV-2
r=-0.1329
p=0.6832
Spike-specific T cells Δ S.F.U/10^6 PBMCs
% of CD57+FcεRIγ- CD56dim
G
2nd dose
PLWH SARS-CoV-2 naive
r=0.4527
p=0.0343
% of CXCR5+CXCR3+CD4 TFH
% of CD57+FcεRIγ- CD56dim
H
2nd dose
PLWH SARS-CoV-2 naive
*
% of CD56dim CD57+FcεRIγ-
<0.5%
>0.5%
% of Spike-specific memory B cells

Figure 6.6. Correlation analysis between adaptive NK cells and SARS-CoV-2 specific responses following vaccination.

Correlation analysis between the frequency of FcεRIγ$^+$CD57$^+$ NK cells and S1 IgG titres after (**A)** one dose or (**B)** two doses of vaccine in PLWH with or without prior infection. Correlation of FcεRIγ$^+$CD57$^+$ NK cells with nAb titres after (**C)** one dose or (**D)** two doses of vaccine. Correlation of FcεRIγ$^+$CD57$^+$ NK cells with spike-specific T-cell responses after (**E)** one dose or (**F)** two doses of vaccine. **(G)** Correlation of the percentage of FcεRIγ$^+$CD57$^+$ NK cells and CXCR3$^+$CXCR5$^+$$T_{FH}$ cells after two doses of vaccine. **(H)** Comparison of the percentage of FcεRIγ$^+$CD57$^+$ NK cells in SARS-CoV-2 naïve PLWH according to their levels of Spike-specific memory B cells. The threshold was set to 0.5% Spike-specific MBCs. Significance determined by two-tailed Mann−Whitney U test. The non-parametric Spearman test was used for correlation analysis (two-tailed).* $p<0.05$.

6.2.4 Antibodies induced by SARS-CoV-2 vaccination can trigger antibody-mediated NK cell responses in PLWH.

Next, I investigated the functional consequences of the observed phenotypic differences in NK cell subsets of PLWH with or without prior SARS-CoV-2 infection following vaccination. Given the importance of ADCC in the control of SARS-CoV-2 (393,397), I established an assay to analyse the Fc receptor-dependent activation of NK cells in response to anti-SARS-CoV-2 antibody stimulation (**Chapter 2, section 2.3.4)**. PBMCs from PLWH were cultured with plate-bound spike glycoprotein in the presence of autologous pre- and post-vaccination serum samples. NK cell activation was measured in response to autologous serum collected at baseline (pre-vaccine), post-first, -second, and -third dose plus immobilised spike glycoprotein for each study participant (SARS-CoV-2 naïve n=14, prior SARS-CoV-2 n=12). Pre-pandemic (serum samples

collected before 2018) or pooled serum (pooled serum after two doses of vaccine) were used as controls. PLWH with prior SARS-CoV-2 infection had a greater magnitude of antibody-dependent NK cell activation, measured by IFN-γ, TNF-α and CD107 expression, at baseline (pre-vaccine) compared to SARS-CoV-2 naïve individuals (**Figure. 6.7A-F**). The frequencies of IFN-γ^+, TNF-α^+, and CD107a^+ NK cells were further increased after one dose of vaccine in PLWH with prior infection and after two doses of vaccine in PLWH without prior SARS-CoV-2 infection (**Figure. 6.7A-F**). Given the considerable heterogeneity in the magnitude of the observed responses to autologous serum in both groups, these responses were related to the pooled serum responses. NK cell responses to autologous serum after two doses of vaccine were comparable in magnitude to responses detected after stimulation with pooled serum (**Figure. 6.7A-F**), suggesting that the differences in responses within individuals were not solely influenced by antibody levels, but could also reflect variations in the NK cell subpopulations following vaccination.

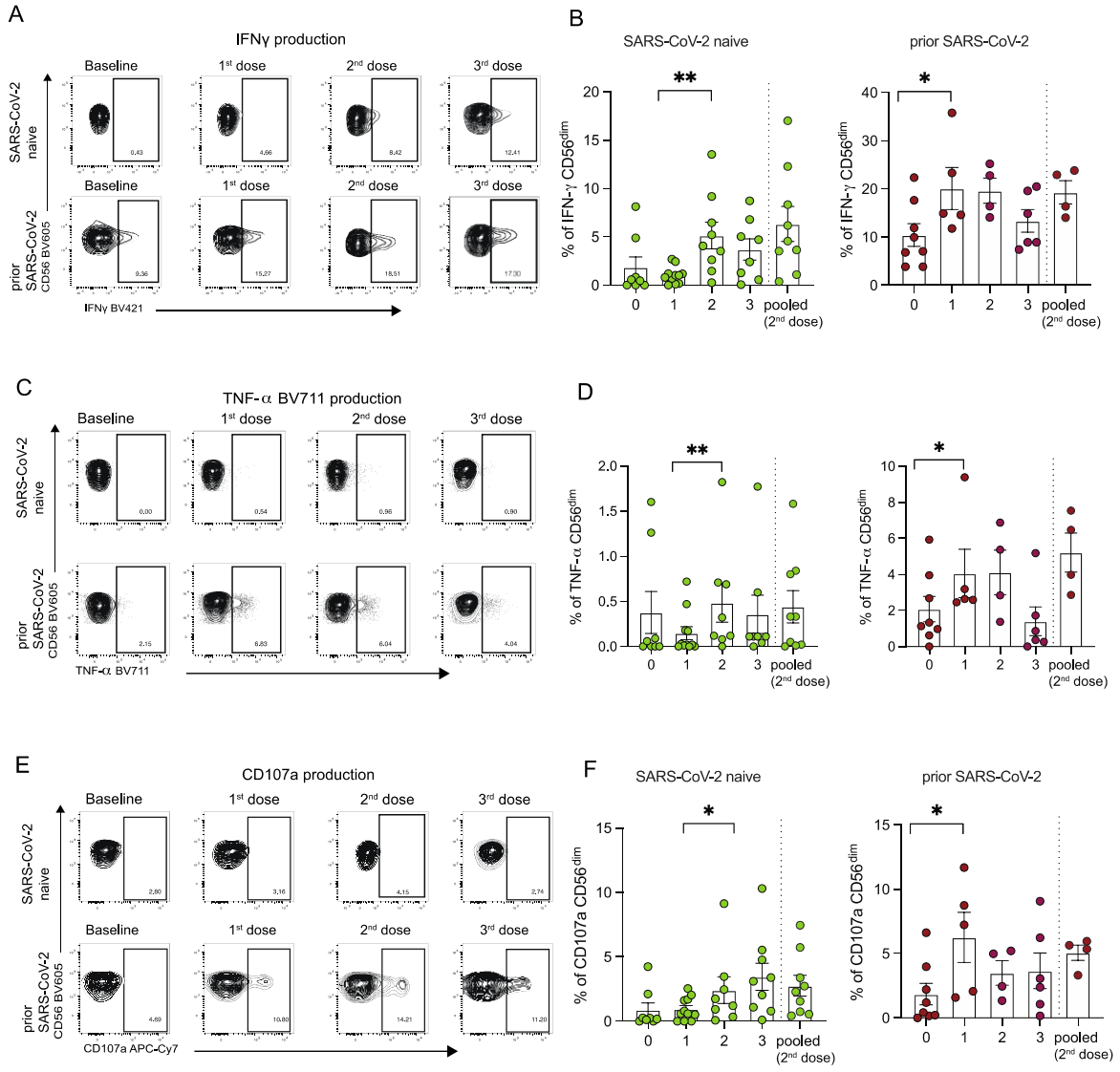


Figure 6.7. Antibody-dependent NK cell responses following SARS-CoV-2 vaccination in PLWH.

(A) Representative plots and (**B)** cross-sectional analysis of t IFN-γ^{+} CD56^{dim} NK cells from PLWH, with or without prior SARS-CoV-2 infection, at baseline (pre-vaccine) and following each dose of vaccine. (SARS-CoV-2 naïve: n=14 baseline, n=9 first dose, n=12 second dose, n=8 third dose; prior SARS-CoV-2 n=12 baseline, n=7 first dose, n=5 second dose, n=7 third dose). (**C)** Representative plots and **(D)** summary analysis of frequencies of TNF-α^{+} CD56^{dim} NK cells. (**E)** Representative flow cytometric plots and **(F)** cross-sectional analysis of frequencies of CD107a^{+} CD56^{dim} NK cells. Significance determined by two-tailed Mann−Whitney U test.* p<0.05, ** p<0.01

Next, the evolution of these responses following SARS-CoV-2 vaccination was examined in longitudinal samples (SARS-CoV-2 naïve n=14, prior SARS-CoV-2 n=12). The frequencies of NK cells producing IFN-γ in response to post-first dose serum were significantly higher than in response to pre-vaccination (baseline), and these responses were further increased post-second dose, reaching a plateau post-third dose in SARS-CoV-2 naïve individuals (**Figure. 6.8A)**. Unlike IFN-γ, NK cell degranulation, measured by CD107a, and TNF-α production were induced only after two doses of vaccine in SARS-CoV-2 naïve individuals and was further boosted by a third dose (**Figure. 6.8B&C)**. PLWH with prior SARS-CoV-2 infection demonstrated higher IFN-γ, TNF-α and CD107a responses at baseline, with a boosting effect observed only after the first dose (**Figure. 6.8A-C)**. In keeping with the observed changes in NK cell function following vaccination, CD16 expression, measured by the median MFI, was lower in response to post-second or -third dose serum compared to baseline in PLWH with no prior SARS-CoV-2 infection and following the first dose in PLWH with prior exposure (**Figure. 6.8D)**.

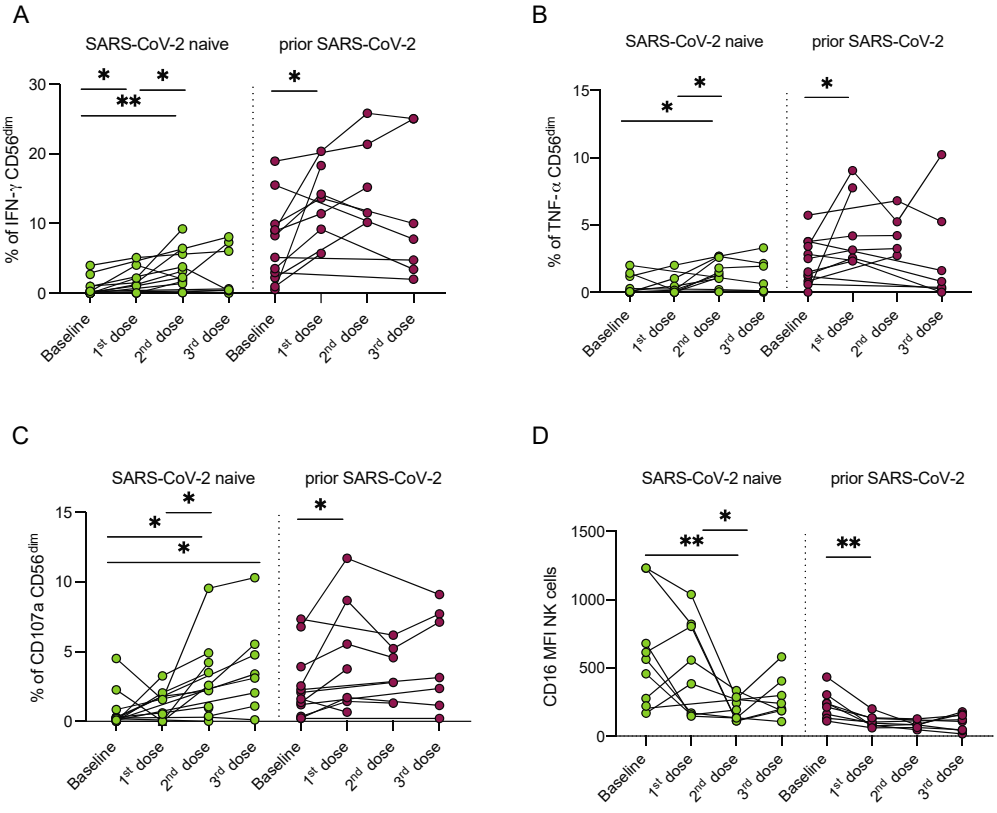


Figure 6.8. Longitudinal assessment of antibody-dependent NK cell responses following SARS-CoV-2 vaccination in PLWH.

Longitudinal analysis of (**A)** IFN-γ^{+} CD56^{dim} NK cells, **(B)** TNF-α^{+} CD56^{dim} NK cells, **(C)** CD107a^{+}CD56^{dim} NK cells, and **(D)** CD16 MFI in PLWH, with or without prior SARS-CoV-2 infection, at baseline (pre-vaccine) and following each dose of vaccine. Significance determined by two-tailed Wilcoxon matched-pairs signed rank test.* p<0.05, ** p<0.01

6.2.5 Antibody-dependent NK cell responses are enriched in adaptive NK cell subsets.

To evaluate the influence of NK cell phenotype variation on the magnitude of antibody-dependent NK cell function, the functional capacity of specific NK cell subsets was analysed. IFN-γ and CD107a responses were examined in differentiated/adaptive CD57^{+}FcεRIγ^{-} CD56^{dim} NK cells that are increased following natural infection/vaccination and in other NK cell subsets including CD56^{bright}, CD57^{-}, CD57^{+}NKG2C^{+} CD56^{dim}, and CD57^{+}FcεRIγ^{+} CD56^{dim}. In SARS-CoV-2 naïve individuals, IFN-γ expression after two doses of vaccine was predominantly mediated by CD57^{+}FcεRIγ^{-}CD56^{dim} NK cells (**Figure. 6.9A&B)**. Given the low-level responses after the first dose in SARS-CoV-2 naïve individuals, no significant differences in the IFN-γ expression between different NK cell subsets were detected (**Figure. 6.9A&B)**. Similar to SARS-CoV-2 naïve, IFN-γ production was significantly enriched within adaptive/differentiated CD57^{+}FcεRIγ^{-} and CD57^{+}NKG2C^{+} subsets in PLWH with prior infection across all time-points analysed (**Figure. 6.9C&D)**. In contrast to IFN-γ expression, no significant differences were observed in CD107a expression between different NK cell subsets (CD56^{bright} vs more differentiated subsets) in PLWH with or without prior SARS-CoV-2 infection (**Figure. 6.10A-D)**. Together, these data demonstrate a stronger antibody-dependent response in terms of cytokine production mediated by more differentiated adaptive NK cells.

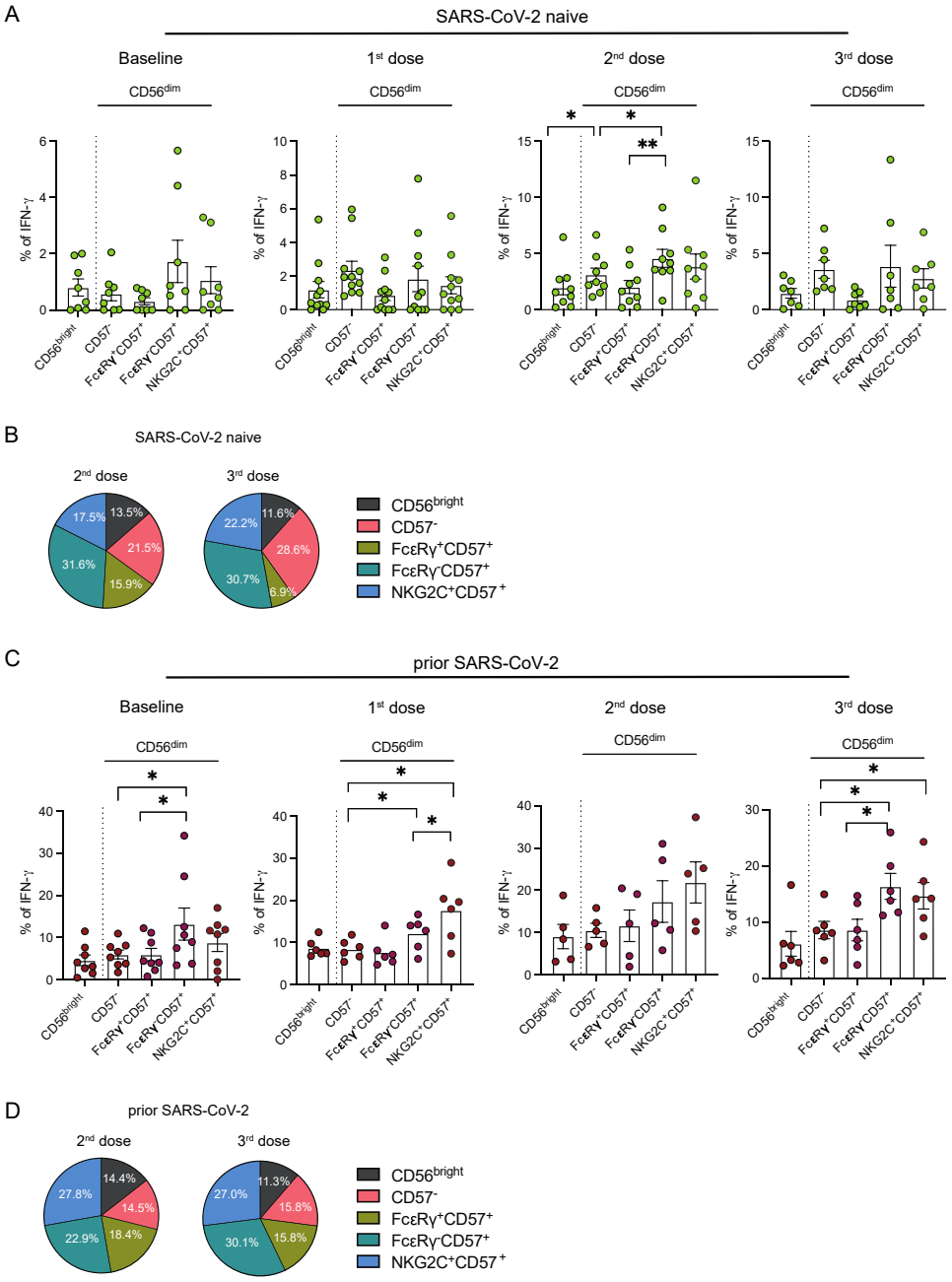


Figure 6.9. IFN-γ⁺ responses within different NK cell subsets in PLWH.

(A) The expression of IFN-γ within CD56^{bright}, CD56^{dim}CD57^{-}, CD56^{dim}CD57^{+}FcεRIγ$^{+/-}$, and CD56^{dim}CD57^{+}NKG2C^{+} cells in SARS-CoV-2 naïve PLWH **(B)** Pie charts representing the percentage of IFN-γ^{+} within different NK cell subsets in SARS-CoV-2 naïve PLWH after two or three doses of vaccine. **(C)** Summary analysis and **(D)** pie charts showing the percentage of IFN-γ^{+} within different NK cell subsets in PLWH with prior infection. Significance determined by two-tailed Wilcoxon matched-pairs signed rank test.* p<0.05, ** p<0.01.

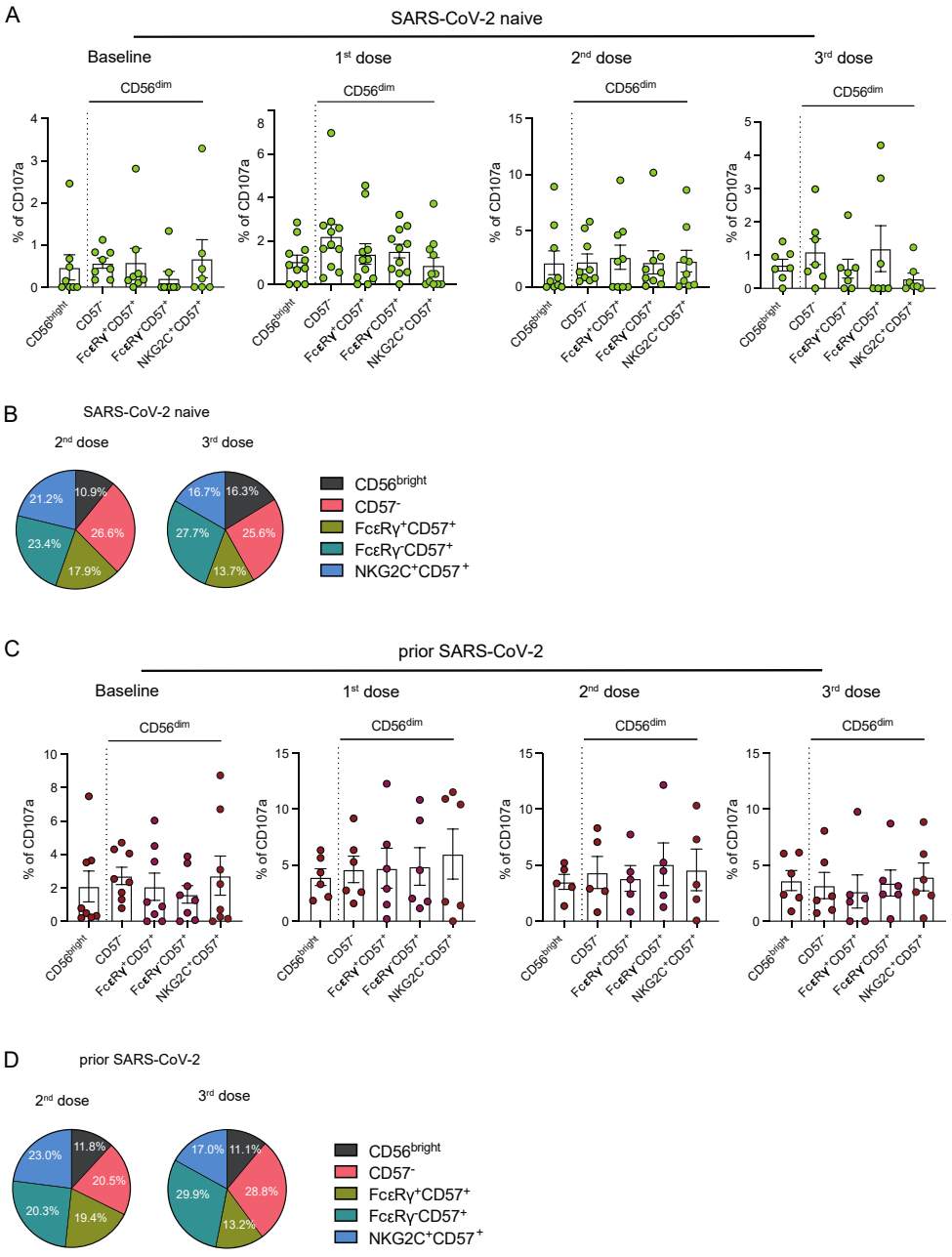


Figure 6.10. CD107a⁺ responses within different NK cell subsets in PLWH.

(A) The expression of CD107a within $CD56^{bright}$, $CD56^{dim}CD57^{-}$,$CD56^{dim}CD57^{+}FcεRIγ^{+/-}$, and $CD56^{dim}CD57^{+}NKG2C^{+}$ cells in SARS-CoV-2 naïve PLWH. **(B)** Pie charts representing the percentage of $CD107a^{+}$ within different NK cell subsets in SARS-CoV-2 naïve PLWH after two or three doses of vaccine. **(C)** Summary analysis and **(D)** pie charts showing the percentage of $CD107a^{+}$ within different NK cell subsets in PLWH with prior infection. Significance determined by two-tailed Wilcoxon matched-pairs signed rank test.* p<0.05, ** p<0.01.

Given that NK cell responses were dominated by adaptive NK cells, the relationship between SARS-CoV-2 antibody titres and adaptive NK cell functional responses was evaluated by comparing antibody and neutralisation levels with the frequency of IFN-γ^+, TNF-α^+, and CD107a$^+$ CD57$^+$FcεRIγ$^+$ CD56^{dim} cells following SARS-CoV-2 vaccination. Overall, antibody-dependent NK cell responses (IFN-γ^+CD57$^+$FcεRIγ$^+$CD56^{dim}) following the first, second, and third vaccine doses correlated positively with S1 IgG binding titres (first dose r = 0.7176, p = 0.0024; second dose r = 0.6631, p = 0.0085; third dose r = 0.7709, p = 0.0018) in PLWH, with or without prior SARS-CoV-2 infection (**Figure. 6.11A-C)**; similar associations were observed for neutralising antibody titres (first dose r = 0.7797, p = 0.0006; second dose r = 0.7670, p = 0.0013; third dose r = 0.4725, p = 0.1057) (**Figure. 6.12A-C)**. Despite these positive associations, some PLWH who lacked neutralising antibody response and/or had low levels of neutralisation (ID_{50}<150) had measurable antibody-dependent NK cell response, in particular those with no prior SARS-CoV-2 infection (**Figure. 6.12A-C)**.

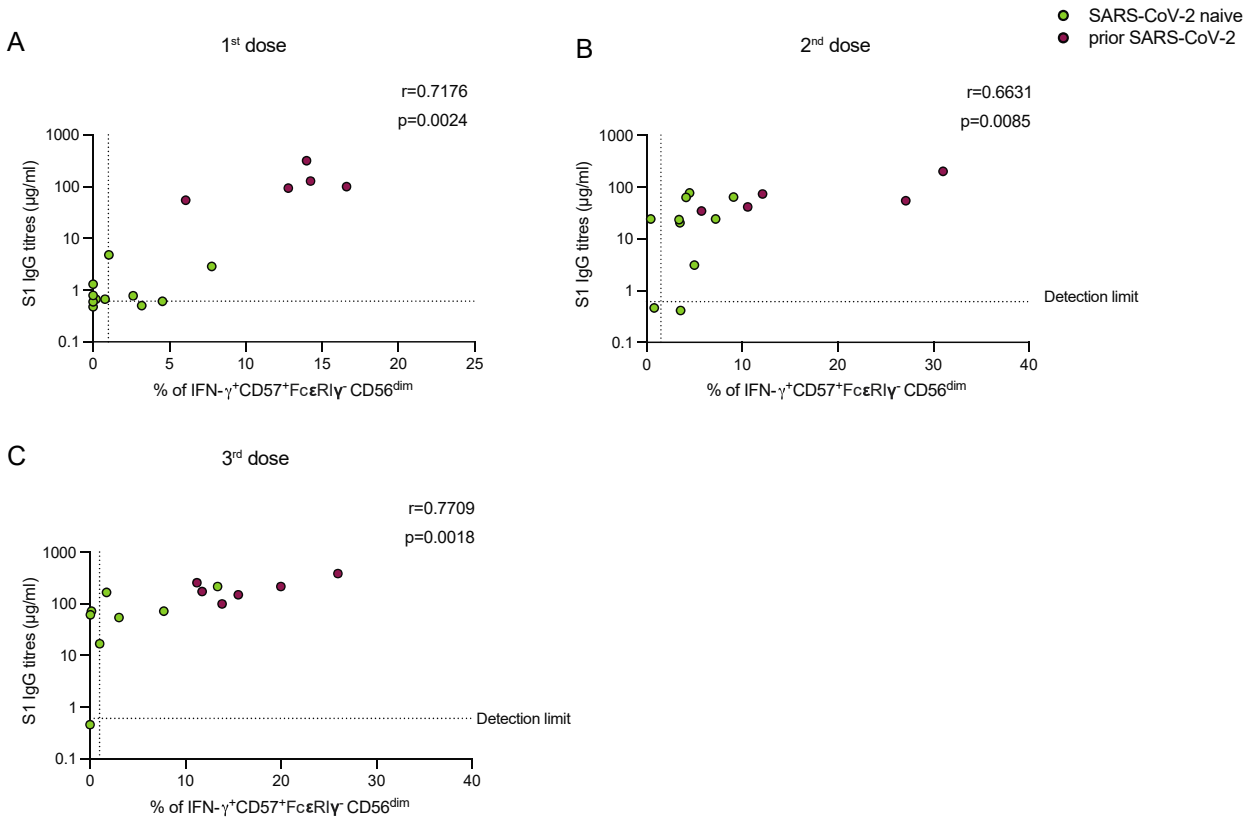


Figure 6.11. Correlation analysis between antibody-dependent NK cell responses and S1 IgG levels in PLWH.

Correlation of IFN-γ^{+} CD57^{+}FcεRIγ^{-} CD56^{dim} NK cell responses with S1 IgG titres after **(A)** one dose, **(B)** two doses, and **(C)** three doses in PLWH, with or without prior SARS-CoV-2 infection (limit of detection 0.6 µg/ml). The non-parametric Spearman test was used for correlation analysis (two-tailed).

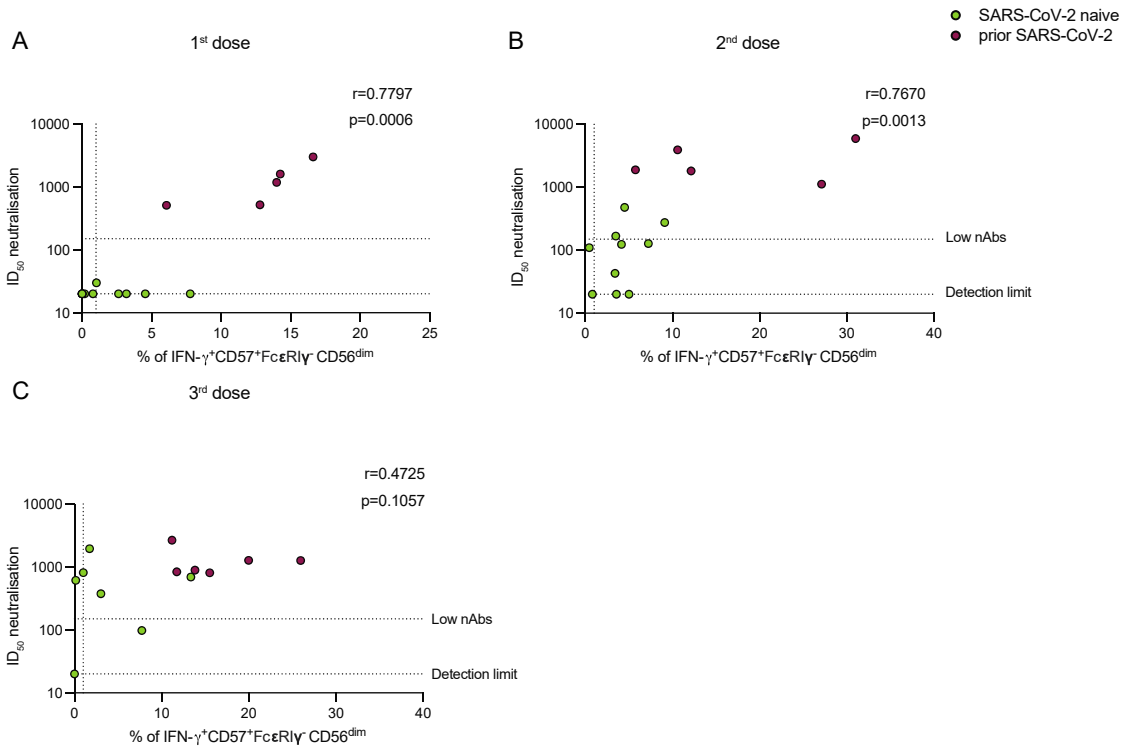


Figure 6.12. Correlation analysis between antibody-dependent NK cell responses and nAbs in PLWH.

Correlation between the frequencies of IFN-γ^{+} CD57^{+}FcεRIγ^{-} CD56^{dim} NK cells and nAb titres (**A)** one dose, **(B)** two doses, and **(C)** three doses in PLWH, with or without prior SARS-CoV-2 infection (limit of detection ID_{50}=20, low nAbs ID_{50}=150). The non-parametric Spearman test was used for correlation analysis (two-tailed).

6.3 Discussion.

NK cell subsets are emerging as attractive vaccine targets owing to their ability to regulate adaptive responses, develop recall responses to antigen re-stimulation and generate Fc effector functions to moderate infection (62,403,405–407). This study suggests that the adaptive NK cell compartment in PLWH, driven by HCMV co-infection and re-shaped by SARS-CoV-2 infection and/or vaccination, influences NK cell antibody-dependent responses and supports the generation of SARS-CoV-2 specific cellular and humoral immunity. These observations provide valuable insights for the manipulation of specific NK cell subsets through novel vaccination strategies to promote NK cell populations with stronger ADCC capacity.

These findings showed that PLWH, with prior exposure to SARS-CoV-2, had a larger proportion of mature/differentiated NK cells that lacked expression of FcεRIγ^{-}. These CD57^{+}FcεRIγ^{-} subsets were detected at least 148 DPSO following predominantly mild infection and were induced post-vaccination in SARS-CoV-2 naïve individuals. In the context of convalescent infection, the frequencies of CD57^{+}FcεRIγ^{-} population are associated with HCMV IgG and CXCL10 (IP-10) levels. The positive associations between adaptive CD57^{+}FcεRIγ^{-} NK cells and HCMV IgG titres in both study groups, SARS-CoV-2 exposed and SARS-CoV-2 naïve PLWH, suggest that the presence of adaptive NK cells in PLWH, are partly driven by HCMV co-infection (84,94,98,408). The higher proportion of adaptive NK cells in SARS-CoV-2 convalescent PLWH suggests that these subsets may also have a direct antiviral role during SARS-

CoV-2 infection. These observations are in line with previous work in the general population showing a higher representation of NK cells with the adaptive phenotype ($CD57^{+}NKG2C^{+}$) in acute and convalescent SARS-CoV-2 infections (189,195,206). The emergence of adaptive NK cells in convalescent PLWH could be triggered by multiple factors. These subsets could result from pre-existing populations following slow homeostatic proliferation mediated by potential HCMV reactivation during heterologous infection or by cross-reactive antigens, in addition to signals received by CD16 and/or cytokine priming (96,103,106,256). In particular, CD16 stimulation has been shown to expand adaptive NK cells *ex vivo* through interactions with CD3z homodimers (96,103,404). In line with these observations, a trend towards lower CD16 expression was observed in PLWH who recovered from COVID-19 disease. Additional work is required to dissect the mechanisms underlying the dynamic adaptations of NK cells in response to SARS-CoV-2 infection/vaccination in PLWH.

The adaptive NK cell subsets described in this study are strongly antibody reactive (103,105,106,409). Durable memory-like NK cell responses have been described following a heterologous prime-boost viral vector-based Ebola virus vaccine resulting in persistent antibody-dependent NK cell activation up to 180 days after the booster dose (410). Interestingly, the presence of adaptive NK cells significantly modified responses to Ebola glycoprotein (Wagstaffe et al. 2021). Consistent with these findings, our data show a durable adaptive NK cell response that was detected up to 148 days post-infection, or 218 days post-

second dose of vaccination, suggesting that these cells could potentially contribute to long-lasting immunity.

While virus neutralisation represents an important correlate of protective antiviral immunity, other non-neutralising Fc effector functions mediated by antibodies, including NK cell-mediated ADCC, could provide additional mechanisms for viral control, especially against emerging variants (397). In keeping with this hypothesis, there was an enhanced capacity for antibody-dependent responses against immobilised spike in the presence of autologous pre- and post-vaccination serum, mediated by adaptive subsets compared to less differentiated NK cells. Individuals with prior exposure to SARS-CoV-2 had higher baseline IFN-γ production, which was further boosted via vaccination and exceeded responses in SARS-CoV-2 naïve individuals even after three vaccine doses. This suggests a stronger antibody-dependent NK cell response in PLWH with hybrid immunity (i.e. natural infection and vaccination) compared to vaccination alone, in keeping with previous observations in the general population (411). While IFN-γ production was more robust in adaptive NK cells, CD107a responses were similarly induced in all NK cell subsets. This is in line with hypomethylated regulatory regions in IFN-γ and the interaction of FcεRγ- with CD3z homodimers in adaptive NK cell subsets providing the mechanisms for stronger induction of cytokine production upon Fc-dependent stimulation (95,96,404). Notably, the magnitude of NK cell activation in response to autologous or pooled serum was comparable in both groups, suggesting that heterogeneity in responses does not solely depend on antibody concentration and could reflect individual variation in

the composition of the adaptive NK cell pool within individuals. Interestingly, Fc-dependent NK cell responses were detected in a small proportion of SARS-CoV-2 naïve PLWH with low or absent neutralising antibodies after vaccination, suggestive of the potential functional contribution of NK cells to vaccine-mediated protection that merits further investigation in larger cohorts.

In addition to their potential to mediate ADCC activity, adaptive NK cells have a reduced ability for immunoregulation and suppression of activated T cells (96) and can modulate the induction of bnAbs in HIV-1 infection through the reduced killing of T_{FH} T cells (84). These findings are consistent with previous reports showing a positive correlation between frequencies of adaptive NK cells and T_{FH} T cells. These adaptive NK cell subpopulations may have the added benefit of supporting the induction of B- and T-cell responses through direct interactions and/or secretion of cytokines (101), which can contribute to virus-specific T-cell expansions and recruitment to the site of infection (101,412,413). These results are in keeping with recent observations showing that an increased frequency of $NKG2C^+$ NK cells correlates with high antibody titres following BNT162b2 mRNA vaccination. Although the full impact of HCMV co-infection on vaccine responses can be broad (reviewed in (414)), these data suggest that the increased NK cell differentiation and presence of adaptive features in PLWH could be advantageous, favouring antibody-mediated activation and induction/ preservation of T-cell and humoral responses. Further research is needed to validate these observations in healthy and/or older HCMV-seropositive

individuals and to refine our understanding of NK cell contributions to vaccine efficacy.

This study has several limitations. It was not possible to determine the effect of different vaccine platforms that may contribute to the variability in the magnitude of responses; this will need to be addressed in future studies. Also, this study reflects changes in the NK cell compartment during the convalescent phase and at least 7 days after vaccination but does not exclude any initial changes during acute SARS-CoV-2 infection or the first few days following vaccination. Additionally, our analysis provides insights into NK cell responses after one, two, or three vaccine doses; future studies are required to assess the durability of these responses and their contribution/complementary role in the longer-term immunity in PLWH, including protection against breakthrough infections and severe disease. Our study focused on antibody-dependent activation against spike, the only antigen in the vaccines received by study participants; thus, further work is required to assess antibody-dependent NK cell activation against non-spike proteins, including nucleoprotein/membrane and accessory proteins (ORFs) which have been shown to activate NK cells in healthy subjects (393,395).

Collectively, the study presented in this chapter demonstrated a robust and durable antibody-dependent NK cell response detectable for at least 148 days after natural infection. These responses were elicited by SARS-CoV-2 vaccination in PLWH with no prior exposure and further boosted in people with

prior infection. Antibody-dependent responses were mediated by mature adaptive NK cell subsets, highlighting the potential to selectively promote these features through vaccination to enhance protection, especially in immunocompromised patients.

Chapter 7: Concluding remarks and future directions.

Chapter 7

7.1 Section 1: acute HIV-1 infection.

7.1.1 Engaging innate immunity in HIV-1 vaccine and cure strategies.

Over thirty years into the HIV-1 pandemic, the need for a globally effective HIV-1 vaccine is more compelling than ever (415). Clinical interventions aimed at reducing HIV-1 acquisition, including pre-and post-exposure prophylaxis for high-risk individuals, large-scale circumcision programmes, and the use of ART therapy as prevention or treatment, have remarkably influenced the trajectory of HIV-1 infection (415). However, despite these advances, the overall population prevalence of HIV-1 remains relatively stable, with ~1.5 million people acquiring HIV-1 each year worldwide (10). Additionally, while ART therapy has significantly improved lifespan and decreased mortality among PLWH, long-term treatment is associated with increased occurrence of a range of serious complications (415–417), and life-long adherence to ART remains a significant challenge, particularly in resource-constrained areas in sub-Saharan Africa (418). Thus, even with antiviral drug therapy (417), there is an unmet need for a preventive or therapeutic HIV-1 vaccine to reduce the global burden of HIV-1 infection.

A central challenge to immune containment and vaccine development is the high genetic diversity within the HIV-1 genome, which is known to be steadily increasing over time, both within and between subtypes. In the light of such variation, different HIV-1 subtypes have been identified, and potential vaccine strategies, to date, have failed to provide adequate protection from infection with any HIV-1 subtype: however, an effective vaccine will need to provide protection against multiple subtypes. While vaccine efforts have been focused on

generating broadly neutralising antibodies, such responses are rarely induced, and the path forward to an effective neutralising antibody-based vaccine remains uncertain (417). Thus, there is an unmet need to define new targets that can be effectively engaged to produce broad and durable immune responses. In addition to developing more effective immunogens, engaging the key components of innate immunity that shape adaptive immune responses and further exploiting immunological memory beyond those driven by B or T cells could be beneficial for HIV-1 vaccine design. NK cells play an important role in antiviral immunity and can confer early host protection against viral infections (62,419). Over the years, insights into their role in controlling HIV-1 replication and their capacity to regulate T- and B-cell responses have put NK cells as a key focus for research. More recently, identifying NK cell subsets with adaptive or “memory” characteristics represents an innovative approach to augmenting memory responses in HIV-1 vaccines/therapies (more details on the implications for vaccine design are included in section 7.1.4) (62,419–421). In this thesis, I provided important insights into the role of NK cells, including adaptive NK cells, in the natural control of HIV-1 viraemia in individuals infected with different HIV-1 subtypes and their interplay with T-cell activation during the early phase of infection. I further showed that individuals infected with HIV-1 subtype A had a preferential expansion of adaptive NK cell subsets with enhanced responses to antibody-coated target cells compared to people infected with other HIV-1 subtypes. These adaptive NK cells were particularly enriched in a small group of subtype A infected individuals who maintained low levels of HIV-1 viraemia in the absence of ART. These data suggest that specific NK cell subsets could contribute to early control of HIV-1

viraemia, highlighting their potential role as a new target to include in the development of novel HIV-1 immunotherapy and preventive vaccination strategies.

The data presented in this thesis focused on NK cell responses in untreated patients after one month of HIV-1 infection. However, whether the expansion of adaptive NK cells in subtype A infection arises during the earlier phase of infection and whether the presence of adaptive NK cell subsets before or at peak viral load is linked to the subsequent control of viraemia is currently unknown. To further examine the early NK cell responses, additional work will be conducted using samples collected at the earlier stage of infection (during the first three weeks of infection, “2-20 days post-EDI”) from a small number of participants from the IAVI Protocol C cohort who were included in our initial study (Chapters 3 and 4) and have donated available PBMC samples. This work aims to longitudinally characterise the phenotypic and functional aspects of NK cell subpopulations, incorporating a detailed dissection of receptor patterns and adaptive features from the earliest time-points and up to three months post-infection. This will allow us to capture and correlate the evolution of NK cell responses and their functional capacity with markers of disease progression (plasma viral load, viral load set-point, $CD4^+$ T-cell count and initiation of ART). The request for additional PBMC samples (n=11) for this work has been approved by IAVI, and the samples have been shipped and are currently stored in Oxford. This work will provide insights into the earliest NK cell responses following HIV-1

infection and their roles in viral control and will have implications for the development of future preventive vaccines.

7.1.2 Future directions in studies of NK cell responses during AHI.

Our knowledge of immune responses during early infection has been hampered by the fact that identifying infected individuals within the first weeks of infection is challenging. This leads to many unanswered questions about the immune dynamics during AHI, particularly for innate immunity, which has been much less investigated than adaptive immune responses. While our study focused on circulating NK cells, a similar analysis will need in future to be performed in tissues to examine the role of tissue-resident NK cells in controlling viral replication, regulating other immune cells, and shaping the overall tissue immune response. However, performing such studies is challenging in humans due to the inherent difficulties in accessing infected tissue samples, the impracticality of sampling tissues for longitudinal studies, and the difficulty of identifying individuals during early infection (422). Nonetheless, NHP models, such as macaques with SIV or SHIV infection, which recapitulate many of the immunological and clinical hallmarks of HIV-1 infection in humans (51), could provide an opportunity to study the functional, actionable significance of early tissue-resident NK cell responses for long-term viral control. This is highly relevant for designing strategies for HIV-1 cure that aim to eradicate latent tissue reservoirs. Given that latent reservoirs are established within days after infection (possibly before the virus is detected in the systemic circulation) (423), future work, likely in NHP models, should aim to identify the role of tissue-resident NK

cells in controlling viral reservoirs and limiting their initial establishment. Critically, innate immune subsets, including NK cells, and their functions during the early stages of infection are poorly described in NHP models. Thus, there is a need for future studies of NK cells and their functional characterisation (including their adaptive features) in SIV/SHIV infection: depletion experiments would also help to contextualise the findings from this thesis. However, such results should be carefully considered, given the biological differences between NHP models and humans, as well as differences in virological properties between HIV-1 and SIV viruses (reviewed in (51,424)). In particular, the lack of several human immune cell lineages, some of which are related to innate immune responses, in NHP models and the subtle differences in virus-host interaction between HIV-1 and SIV could limit the use of such models in acute infection (51). Thus, increasing efforts are required to develop models that recapitulate the complexity of virus-host interactions in HIV-1 infection and the diversity of viral components naturally found in HIV-1, with the aim of improving the relevance of animal models for HIV-1 pathogenesis studies and helping the global effort to achieve the development of efficient preventive and cure strategies.

With improved NK cell manipulation in NHP models, it will also be important to test the impact of early viral suppression (i.e. early ART initiation) on the NK cell compartment. These early treatment conditions can be utilised to compare NK cell responses in early viraemia suppression (i.e. the absence of ongoing viral replication) versus progressive infection to identify the timing and quality of viral spread, as well as to observe the impact of hyperactivated and/or dysfunctional

NK cell responses during acute infection. It is important to further distinguish molecular and functional differences in NK cells in the earliest stages of HIV-1 infection, before complete suppression of viraemia, between early treated and untreated individuals (although this approach may be limited by the current recommendation to treat all HIV-infected people when first diagnosed with infection). These earliest time-points provide the best opportunity to discern how mitigating HIV-1 viraemia and potential inflammation would affect the longevity and quality of both NK cell responses and other immune subsets. Linking these events to long-term viral control and disease progression could inform clinical or cellular metrics and identify targets for preventive or therapeutic vaccines.

7.1.3 Antigen-specific NK cell responses in AHI, so much more to learn.

If the design of HIV-1 vaccines were to aim to induce memory NK cell responses alongside the induction of B- and T-cell responses, viral antigens promoting memory responses need to be identified. While the data described in this thesis provide some insights into the role of adaptive NK cells in AHI, questions remain regarding the viral antigen specificity of these subsets. Given that PLZF^{-} FcεRIγ^{-}NK cells exhibited a higher expression of NKG2C, an activating receptor which recognises a limited set of viral peptides presented by human leukocyte antigen E (HLA-E) (93,103), it is possible that these cells can mediate antigen-specific responses (96). However, future studies will be necessary to examine antigen-specific responses within these adaptive NK cell subsets and their roles in antiviral activity and disease progression.

Adaptive NK cells consist of distinct but largely overlapping NK cell subsets, with FcεRIγ^{-} adaptive NK subsets containing higher levels of NKG2C^{+} cells, including in the peripheral blood and tissues of healthy individuals (425,426). NKG2C^{+} NK cells have been described to mount antigen-specific responses in HIV-1 infection (128) and were associated with long-term viral suppression (in elite controllers (128) and a post-treatment controller (230)). In the context of vaccination, NKG2C^{+} NK cells have been described to mount vaccination-dependent, antigen-specific recall responses in humanised mice previously vaccinated with an HIV-encoded envelope protein (86). These NK cell memory responses were detected up to 5 years following vaccination in rhesus macaques, indicating that antigen-specific NK cell memory is durable and does not require ongoing antigenic stimulation (87). Identifying peptides that stabilise HLA-E molecules and favour NKG2C responses in early HIV-1 infection would represent a first step in targeting these subsets. Experimentally, these peptides could initially be identified by screening for epitopes with features similar to the leader sequence peptide (referred to as VL9) that binds efficiently to HLA-E (as previously used in HLA-E restricted T cells work in HIV-1 by Yang *et al.* (427)). Peptides would be derived from different HIV-1 subtypes (Env or Gag) and shown to stabilise HLA-E at the surface of human cell lines stably expressing HLA-E (such as K562). Evaluation of HIV-1 specific responses could be performed by stimulating primary NK cells from acutely infected individuals with HIV-1 peptides presented by antigen-presenting cells (such as autologous B cells) and measuring cytokine production and/or degranulation (as previously used in (128)). Additional work in NHP models could also provide insights into the antigen specificity of NK cells,

especially within key tissue compartments (mucosal tissues and lymph nodes), during acute infection. Recently, antigen-specific NK cell responses have been described in SIV infection in the natural host, African green monkey (a model for non-pathogenic SIV infection), and rhesus macaques (a model for pathogenic SIV infection) (132). These data showed that MHC-E-restricted SIV-specific NK cell responses increased after SIV infection in the natural host, and these responses were linked to the natural control of SIV infection (132). Additional work is needed to further define viral antigens, molecular pathways, co-stimulatory molecules, and/or inflammatory cytokines that selectively target antigen-specific NK cell responses, with implications for developing NK cell-based vaccines/immunotherapies.

7.1.4 Implications for vaccine design.

Vaccination strategies aimed at inducing adaptive NK cell responses in combination with the induction of classical memory responses (virus-specific B or T cells) represent an exciting area that can circumvent some of the unwanted immunoregulatory effects of conventional NK cells (305,407,419,428,429). Adaptive NK cells described in this thesis (PLZF^{-}FcεRIγ^{-} CD57^{+} NK cells) could expand in response to multiple factors, including systemic inflammation, antibody-opsonised targets, and/or exposure to HIV-1 antigens (98,105,106,229). Identifying agents (viral ligands, molecular pathways, co-stimulatory signals, and proinflammatory cytokines) that selectively promote adaptive NK cell expansion will aid in manipulating their beneficial properties, providing a complementary approach for vaccine strategies. Given that these

adaptive NK cells exhibited enhanced ADCC capacity (as presented in Chapter 3), these NK cell subpopulations can potentially be targeted for designing preventive or therapeutic vaccines aimed at generating ADCC-promoting antibody responses or in combination with broadly neutralising antibodies. Additionally, the specificity of adaptive NK cells responding to HLA-E presented peptides (93), including the previously unappreciated ability of HLA-E to bind HIV-1 peptides (128), leading to activation of virus-specific NK cell responses, opens up the possibility for further refining approaches targeting HLA-E for vaccine development. The significance of HLA-E-restricted responses has received significant attention in the HIV-1 vaccine field (430). This follows observations of broadly-targeted HLA-E-restricted $CD8^+$ T cells as important correlates of immune protection in macaques vaccinated with a CMV-vectored SIV vaccine (427,431,432). Such strategies that encourage HLA-E-dependent responses could lead to the induction of HIV-1-specific memory NK cells with the ability to react to a broader range of antigens from the same or different viruses, complementing T-cell responses (132,432).

7.1.4 Implications for therapeutic strategies.

As previously mentioned, there is currently no effective cure strategy for HIV-1 infection, and ART treatment is essential to maintain long-term viral suppression, owing to viral persistence in latent reservoirs (433). Given the necessity of life-long adherence, the high cost associated with ART, and limited accessibility in rural areas, only 75% of PLWH currently receive ART (434), and the sustainability of the current ART programme remains unknown. With the complexities and

expenses associated with life-long treatment, developing an effective curative intervention is a global priority. Several strategies have been proposed for HIV-1 cure, including approaches aimed at achieving either durable control of viral replication without ART treatment (functional cure) or complete viral eradication (sterilising cure) (reviewed in (302,419,420,433,435)). Mechanisms of HIV-1 persistence, including viral latency, immune evasion and dysfunction, target cell-intrinsic immune resistance, and, potentially, target cell distraction of immune effectors, likely need to be overcome in order to achieve an HIV-1 cure (436). The current efforts to eliminate HIV-1 reservoirs have been focused on harnessing adaptive immune systems, including broadly neutralising antibodies and $CD8^+$ T-cell responses. Despite some progress, a number of fundamental issues with B- or T-cell-based treatment still exist, and the path forwards for an effective and safe antibody or T-cell-based treatment is unclear. In addition to improving current strategies, engaging innate immune responses that regulate adaptive immunity and mediate potent and broad responses, holds promise for advancing towards an HIV-1 cure. As shown in this thesis, the ability of NK cells to potently control viral replication, generate immunological memory responses, and shape overall immune responses, opens new avenues for novel therapeutic approaches that either manipulate or use NK cell antiviral properties. While current NK cell-based immunotherapies have focused on cancer biology, these advances can be readily applied to target HIV-1 infection (302,419,420,435,437). Promising developments include the recently reported data demonstrating that CAR NK cells are capable of targeted responses while inducing less off-target and toxic side effects compared to CAR T-cell therapies (302,419,420,435,437).

Further CAR NK cells derived from NK cell lines or inducible stem cells may allow for more rapid “off-the-shelf” access. These data demonstrate the potential of CAR NK cells as a promising alternative, highlighting their ability to achieve desired therapeutic outcomes while minimising the associated adverse effects commonly observed in CAR T-cell treatments (302,419,420,435,437). Other work in investigating the use of latency-reversing agents (LRAs) to induce HIV-1 transcription in latent reservoirs, allowing for latently-infected cells to be recognised and killed by cytotoxic cells (441,442), may also provide a resource for enhancing NK cell clearance of HIV-1 reservoirs. Interestingly, NK cells have been reported to modulate the effects of LRAs on the viral reservoir, and their activity was linked to a decline in the HIV-1 DVA level during treatment with LRAs (302). In a clinical trial, the administration of panobinostat or pegylated interferon-α (PEG-IFNα) induced NK cell activation, reduced levels of cell-associated proviral DNA, and delayed viral rebound following analytical treatment interruption (443,444). The impact of LRAs on NK cells could be due to the direct activation of NK cells and/or alternations in the levels of germline-encoded NK cell receptor ligands on HIV-1 infected cells. It is also worth noting that targeting NK cell subsets to restore any residual dysfunction could enhance their antiviral functions and clearance of HIV-1 reservoirs.

In addition to LRAs, the passive administration of antibodies that are capable of mediating strong ADCC is a strategy under consideration and can be combined with NK cell-based therapies to enhance the clearance of HIV-1 infected cells (445–447). Evidence from treatment with bNAbs in *in vivo* SHIV models suggests

that NK cell-mediated ADCC responses can contribute to the elimination of HIV-1 infected cells and reduce viraemia (448–450). Similar to bNAbs, the administration of non-neutralising antibodies has been associated with a reduction in viral load and the size of viral reservoirs, as well as the clonal restriction of transmitted viruses (451–453). Given that non-neutralising antibodies cannot prevent infection by cell-free virions, these effects of non-neutralising antibodies may be attributed to Fc-mediated NK cell activity. Thus, modifying existing antibodies to better elicit ADCC functions, combined with therapies aimed at inducing NK-cell mediated ADCC, could be an attractive candidate for an HIV-1 cure.

Further, with the identification of adaptive NK cells against HIV-1, it is possible that targeting MHC-E peptide presentation to NKG2C and/or enhanced NK cell memory via specific cytokines to promote cytokine-induced memory responses could be achieved with therapeutic approaches. Adaptive NK cells have *in vitro* expansion capability with predictable selectivity as an alternative or combination strategy for a functional cure. Utilising HLA-E expressing transfectants has been a successful strategy for obtaining robust proliferation of functional adaptive NK cells, with profound skewing toward a single self KIR, and enhanced NKG2C effector potential against allogeneic acute lymphoblastic leukaemia primary blasts (454). The exquisite specificity of adaptive NK cells for HLA-E presented peptides (92,93), opens up the possibility for further refinement of these approaches by tailoring the peptide ligand on HLA-E. Various combinations of specific cytokines have also been demonstrated to induce expansions of

cytokine-induced memory-like NK cells with increased responsiveness (108). In particular, IL-15 stimulated NK cells from HIV-infected donors on suppressive ART were able to recognise and kill autologous latently HIV-infected $CD4^+$ T cells following exposure to the potent latency reversal histone deacetylase inhibitor (HDACi), Vorinostat (455). The induction of memory NK cells can also be achieved by *ex vivo* priming with a combination of cytokines, including IL-12, IL-15 and IL-18 (107). Adoptive transfer of these cytokine-induced adaptive NK cells is being tested in phase I clinical trials in AML patients (456). Such an approach could, therefore, be tailored to direct/boost specific adaptive NK cell subpopulations for HIV-1 functional cure strategies but, so far, has remained unexplored.

7.1.5 Virus-specific T-cell responses to different HIV-1 subtypes.

After activation of innate immune responses, HIV-specific T-cell responses arise in the days to weeks after peak plasma viraemia and contribute to viraemia control. The development of an effective vaccine will likely require the induction of both innate and adaptive immune responses to provide adequate immune protection before transmission, enabling earlier, broader and more effective secondary responses for preventing or controlling AHI (48,457). The relationship between the infecting subtype, adaptive immunity, and subsequent viral control has not been well defined due to the difficulty in obtaining samples during the first weeks of infection from individuals infected with different HIV-1 subtypes. In Chapter 4, I showed that AHI elicited robust $CD4^+$ and $CD8^+$ T-cell activation, with up to 60% of peripheral $CD8^+$ T cells expressing HLA-DR and CD38. In addition,

these data demonstrated that different HIV-1 subtypes induce similar magnitudes of $CD4^+$ and $CD8^+$ T-cell activation, and these responses were associated with the levels of HIV-1 viraemia. These findings highlighted the early interactions between adaptive immune responses and different HIV-1 subtypes and suggested that the impact of genetic heterogeneity between different subtypes on T-cell activation is minimal.

Given the important role of virus-specific T-cell responses in the control of HIV-1, future studies should assess whether these activated $CD8^+$ T cells represent virus-specific populations in acute infection and determine their contribution to subsequent viral control. An important issue for T cell-based vaccine design is the increasing antigenic diversity between and within HIV-1 subtypes. Thus, in order to confer protection against the majority of circulating HIV-1 variants, immunogens able to induce broadly cross-reactive T cells are required. Currently, the efforts to develop vaccines that elicit T-cell responses primarily rely on immunogens/peptides derived from a single variant of HIV-1 and the outcomes of human trials of these T cell-based vaccines have been unsatisfactory, as evidenced by the available literature (reviewed in (272)). This includes the STEP and HVTN505 clinical trials, both of which were based on adenovirus serotype 5 (Ad5) vectors encoding HIV-1 antigens (Gag, Nef, and Pol) that are commonly recognised across different HIV-1 subtypes (458). However, in STEP, the encoded proteins induced HIV-specific $CD8^+$ T-cell responses that were low in magnitude, targeted a limited range of epitopes, and didn't improve the prevention of HIV-1 acquisition or control of subsequent infection (one caveat is

that this trial was conducted in a region where subtype B is the predominant HIV-1 subtype) (272,458,459). Similar results were observed in HVTN505, where T-cell responses were primarily directed against the Env protein, which is among the most variable viral proteins between different HIV-1 subtypes (459).

To induce broad, protective responses, additional efforts should be dedicated to improving the breadth of T cell-based antigens, with the aim of mitigating the possibility of a mismatch between the vaccine immunogen and circulating virus variants. One promising strategy involves the use of a conserved region vaccine approach utilising a 'mosaic' of viral sequences, which consist of naturally occurring epitope sequences and prevalent HIV-1 variants (460,461). These antigens have been tested in human trials and have demonstrated safety and tolerability with a highly immunogenic profile(462–464). As a complementary strategy, the design of immunogens has also focused on inducing broad cellular immune responses, solely directed against sequence-conserved regions of the virus (tHIVConsvX) (462,464). Such findings add support to the notion that vaccine candidates designed to elicit T-cell responses may have more chance of success where broad epitope recognition is induced. The simultaneous assessment of T-cell responses in different HIV-1 subtypes, as described in this thesis, can be developed further to characterise the specificity and breadth of T-cell responses in individuals infected with different HIV-1 subtypes, especially in subtype A infection where disease outcome is more favourable. One approach that can be taken to comprehensively assess T-cell functions, without the need for excessive blood volume/samples, involves a polyclonal $CD8^+$ T-cell expansion

technique (465). This approach includes the expansion of T cells from one cryopreserved PBMC sample to generate sufficient T cells to allow the identification of individual peptides and assessment of $CD8^+$ T cell-mediated inhibition of HIV-1 replication (465). This methodology has been recently designed and tested in 14 acutely HIV-1 infected donors from the IAVI Protocol C cohort to characterise HIV-1-specific $CD8^+$ T-cell responses by different functional readouts within the context of extreme HIV-1 diversity and proved to be a successful strategy that addressed the issue of sample constraints (465). The ability to assess T-cell mediated control of diverse HIV-1 isolates and link this with recognition of individual viral epitopes would aid the understanding of potential correlates of immune protection and identification of broadly effective T-cell targets, thereby providing tools for rational T-cell immunogen design for effective vaccine candidates.

7.1.6 The interaction of NK cells with other immune cells and their impact on lymphoid organs.

It is likely that the importance of crosstalk between NK cells and other immune cells, including innate and adaptive cells, and the engagement of NK cells in regulating overall immune cell homeostasis and the outcomes of disease progression will be increasingly appreciated as studies in early HIV-1 infection occur. In addition to peripheral tissues, NK cells interact with other immune cells in inflamed tissues and in secondary lymphoid organs leading to the modulation or amplification of different effector mechanisms and impacting overall functions in lymphoid organs (466). The fact that NK cells are regulatory cells engaged in

reciprocal interactions with dendritic cells, macrophages, T cells and endothelial cells, has put NK cells as a key focus in manipulating effective immune responses to viral infections. DCs activated by microbial stimuli may represent a common stimulus for the activation of NK cell responses in AHI. Conversely, by contributing to the maturation of DCs (as detailed in Chapter 1, section 1.1.6.2.2), NK cells may amplify or limit T cell activation, serving as one of several “alarm systems” that effectively regulate responses of the adaptive immune system and can potentially be targeted to manipulate an efficient antiviral response (reviewed in (62,412,467). In other contexts, the elimination of immature DCs by NK cells may repress adaptive immune cell responses. A key unanswered question is what the balance or choice between these two opposing outcomes is and how these NK cell immunoregulatory functions are regulated in HIV-1 infection, especially in the early stage of infection where the early development of virus-specific responses are key to controlling viral replication. Finally, an important challenge will be to clarify the physiological significance of NK receptors expressed by T cells. In the longer term, the bigger challenge will be to develop new approaches to understand how these complex cellular and receptor interactions between NK cells and the adaptive immune system are integrated to yield beneficial immune responses. Circumventing and ablating these barriers should be the focus of research efforts and must continue to be studied as NK-cell-based therapies evolve.

7.1.7 Defining the balance between protective versus pathological/ immunoregulatory responses of NK cells.

In addition to their direct antiviral role, NK cells have important immunoregulatory roles that can shape the overall magnitude of adaptive immune responses to viral infection. In Chapter 4, I showed that, while infection by different HIV-1 subtypes induced a similar magnitude of T-cell activation during AHI, the relationship between NK cell responses and T-cell activation was different between subtype A and non-A subtype infections. NK cell activation (measured by CD38) was positively correlated with $CD8^+$ T-cell activation (measured by CD38 and HLA-DR co-expression) during the first month of infection in individuals infected with subtype A. Such an association was lacking in non-A subtype infection. Instead, a negative association was observed between cytotoxic NK cell subsets, $CD56^{dim}$ cells, and $CD8^+$ T-cell activation in non-A subtype infection, which could suggest that NK cells may negatively impact T-cell activation, a feature that is more prominent in non-A subtype infection. Further research is necessary to validate these findings in a larger cohort and to conduct a more comprehensive examination of the association between early NK cell responses and the subsequent emergence of virus-specific T-cell responses. The immunoregulatory and cytolytic functions of NK cells in suppressing adaptive immune responses after viral infections have been described in a number of published studies (84,287,288,304,407,468). The perforin-dependent delivery of granzymes via the cytolytic granules of NK cells and the interaction between death receptors such as TRAIL and its ligand constitute some of the underlying mechanisms of the immunoregulatory killing by NK cells (83,469). Elimination of activated $CD4^+$ and

$CD8^+$ T cells could constrain both the quantity and quality of subsequent memory T-cell responses (287,288,304,407,468). Similarly, NK cell-mediated killing of activated $CD4^+$ T cells reduces the magnitude of T follicular helper cell (T_{FH}) responses, thereby limiting the quantity and quality of germinal centre responses and the development of broadly neutralising antibodies (currently the main target for HIV-1 vaccine design) (84). The observed association between NK cell responses, T-cell activation, and HIV-1 viral load in our study raises the possibility that there are unexpected functional specialisations and distinct immunoregulatory capabilities among NK cell subpopulations in response to different HIV-1 subtypes, a mechanism which could be exploited to promote antiviral immunity in acute infection. In-depth characterisation of functional HIV-1-specific T-cell responses during acute infection in different HIV-1 subtypes, including evaluation of T-cell cross-recognition between subtypes, while simultaneously assessing early NK cell responses, would provide valuable insights into the relationship between NK cells and virus-specific T-cell responses. Further investigation of the magnitude and quality of HIV-1 specific T-cell responses in the presence or absence of NK cells (in animal models as described in (83) or *in vitro* culture (469)) could be used to study the impact of NK cells on antiviral T-cell responses in the setting of AHI. To understand the persistent role of NK cell subsets in improving or impeding adaptive responses and/or directly fighting viraemia, more granular characterisation of these cells across tissue compartments will need to be performed, likely in NHP models, given that the current standard of care requires treatment initiation at HIV-1 detection and the shortage of available samples. NHP models also provide

opportunities to functionally test both already established crosstalk between NK cells and other immune cells, their antiviral contributions, and those yet to be defined. An improved understanding of the immunoregulatory activity of NK cells during the early stage of infection, as well as their contribution to the development of effective adaptive immune responses and the impact of such associations on subsequent viral control, could assist in the development of novel adjuvants that promote the beneficial properties of NK cells while inhibiting their immunosuppressive/pathological functions. This would serve as an innovative approach to augment the effectiveness of HIV-1 vaccines.

As multiple measurements accumulate from the same individuals in the IAVI Protocol C cohort, unsupervised or supervised approaches using machine learning-based computational techniques, commonly used in the systems biology (58,457), could begin to link epidemiological, virological, cellular and molecular features of acute infection to clinical features such as disease outcome. Machine learning models using unsupervised approaches that explore the immunological, virological, and clinical features without pre-defining groups for analysis allow the identification of natural similarities or differences within the dataset. Such an approach is powerful in its ability to comprehensively explore the virological features or immunological signatures in an unbiased manner, potentially uncovering novel linkages that would not be identified through traditional methods (470). This integration of the multiple layers of information from the same participants in the IAVI Protocol C cohort within an unsupervised machine learning framework would provide a new, objective approach to identifying

important signatures associated with natural control of viraemia and/or disease progression (31,210). Supervised machine-learning approaches include adding pre-defined groups or classifications, from which the subsequent analysis is based, with the goal of identifying key features associated with the pre-defined groups (470). In the context of acute infection, these groups may be related to a specific subtype (A, C, D, or recombinant subtypes) or clinical features (viral controllers versus non-controllers), with the aim of identifying novel correlates of protection or key signatures associated with HIV-1 subtypes and/or natural control of HIV-1 infection. The strength of this approach is that it is useful for defining immunological or clinical features linked to a specific class and helps in reducing the complexity of the data (470). Overall, the application of these machine learning approaches to the data collected from the IAVI Protocol C study could integrate and highlight the most critical associations between virological, immunological, and clinical features during AHI with protection from disease progression, thus becoming a highly targeted and comprehensive hypothesis-driving tool that can accelerate the identification of key targets for further experimentation, vaccine testing or exploration by additional quantitative models.

7.2 Section 2: SARS-CoV-2 infection and vaccination in PLWH.

7.2.1 Future studies in T-cell responses to SARS-CoV-2 in PLWH.

PLWH seem to be at increased risk of worse disease outcomes (168,309,310). However, due to the scarcity of data and exclusion from the initial vaccine trials, it remains unclear whether immune responses induced by SARS-CoV-2 infection or vaccination are compromised and/or less durable in PLWH. Such knowledge is crucial for clinical management and optimising vaccine strategies in this patient group. In Chapter 6, I showed that the majority of PLWH with an undetectable HIV-1 viral load on ART could mount a robust adaptive immune response to SARS-CoV-2. Humoral and cellular responses are comparable between PLWH and HIV-negative individuals and persist 5-7 months following predominately mild COVID-19 disease, providing evidence for medium-term durable immune responses. However, in SARS-CoV-2 vaccination, antibody responses, including neutralisation levels, were reduced in PLWH compared to HIV-negative donors following each dose of vaccine (i.e. one, two, or three doses). Despite these reduced humoral responses, T-cell mediated immunity was preserved across all time-points, suggesting that vaccinating PLWH is still likely to provide some measure of immunity to SARS-CoV-2 (367,368).

In order to fully uncover the importance of T cells for protection, some critical questions need to be resolved about T-cell immunity to SARS-CoV-2 in PLWH. The features of an optimally coordinated cellular response at primary infection and the relative contribution of pre-existing/cross-reactive T-cell responses generated by exposure to other human coronaviruses remain uncertain in PLWH.

The presence of pre-existing T-cell responses has been described in HIV-negative individuals with substantial exposure to SARS-CoV-2, such as healthcare workers, without evidence of established infection, indicating a potential role for pre-existing cellular responses in clearing infection before it is fully established (186,366,471,472). Detailed assessment of pre-existing T-cell responses in PLWH, including identification of the epitopes recognised by these responses and evaluation of T-cell cross-reactivity to wild-type and emerging VOCs, and their contribution as a correlate of protection against SARS-CoV-2, would help in defining new targets for future vaccines. Experimentally, in-depth characterisation of pre-existing $CD4^+$ and $CD8^+$ T-cell immune responses in samples from exposed but uninfected HIV-1 positive individuals (such as healthcare workers living with HIV-1) and SARS-CoV-2 infected HIV-1 positive patients with a range of disease severity (asymptomatic, mild, and severe/critical infection), would provide valuable insights into their role in protective immunity.

One unexpected finding in our study was the enrichment of $CXCR3^+CD127^+CD8^+$ T-cell responses after two doses of SARS-CoV-2 vaccination in those PLWH who failed to generate an optimal neutralising response. These $CD8^+$ T cells could play a complementary role in protecting against severe disease, as previously described in critically-ill SARS-CoV-2 infected patients (344). The positive association between virus-specific responses and the proportion of $CXCR3^+CD127^+CD8^+$ T cells supports the notion that these subsets could contribute to the observed induction of T-cell responses in PLWH, who lacked optimal serological responses. However, an open question from these data is the

viral specificity of these subsets. Virus-specific responses can be assessed using multi-colour flow cytometry analysis, incorporating key functional readouts (such as activation markers and/or cytokine production/degranulation) of $CD4^+$ and $CD8^+$ T-cell responses. Due to the limited sample availability, it was not possible to perform additional work to further characterise virus-specific responses in our cohort, especially in PLWH who lacked effective serological response. Characterising virus-specific responses within $CXCR3^+CD127^+$ $CD8^+$ T cells could provide further insights into the nature of these augmented $CD8^+$ T-cell responses, including their antiviral capacity and viral specificity. Improving our understanding of the role of $CXCR3^+CD127^+$ $CD8^+$ T cells in immunity against SARS-CoV-2, and how these may contribute to protection against viral variants, is critical to define the utility of these cells in future vaccine design.

With regard to global T-cell responses, future longitudinal studies are needed to assess the dynamics of T-cell responses against SARS-CoV-2 in PLWH (with suppressed or unsuppressed viraemia) over time, and to determine what treatments/co-morbidities influence these responses and what level of T-cell dysfunction results in poorer long-term clinical outcomes, particularly in those with advanced infection Additionally, $CD8^+$ T-cell profiles and antiviral activity should be monitored in PLWH to understand whether these cells do provide the proposed immunological compensation for defects in the B-cell compartment.

7.2.2 NK cell responses in the context of introducing another virus in PLWH.

Having previously reported a reduced neutralising antibody response against SARS-CoV-2 in PLWH, I sought to investigate the contribution of other immune

cell components with antiviral and immunoregulatory capabilities. NK cells are key regulators of vaccine-induced T and B cell responses with the potential to develop memory responses that can contribute to viral clearance. I have previously described the accumulation of adaptive NK cells in PLWH (acute infection) and their role in the natural control of HIV-1 viraemia (Chapter 3). Building on this work and further expanding our findings in the setting of HIV-1/SARS-CoV-2 co-infection, I assessed how SARS-CoV-2 infection/vaccination further shapes the NK cell repertoire and functional capacity in PLWH and how these responses relate to the development of adaptive immunity. Our data show that SARS-CoV-2 infection skews NK cells towards a more differentiated/adaptive phenotype and further expands adaptive NK cells lacking FcεRIγ. Longitudinal analysis of pre- and post-vaccination samples further demonstrated an expansion of adaptive NK cells in PLWH following vaccination. Notably, adaptive NK cell subsets ($CD57^{+}Fc\varepsilon RI\gamma^{-}$) demonstrated a stronger functional capacity, with increased antibody-dependent responses to immobilised spike glycoprotein in PLWH. The increased frequencies of adaptive NK cells in SARS-CoV-2 are associated with the magnitude of T-cell and antibody responses to SARS-CoV-2, suggesting that features of adaptive NK cells could be harnessed to complement and boost vaccine-induced adaptive immunity.

7.2.3 Remaining questions in NK cell responses during SARS-CoV-2 infection.

The findings from Chapter 6 (NK cell responses in SARS-CoV-2 infection/vaccination in PLWH) complement our previous observations in AHI and

provide further evidence for the beneficial role of adaptive NK cells in controlling viral infections. However, in contrast to our acute HIV-1 study, these data reflect changes in the NK cell responses during the convalescent phase and do not exclude any initial changes over the first days/weeks following SARS-CoV-2 infection. Future longitudinal studies are required to assess the evolution of NK cell responses from the acute to convalescent phases of infection and to dissect the mechanisms underlying the dynamic adaptations of NK cells in response to SARS-CoV-2 infection in PLWH. A better understanding of the role of early NK cell responses in viral control and their evolution over the course of infection, and mechanisms underlying the early induction and durability of these responses, as well as the identification of optimal strategies for triggering these responses, could inform the development of new vaccine approaches.

Our findings describe the NK cell responses in PLWH who recovered from mild COVID-19 disease, and further investigations are needed to assess NK cell responses in severe disease (189,192). Recently, NK cells have emerged as one of the immune components that shape/modulate the clinical severity of SARS-CoV-2 infection, with some studies demonstrating an association between specific NK cell proinflammatory phenotypes and severe outcomes (187–189,195,390–392). As PLWH appear to be at elevated risk of severe COVID-19 infection (310) and HIV-1 infection is associated with inflammatory NK cell responses (39), the pre-existing NK cell dysregulation in PLWH could play a role in the progression of COVID-19 disease. Understanding the role of NK cells in

SARS-CoV-2-associated immunopathology in PLWH may guide the design of effective therapeutic interventions.

This study reported an increased frequency of adaptive NK cells, characterised by high CD57 and low FcεRIγ expression, in PLWH who recovered from mild infection. It remains unclear whether the increased frequency of adaptive NK cells in SARS-CoV-2 in PLWH is because of a direct effect of SARS-CoV-2 or whether this is a bystander phenomenon driven by HCMV reactivation and/or inflammatory responses (189). SARS-CoV-2 has been shown to induce HLA-E expression, and both immune and parenchymal cells in the lungs of patients with COVID-19 disease have elevated HLA-E expression (189,194,473). Whether this upregulated HLA-E expression will induce adaptive NK cell expansion in PLWH is still unknown. Additionally, while the data in Chapter 6 show an association between adaptive NK cells and the magnitude of virus-specific immunity, the exact mechanisms underlying these associations are currently unknown. Adaptive NK cells have been described to regulate T-cell expansion and trafficking to the site of infection through cytokine production, including IFN-γ, IP-10/CXCL10, and CCL4 (101). The increased T-cell exposure to antigens could contribute to the enhanced virus-specific responses observed in individuals with higher frequencies of adaptive NK cells (101). Additionally, adaptive NK cells have a more specialised receptor repertoire and exhibit less reactivity to activated T cells than canonical NK cells, thus sparing a larger pool of uninfected T cells from bystander killing (96). A more detailed understanding of the role of adaptive NK cells in SARS-CoV-2 responses and the development of adaptive immunity

in PLWH might help define targets that could improve antiviral responses against SARS-CoV-2 in this patient group.

7.2.4 Adaptive NK cell responses: implication for future vaccine strategies.

Beyond enhancing our understanding of adaptive immunity to SARS-CoV-2 in PLWH, it will also be important to evaluate the innate immune activation and Fc-mediated effector functions of NK cells, including antibody-dependent cellular cytotoxicity (ADCC), which has been associated with improved COVID-19 outcomes and vaccine protection (393,394,397,474). This is particularly relevant for PLWH, in whom the neutralising antibody response was found to be reduced after the primary vaccination cycle and additional/booster doses (data presented in Chapter 5), and the non-neutralising effector functions of antibodies could provide an extra layer of protection. Our data demonstrating the superior capacity of adaptive NK cells for antibody-mediated Fc-effector responses elicited by natural infection or vaccination may inform future vaccine design. These subsets can be considered as potential targets for therapeutic interventions or vaccination aimed at generating ADCC-promoting antibody responses. Given that ADCC responses are preserved against all of the tested SARS-CoV-2 variants (475), eliciting these responses via vaccination could overcome the challenges associated with the emergence of VOCs that escape neutralising responses. As new variants continue to emerge, it will be important to continue to assess the additional modes of antibody-mediated protection, including antibody-dependent NK cell responses, to better understand the immunogenicity and efficacy of the current vaccines, especially in this patient group.

Vaccination strategies aimed at inducing memory NK cell subpopulations, in combination with the induction of classical memory responses (memory B- and T- cell responses), present an exciting opportunity to overcome the limitations of conventional memory responses. The contribution of memory NK cells to vaccine-induced responses is supported by studies showing antigen-specific recall responses to other viral antigens. With relevance to PLWH, human NK cells in humanised mice exhibited vaccine-dependent, antigen-specific NK cell responses following immunisation with an HIV-encoded envelope protein (86). Similarly, NK cells from macaques infected with SIV and SHIV or adenovirus vector-vaccinated animals demonstrated long-term antigen specificity (87). Recently, such NK cell phenomena have also been reported following SARS-CoV-2 infection and vaccination. NK cells from convalescent individuals exhibited memory responses and suppressed viral replication through direct recognition of SARS-CoV-2 peptides, particularly SARS-CoV-2 Nsp13, presented via HLA-E (194). The specificity of adaptive NK cells for HLA-E-presented peptides (93), including the previously unappreciated ability of HLA-E to bind viral peptides, leading to activation of virus-specific responses, opens up the possibility for further refining these approaches. The significant role of HLA-E-restricted responses, particularly in the context of broadly reactive HLA-E-restricted T cells as key immune protection correlates in vaccinated macaques (476,477), highlights the importance of incorporating HLA-E-dependent responses in SARS-CoV-2 vaccine design. Such strategies that encourage HLA-E-dependent responses could lead to the induction of SARS-CoV-2-specific memory NK cells

with the ability to react to a wider range of antigens from different variants, complementing B- and T-cell responses.

7.3 Overall contribution.

More broadly, the findings from this thesis provide important insights into early innate and adaptive immune responses during acute viral infections, their persistence after the resolution of viral infection, and how they work together to promote viral clearance after infection and vaccination. These findings can be integrated into a large dataset to inform future vaccines or therapeutics for viral infections.

7.4 Conferences, symposiums and publications during D.Phil. studies.

7.4.1 Publications.

7.4.1.1 Primary research articles.

1. Touizer E*, **Alrubayyi A***, et al. Attenuated humoral responses in HIV after SARS-CoV-2 vaccination linked to B cell defects and altered immune profiles. iScience. 2023 Jan 20;26(1):105862. * joint authorship
2. **Alrubayyi A**, et al. Functional Restoration of Exhausted CD8 T Cells in Chronic HIV-1 Infection by Targeting Mitochondrial Dysfunction. Front Immunol. 2022;13:908697. Published 2022 Jul 5.
3. **Alrubayyi A**, et al. Characterization of humoral and SARS-CoV-2 specific T cell responses in people living with HIV. Nat Commun. Published 2021 Oct 5.
4. Touizer E*, **Alrubayyi A***, et al. Failure to seroconvert after two doses of BNT162b2 SARS-CoV-2 vaccine in a patient with uncontrolled HIV. Lancet HIV. 2021;8(6):e317-e318. *** joint authorship**

5. Gupta RK, Peppa D, Hill AL, Gálvez C, Salgado M, Pace M, McCoy L, Griffith S A, Thornhill J, **Alrubayyi A** et al. Evidence for HIV-1 cure after CCR5Δ32/Δ32 allogeneic haemopoietic stem-cell transplantation 30 months post analytical treatment interruption: a case report. Lancet HIV. 2020;7(5):e340-e347.

7.4.1.2 Review articles.

1. **Alrubayyi A**, Peppa D. Seeing SARS-CoV-2 variants through the eyes of T cells. Nat Rev Immunol. 2021;21(5):274.
2. **Alrubayyi A**. B cell persistence and evolution to SARS-CoV-2. Nat Rev Immunol. 2021;21(1):3.
3. **Alrubayyi A**. Intestinal attenuation of COVID-19 inflammation. Nat Rev Immunol. 2020;20(12):719.
4. Richter FC*, **Alrubayyi A***, et al. Impact of obesity and SARS-CoV-2 infection: implications for host defence-COVID-19 living review. Oxf Open Immunol. Published 2021 Jan 21. * joint authorship
5. Rodrigues PRS*, **Alrubayyi A***, et al. Innate immunology in COVID-19-a living review. Part II: dysregulated inflammation drives immunopathology. Oxf Open Immunol. Published 2020 Dec 8. * joint authorship
6. **Alrubayyi A**. Coordinated and sustained immune memory responses after mild COVID-19. Nat Rev Immunol. 2020;20(11):648.
7. **Alrubayyi A**. NK cells in COVID-19: protectors or opponents? [published correction appears in Nat Rev Immunol. 2020 Aug 4]. Nat Rev Immunol. 2020;20(9):520.
8. **Alrubayyi A**, et al. Harnessing Natural Killer Cell Innate and Adaptive Traits in HIV Infection. Front Cell Infect Microbiol. 2020;10:395. Published 2020 Aug 4.

7.4.2 Conferences and workshops.

1. **British HIV Association Spring Conference 2022**

Poster presentation, “SARS-CoV-2 vaccine-induced cellular immune responses in people living with HIV-1”.

2. **The 19th Meeting of the Society for Natural Immunity (SNI)- NK2022**

Two Poster presentations, “The role of adaptive NK cells during acute HIV-1 infection with different subtypes”, and “Natural Killer cell subset perturbations and functional potency in HIV/HBV co-infection”.

3. **Conference for Retroviruses and Opportunistic Infections (CROI) 2022**

Poster presentation, “The role of adaptive NK cells during acute HIV-1 infection with different subtypes”.

4. **The British Society for Immunology Congress 2021**

Joined poster presentation,“Evaluation of COVID-19 vaccine-induced immune responses in people living with HIV”.

5. **Conference for Retroviruses and Opportunistic Infections (CROI) 2021**

Selected for research highlight, Oral presentation,”Characterisation of humoral and SARS-CoV-2 specific T cell responses in people living with HIV”.

6. **Keystone Symposia for HIV Pathogenesis and Cure**

Poster presentation, “Characterisation of metabolic circuits in exhausted CD8 T cells during HIV infection”.

7. **The British Society for Immunology Congress 2019**
   Poster presentation “Characterisation of metabolic circuits in exhausted CD8 T cells during HIV-1 Infection”.

8. **VISTA and Sub Saharan African Network meeting**

Oral and poster presentation “Characterisation of Natural Killer Cell Subpopulations During Acute HIV-1 Infection and their Association with Presentation of ARS Symptoms”.

9. **EMBO workshop, CD1-MR1: Beyond MHC-restricted lymphocytes**

Poster presentation, “Characterisation of CD8 T cells acquisition of NK-like Features in Chronic HIV-1 Infection”.

7.4.3 Awards.

1. The Nuffield Department of Medicine. Graduate Student Prize (2021)
2. New Investigator Scholarship - CROI Conference (2021)
3. The British Society for Immunology Congress, Travel Bursary (2019).

Approximate word count: 48,000

References.

1. Cohen MS, Shaw GM, McMichael AJ, Haynes BF. Acute HIV-1 Infection. N Engl J Med. 2011 May 19;364(20):1943–54.

2. Cohen MS, Gay CL, Busch MP, Hecht FM. The Detection of Acute HIV Infection. The Journal of Infectious Diseases. 2010 Oct 1;202(Supplement_2):S270–7.

3. Robb ML, Eller LA, Kibuuka H, Rono K, Maganga L, Nitayaphan S, et al. Prospective Study of Acute HIV-1 Infection in Adults in East Africa and Thailand. N Engl J Med. 2016 Jun 2;374(22):2120–30.

4. Price MA, Kilembe W, Ruzagira E, Karita E, Inambao M, Sanders EJ, et al. Cohort Profile: IAVI's HIV epidemiology and early infection cohort studies in Africa to support vaccine discovery. International Journal of Epidemiology. 2021 Feb 1;50(1):29–30.

5. Hassan AS, Hare J, Gounder K, Nazziwa J, Karlson S, Olsson L, et al. A Stronger Innate Immune Response During Hyperacute HIV-1 Infection is associated with ACUTE retroviral syndrome. Clinical Infectious Diseases [Internet]. 2021 Feb 15 [cited 2021 Apr 7];(ciab139). Available from: https://doi.org/10.1093/cid/ciab139

6. Kazer SW, Walker BD, Shalek AK. Evolution and Diversity of Immune Responses during Acute HIV Infection. Immunity. 2020 Nov 17;53(5):908–24.

7. Deeks SG, Overbaugh J, Phillips A, Buchbinder S. HIV infection. Nat Rev Dis Primers. 2015 Oct 1;1(1):1–22.

8. Human Immunodeficiency Virus (HIV). Transfus Med Hemother. 2016 May;43(3):203–22.

9. Pandey A, Galvani AP. The global burden of HIV and prospects for control. The Lancet HIV. 2019 Dec 1;6(12):e809–11.

10. Global HIV & AIDS statistics — 2019 fact sheet [Internet]. [cited 2019 Sep 12]. Available from: https://www.unaids.org/en/resources/fact-sheet

11. Frank TD, Carter A, Jahagirdar D, Biehl MH, Douwes-Schultz D, Larson SL, et al. Global, regional, and national incidence, prevalence, and mortality of HIV, 1980–2017, and forecasts to 2030, for 195 countries and territories: a systematic analysis for the Global Burden of Diseases, Injuries, and Risk Factors Study 2017. The Lancet HIV. 2019 Dec 1;6(12):e831–59.

12. Global, regional, and national age–sex specific all-cause and cause-specific mortality for 240 causes of death, 1990–2013: a systematic analysis for the Global Burden of Disease Study 2013. The Lancet. 2015 Jan 10;385(9963):117–71.

13. Pantaleo G, Fauci AS. Immunopathogenesis of Hiv Infection. Annual Review of Microbiology. 1996;50(1):825–54.

14. Maher D, Wu X, Schacker T, Horbul J, Southern P. HIV binding, penetration, and primary infection in human cervicovaginal tissue. Proc Natl Acad Sci U S A. 2005 Aug 9;102(32):11504–9.

15. Mellors JW, Rinaldo CR, Gupta P, White RM, Todd JA, Kingsley LA. Prognosis in HIV-1 infection predicted by the quantity of virus in plasma. Science. 1996 May 24;272(5265):1167–70.

16. Sengupta S, Siliciano RF. Targeting the Latent Reservoir for HIV-1. Immunity. 2018 May 15;48(5):872–95.

17. Eisinger RW, Dieffenbach CW, Fauci AS. HIV Viral Load and Transmissibility of HIV Infection: Undetectable Equals Untransmittable. JAMA. 2019 Feb 5;321(5):451–2.

18. Hemelaar J, Gouws E, Ghys PD, Osmanov S. Global and regional distribution of HIV-1 genetic subtypes and recombinants in 2004. AIDS. 2006 Oct 24;20(16):W13-23.

19. Hemelaar J, Elangovan R, Yun J, Dickson-Tetteh L, Fleminger I, Kirtley S, et al. Global and regional molecular epidemiology of HIV-1, 1990–2015: a systematic review, global survey, and trend analysis. The Lancet Infectious Diseases. 2019 Feb 1;19(2):143–55.

20. Geretti AM. HIV-1 subtypes: epidemiology and significance for HIV management. Current Opinion in Infectious Diseases. 2006 Feb;19(1):1–7.

21. Bbosa N, Kaleebu P, Ssemwanga D. HIV subtype diversity worldwide. Current Opinion in HIV and AIDS. 2019 May;14(3):153–60.

22. Taylor BS, Sobieszczyk ME, McCutchan FE, Hammer SM. The Challenge of HIV-1 Subtype Diversity. N Engl J Med. 2008 Apr 10;358(15):1590–602.

23. Santoro MM, Perno CF. HIV-1 Genetic Variability and Clinical Implications. ISRN Microbiol. 2013 Jun 17;2013:481314.

24. Billings E, Sanders-Buell E, Bose M, Kijak GH, Bradfield A, Crossler J, et al. HIV-1 Genetic Diversity Among Incident Infections in Mbeya, Tanzania. AIDS Res Hum Retroviruses. 2017 Apr;33(4):373–81.

25. Gounder K, Oyaro M, Padayachi N, Zulu TM, de Oliveira T, Wylie J, et al. Complex Subtype Diversity of HIV-1 Among Drug Users in Major Kenyan Cities. AIDS Res Hum Retroviruses. 2017 May;33(5):500–10.

26. Kiwanuka N, Laeyendecker O, Robb M, Kigozi G, Arroyo M, McCutchan F, et al. Effect of human immunodeficiency virus Type 1 (HIV-1) subtype on disease progression in persons from Rakai, Uganda, with incident HIV-1 infection. J Infect Dis. 2008 Mar 1;197(5):707–13.

27. Kaleebu P, French N, Mahe C, Yirrell D, Watera C, Lyagoba F, et al. Effect of human immunodeficiency virus (HIV) type 1 envelope subtypes A and D on disease progression in a large cohort of HIV-1-positive persons in Uganda. J Infect Dis. 2002 May 1;185(9):1244–50.

28. Vasan A, Renjifo B, Hertzmark E, Chaplin B, Msamanga G, Essex M, et al. Different rates of disease progression of HIV type 1 infection in Tanzania based on infecting subtype. Clin Infect Dis. 2006 Mar 15;42(6):843–52.

29. Baeten JM, Chohan B, Lavreys L, Chohan V, McClelland RS, Certain L, et al. HIV-1 subtype D infection is associated with faster disease progression than subtype A in spite of similar plasma HIV-1 loads. J Infect Dis. 2007 Apr 15;195(8):1177–80.

30. Palm AA, Esbjörnsson J, Månsson F, Kvist A, Isberg PE, Biague A, et al. Faster Progression to AIDS and AIDS-Related Death Among Seroincident Individuals Infected With Recombinant HIV-1 A3/CRF02_AG Compared With Sub-subtype A3. The Journal of Infectious Diseases. 2014 Mar 1;209(5):721–8.

31. Amornkul PN, Karita E, Kamali A, Rida WN, Sanders EJ, Lakhi S, et al. Disease progression by infecting HIV-1 subtype in a seroconverter cohort in sub-Saharan Africa. AIDS. 2013 Nov 13;27(17):2775–86.

32. Ssemwanga D, Nsubuga RN, Mayanja BN, Lyagoba F, Magambo B, Yirrell D, et al. Effect of HIV-1 Subtypes on Disease Progression in Rural Uganda: A Prospective Clinical Cohort Study. PLOS ONE. 2013 Aug 12;8(8):e71768.

33. Price MA, Rida W, Kilembe W, Karita E, Inambao M, Ruzagira E, et al. Control of the HIV-1 Load Varies by Viral Subtype in a Large Cohort of African Adults With Incident HIV-1 Infection. The Journal of Infectious Diseases. 2019 Jul 2;220(3):432–41.

34. Sanders EJ, Price MA, Karita E, Kamali A, Kilembe W, Bekker LG, et al. Differences in acute retroviral syndrome by HIV-1 subtype in a multicentre cohort study in Africa. AIDS. 2017 Nov 28;31(18):2541–6.

35. Siemieniuk RA, Beckthold B, Gill MJ. Increasing HIV subtype diversity and its clinical implications in a sentinel North American population. Can J Infect Dis Med Microbiol. 2013;24(2):69–73.

36. Ball SC, Abraha A, Collins KR, Marozsan AJ, Baird H, Quiñones-Mateu ME, et al. Comparing the ex vivo fitness of CCR5-tropic human immunodeficiency virus type 1 isolates of subtypes B and C. J Virol. 2003 Jan;77(2):1021–38.

37. Abraha A, Nankya IL, Gibson R, Demers K, Tebit DM, Johnston E, et al. CCR5- and CXCR4-tropic subtype C human immunodeficiency virus type 1 isolates have a lower level of pathogenic fitness than other dominant group M subtypes: implications for the epidemic. J Virol. 2009 Jun;83(11):5592–605.

38. Ariën KK, Abraha A, Quiñones-Mateu ME, Kestens L, Vanham G, Arts EJ. The replicative fitness of primary human immunodeficiency virus type 1 (HIV-1) group M, HIV-1 group O, and HIV-2 isolates. J Virol. 2005 Jul;79(14):8979–90.

39. Njai HF, Gali Y, Vanham G, Clybergh C, Jennes W, Vidal N, et al. The predominance of Human Immunodeficiency Virus type 1 (HIV-1) circulating recombinant form 02 (CRF02_AG) in West Central Africa may be related to its replicative fitness. Retrovirology. 2006 Jul 3;3:40.

40. Konings FAJ, Burda ST, Urbanski MM, Zhong P, Nadas A, Nyambi PN. Human immunodeficiency virus type 1 (HIV-1) circulating recombinant form 02_AG (CRF02_AG) has a higher in vitro replicative capacity than its parental subtypes A and G. J Med Virol. 2006 May;78(5):523–34.

41. Ng OT, Laeyendecker O, Redd AD, Munshaw S, Grabowski MK, Paquet AC, et al. HIV type 1 polymerase gene polymorphisms are associated with phenotypic differences in replication capacity and disease progression. J Infect Dis. 2014 Jan 1;209(1):66–73.

42. Mann JK, Chopera D, Omarjee S, Kuang XT, Le AQ, Anmole G, et al. Nef-mediated down-regulation of CD4 and HLA class I in HIV-1 subtype C infection: association with disease progression and influence of immune pressure. Virology. 2014 Nov;468–470:214–25.

43. Mann JK, Byakwaga H, Kuang XT, Le AQ, Brumme CJ, Mwimanzi P, et al. Ability of HIV-1 Nef to downregulate CD4 and HLA class I differs among viral subtypes. Retrovirology. 2013 Sep 16;10:100.

44. Chen Q, Zeng D, She Y, Lyu Y, Gong X, Feinstein MJ, et al. Different transmission routes and the risk of advanced HIV disease: A systematic review and network meta-analysis of observational studies. eClinicalMedicine. 2019 Nov 1;16:121–8.

45. Parrish NF, Gao F, Li H, Giorgi EE, Barbian HJ, Parrish EH, et al. Phenotypic properties of transmitted founder HIV-1. Proceedings of the National Academy of Sciences. 2013 Apr 23;110(17):6626–33.

46. Salazar-Gonzalez JF, Salazar MG, Keele BF, Learn GH, Giorgi EE, Li H, et al. Genetic identity, biological phenotype, and evolutionary pathways of transmitted/founder viruses in acute and early HIV-1 infection. J Exp Med. 2009 Jun 8;206(6):1273–89.

47. Lumngwena EN, Metenou S, Masson L, Cicala C, Arthos J, Woodman Z. HIV-1 subtype C transmitted founders modulate dendritic cell inflammatory responses. Retrovirology. 2020 Jul 2;17:17.

48. McMichael AJ, Borrow P, Tomaras GD, Goonetilleke N, Haynes BF. The immune response during acute HIV-1 infection: clues for vaccine development. Nat Rev Immunol. 2010;10(1):11–23.

49. Schacker TW, Hughes JP, Shea T, Coombs RW, Corey L. Biological and virologic characteristics of primary HIV infection. Ann Intern Med. 1998 Apr 15;128(8):613–20.

50. Ho DD, Neumann AU, Perelson AS, Chen W, Leonard JM, Markowitz M. Rapid turnover of plasma virions and CD4 lymphocytes in HIV-1 infection. Nature. 1995 Jan 12;373(6510):123–6.

51. Garcia-Tellez T, Huot N, Ploquin MJ, Rascle P, Jacquelin B, Müller-Trutwin M. Non-human primates in HIV research: Achievements, limits and alternatives. Infect Genet Evol. 2016 Dec;46:324–32.

52. Dong KL, Moodley A, Kwon DS, Ghebremichael MS, Dong M, Ismail N, et al. Detection and treatment of Fiebig stage I HIV-1 infection in young at-risk women in South Africa: a prospective cohort study. The Lancet HIV. 2018 Jan 1;5(1):e35–44.

53. Sanders EJ, Mugo P, Prins HAB, Wahome E, Thiong'o AN, Mwashigadi G, et al. Acute HIV-1 infection is as common as malaria in young febrile adults seeking care in coastal Kenya. AIDS. 2014 Jun 1;28(9):1357–63.

54. Stacey AR, Norris PJ, Qin L, Haygreen EA, Taylor E, Heitman J, et al. Induction of a Striking Systemic Cytokine Cascade prior to Peak Viremia in Acute Human Immunodeficiency Virus Type 1 Infection, in Contrast to More Modest and Delayed Responses in Acute Hepatitis B and C Virus Infections. Journal of Virology. 2009 Apr 15;83(8):3719–33.

55. Haase AT. Early Events in Sexual Transmission of HIV and SIV and Opportunities for Interventions. Annu Rev Med. 2011 Feb 18;62(1):127–39.

56. Muema DM, Akilimali NA, Ndumnego OC, Rasehlo SS, Durgiah R, Ojwach DBA, et al. Association between the cytokine storm, immune cell dynamics, and viral replicative capacity in hyperacute HIV infection. BMC Med. 2020 Mar 25;18(1):81.

57. Bosinger SE, Utay NS. Type I Interferon: Understanding Its Role in HIV Pathogenesis and Therapy. Curr HIV/AIDS Rep. 2015 Mar 1;12(1):41–53.

58. Kazer SW, Aicher TP, Muema DM, Carroll SL, Ordovas-Montanes J, Miao VN, et al. Integrated single-cell analysis of multicellular immune dynamics during hyperacute HIV-1 infection. Nature Medicine. 2020 Apr;26(4):511–8.

59. Breen EC. Pro- and anti-inflammatory cytokines in human immunodeficiency virus infection and acquired immunodeficiency syndrome. Pharmacol Ther. 2002 Sep;95(3):295–304.

60. Kapaata A, Balinda SN, Hare J, Leonova O, Kikaire B, Egesa M, et al. Infection with HIV-1 subtype D among acutely infected Ugandans is associated with higher median concentration of cytokines compared to subtype A. IJID Regions. 2022 Jun 1;3:89–95.

61. Borrow P. Innate immunity in acute HIV-1 infection. Curr Opin HIV AIDS. 2011 Sep;6(5):353–63.

62. Björkström NK, Strunz B, Ljunggren HG. Natural killer cells in antiviral immunity. Nat Rev Immunol. 2021 Jun 11;1–12.

63. Scully E, Alter G. NK Cells in HIV Disease. Curr HIV/AIDS Rep. 2016 Apr;13(2):85–94.

64. Sun JC, Lanier LL. NK cell development, homeostasis and function: parallels with CD8$^+$ T cells. Nat Rev Immunol. 2011 Aug 26;11(10):645–57.

65. Long EO, Kim HS, Liu D, Peterson ME, Rajagopalan S. Controlling natural killer cell responses: integration of signals for activation and inhibition. Annu Rev Immunol. 2013;31:227–58.

66. Orr MT, Lanier LL. Natural killer cell education and tolerance. Cell. 2010 Sep 17;142(6):847–56.

67. Lanier LL. Evolutionary struggles between NK cells and viruses. Nat Rev Immunol. 2008 Apr;8(4):259–68.

68. Elliott JM, Yokoyama WM. Unifying concepts of MHC-dependent natural killer cell education. Trends Immunol. 2011 Aug;32(8):364–72.

69. Boudreau JE, Hsu KC. Natural killer cell education in human health and disease. Curr Opin Immunol. 2018;50:102–11.

70. Hammer Q, Rückert T, Romagnani C. Natural killer cell specificity for viral infections. Nat Immunol. 2018 Aug;19(8):800–8.

71. van Erp EA, van Kampen MR, van Kasteren PB, de Wit J. Viral Infection of Human Natural Killer Cells. Viruses [Internet]. 2019 Mar 12 [cited 2020 Dec 27];11(3). Available from: https://www.ncbi.nlm.nih.gov/pmc/articles/PMC6466310/

72. Peppa D, Gill US, Reynolds G, Easom NJW, Pallett LJ, Schurich A, et al. Up-regulation of a death receptor renders antiviral T cells susceptible to NK cell-mediated deletion. J Exp Med. 2013 Jan 14;210(1):99–114.

73. Chen X, Lin M, Qian S, Zhang Z, Fu Y, Xu J, et al. The Early Antibody-Dependent Cell-Mediated Cytotoxicity Response Is Associated With Lower Viral Set Point in Individuals With Primary HIV Infection. Front Immunol [Internet]. 2018 Oct 9 [cited 2020 Apr 22];9. Available from: https://www.ncbi.nlm.nih.gov/pmc/articles/PMC6189277/

74. Brandstadter JD, Yang Y. Natural Killer Cell Responses to Viral Infection. J Innate Immun. 2011 Apr;3(3):274–9.

75. Rydyznski CE, Waggoner SN. Boosting vaccine efficacy the natural (killer) way. Trends Immunol. 2015 Sep;36(9):536–46.

76. Piccioli D, Sbrana S, Melandri E, Valiante NM. Contact-dependent stimulation and inhibition of dendritic cells by natural killer cells. J Exp Med. 2002 Feb 4;195(3):335–41.

77. Gray JD, Hirokawa M, Ohtsuka K, Horwitz DA. Generation of an Inhibitory Circuit Involving CD8+ T Cells, IL-2, and NK Cell-Derived TGF-β: Contrasting Effects of Anti-CD2 and Anti-CD3. The Journal of Immunology. 1998 Mar 1;160(5):2248–54.

78. Morandi B, Bougras G, Muller WA, Ferlazzo G, Münz C. NK cells of human secondary lymphoid tissues enhance T cell polarization via IFN-γ secretion. European Journal of Immunology. 2006;36(9):2394–400.

79. Martín-Fontecha A, Thomsen LL, Brett S, Gerard C, Lipp M, Lanzavecchia A, et al. Induced recruitment of NK cells to lymph nodes provides IFN-γ for TH1 priming. Nat Immunol. 2004 Dec;5(12):1260–5.

80. Adam C, King S, Allgeier T, Braumüller H, Lüking C, Mysliwietz J, et al. DC-NK cell cross talk as a novel CD4+ T-cell–independent pathway for antitumor CTL induction. Blood. 2005 Jul 1;106(1):338–44.

81. Mocikat R, Braumüller H, Gumy A, Egeter O, Ziegler H, Reusch U, et al. Natural Killer Cells Activated by MHC Class ILow Targets Prime Dendritic Cells to Induce Protective CD8 T Cell Responses. Immunity. 2003 Oct 1;19(4):561–9.

82. Joshi NS, Cui W, Chandele A, Lee HK, Urso DR, Hagman J, et al. Inflammation Directs Memory Precursor and Short-Lived Effector CD8+ T Cell Fates via the Graded Expression of T-bet Transcription Factor. Immunity. 2007 Aug 24;27(2):281–95.

83. Ali A, Canaday LM, Feldman HA, Cevik H, Moran MT, Rajaram S, et al. Natural killer cell immunosuppressive function requires CXCR3-dependent redistribution within lymphoid tissues. J Clin Invest [Internet]. 2021 Jul 27 [cited 2021 Aug 16]; Available from: https://www.jci.org/articles/view/146686

84. Bradley T, Peppa D, Pedroza-Pacheco I, Li D, Cain DW, Henao R, et al. RAB11FIP5 Expression and Altered Natural Killer Cell Function Are Associated with Induction of HIV Broadly Neutralizing Antibody Responses. Cell. 2018 04;175(2):387-399.e17.

85. Rydyznski C, Daniels KA, Karmele EP, Brooks TR, Mahl SE, Moran MT, et al. Generation of cellular immune memory and B-cell immunity is impaired by natural killer cells. Nature Communications. 2015 Feb 27;6(1):1–14.

86. Nikzad R, Angelo LS, Aviles-Padilla K, Le DT, Singh VK, Bimler L, et al. Human natural killer cells mediate adaptive immunity to viral antigens. Science Immunology [Internet]. 2019 May 10 [cited 2020 Feb 26];4(35).

87. Reeves RK, Li H, Jost S, Blass E, Li H, Schafer JL, et al. Antigen-specific NK cell memory in rhesus macaques. Nature Immunology. 2015 Sep;16(9):927–32.

88. O'Sullivan TE, Sun JC, Lanier LL. Natural Killer Cell Memory. Immunity. 2015 Oct 20;43(4):634–45.

89. Gumá M, Budt M, Sáez A, Brckalo T, Hengel H, Angulo A, et al. Expansion of CD94/NKG2C+ NK cells in response to human cytomegalovirus-infected fibroblasts. Blood. 2006 May 1;107(9):3624–31.

90. Béziat V, Liu LL, Malmberg JA, Ivarsson MA, Sohlberg E, Björklund AT, et al. NK cell responses to cytomegalovirus infection lead to stable imprints in the human KIR repertoire and involve activating KIRs. Blood. 2013 Apr 4;121(14):2678–88.

91. Peppa D, Pedroza-Pacheco I, Pellegrino P, Williams I, Maini MK, Borrow P. Adaptive Reconfiguration of Natural Killer Cells in HIV-1 Infection. Front Immunol. 2018;9:474.

92. Hammer Q, Rückert T, Borst EM, Dunst J, Haubner A, Durek P, et al. Peptide-specific recognition of human cytomegalovirus strains controls adaptive natural killer cells. Nat Immunol. 2018;19(5):453–63.

93. Rölle A, Meyer M, Calderazzo S, Jäger D, Momburg F. Distinct HLA-E Peptide Complexes Modify Antibody-Driven Effector Functions of Adaptive NK Cells. Cell Rep. 2018 21;24(8):1967-1976.e4.

94. Gumá M, Angulo A, Vilches C, Gómez-Lozano N, Malats N, López-Botet M. Imprint of human cytomegalovirus infection on the NK cell receptor repertoire. Blood. 2004 Dec 1;104(12):3664–71.

95. Luetke-Eversloh M, Hammer Q, Durek P, Nordström K, Gasparoni G, Pink M, et al. Human cytomegalovirus drives epigenetic imprinting of the IFNG locus in NKG2Chi natural killer cells. PLoS Pathog. 2014 Oct;10(10):e1004441.

96. Schlums H, Cichocki F, Tesi B, Theorell J, Beziat V, Holmes TD, et al. Cytomegalovirus infection drives adaptive epigenetic diversification of NK cells with altered signaling and effector function. Immunity. 2015 Mar 17;42(3):443–56.

97. Gyurova IE, Schlums H, Sucharew H, Ambroggio L, Ochayon DE, Win HT, et al. Dynamic Changes in Natural Killer Cell Subset Frequencies in the Absence of Cytomegalovirus Infection. Front Immunol. 2019;10:2728.

98. Zhou J, Amran FS, Kramski M, Angelovich TA, Elliott J, Hearps AC, et al. An NK Cell Population Lacking FcRγ Is Expanded in Chronically Infected HIV Patients. The Journal of Immunology. 2015 May 15;194(10):4688–97.

99. Lee S, Doualeh M, Affandi JS, Makwana N, Irish A, Price P. Functional and clinical consequences of changes to natural killer cell phenotypes driven by chronic cytomegalovirus infections. J Med Virol. 2019 Jun;91(6):1120–7.

100. Rölle A, Pollmann J, Ewen EM, Le VTK, Halenius A, Hengel H, et al. IL-12-producing monocytes and HLA-E control HCMV-driven NKG2C+ NK cell expansion. J Clin Invest. 2014 Dec;124(12):5305–16.

101. Basílio-Queirós D, Venturini L, Luther-Wolf S, Dammann E, Ganser A, Stadler M, et al. Adaptive NK cells undergo a dynamic modulation in response to human cytomegalovirus and recruit T cells in in vitro migration assays. Bone Marrow Transplant. 2022 May;57(5):712–20.

102. Duhan V, Hamdan TA, Xu HC, Shinde P, Bhat H, Li F, et al. NK cell–intrinsic FcεRIγ limits CD8+ T-cell expansion and thereby turns an acute into a chronic viral infection. PLoS Pathog [Internet]. 2019 Jun 20 [cited 2020 May 26];15(6). Available from: https://www.ncbi.nlm.nih.gov/pmc/articles/PMC6605677/

103. Lee J, Zhang T, Hwang I, Kim A, Nitschke L, Kim M, et al. Epigenetic modification and antibody-dependent expansion of memory-like NK cells in human cytomegalovirus-infected individuals. Immunity. 2015 Mar 17;42(3):431–42.

104. Lanier LL, Le AM, Civin CI, Loken MR, Phillips JH. The relationship of CD16 (Leu-11) and Leu-19 (NKH-1) antigen expression on human peripheral blood NK cells and cytotoxic T lymphocytes. J Immunol. 1986 Jun 15;136(12):4480–6.

105. Liu W, Scott JM, Langguth E, Chang H, Park PH, Kim S. FcRγ Gene Editing Reprograms Conventional NK Cells to Display Key Features of Adaptive Human NK Cells. iScience. 2020 Oct 20;23(11):101709.

106. Hwang I, Zhang T, Scott JM, Kim AR, Lee T, Kakarla T, et al. Identification of human NK cells that are deficient for signaling adaptor FcRγ and specialized for antibody-dependent immune functions. Int Immunol. 2012 Dec;24(12):793–802.

107. Berrien-Elliott MM, Wagner JA, Fehniger TA. Human Cytokine-Induced Memory-Like Natural Killer Cells. J Innate Immun. 2015 Oct;7(6):563–71.

108. Romee R, Schneider SE, Leong JW, Chase JM, Keppel CR, Sullivan RP, et al. Cytokine activation induces human memory-like NK cells. Blood. 2012 Dec 6;120(24):4751–60.

109. Wang Y, Lifshitz L, Gellatly K, Vinton CL, Busman-Sahay K, McCauley S, et al. HIV-1-induced cytokines deplete homeostatic innate lymphoid cells and expand TCF7-dependent memory NK cells. Nat Immunol. 2020 Mar;21(3):274–86.

110. Gang M, Wong P, Berrien-Elliott MM, Fehniger TA. Memory-like natural killer cells for cancer immunotherapy. Semin Hematol. 2020 Oct;57(4):185–93.

111. Zapata W, Aguilar-Jiménez W, Pineda-Trujillo N, Rojas W, Estrada H, Rugeles MT. Influence of CCR5 and CCR2 genetic variants in the resistance/susceptibility to HIV in serodiscordant couples from Colombia. AIDS Res Hum Retroviruses. 2013 Dec;29(12):1594–603.

112. Martin MP, Gao X, Lee JH, Nelson GW, Detels R, Goedert JJ, et al. Epistatic interaction between KIR3DS1 and HLA-B delays the progression to AIDS. Nat Genet. 2002 Aug;31(4):429–34.

113. Martin MP, Qi Y, Gao X, Yamada E, Martin JN, Pereyra F, et al. Innate partnership of HLA-B and KIR3DL1 subtypes against HIV-1. Nat Genet. 2007 Jun;39(6):733–40.

114. Alter G, Teigen N, Ahern R, Streeck H, Meier A, Rosenberg ES, et al. Evolution of innate and adaptive effector cell functions during acute HIV-1 infection. J Infect Dis. 2007 May 15;195(10):1452–60.

115. Alter G, Teigen N, Davis BT, Addo MM, Suscovich TJ, Waring MT, et al. Sequential deregulation of NK cell subset distribution and function starting in acute HIV-1 infection. Blood. 2005 Nov 15;106(10):3366–9.

116. Naranbhai V, Altfeld M, Karim SSA, Ndung'u T, Karim QA, Carr WH. Changes in Natural Killer cell activation and function during primary HIV-1 Infection. PLoS ONE. 2013;8(1):e53251.

117. Sawyer LA, Katzenstein DA, Hendry RM, Boone EJ, Vujcic LK, Williams CC, et al. Possible beneficial effects of neutralizing antibodies and antibody-dependent, cell-mediated cytotoxicity in human immunodeficiency virus infection. AIDS Res Hum Retroviruses. 1990 Mar;6(3):341–56.

118. Mavilio D, Lombardo G, Benjamin J, Kim D, Follman D, Marcenaro E, et al. Characterization of CD56-/CD16+ natural killer (NK) cells: a highly dysfunctional NK subset expanded in HIV-infected viremic individuals. Proc Natl Acad Sci USA. 2005 Feb 22;102(8):2886–91.

119. Jost S, Moreno-Nieves UY, Garcia-Beltran WF, Rands K, Reardon J, Toth I, et al. Dysregulated Tim-3 expression on natural killer cells is associated with increased Galectin-9 levels in HIV-1 infection. Retrovirology. 2013 Jul 18;10:74.

120. Zhang X, Lu X, Cheung AKL, Zhang Q, Liu Z, Li Z, et al. Analysis of the Characteristics of TIGIT-Expressing CD3−CD56+NK Cells in Controlling Different Stages of HIV-1 Infection. Front Immunol [Internet]. 2021 Feb 26 [cited 2021 Apr 4];12. Available from: https://www.ncbi.nlm.nih.gov/pmc/articles/PMC7953050/

121. Crocker PR, Paulson JC, Varki A. Siglecs and their roles in the immune system. Nat Rev Immunol. 2007 Apr;7(4):255–66.

122. Brunetta E, Fogli M, Varchetta S, Bozzo L, Hudspeth KL, Marcenaro E, et al. The decreased expression of Siglec-7 represents an early marker of dysfunctional natural killer-cell subsets associated with high levels of HIV-1 viremia. Blood. 2009 Oct 29;114(18):3822–30.

123. Mela CM, Burton CT, Imami N, Nelson M, Steel A, Gazzard BG, et al. Switch from inhibitory to activating NKG2 receptor expression in HIV-1 infection: lack of reversion with highly active antiretroviral therapy. AIDS. 2005 Nov 4;19(16):1761–9.

124. Peppa D, Pedroza-Pacheco I, Pellegrino P, Williams I, Maini MK, Borrow P. Adaptive Reconfiguration of Natural Killer Cells in HIV-1 Infection. Front Immunol [Internet]. 2018 Mar 16 [cited 2019 Sep 17];9.

125. Bachtel ND, Umviligihozo G, Pickering S, Mota TM, Liang H, Prete GQD, et al. HLA-C downregulation by HIV-1 adapts to host HLA genotype. PLOS Pathogens. 2018 Sep 4;14(9):e1007257.

126. Ma M, Wang Z, Chen X, Tao A, He L, Fu S, et al. NKG2C+NKG2A− Natural Killer Cells are Associated with a Lower Viral Set Point and may Predict Disease Progression in Individuals with Primary HIV Infection. Front Immunol [Internet]. 2017 Sep 20 [cited 2019 Feb 19];8. Available from: https://www.ncbi.nlm.nih.gov/pmc/articles/PMC5611385/

127. Gondois-Rey F, Chéret A, Mallet F, Bidaut G, Granjeaud S, Lécuroux C, et al. A Mature NK Profile at the Time of HIV Primary Infection Is Associated with an Early Response to cART. Front Immunol. 2017;8:54.

128. Jost S, Lucar O, Yoder T, Kroll K, Sugawara S, Smith S, et al. Human antigen-specific memory natural killer cell responses develop against HIV-1 and influenza virus and are dependent on MHC-E restriction [Internet]. Immunology; 2020 Nov [cited 2020 Dec 27]. Available from: http://biorxiv.org/lookup/doi/10.1101/2020.11.09.374348

129. Wijaya RS, Read SA, Truong NR, Han S, Chen D, Shahidipour H, et al. HBV vaccination and HBV infection induces HBV-specific natural killer cell memory. Gut. 2021 Feb 1;70(2):357–69.

130. Reeves RK, Evans TI, Gillis J, Johnson RP. Simian immunodeficiency virus infection induces expansion of alpha4beta7+ and cytotoxic CD56+ NK cells. J Virol. 2010 Sep;84(17):8959–63.

131. Sips M, Sciaranghella G, Diefenbach T, Dugast AS, Berger CT, Liu Q, et al. Altered distribution of mucosal NK cells during HIV infection. Mucosal Immunol. 2012 Jan;5(1):30–40.

132. Huot N, Rascle P, Petitdemange C, Contreras V, Stürzel CM, Baquero E, et al. SIV-induced terminally differentiated adaptive NK cells in lymph nodes associated with enhanced MHC-E restricted activity. Nature Communications. 2021 Feb 24;12(1):1282.

133. Rasid O, Chevalier C, Camarasa TMN, Fitting C, Cavaillon JM, Hamon MA. H3K4me1 Supports Memory-like NK Cells Induced by Systemic Inflammation. Cell Reports. 2019 Dec;29(12):3933-3945.e3.

134. Rosendahl Huber S, van Beek J, de Jonge J, Luytjes W, van Baarle D. T Cell Responses to Viral Infections – Opportunities for Peptide Vaccination. Front Immunol. 2014 Apr 16;5:171.

135. Blank CU, Haining WN, Held W, Hogan PG, Kallies A, Lugli E, et al. Defining 'T cell exhaustion'. Nat Rev Immunol. 2019 Nov;19(11):665–74.

136. A H, V D, C C, Pa B, Ra DP, G P. Functional Signatures of Protective Antiviral T-cell Immunity in Human Virus Infections [Internet]. Vol. 211, Immunological reviews. Immunol Rev; 2006 [cited 2020 May 20]. Available from: https://pubmed.ncbi.nlm.nih.gov/16824132/

137. Kim TS, Shin EC. The activation of bystander CD8+ T cells and their roles in viral infection. Exp Mol Med. 2019 Dec;51(12):1–9.

138. Jagadeesh A, Prathyusha AMVN, Sheela GM, Bramhachari PV. T Cells in Viral Infections: The Myriad Flavours of Antiviral Immunity. Dynamics of Immune Activation in Viral Diseases. 2019 Nov 5;139–48.

139. Moss P. The T cell immune response against SARS-CoV-2. Nat Immunol. 2022 Feb;23(2):186–93.

140. Walker B, McMichael A. The T-Cell Response to HIV. Cold Spring Harb Perspect Med. 2012 Nov;2(11):a007054.

141. Rouse BT, Sehrawat S. Immunity and immunopathology to viruses: what decides the outcome? Nat Rev Immunol. 2010 Jul;10(7):514–26.

142. Appay V, Papagno L, Spina CA, Hansasuta P, King A, Jones L, et al. Dynamics of T cell responses in HIV infection. J Immunol. 2002 Apr 1;168(7):3660–6.

143. Pantaleo G, Demarest JF, Soudeyns H, Graziosi C, Denis F, Adelsberger JW, et al. Major expansion of CD8+ T cells with a predominant V beta usage during the primary immune response to HIV. Nature. 1994 Aug 11;370(6489):463–7.

144. Takata H, Buranapraditkun S, Kessing C, Fletcher JLK, Muir R, Tardif V, et al. Delayed differentiation of potent effector CD8+ T cells reducing viremia and reservoir seeding in acute HIV infection. Science Translational Medicine. 2017 Feb 15;9(377):eaag1809.

145. Ndhlovu ZM, Kamya P, Mewalal N, Kløverpris HN, Nkosi T, Pretorius K, et al. Magnitude and Kinetics of CD8+ T Cell Activation during Hyperacute HIV Infection Impact Viral Set Point. Immunity. 2015 Sep 15;43(3):591–604.

146. Demers KR, Makedonas G, Buggert M, Eller MA, Ratcliffe SJ, Goonetilleke N, et al. Temporal Dynamics of CD8+ T Cell Effector Responses during Primary HIV Infection. PLOS Pathogens. 2016 Aug 3;12(8):e1005805.

147. Streeck H, Lu R, Beckwith N, Milazzo M, Liu M, Routy JP, et al. Emergence of Individual HIV-Specific CD8 T Cell Responses during Primary HIV-1 Infection Can Determine Long-Term Disease Outcome. Journal of Virology. 2014 Nov;88(21):12793–801.

148. Ndhlovu Z, Kamya P, Mewalal N, Kløverpris HN, Nkosi T, Pretorius K, et al. Magnitude and kinetics of CD8+ T cell activation during hyperacute HIV infection impacts viral set point. Immunity. 2015 Sep 15;43(3):591–604.

149. Streeck H, Jolin JS, Qi Y, Yassine-Diab B, Johnson RC, Kwon DS, et al. Human immunodeficiency virus type 1-specific CD8+ T-cell responses during primary infection are

major determinants of the viral set point and loss of CD4+ T cells. J Virol. 2009 Aug;83(15):7641–8.

150. Streeck H, Nixon DF. T cell immunity in acute HIV-1 infection. J Infect Dis. 2010 Oct 15;202(Suppl 2):S302–8.

151. Beltra JC, Manne S, Abdel-Hakeem MS, Kurachi M, Giles JR, Chen Z, et al. Developmental Relationships of Four Exhausted CD8+ T Cell Subsets Reveals Underlying Transcriptional and Epigenetic Landscape Control Mechanisms. Immunity [Internet]. 2020 May 11 [cited 2020 May 19];

152. Alrubayyi A, Moreno-Cubero E, Hameiri-Bowen D, Matthews R, Rowland-Jones S, Schurich A, et al. Functional Restoration of Exhausted CD8 T Cells in Chronic HIV-1 Infection by Targeting Mitochondrial Dysfunction. Frontiers in Immunology [Internet]. 2022 [cited 2022 Sep 12];13.

153. Arthos J, Cicala C, Martinelli E, Macleod K, Van Ryk D, Wei D, et al. HIV-1 envelope protein binds to and signals through integrin α4β7, the gut mucosal homing receptor for peripheral T cells. Nat Immunol. 2008 Mar;9(3):301–9.

154. Chevalier MF, Didier C, Girard PM, Manea ME, Campa P, Barré-Sinoussi F, et al. CD4 T-Cell Responses in Primary HIV Infection: Interrelationship with Immune Activation and Virus Burden. Frontiers in Immunology [Internet]. 2016 [cited 2022 Sep 10];7. Available from: https://www.frontiersin.org/articles/10.3389/fimmu.2016.00395

155. Soghoian DZ, Jessen H, Flanders M, Sierra-Davidson K, Cutler S, Pertel T, et al. HIV-Specific Cytolytic CD4 T Cell Responses During Acute HIV Infection Predict Disease Outcome. Science Translational Medicine. 2012 Feb 29;4(123):123ra25-123ra25.

156. Maenetje P, Riou C, Casazza JP, Ambrozak D, Hill B, Gray G, et al. A steady state of CD4+ T cell memory maturation and activation is established during primary subtype C HIV-1 infection. J Immunol. 2010 May 1;184(9):4926–35.

157. WHO Coronavirus (COVID-19) Dashboard [Internet]. [cited 2022 Aug 19]. Available from: https://covid19.who.int

158. Hu B, Guo H, Zhou P, Shi ZL. Characteristics of SARS-CoV-2 and COVID-19. Nat Rev Microbiol. 2021 Mar;19(3):141–54.

159. Williamson EJ, Walker AJ, Bhaskaran K, Bacon S, Bates C, Morton CE, et al. Factors associated with COVID-19-related death using OpenSAFELY. Nature. 2020 Aug;584(7821):430–6.

160. Wu Z, McGoogan JM. Characteristics of and Important Lessons From the Coronavirus Disease 2019 (COVID-19) Outbreak in China: Summary of a Report of 72 314 Cases From the Chinese Center for Disease Control and Prevention. JAMA. 2020 Apr 7;323(13):1239–42.

161. De Francesco D, Wit FW, Bürkle A, Oehlke S, Kootstra NA, Winston A, et al. Do people living with HIV experience greater age advancement than their HIV-negative counterparts? AIDS. 2019 Feb 1;33(2):259–68.

162. Guaraldi G, Orlando G, Zona S, Menozzi M, Carli F, Garlassi E, et al. Premature age-related comorbidities among HIV-infected persons compared with the general population. Clin Infect Dis. 2011 Dec;53(11):1120–6.

163. Deeks SG, Phillips AN. HIV infection, antiretroviral treatment, ageing, and non-AIDS related morbidity. BMJ. 2009 Jan 26;338:a3172.

164. Blanco JL, Ambrosioni J, Garcia F, Martínez E, Soriano A, Mallolas J, et al. COVID-19 in patients with HIV: clinical case series. Lancet HIV. 2020 May;7(5):e314–6.

165. Hoffmann C, Casado JL, Härter G, Vizcarra P, Moreno A, Cattaneo D, et al. Immune deficiency is a risk factor for severe COVID-19 in people living with HIV. HIV Medicine [Internet]. 2021 May 22 [cited 2020 Dec 31];n/a(n/a). Available from: https://onlinelibrary.wiley.com/doi/abs/10.1111/hiv.13037

166. Maciel RA, Klück HM, Durand M, Sprinz E. Comorbidity is more common and occurs earlier in persons living with HIV than in HIV-uninfected matched controls, aged 50 years and older: A cross-sectional study. International Journal of Infectious Diseases. 2018 May 1;70:30–5.

167. Ssentongo P, Heilbrunn ES, Ssentongo AE, Advani S, Chinchilli VM, Nunez JJ, et al. Epidemiology and outcomes of COVID-19 in HIV-infected individuals: a systematic review and meta-analysis. Sci Rep. 2021 Mar 18;11(1):6283.

168. Tesoriero JM, Swain CAE, Pierce JL, Zamboni L, Wu M, Holtgrave DR, et al. COVID-19 Outcomes Among Persons Living With or Without Diagnosed HIV Infection in New York State. JAMA Netw Open. 2021 Feb 1;4(2):e2037069.

169. Park A, Iwasaki A. Type I and Type III Interferons - Induction, Signaling, Evasion, and Application to Combat COVID-19. Cell Host Microbe. 2020 Jun 10;27(6):870–8.

170. Boucau J, Le Gall S. Antigen processing and presentation in HIV infection. Mol Immunol. 2019 Sep;113:67–74.

171. Wonderlich ER, Leonard JA, Collins KL. HIV Immune Evasion: Disruption of antigen presentation by the HIV Nef protein. Adv Virus Res. 2011;80:103–27.

172. Naidoo KK, Ndumnego OC, Ismail N, Dong KL, Ndung'u T. Antigen Presenting Cells Contribute to Persistent Immune Activation Despite Antiretroviral Therapy Initiation During Hyperacute HIV-1 Infection. Frontiers in Immunology [Internet]. 2021 [cited 2023 Mar 13];12. Available from: https://www.frontiersin.org/articles/10.3389/fimmu.2021.738743

173. Yang Y, Iwasaki A. Impact of Chronic HIV Infection on SARS-CoV-2 Infection, COVID-19 Disease and Vaccines. Curr HIV/AIDS Rep. 2022 Feb 1;19(1):5–16.

174. Mullender C, da Costa KAS, Alrubayyi A, Pett SL, Peppa D. SARS-CoV-2 immunity and vaccine strategies in people with HIV. Oxford Open Immunology. 2022 Jan 1;3(1):iqac005.

175. Zheng M, Gao Y, Wang G, Song G, Liu S, Sun D, et al. Functional exhaustion of antiviral lymphocytes in COVID-19 patients. Cell Mol Immunol. 2020 May;17(5):533–5.

176. Zheng HY, Zhang M, Yang CX, Zhang N, Wang XC, Yang XP, et al. Elevated exhaustion levels and reduced functional diversity of T cells in peripheral blood may predict severe progression in COVID-19 patients. Cell Mol Immunol. 2020 May;17(5):541–3.

177. Yu K, He J, Wu Y, Xie B, Liu X, Wei B, et al. Dysregulated adaptive immune response contributes to severe COVID-19. Cell Res. 2020 Sep;30(9):814–6.

178. Kusnadi A, Ramírez-Suástegui C, Fajardo V, Chee SJ, Meckiff BJ, Simon H, et al. Severely ill patients with COVID-19 display impaired exhaustion features in SARS-CoV-2–reactive CD8+ T cells. Science Immunology. 2021 Jan 21;6(55):eabe4782.

179. Rydyznski Moderbacher C, Ramirez SI, Dan JM, Grifoni A, Hastie KM, Weiskopf D, et al. Antigen-Specific Adaptive Immunity to SARS-CoV-2 in Acute COVID-19 and Associations with Age and Disease Severity. Cell. 2020 Nov 12;183(4):996-1012.e19.

180. Sharov KS. HIV/SARS-CoV-2 co-infection: T cell profile, cytokine dynamics and role of exhausted lymphocytes. Int J Infect Dis. 2021 Jan;102:163–9.

181. Nkosi T, Chasara C, Papadopoulos AO, Nguni TL, Karim F, Moosa MYS, et al. Unsuppressed HIV infection impairs T cell responses to SARS-CoV-2 infection and abrogates T cell cross-recognition. Schiffer JT, Taniguchi T, Schiffer JT, editors. eLife. 2022 Jul 26;11:e78374.

182. Levy I, Wieder-Finesod A, Litchevsky V, Biber A, Indenbaum V, Olmer L, et al. Immunogenicity and safety of the BNT162b2 mRNA COVID-19 vaccine in people living with HIV-1. Clinical Microbiology and Infection. 2021 Dec 1;27(12):1851–5.

183. Vergori A, Cozzi Lepri A, Cicalini S, Matusali G, Bordoni V, Lanini S, et al. Immunogenicity to COVID-19 mRNA vaccine third dose in people living with HIV. Nat Commun. 2022 Aug 22;13(1):4922.

184. Frater J, Ewer KJ, Ogbe A, Pace M, Adele S, Adland E, et al. Safety and immunogenicity of the ChAdOx1 nCoV-19 (AZD1222) vaccine against SARS-CoV-2 in HIV infection: a single-arm substudy of a phase 2/3 clinical trial. The Lancet HIV. 2021 Aug 1;8(8):e474–85.

185. Ogbe A, Pace M, Bittaye M, Tipoe T, Adele S, Alagaratnam J, et al. Durability of ChAdOx1 nCoV-19 vaccination in people living with HIV. JCI Insight. 2022 Apr 8;7(7):e157031.

186. Antinori A, Cicalini S, Meschi S, Bordoni V, Lorenzini P, Vergori A, et al. Humoral and Cellular Immune Response Elicited by mRNA Vaccination Against Severe Acute Respiratory Syndrome Coronavirus 2 (SARS-CoV-2) in People Living With Human Immunodeficiency Virus Receiving Antiretroviral Therapy Based on Current CD4 T-Lymphocyte Count. Clinical Infectious Diseases. 2022 Jul 1;75(1):e552–63.

187. Krämer B, Knoll R, Bonaguro L, ToVinh M, Raabe J, Astaburuaga-García R, et al. Early IFN-α signatures and persistent dysfunction are distinguishing features of NK cells in severe COVID-19. Immunity. 2021 Nov 9;54(11):2650-2669.e14.

188. Bi J. NK cell dysfunction in patients with COVID-19. Cell Mol Immunol. 2022 Feb;19(2):127–9.

189. Maucourant C, Filipovic I, Ponzetta A, Aleman S, Cornillet M, Hertwig L, et al. Natural killer cell immunotypes related to COVID-19 disease severity. Science Immunology [Internet]. 2020 Aug 21 [cited 2020 Oct 10];5(50).

190. Chua RL, Lukassen S, Trump S, Hennig BP, Wendisch D, Pott F, et al. COVID-19 severity correlates with airway epithelium-immune cell interactions identified by single-cell analysis. Nat Biotechnol. 2020 Aug;38(8):970–9.

191. Liao M, Liu Y, Yuan J, Wen Y, Xu G, Zhao J, et al. Single-cell landscape of bronchoalveolar immune cells in patients with COVID-19. Nature Medicine. 2020 Jun;26(6):842–4.

192. Osman M, Faridi RM, Sligl W, Shabani-Rad MT, Dharmani-Khan P, Parker A, et al. Impaired natural killer cell counts and cytolytic activity in patients with severe COVID-19. Blood Adv. 2020 Oct 19;4(20):5035–9.

193. Lee MJ, Leong MW, Rustagi A, Beck A, Zeng L, Holmes S, et al. SARS-CoV-2 escapes direct NK cell killing through Nsp1-mediated downregulation of ligands for NKG2D. Cell Rep. 2022 Dec 27;41(13):111892.

194. Hammer Q, Dunst J, Christ W, Picarazzi F, Wendorff M, Momayyezi P, et al. SARS-CoV-2 Nsp13 encodes for an HLA-E-stabilizing peptide that abrogates inhibition of NKG2A-expressing NK cells. Cell Rep. 2022 Mar 8;38(10):110503.

195. Witkowski M, Tizian C, Ferreira-Gomes M, Niemeyer D, Jones TC, Heinrich F, et al. Untimely TGFβ responses in COVID-19 limit antiviral functions of NK cells. Nature. 2021 Dec;600(7888):295–301.

196. Gorman MJ, Patel N, Guebre-Xabier M, Zhu AL, Atyeo C, Pullen KM, et al. Fab and Fc contribute to maximal protection against SARS-CoV-2 following NVX-CoV2373 subunit vaccine with Matrix-M vaccination. Cell Rep Med. 2021 Sep 21;2(9):100405.

197. Schäfer A, Muecksch F, Lorenzi JCC, Leist SR, Cipolla M, Bournazos S, et al. Antibody potency, effector function, and combinations in protection and therapy for SARS-CoV-2 infection in vivo. J Exp Med. 2021 Mar 1;218(3):e20201993.

198. Suryadevara N, Shrihari S, Gilchuk P, VanBlargan LA, Binshtein E, Zost SJ, et al. Neutralizing and protective human monoclonal antibodies recognizing the N-terminal domain of the SARS-CoV-2 spike protein. Cell. 2021 Apr 29;184(9):2316-2331.e15.

199. Winkler ES, Gilchuk P, Yu J, Bailey AL, Chen RE, Zost SJ, et al. Human neutralizing antibodies against SARS-CoV-2 require intact Fc effector functions and monocytes for optimal therapeutic protection. bioRxiv. 2020 Dec 28;2020.12.28.424554.

200. Yamin R, Jones AT, Hoffmann HH, Schäfer A, Kao KS, Francis RL, et al. Fc-engineered antibody therapeutics with improved anti-SARS-CoV-2 efficacy. Nature. 2021 Nov;599(7885):465–70.

201. Dufloo J, Grzelak L, Staropoli I, Madec Y, Tondeur L, Anna F, et al. Asymptomatic and symptomatic SARS-CoV-2 infections elicit polyfunctional antibodies. Cell Rep Med. 2021 May 18;2(5):100275.

202. Lee WS, Selva KJ, Davis SK, Wines BD, Reynaldi A, Esterbauer R, et al. Decay of Fc-dependent antibody functions after mild to moderate COVID-19. Cell Rep Med. 2021 Jun 15;2(6):100296.

203. Anand SP, Prévost J, Nayrac M, Beaudoin-Bussières G, Benlarbi M, Gasser R, et al. Longitudinal analysis of humoral immunity against SARS-CoV-2 Spike in convalescent individuals up to 8 months post-symptom onset. Cell Rep Med. 2021 May 5;2(6):100290.

204. Herman JD, Wang C, Loos C, Yoon H, Rivera J, Eugenia Dieterle M, et al. Functional convalescent plasma antibodies and pre-infusion titers shape the early severe COVID-19 immune response. Nat Commun. 2021 Nov 25;12(1):6853.

205. Fielding CA, Sabberwal P, Williamson JC, Greenwood EJ, Crozier TW, Zelek W, et al. SARS-CoV-2 host-shutoff impacts innate NK cell functions, but antibody-dependent NK activity is strongly activated through non-spike antibodies. eLife. 11:e74489.

206. Herrera L, Martin-Inaraja M, Santos S, Inglés-Ferrándiz M, Azkarate A, Perez-Vaquero MA, et al. Identifying SARS-CoV-2 ‘memory’ NK cells from COVID-19 convalescent donors for adoptive cell therapy. Immunology. 2022 Feb;165(2):234–49.

207. Vietzen H, Zoufaly A, Traugott M, Aberle J, Aberle SW, Puchhammer-Stöckl E. Deletion of the NKG2C receptor encoding KLRC2 gene and HLA-E variants are risk factors for severe COVID-19. Genet Med. 2021 May;23(5):963–7.

208. Van Gassen S, Callebaut B, Van Helden MJ, Lambrecht BN, Demeester P, Dhaene T, et al. FlowSOM: Using self-organizing maps for visualization and interpretation of cytometry data. Cytometry A. 2015 Jul;87(7):636–45.

209. Zhang Z, Mateus J, Coelho CH, Dan JM, Moderbacher CR, Gálvez RI, et al. Humoral and cellular immune memory to four COVID-19 vaccines. Cell. 2022 Jul 7;185(14):2434-2451.e17.

210. Kamali A, Price MA, Lakhi S, Karita E, Inambao M, Sanders EJ, et al. Creating an African HIV clinical research and prevention trials network: HIV prevalence, incidence and transmission. PLoS One. 2015;10(1):e0116100.

211. Price MA, Wallis CL, Lakhi S, Karita E, Kamali A, Anzala O, et al. Transmitted HIV type 1 drug resistance among individuals with recent HIV infection in East and Southern Africa. AIDS Res Hum Retroviruses. 2011 Jan;27(1):5–12.

212. Alrubayyi A, Gea-Mallorquí E, Touizer E, Hameiri-Bowen D, Kopycinski J, Charlton B, et al. Characterization of humoral and SARS-CoV-2 specific T cell responses in people living with HIV. Nat Commun. 2021 Oct 5;12(1):5839.

213. Zufferey R, Nagy D, Mandel RJ, Naldini L, Trono D. Multiply attenuated lentiviral vector achieves efficient gene delivery in vivo. Nature Biotechnology. 1997 Sep;15(9):871–5.

214. Seow J, Graham C, Merrick B, Acors S, Pickering S, Steel KJA, et al. Longitudinal observation and decline of neutralizing antibody responses in the three months following SARS-CoV-2 infection in humans. Nature Microbiology. 2020 Dec;5(12):1598–607.

215. Reynolds CJ, Pade C, Gibbons JM, Butler DK, Otter AD, Menacho K, et al. Prior SARS-CoV-2 infection rescues B and T cell responses to variants after first vaccine dose. Science. 2021 Jun 25;372(6549):1418–23.

216. Kharsany ABM, Karim QA. HIV Infection and AIDS in Sub-Saharan Africa: Current Status, Challenges and Opportunities. Open AIDS J. 2016 Apr 8;10:34–48.

217. Ankomah A, Ganle JK, Lartey MY, Kwara A, Nortey PA, Okyerefo MPK, et al. ART access-related barriers faced by HIV-positive persons linked to care in southern Ghana: a mixed method study. BMC Infect Dis. 2016 Dec 7;16:738.

218. HIV/AIDS [Internet]. WHO | Regional Office for Africa. [cited 2022 Dec 14]. Available from: https://www.afro.who.int/health-topics/hivaids

219. Alter G, Martin MP, Teigen N, Carr WH, Suscovich TJ, Schneidewind A, et al. Differential natural killer cell-mediated inhibition of HIV-1 replication based on distinct KIR/HLA subtypes. J Exp Med. 2007 Nov 26;204(12):3027–36.

220. Shah AH, Sowrirajan B, Davis ZB, Ward JP, Campbell EM, Planelles V, et al. Degranulation of natural killer cells following interaction with HIV-1-infected cells is hindered by downmodulation of NTB-A by Vpu. Cell Host Microbe. 2010 Nov 18;8(5):397–409.

221. Boudreau JE, Mulrooney TJ, Le Luduec JB, Barker E, Hsu KC. KIR3DL1 and HLA-B Density and Binding Calibrate NK Education and Response to HIV. J Immunol. 2016 Apr 15;196(8):3398–410.

222. Haynes BF, Gilbert PB, McElrath MJ, Zolla-Pazner S, Tomaras GD, Alam SM, et al. Immune-Correlates Analysis of an HIV-1 Vaccine Efficacy Trial. New England Journal of Medicine. 2012 Apr 5;366(14):1275–86.

223. Wren LH, Chung AW, Isitman G, Kelleher AD, Parsons MS, Amin J, et al. Specific antibody-dependent cellular cytotoxicity responses associated with slow progression of HIV infection. Immunology. 2013 Feb;138(2):116–23.

224. Kulkarni A, Kurle S, Shete A, Ghate M, Godbole S, Madhavi V, et al. Indian Long-term Non-Progressors Show Broad ADCC Responses with Preferential Recognition of V3 Region of Envelope and a Region from Tat Protein. Front Immunol. 2017;8:5.

225. Madhavi V, Wines BD, Amin J, Emery S, ENCORE1 Study Group, Lopez E, et al. HIV-1 Env- and Vpu-Specific Antibody-Dependent Cellular Cytotoxicity Responses Associated with Elite Control of HIV. J Virol. 2017 15;91(18).

226. Li SS, Hickey A, Shangguan S, Ehrenberg PK, Geretz A, Butler L, et al. HLA-B∗46 associates with rapid HIV disease progression in Asian cohorts and prominent differences in NK cell phenotype. Cell Host & Microbe. 2022 Aug 10;30(8):1173-1185.e8.

227. Barnes S, Schilizzi O, Audsley KM, Newnes HV, Foley B. Deciphering the Immunological Phenomenon of Adaptive Natural Killer (NK) Cells and Cytomegalovirus (CMV). Int J Mol Sci. 2020 Nov 23;21(22):8864.

228. Govender K, Msomi N, Moodley P, Parboosing R. Cytomegalovirus pneumonia of infants in Africa: a narrative literature review. Future Microbiology. 2021 Dec;16(18):1401–14.

229. Zhang T, Scott JM, Hwang I, Kim S. Cutting edge: antibody-dependent memory-like NK cells distinguished by FcRγ deficiency. J Immunol. 2013 Feb 15;190(4):1402–6.

230. Climent N, Ambrosioni J, González T, Xufré C, Casadellà M, Noguera-Julian M, et al. Immunological and virological findings in a patient with exceptional post-treatment control: a case report. The Lancet HIV [Internet]. 2022 Oct 27 [cited 2022 Oct 29]; Available from: https://www.sciencedirect.com/science/article/pii/S2352301822003022

231. Rainwater S, DeVange S, Sagar M, Ndinya-Achola J, Mandaliya K, Kreiss JK, et al. No evidence for rapid subtype C spread within an epidemic in which multiple subtypes and intersubtype recombinants circulate. AIDS Res Hum Retroviruses. 2005 Dec;21(12):1060–5.

232. Kanki PJ, Hamel DJ, Sankalé JL, Hsieh C c, Thior I, Barin F, et al. Human immunodeficiency virus type 1 subtypes differ in disease progression. J Infect Dis. 1999 Jan;179(1):68–73.

233. Kiwanuka N, Robb M, Laeyendecker O, Kigozi G, Wabwire-Mangen F, Makumbi FE, et al. HIV-1 viral subtype differences in the rate of CD4+ T-cell decline among HIV seroincident antiretroviral naive persons in Rakai district, Uganda. J Acquir Immune Defic Syndr. 2010 Jun;54(2):180–4.

234. Prentice HA, Price MA, Porter TR, Cormier E, Mugavero MJ, Kamali A, et al. Dynamics of Viremia in Primary HIV-1 infection in Africans: Insights from Analyses of Host and Viral Correlates. Virology. 2014 Jan 20;449:254–62.

235. Tang J, Cormier E, Gilmour J, Price MA, Prentice HA, Song W, et al. Human leukocyte antigen variants B*44 and B*57 are consistently favorable during two distinct phases of primary HIV-1 infection in sub-Saharan Africans with several viral subtypes. J Virol. 2011 Sep;85(17):8894–902.

236. Yaffe ZA, Naiman NE, Slyker J, Wines BD, Richardson BA, Hogarth PM, et al. Improved HIV-positive infant survival is correlated with high levels of HIV-specific ADCC activity in multiple cohorts. Cell Reports Medicine. 2021 Apr 20;2(4):100254.

237. Ackerman ME, Mikhailova A, Brown EP, Dowell KG, Walker BD, Bailey-Kellogg C, et al. Polyfunctional HIV-Specific Antibody Responses Are Associated with Spontaneous HIV Control. PLoS Pathog. 2016 Jan;12(1):e1005315.

238. O'Sullivan TE, Sun JC, Lanier LL. Natural Killer Cell Memory. Immunity. 2015 Oct 20;43(4):634–45.

239. Littwitz-Salomon E, Moreira D, Frost JN, Choi C, Liou KT, Ahern DK, et al. Metabolic requirements of NK cells during the acute response against retroviral infection. Nat Commun. 2021 Sep 10;12(1):5376.

240. Cubero EM, Balint S, Alrubayyi A, Ogbe A, Matthews R, Burns F, et al. IL-15 re-programming compensates for NK cell mitochondrial dysfunction in HIV-1 infection. bioRxiv. 2019 Oct 21;811117.

241. Foo J, Bellot G, Pervaiz S, Alonso S. Mitochondria-mediated oxidative stress during viral infection. Trends in Microbiology. 2022 Jul 1;30(7):679–92.

242. van der Windt GJW, Everts B, Chang CH, Curtis JD, Freitas TC, Amiel E, et al. Mitochondrial respiratory capacity is a critical regulator of CD8+ T cell memory development. Immunity. 2012 Jan 27;36(1):68–78.

243. Surace L, Doisne JM, Escoll P, Marie S, Dardalhon V, Croft C, et al. Polarized mitochondria as guardians of NK cell fitness. Blood Advances. 2020 Dec 29;5(1):26–38.

244. Mitchell P, Moyle J. Evidence discriminating between the Chemical and the Chemiosmotic Mechanisms of Electron Transport Phosphorylation. Nature. 1965 Dec;208(5016):1205–6.

245. Momcilovic M, Jones A, Bailey ST, Waldmann CM, Li R, Lee JT, et al. In vivo imaging of mitochondrial membrane potential in non-small-cell lung cancer. Nature. 2019 Nov;575(7782):380–4.

246. Flow-cytometry-based protocol to analyze respiratory chain function in mouse microglia: STAR Protocols [Internet]. [cited 2022 Oct 31]. Available from: https://star-protocols.cell.com/protocols/1447

247. Terrén I, Orrantia A, Mosteiro A, Vitallé J, Zenarruzabeitia O, Borrego F. Metabolic changes of Interleukin-12/15/18-stimulated human NK cells. Sci Rep. 2021 Mar 19;11(1):1–15.

248. Gurdasani D, Iles L, Dillon DG, Young EH, Olson AD, Naranbhai V, et al. A systematic review of definitions of extreme phenotypes of HIV control and progression. AIDS. 2014 Jan 14;28(2):149–62.

249. Neilson JR, John GC, Carr JK, Lewis P, Kreiss JK, Jackson S, et al. Subtypes of Human Immunodeficiency Virus Type 1 and Disease Stage among Women in Nairobi, Kenya. J Virol. 1999 May;73(5):4393–403.

250. Prado JG, Prendergast A, Thobakgale C, Molina C, Tudor-Williams G, Ndung'u T, et al. Replicative capacity of human immunodeficiency virus type 1 transmitted from mother to child is associated with pediatric disease progression rate. J Virol. 2010 Jan;84(1):492–502.

251. Kaleebu P, Nankya IL, Yirrell DL, Shafer LA, Kyosiimire-Lugemwa J, Lule DB, et al. Relation Between Chemokine Receptor Use, Disease Stage, and HIV-1 Subtypes A and D: Results From a Rural Ugandan Cohort. JAIDS Journal of Acquired Immune Deficiency Syndromes. 2007 May 1;45(1):28–33.

252. Esbjörnsson J, Månsson F, Martínez-Arias W, Vincic E, Biague AJ, da Silva ZJ, et al. Frequent CXCR4 tropism of HIV-1 subtype A and CRF02_AG during late-stage disease--indication of an evolving epidemic in West Africa. Retrovirology. 2010 Mar 22;7:23.

253. Fenyö EM, Esbjörnsson J, Medstrand P, Jansson M. Human immunodeficiency virus type 1 biological variation and coreceptor use: from concept to clinical significance. J Intern Med. 2011 Dec;270(6):520–31.

254. Fourati S, Ribeiro SP, Blasco Tavares Pereira Lopes F, Talla A, Lefebvre F, Cameron M, et al. Integrated systems approach defines the antiviral pathways conferring protection by the RV144 HIV vaccine. Nat Commun [Internet]. 2019 Feb 20 [cited 2019 Nov 12];10. Available from: https://www.ncbi.nlm.nih.gov/pmc/articles/PMC6382801/

255. Sun JC, Beilke JN, Bezman NA, Lanier LL. Homeostatic proliferation generates long-lived natural killer cells that respond against viral infection. J Exp Med. 2011 Feb 14;208(2):357–68.

256. Shemesh A, Su Y, Calabrese DR, Chen D, Arakawa-Hoyt J, Roybal KT, et al. Diminished cell proliferation promotes natural killer cell adaptive-like phenotype by limiting FcεRIγ expression. J Exp Med [Internet]. 2022 Nov 7 [cited 2022 Sep 6];219(11). Available from: https://rupress.org/jem/article/219/11/e20220551/213443/Diminished-cell-proliferation-promotes-natural

257. Lynch RM, Shen T, Gnanakaran S, Derdeyn CA. Appreciating HIV Type 1 Diversity: Subtype Differences in Env. AIDS Res Hum Retroviruses. 2009 Mar;25(3):237–48.

258. Mogensen TH, Melchjorsen J, Larsen CS, Paludan SR. Innate immune recognition and activation during HIV infection. Retrovirology. 2010 Jun 22;7:54.

259. Go EP, Hewawasam G, Liao HX, Chen H, Ping LH, Anderson JA, et al. Characterization of Glycosylation Profiles of HIV-1 Transmitted/Founder Envelopes by Mass Spectrometry ▿. J Virol. 2011 Aug;85(16):8270–84.

260. Liao HX, Sutherland LL, Xia SM, Brock ME, Scearce RM, Vanleeuwen S, et al. A group M consensus envelope glycoprotein induces antibodies that neutralize subsets of subtype B and C HIV-1 primary viruses. Virology. 2006 Sep 30;353(2):268–82.

261. Li M, Salazar-Gonzalez JF, Derdeyn CA, Morris L, Williamson C, Robinson JE, et al. Genetic and neutralization properties of subtype C human immunodeficiency virus type 1 molecular env clones from acute and early heterosexually acquired infections in Southern Africa. J Virol. 2006 Dec;80(23):11776–90.

262. Madhavi V, Wren LH, Center RJ, Gonelli C, Winnall WR, Parsons MS, et al. Breadth of HIV-1 Env-specific antibody-dependent cellular cytotoxicity: relevance to global HIV vaccine design. AIDS. 2014 Aug 24;28(13):1859.

263. Landais E, Huang X, Havenar-Daughton C, Murrell B, Price MA, Wickramasinghe L, et al. Broadly Neutralizing Antibody Responses in a Large Longitudinal Sub-Saharan HIV Primary Infection Cohort. PLOS Pathogens. 2016 Jan 14;12(1):e1005369.

264. Gondois-Rey F, Chéret A, Granjeaud S, Mallet F, Bidaut G, Lécuroux C, et al. NKG2C+ memory-like NK cells contribute to the control of HIV viremia during primary infection: Optiprim-ANRS 147. Clin Transl Immunology. 2017 Jul 7;6(7):e150.

265. Bates M, Brantsaeter AB. Human cytomegalovirus (CMV) in Africa: a neglected but important pathogen. Journal of Virus Eradication. 2016 Jul 1;2(3):136–42.

266. Shah SV, Manickam C, Ram DR, Kroll K, Itell H, Permar SR, et al. CMV Primes Functional Alternative Signaling in Adaptive Δg NK Cells but Is Subverted by Lentivirus Infection in Rhesus Macaques. Cell Reports. 2018 Dec 4;25(10):2766-2774.e3.

267. Sinclair LV, Barthelemy C, Cantrell DA. Single Cell Glucose Uptake Assays: A Cautionary Tale. Immunometabolism. 2020;2(4):e200029.

268. Weinberg SE, Sena LA, Chandel NS. Mitochondria in the regulation of innate and adaptive immunity. Immunity. 2015 Mar 17;42(3):406–17.

269. Sena LA, Li S, Jairaman A, Prakriya M, Ezponda T, Hildeman DA, et al. Mitochondria are required for antigen-specific T cell activation through reactive oxygen species signaling. Immunity. 2013 Feb 21;38(2):225–36.

270. Sukumar M, Liu J, Mehta GU, Patel SJ, Roychoudhuri R, Crompton JG, et al. Mitochondrial Membrane Potential Identifies Cells with Enhanced Stemness for Cellular Therapy. Cell Metabolism. 2016 Jan 12;23(1):63–76.

271. McElrath MJ, Haynes BF. Induction of immunity to human immunodeficiency virus type-1 by vaccination. Immunity. 2010 Oct 29;33(4):542–54.

272. Collins DR, Gaiha GD, Walker BD. CD8+ T cells in HIV control, cure and prevention. Nat Rev Immunol. 2020 Aug;20(8):471–82.

273. Borrow P, Lewicki H, Hahn BH, Shaw GM, Oldstone MB. Virus-specific CD8+ cytotoxic T-lymphocyte activity associated with control of viremia in primary human immunodeficiency virus type 1 infection. J Virol. 1994 Sep;68(9):6103–10.

274. Schmitz JE, Kuroda MJ, Santra S, Sasseville VG, Simon MA, Lifton MA, et al. Control of viremia in simian immunodeficiency virus infection by CD8+ lymphocytes. Science. 1999 Feb 5;283(5403):857–60.

275. Lambotte O, Boufassa F, Madec Y, Nguyen A, Goujard C, Meyer L, et al. HIV controllers: a homogeneous group of HIV-1-infected patients with spontaneous control of viral replication. Clin Infect Dis. 2005 Oct 1;41(7):1053–6.

276. Trautmann L, Mbitikon-Kobo FM, Goulet JP, Peretz Y, Shi Y, Van Grevenynghe J, et al. Profound metabolic, functional, and cytolytic differences characterize HIV-specific CD8 T cells in primary and chronic HIV infection. Blood. 2012 Oct 25;120(17):3466–77.

277. Emergence of Individual HIV-Specific CD8 T Cell Responses during Primary HIV-1 Infection Can Determine Long-Term Disease Outcome | Journal of Virology [Internet]. [cited 2022 Nov 14]. Available from: https://journals.asm.org/doi/full/10.1128/JVI.02016-14

278. Gloster SE, Newton P, Cornforth D, Lifson JD, Williams I, Shaw GM, et al. Association of strong virus-specific CD4 T cell responses with efficient natural control of primary HIV-1 infection. AIDS. 2004 Mar 26;18(5):749.

279. Rerks-Ngarm S, Pitisuttithum P, Nitayaphan S, Kaewkungwal J, Chiu J, Paris R, et al. Vaccination with ALVAC and AIDSVAX to Prevent HIV-1 Infection in Thailand. New England Journal of Medicine. 2009 Dec 3;361(23):2209–20.

280. Schieffer M, Jessen HK, Oster AF, Pissani F, Soghoian DZ, Lu R, et al. Induction of Gag-Specific CD4 T Cell Responses during Acute HIV Infection Is Associated with Improved Viral Control. Journal of Virology. 2014 Jul;88(13):7357–66.

281. Sant AJ, McMichael A. Revealing the role of CD4+ T cells in viral immunity. Journal of Experimental Medicine. 2012 Jul 30;209(8):1391–5.

282. Casazza JP, Betts MR, Price DA, Precopio ML, Ruff LE, Brenchley JM, et al. Acquisition of direct antiviral effector functions by CMV-specific CD4+ T lymphocytes with cellular maturation. Journal of Experimental Medicine. 2006 Dec 11;203(13):2865–77.

283. Welsh RM, Waggoner SN. NK cells controlling virus-specific T cells: Rheostats for acute vs. persistent infections. Virology. 2013 Jan 5;435(1):37–45.

284. Whitmire JK, Eam B, Benning N, Whitton JL. Direct Interferon-γ Signaling Dramatically Enhances CD4+ and CD8+ T Cell Memory. The Journal of Immunology. 2007 Jul 15;179(2):1190–7.

285. Andrews DM, Estcourt MJ, Andoniou CE, Wikstrom ME, Khong A, Voigt V, et al. Innate immunity defines the capacity of antiviral T cells to limit persistent infection. J Exp Med. 2010 Jun 7;207(6):1333–43.

286. Lee SH, Kim KS, Fodil-Cornu N, Vidal SM, Biron CA. Activating receptors promote NK cell expansion for maintenance, IL-10 production, and CD8 T cell regulation during viral infection. J Exp Med. 2009 Sep 28;206(10):2235–51.

287. Cook KD, Waggoner SN, Whitmire JK. NK cells and their ability to modulate T cells during virus infections. Crit Rev Immunol. 2014;34(5):359–88.

288. Lang PA, Lang KS, Xu HC, Grusdat M, Parish IA, Recher M, et al. Natural killer cell activation enhances immune pathology and promotes chronic infection by limiting CD8+ T-cell immunity. Proc Natl Acad Sci U S A. 2012 Jan 24;109(4):1210–5.

289. Waggoner SN, Daniels KA, Welsh RM. Therapeutic depletion of natural killer cells controls persistent infection. J Virol. 2014 Feb;88(4):1953–60.

290. Rydyznski C, Daniels KA, Karmele EP, Brooks TR, Mahl SE, Moran MT, et al. Generation of cellular immune memory and B-cell immunity are impaired by natural killer cells. Nat Commun. 2015 Feb 27;6:6375.

291. Perreau M, Savoye AL, De Crignis E, Corpataux JM, Cubas R, Haddad EK, et al. Follicular helper T cells serve as the major CD4 T cell compartment for HIV-1 infection, replication, and production. J Exp Med. 2013 Jan 14;210(1):143–56.

292. Chomont N, El-Far M, Ancuta P, Trautmann L, Procopio FA, Yassine-Diab B, et al. HIV reservoir size and persistence are driven by T cell survival and homeostatic proliferation. Nat Med. 2009 Aug;15(8):893–900.

293. Huot N, Jacquelin B, Garcia-Tellez T, Rascle P, Ploquin MJ, Madec Y, et al. Natural killer cells migrate into and control simian immunodeficiency virus replication in lymph node follicles in African green monkeys. Nat Med. 2017 Nov;23(11):1277–86.

294. Guo AL, Jiao YM, Zhao QW, Huang HH, Deng JN, Zhang C, et al. Implications of the accumulation of CXCR5+ NK cells in lymph nodes of HIV-1 infected patients. EBioMedicine [Internet]. 2022 Jan 1 [cited 2022 Jan 5];75.

295. Froebel KS, Raab GM, D'alessandro C, Armitage MP, Mackenzie KM, Struthers M, et al. A single measurement of CD38CD8 cells in HIV+, long-term surviving injecting drug users distinguishes those who will progress to AIDS from those who will remain stable. Clin Exp Immunol. 2000 Oct;122(1):72–8.

296. Meditz AL, Haas MK, Folkvord JM, Melander K, Young R, McCarter M, et al. HLA-DR+ CD38+ CD4+ T Lymphocytes Have Elevated CCR5 Expression and Produce the Majority of R5-Tropic HIV-1 RNA In Vivo ▿. J Virol. 2011 Oct;85(19):10189–200.

297. Xia H, Jiang W, Zhang X, Qin L, Su B, Li Z, et al. Elevated Level of CD4+ T Cell Immune Activation in Acutely HIV-1-Infected Stage Associates With Increased IL-2 Production and Cycling Expression, and Subsequent CD4+ T Cell Preservation. Frontiers in Immunology [Internet]. 2018 [cited 2022 Nov 21];9.

298. Koup RA, Safrit JT, Cao Y, Andrews CA, McLeod G, Borkowsky W, et al. Temporal association of cellular immune responses with the initial control of viremia in primary human immunodeficiency virus type 1 syndrome. J Virol. 1994 Jul;68(7):4650–5.

299. Utzschneider DT, Charmoy M, Chennupati V, Pousse L, Ferreira DP, Calderon-Copete S, et al. T Cell Factor 1-Expressing Memory-like CD8+ T Cells Sustain the Immune Response to Chronic Viral Infections. Immunity. 2016 Aug 16;45(2):415–27.

300. Takata H, Trautmann L. Transforming dysfunctional CD8+ T cells into natural controller–like CD8+ T cells: can TCF-1 be the magic wand? Journal of Clinical Investigation. 2022 Jun 1;132(11):e160474.

301. Johnson S, Eller M, Teigler JE, Maloveste SM, Schultz BT, Soghoian DZ, et al. Cooperativity of HIV-Specific Cytolytic CD4 T Cells and CD8 T Cells in Control of HIV Viremia. J Virol. 2015 May 13;89(15):7494–505.

302. Flórez-Álvarez L, Hernandez JC, Zapata W. NK Cells in HIV-1 Infection: From Basic Science to Vaccine Strategies. Front Immunol. 2018;9:2290.

303. Alrubayyi A, Rowland-Jones S, Peppa D. Natural killer cells during acute HIV-1 infection: clues for HIV-1 prevention and therapy. AIDS. 2022 Jul 11;

304. Uzhachenko RV, Shanker A. CD8+ T Lymphocyte and NK Cell Network: Circuitry in the Cytotoxic Domain of Immunity. Frontiers in Immunology [Internet]. 2019 [cited 2022 Nov 22];10. Available from: https://www.frontiersin.org/articles/10.3389/fimmu.2019.01906

305. Waggoner SN, Cornberg M, Selin LK, Welsh RM. Natural killer cells act as rheostats modulating antiviral T cells. Nature. 2011 Nov 20;481(7381):394–8.

306. Björkström NK, Ljunggren HG, Sandberg JK. CD56 negative NK cells: origin, function, and role in chronic viral disease. Trends in Immunology. 2010 Nov 1;31(11):401–6.

307. Koff WC, Schenkelberg T, Williams T, Baric RS, McDermott A, Cameron CM, et al. Development and deployment of COVID-19 vaccines for those most vulnerable. Science Translational Medicine. 2021 Feb 3;13(579):eabd1525.

308. Cooper TJ, Woodward BL, Alom S, Harky A. Coronavirus disease 2019 (COVID-19) outcomes in HIV/AIDS patients: a systematic review. HIV Med. 2020 Oct;21(9):567–77.

309. Geretti AM, Stockdale AJ, Kelly SH, Cevik M, Collins S, Waters L, et al. Outcomes of Coronavirus Disease 2019 (COVID-19) Related Hospitalization Among People With Human Immunodeficiency Virus (HIV) in the ISARIC World Health Organization (WHO) Clinical Characterization Protocol (UK): A Prospective Observational Study. Clinical Infectious Diseases [Internet]. 2020 Oct 23 [cited 2021 Feb 2];(ciaa1605). Available from: https://doi.org/10.1093/cid/ciaa1605

310. Bhaskaran K, Rentsch CT, MacKenna B, Schultze A, Mehrkar A, Bates CJ, et al. HIV infection and COVID-19 death: a population-based cohort analysis of UK primary care data and linked national death registrations within the OpenSAFELY platform. The Lancet HIV. 2021 Jan 1;8(1):e24–32.

311. Riou C, Bruyn E du, Stek C, Daroowala R, Goliath RT, Abrahams F, et al. Relationship of SARS-CoV-2–specific CD4 response to COVID-19 severity and impact of HIV-1 and tuberculosis coinfection. J Clin Invest [Internet]. 2021 Jun 15 [cited 2022 Aug 31];131(12). Available from: https://www.jci.org/articles/view/149125

312. Bertagnolio S, Thwin SS, Silva R, Nagarajan S, Jassat W, Fowler R, et al. Clinical features of, and risk factors for, severe or fatal COVID-19 among people living with HIV admitted to hospital: analysis of data from the WHO Global Clinical Platform of COVID-19. The Lancet HIV. 2022 Jul 1;9(7):e486–95.

313. Hensley KS, Jongkees MJ, Geers D, GeurtsvanKessel CH, Mueller YM, Dalm VASH, et al. Immunogenicity and reactogenicity of SARS-CoV-2 vaccines in people living with HIV in the Netherlands: A nationwide prospective cohort study. PLoS Med. 2022 Oct;19(10):e1003979.

314. Dan JM, Mateus J, Kato Y, Hastie KM, Yu ED, Faliti CE, et al. Immunological memory to SARS-CoV-2 assessed for up to 8 months after infection. Science. 2021 Feb 5;371(6529):eabf4063.

315. Oja AE, Saris A, Ghandour CA, Kragten NAM, Hogema BM, Nossent EJ, et al. Divergent SARS-CoV-2-specific T- and B-cell responses in severe but not mild COVID-19 patients. Eur J Immunol. 2020 Dec;50(12):1998–2012.

316. Tan AT, Linster M, Tan CW, Le Bert N, Chia WN, Kunasegaran K, et al. Early induction of functional SARS-CoV-2-specific T cells associates with rapid viral clearance and mild disease in COVID-19 patients. Cell Rep. 2021 Feb 9;34(6):108728.

317. Boppana S, Qin K, Files JK, Russell RM, Stoltz R, Bibollet-Ruche F, et al. SARS-CoV-2-specific circulating T follicular helper cells correlate with neutralizing antibodies and increase during early convalescence. PLoS Pathog. 2021 Jul;17(7):e1009761.

318. Juno JA, Tan HX, Lee WS, Reynaldi A, Kelly HG, Wragg K, et al. Humoral and circulating follicular helper T cell responses in recovered patients with COVID-19. Nat Med. 2020 Sep;26(9):1428–34.

319. Crotty S. A brief history of T cell help to B cells. Nat Rev Immunol. 2015 Mar;15(3):185–9.

320. Notarbartolo S, Ranzani V, Bandera A, Gruarin P, Bevilacqua V, Putignano AR, et al. Integrated longitudinal immunophenotypic, transcriptional and repertoire analyses delineate immune responses in COVID-19 patients. Sci Immunol. 2021 Aug 10;6(62):eabg5021.

321. Tarke A, Coelho CH, Zhang Z, Dan JM, Yu ED, Methot N, et al. SARS-CoV-2 vaccination induces immunological T cell memory able to cross-recognize variants from Alpha to Omicron. Cell. 2022 Mar 3;185(5):847-859.e11.

322. Cohen B, Rubinstein R, Gans MD, Deng L, Rubinstein A, Eisenberg R. COVID-19 infection in 10 common variable immunodeficiency patients in New York City. J Allergy Clin Immunol Pract. 2021 Jan;9(1):504-507.e1.

323. Bange EM, Han NA, Wileyto P, Kim JY, Gouma S, Robinson J, et al. CD8+ T cells contribute to survival in COVID-19 patients with hematologic cancers. Nat Med. 2021 Jul;27(7):1280–9.

324. Mathew D, Giles JR, Baxter AE, Oldridge DA, Greenplate AR, Wu JE, et al. Deep immune profiling of COVID-19 patients reveals distinct immunotypes with therapeutic implications. Science [Internet]. 2020 Sep 4 [cited 2020 Dec 30];369(6508). Available from: https://science.sciencemag.org/content/369/6508/eabc8511

325. Vergori A, Cozzi-Lepri A, Matusali G, Colavita F, Cicalini S, Gallì P, et al. SARS-CoV-2 Omicron Variant Neutralization after Third Dose Vaccination in PLWH. Viruses. 2022 Aug 3;14(8):1710.

326. Ng KW, Faulkner N, Cornish GH, Rosa A, Harvey R, Hussain S, et al. Preexisting and de novo humoral immunity to SARS-CoV-2 in humans. Science. 2020 Dec 11;370(6522):1339–43.

327. Harrington P, Doores KJ, Radia D, O'Reilly A, Lam HPJ, Seow J, et al. Single dose of BNT162b2 mRNA vaccine against severe acute respiratory syndrome coronavirus-2 (SARS-CoV-2) induces neutralising antibody and polyfunctional T-cell responses in patients with chronic myeloid leukaemia. Br J Haematol. 2021 Jun 3;

328. Pickering S, Betancor G, Galão RP, Merrick B, Signell AW, Wilson HD, et al. Comparative assessment of multiple COVID-19 serological technologies supports continued evaluation of point-of-care lateral flow assays in hospital and community healthcare settings. PLoS Pathog [Internet]. 2020 Sep 24 [cited 2021 Jan 15];16(9). Available from: https://www.ncbi.nlm.nih.gov/pmc/articles/PMC7514033/

329. Peng Y, Mentzer AJ, Liu G, Yao X, Yin Z, Dong D, et al. Broad and strong memory CD4+ and CD8+ T cells induced by SARS-CoV-2 in UK convalescent individuals following COVID-19. Nat Immunol. 2020 Nov;21(11):1336–45.

330. Rydyznski Moderbacher C, Ramirez SI, Dan JM, Grifoni A, Hastie KM, Weiskopf D, et al. Antigen-Specific Adaptive Immunity to SARS-CoV-2 in Acute COVID-19 and Associations with Age and Disease Severity. Cell. 2020 Nov 12;183(4):996-1012.e19.

331. Sette A, Crotty S. Adaptive immunity to SARS-CoV-2 and COVID-19. Cell. 2021 Feb 18;184(4):861–80.

332. Reynolds CJ, Swadling L, Gibbons JM, Pade C, Jensen MP, Diniz MO, et al. Discordant neutralizing antibody and T cell responses in asymptomatic and mild SARS-CoV-2 infection. Science Immunology [Internet]. 2020 Dec 23 [cited 2021 Jan 1];5(54). Available from: https://immunology.sciencemag.org/content/5/54/eabf3698

333. De Biasi S, Meschiari M, Gibellini L, Bellinazzi C, Borella R, Fidanza L, et al. Marked T cell activation, senescence, exhaustion and skewing towards TH17 in patients with COVID-19 pneumonia. Nature Communications. 2020 Jul 6;11(1):3434.

334. Douek DC, McFarland RD, Keiser PH, Gage EA, Massey JM, Haynes BF, et al. Changes in thymic function with age and during the treatment of HIV infection. Nature. 1998 Dec 17;396(6712):690–5.

335. Hazenberg MD, Otto SA, Cohen Stuart JW, Verschuren MC, Borleffs JC, Boucher CA, et al. Increased cell division but not thymic dysfunction rapidly affects the T-cell receptor excision circle content of the naive T cell population in HIV-1 infection. Nat Med. 2000 Sep;6(9):1036–42.

336. Zhang L, Lewin SR, Markowitz M, Lin HH, Skulsky E, Karanicolas R, et al. Measuring recent thymic emigrants in blood of normal and HIV-1-infected individuals before and after effective therapy. J Exp Med. 1999 Sep 6;190(5):725–32.

337. Yin J, Chen Y, Li Y, Wang C, Zhang X. Immunogenicity and efficacy of COVID-19 vaccines in people living with HIV: a systematic review and meta-analysis. International Journal of Infectious Diseases. 2022 Nov 1;124:212–23.

338. Goel RR, Painter MM, Apostolidis SA, Mathew D, Meng W, Rosenfeld AM, et al. mRNA Vaccination Induces Durable Immune Memory to SARS-CoV-2 with Continued Evolution to Variants of Concern [Internet]. Immunology; 2021 Aug [cited 2021 Sep 16]. Available from: http://biorxiv.org/lookup/doi/10.1101/2021.08.23.457229

339. Le Bert N, Tan AT, Kunasegaran K, Tham CYL, Hafezi M, Chia A, et al. SARS-CoV-2-specific T cell immunity in cases of COVID-19 and SARS, and uninfected controls. Nature. 2020 Aug;584(7821):457–62.

340. Grifoni A, Weiskopf D, Ramirez SI, Mateus J, Dan JM, Moderbacher CR, et al. Targets of T Cell Responses to SARS-CoV-2 Coronavirus in Humans with COVID-19 Disease and Unexposed Individuals. Cell. 2020 Jun 25;181(7):1489-1501.e15.

341. Mateus J, Grifoni A, Tarke A, Sidney J, Ramirez SI, Dan JM, et al. Selective and cross-reactive SARS-CoV-2 T cell epitopes in unexposed humans. Science. 2020 Oct 2;370(6512):89–94.

342. Braun J, Loyal L, Frentsch M, Wendisch D, Georg P, Kurth F, et al. SARS-CoV-2-reactive T cells in healthy donors and patients with COVID-19. Nature. 2020 Nov;587(7833):270–4.

343. Casado JL, Vizcarra P, Haemmerle J, Velasco H, Martín-Hondarza A, Rodríguez-Domínguez MJ, et al. Pre-existing T cell immunity determines the frequency and magnitude of cellular immune response to two doses of mRNA vaccine against SARS-CoV-2. Vaccine X. 2022 Aug;11:100165.

344. Adam L, Rosenbaum P, Quentric P, Parizot C, Bonduelle O, Guillou N, et al. CD8+PD-L1+CXCR3+ polyfunctional T cell abundances are associated with survival in critical SARS-CoV-2–infected patients. JCI Insight. 2021 Sep 22;6(18):e151571.

345. Lopez Bernal J, Andrews N, Gower C, Gallagher E, Simmons R, Thelwall S, et al. Effectiveness of Covid-19 Vaccines against the B.1.617.2 (Delta) Variant. N Engl J Med. 2021 Aug 12;385(7):585–94.

346. Nasreen S, Chung H, He S, Brown KA, Gubbay JB, Buchan SA, et al. Effectiveness of mRNA and ChAdOx1 COVID-19 vaccines against symptomatic SARS-CoV-2 infection and severe outcomes with variants of concern in Ontario [Internet]. medRxiv; 2021 [cited 2022 Dec 31]. p. 2021.06.28.21259420.

347. Yu J, Tostanoski LH, Peter L, Mercado NB, McMahan K, Mahrokhian SH, et al. DNA vaccine protection against SARS-CoV-2 in rhesus macaques. Science. 2020 Aug 14;369(6505):806–11.

348. Wajnberg A, Amanat F, Firpo A, Altman DR, Bailey MJ, Mansour M, et al. Robust neutralizing antibodies to SARS-CoV-2 infection persist for months. Science. 2020 Dec 4;370(6521):1227–30.

349. Robbiani DF, Gaebler C, Muecksch F, Lorenzi JCC, Wang Z, Cho A, et al. Convergent antibody responses to SARS-CoV-2 in convalescent individuals. Nature. 2020 Aug;584(7821):437–42.

350. Spinelli MA, Lynch KL, Yun C, Glidden DV, Peluso MJ, Henrich TJ, et al. SARS-CoV-2 seroprevalence, and IgG concentration and pseudovirus neutralising antibody titres after infection, compared by HIV status: a matched case-control observational study. Lancet HIV. 2021 Jun;8(6):e334–41.

351. Jeger-Madiot R, Heredia M, Graff-Dubois S. Germinal centers B-cell reaction and T follicular helper cells in response to HIV-1 infection. Curr Opin HIV AIDS. 2019 Jul;14(4):246–52.

352. Moir S, Fauci AS. Insights into B cells and HIV-specific B-cell responses in HIV-infected individuals. Immunol Rev. 2013 Jul;254(1):207–24.

353. Touizer E, Alrubayyi A, Ford R, Hussain N, Gerber PP, Shum HL, et al. Attenuated humoral responses in HIV after SARS-CoV-2 vaccination linked to B cell defects and altered immune profiles. iScience. 2023 Jan 20;26(1):105862.

354. Sheth AN, Althoff KN, Brooks JT. Influenza Susceptibility, Severity, and Shedding in HIV-Infected Adults: A Review of the Literature. Clinical Infectious Diseases. 2011 Jan 15;52(2):219–27.

355. Catherine FX, Piroth L. Hepatitis B virus vaccination in HIV-infected people: A review. Hum Vaccin Immunother. 2017 Feb 16;13(6):1304–13.

356. Assis R, Jain A, Nakajima R, Jasinskas A, Khan S, Palma A, et al. Distinct SARS-CoV-2 antibody reactivity patterns elicited by natural infection and mRNA vaccination. npj Vaccines. 2021 Nov 4;6(1):1–10.

357. Altawalah H. Antibody Responses to Natural SARS-CoV-2 Infection or after COVID-19 Vaccination. Vaccines (Basel). 2021 Aug 16;9(8):910.

358. Kojima N, Klausner JD. Protective immunity after recovery from SARS-CoV-2 infection. The Lancet Infectious Diseases. 2022 Jan 1;22(1):12–4.

359. Milne G, Hames T, Scotton C, Gent N, Johnsen A, Anderson RM, et al. Does infection with or vaccination against SARS-CoV-2 lead to lasting immunity? The Lancet Respiratory Medicine. 2021 Dec 1;9(12):1450–66.

360. Hall V, Foulkes S, Insalata F, Kirwan P, Saei A, Atti A, et al. Protection against SARS-CoV-2 after Covid-19 Vaccination and Previous Infection. New England Journal of Medicine. 2022 Mar 31;386(13):1207–20.

361. Crotty S. Hybrid immunity. Science. 2021 Jun 25;372(6549):1392–3.

362. Niessl J, Sekine T, Buggert M. T cell immunity to SARS-CoV-2. Semin Immunol. 2021 Jun;55:101505.

363. Chen Z, John Wherry E. T cell responses in patients with COVID-19. Nature Reviews Immunology. 2020 Sep;20(9):529–36.

364. Kedzierska K, Thomas PG. Count on us: T cells in SARS-CoV-2 infection and vaccination. Cell Rep Med. 2022 Mar 15;3(3):100562.

365. Murray SM, Ansari AM, Frater J, Klenerman P, Dunachie S, Barnes E, et al. The impact of pre-existing cross-reactive immunity on SARS-CoV-2 infection and vaccine responses. Nat Rev Immunol. 2022 Dec 20;1–13.

366. Sekine T, Perez-Potti A, Rivera-Ballesteros O, Strålin K, Gorin JB, Olsson A, et al. Robust T Cell Immunity in Convalescent Individuals with Asymptomatic or Mild COVID-19. Cell. 2020 Oct 1;183(1):158-168.e14.

367. Geers D, Shamier MC, Bogers S, den Hartog G, Gommers L, Nieuwkoop NN, et al. SARS-CoV-2 variants of concern partially escape humoral but not T-cell responses in COVID-19 convalescent donors and vaccinees. Sci Immunol. 2021 May 25;6(59):eabj1750.

368. Tarke A, Sidney J, Methot N, Yu ED, Zhang Y, Dan JM, et al. Impact of SARS-CoV-2 variants on the total CD4+ and CD8+ T cell reactivity in infected or vaccinated individuals. Cell Rep Med. 2021 Jul 2;2(7):100355.

369. Maringer Y, Nelde A, Schroeder SM, Schuhmacher J, Hörber S, Peter A, et al. Durable spike-specific T cell responses after different COVID-19 vaccination regimens are not further enhanced by booster vaccination. Science Immunology. 2022 Nov;7(78):eadd3899.

370. Keeton R, Tincho MB, Ngomti A, Baguma R, Benede N, Suzuki A, et al. T cell responses to SARS-CoV-2 spike cross-recognize Omicron. Nature. 2022 Mar;603(7901):488–92.

371. Feng Y, Zhang Y, He Z, Huang H, Tian X, Wang G, et al. Immunogenicity of an inactivated SARS-CoV-2 vaccine in people living with HIV-1: a non-randomized cohort study. eClinicalMedicine [Internet]. 2022 Jan 1 [cited 2023 Jan 1];43. Available from: https://www.thelancet.com/journals/eclinm/article/PIIS2589-5370(21)00507-1/fulltext

372. Fidler S, Fox J, Tipoe T, Longet S, Tipton T, Abeywickrema M, et al. Booster vaccination against SARS-CoV-2 induces potent immune responses in people with HIV. Clin Infect Dis. 2022 Oct 5;ciac796.

373. Wen X song, Jiang D, Gao L, Zhou J zhong, Xiao J, Cheng X cheng, et al. Clinical characteristics and predictive value of lower CD4+T cell level in patients with moderate and severe COVID-19: a multicenter retrospective study. BMC Infectious Diseases. 2021 Jan 12;21(1):57.

374. BHIVA statement on JCVI recommendations for a third COVID-19 vaccine dose [Internet]. 2021 [cited 2022 Aug 19]. Available from: https://www.bhiva.org/BHIVA-statement-on-JCVI-recommendations-for-a-third-COVID-19-vaccine-dose

375. Pérez-Alós L, Armenteros JJA, Madsen JR, Hansen CB, Jarlhelt I, Hamm SR, et al. Modeling of waning immunity after SARS-CoV-2 vaccination and influencing factors. Nat Commun. 2022 Mar 28;13(1):1614.

376. Jeyanathan M, Afkhami S, Khera A, Mandur T, Damjanovic D, Yao Y, et al. CXCR3 Signaling Is Required for Restricted Homing of Parenteral Tuberculosis Vaccine-Induced T Cells to Both the Lung Parenchyma and Airway. J Immunol. 2017 Oct 1;199(7):2555–69.

377. Bangs DJ, Tsitsiklis A, Steier Z, Chan SW, Kaminski J, Streets A, et al. CXCR3 regulates stem and proliferative CD8+ T cells during chronic infection by promoting interactions with DCs in splenic bridging channels. Cell Reports. 2022 Jan;38(3):110266.

378. De Simone G, Mazza EMC, Cassotta A, Davydov AN, Kuka M, Zanon V, et al. CXCR3 Identifies Human Naive CD8+ T Cells with Enhanced Effector Differentiation Potential. The Journal of Immunology. 2019 Dec 15;203(12):3179–89.

379. Kurachi M, Kurachi J, Suenaga F, Tsukui T, Abe J, Ueha S, et al. Chemokine receptor CXCR3 facilitates CD8+ T cell differentiation into short-lived effector cells leading to memory degeneration. J Exp Med. 2011 Aug 1;208(8):1605–20.

380. Hickman HD, Reynoso GV, Ngudiankama BF, Cush SS, Gibbs J, Bennink JR, et al. CXCR3 chemokine receptor enables local CD8(+) T cell migration for the destruction of virus-infected cells. Immunity. 2015 Mar 17;42(3):524–37.

381. Slütter B, Pewe LL, Kaech SM, Harty JT. Lung airway-surveilling CXCR3hi memory CD8+ T cells are critical for protection against Influenza A virus. Immunity. 2013 Nov 14;39(5):10.1016/j.immuni.2013.09.013.

382. Apostolidis SA, Kakara M, Painter MM, Goel RR, Mathew D, Lenzi K, et al. Cellular and humoral immune responses following SARS-CoV-2 mRNA vaccination in patients with multiple sclerosis on anti-CD20 therapy. Nat Med. 2021 Sep 14;1–12.

383. Liu J, Yu J, McMahan K, Jacob-Dolan C, He X, Giffin V, et al. CD8 T cells contribute to vaccine protection against SARS-CoV-2 in macaques. Science Immunology. 2022 Aug 9;7(77):eabq7647.

384. Pozzetto B, Legros V, Djebali S, Barateau V, Guibert N, Villard M, et al. Immunogenicity and efficacy of heterologous ChAdOx1–BNT162b2 vaccination. Nature. 2021 Dec;600(7890):701–6.

385. Stuart ASV, Shaw RH, Liu X, Greenland M, Aley PK, Andrews NJ, et al. Immunogenicity, safety, and reactogenicity of heterologous COVID-19 primary vaccination incorporating mRNA, viral-vector, and protein-adjuvant vaccines in the UK (Com-COV2): a single-blind, randomised, phase 2, non-inferiority trial. The Lancet. 2022 Jan 1;399(10319):36–49.

386. Liu X, Shaw RH, Stuart ASV, Greenland M, Aley PK, Andrews NJ, et al. Safety and immunogenicity of heterologous versus homologous prime-boost schedules with an adenoviral vectored and mRNA COVID-19 vaccine (Com-COV): a single-blind, randomised, non-inferiority trial. The Lancet. 2021 Sep 4;398(10303):856–69.

387. Atmar RL, Lyke KE, Deming ME, Jackson LA, Branche AR, El Sahly HM, et al. Homologous and Heterologous Covid-19 Booster Vaccinations. N Engl J Med. 2022 Mar 17;386(11):1046–57.

388. Khoo NKH, Lim JME, Gill US, de Alwis R, Tan N, Toh JZN, et al. Differential immunogenicity of homologous versus heterologous boost in Ad26.COV2.S vaccine recipients. Med. 2022 Feb 11;3(2):104-118.e4.

389. Touizer E, Alrubayyi A, Rees-Spear C, Fisher-Pearson N, Griffith SA, Muir L, et al. Failure to seroconvert after two doses of BNT162b2 SARS-CoV-2 vaccine in a patient with uncontrolled HIV. Lancet HIV. 2021 Jun;8(6):e317–8.

390. Narni-Mancinelli E, Vivier E. Clues that natural killer cells help to control COVID. Nature. 2021 Dec;600(7888):226–7.

391. Bao C, Tao X, Cui W, Hao Y, Zheng S, Yi B, et al. Natural killer cells associated with SARS-CoV-2 viral RNA shedding, antibody response and mortality in COVID-19 patients. Exp Hematol Oncol. 2021 Jan 27;10(1):5.

392. Kučan Brlić P, Brizić I. Taking on SARS-CoV-2. eLife. 2022 Jun 28;11:e80552.

393. Hagemann K, Riecken K, Jung JM, Hildebrandt H, Menzel S, Bunders MJ, et al. Natural killer cell-mediated ADCC in SARS-CoV-2-infected individuals and vaccine recipients. European Journal of Immunology. 2022;52(8):1297–307.

394. Tso FY, Lidenge SJ, Poppe LK, Peña PB, Privatt SR, Bennett SJ, et al. Presence of antibody-dependent cellular cytotoxicity (ADCC) against SARS-CoV-2 in COVID-19 plasma. PLoS One. 2021;16(3):e0247640.

395. Fielding CA, Sabberwal P, Williamson JC, Greenwood EJ, Crozier TW, Zelek W, et al. SARS-CoV-2 host-shutoff impacts innate NK cell functions, but antibody-dependent NK activity is strongly activated through non-spike antibodies. Jonjic S, Diamond B, Mavilio D, editors. eLife. 2022 May 19;11:e74489.

396. Rieke GJ, van Bremen K, Bischoff J, ToVinh M, Monin MB, Schlabe S, et al. Natural Killer Cell-Mediated Antibody-Dependent Cellular Cytotoxicity Against SARS-CoV-2 After Natural Infection Is More Potent Than After Vaccination. J Infect Dis. 2022 May 16;225(10):1688–93.

397. Yu Y, Wang M, Zhang X, Li S, Lu Q, Zeng H, et al. Antibody-dependent cellular cytotoxicity response to SARS-CoV-2 in COVID-19 patients. Sig Transduct Target Ther. 2021 Sep 24;6(1):1–10.

398. Mercado NB, Zahn R, Wegmann F, Loos C, Chandrashekar A, Yu J, et al. Single-Shot Ad26 Vaccine Protects Against SARS-CoV-2 in Rhesus Macaques. Nature. 2020 Oct;586(7830):583–8.

399. Duhan V, Hamdan TA, Xu HC, Shinde P, Bhat H, Li F, et al. NK cell-intrinsic FcεRIγ limits CD8+ T-cell expansion and thereby turns an acute into a chronic viral infection. PLoS Pathog. 2019 Jun;15(6):e1007797.

400. Herrera L, Martin-Inaraja M, Santos S, Inglés-Ferrándiz M, Azkarate A, Perez-Vaquero MA, et al. Identifying SARS-CoV-2 'memory' NK cells from COVID-19 convalescent donors for adoptive cell therapy. Immunology. 2022;165(2):234–49.

401. Cuapio A, Boulouis C, Filipovic I, Wullimann D, Kammann T, Parrot T, et al. NK cell frequencies, function and correlates to vaccine outcome in BNT162b2 mRNA anti-SARS-CoV-2 vaccinated healthy and immunocompromised individuals. Molecular Medicine. 2022 Feb 8;28(1):20.

402. Fielding C, Sabberwal P, Williamson J, Greenwood E, Crozier T, Zelek W, et al. ADNKA overcomes SARS-CoV2-mediated NK cell inhibition through non-spike antibodies [Internet]. Immunology; 2021 Apr [cited 2021 Dec 3]. Available from: http://biorxiv.org/lookup/doi/10.1101/2021.04.06.438630

403. Di Vito C, Calcaterra F, Coianiz N, Terzoli S, Voza A, Mikulak J, et al. Natural Killer Cells in SARS-CoV-2 Infection: Pathophysiology and Therapeutic Implications. Frontiers in Immunology [Internet]. 2022 [cited 2023 Jan 20];13. Available from: https://www.frontiersin.org/articles/10.3389/fimmu.2022.888248

404. Liu W, Scott JM, Langguth E, Chang H, Park PH, Kim S. FcRγ Gene Editing Reprograms Conventional NK Cells to Display Key Features of Adaptive Human NK Cells. iScience. 2020 Oct 20;23(11):101709.

405. Deng X, Terunuma H, Nieda M. Exploring the Utility of NK Cells in COVID-19. Biomedicines. 2022 Apr 26;10(5):1002.

406. Pierce S, Geanes ES, Bradley T. Targeting Natural Killer Cells for Improved Immunity and Control of the Adaptive Immune Response. Front Cell Infect Microbiol [Internet]. 2020 [cited 2021 Apr 7];10.

407. Cox A, Cevik H, Feldman HA, Canaday LM, Lakes N, Waggoner SN. Targeting natural killer cells to enhance vaccine responses. Trends in Pharmacological Sciences. 2021 Sep 1;42(9):789–801.

408. Comeau EM, Holder KA, Fudge NJ, Grant MD. Cytomegalovirus-Driven Adaption of Natural Killer Cells in NKG2Cnull Human Immunodeficiency Virus-Infected Individuals. Viruses. 2019 09;11(3).

409. Costa-Garcia M, Vera A, Moraru M, Vilches C, López-Botet M, Muntasell A. Antibody-mediated response of NKG2Cbright NK cells against human cytomegalovirus. J Immunol. 2015 Mar 15;194(6):2715–24.

410. Wagstaffe HR, Susannini G, Thiébaut R, Richert L, Lévy Y, Bockstal V, et al. Durable natural killer cell responses after heterologous two-dose Ebola vaccination. npj Vaccines. 2021 Jan 29;6(1):1–10.

411. Rieke GJ, van Bremen K, Bischoff J, To Vinh M, Monin MB, Schlabe S, et al. Induction of NK cell-mediated antibody-dependent cellular cytotoxicity (ADCC) against SARS-CoV-2 after natural infection is more potent than after vaccination. J Infect Dis. 2022 Mar 22;jiac060.

412. Vivier E, Tomasello E, Baratin M, Walzer T, Ugolini S. Functions of natural killer cells. Nat Immunol. 2008 May;9(5):503–10.

413. Schuster IS, Coudert JD, Andoniou CE, Degli-Esposti MA. “Natural Regulators”: NK Cells as Modulators of T Cell Immunity. Front Immunol. 2016 Jun 14;7:235.

414. Goodier MR, Jonjić S, Riley EM, Juranić Lisnić V. CMV and natural killer cells: shaping the response to vaccination. Eur J Immunol. 2018 Jan;48(1):50–65.

415. Corey L, Gilbert PB, Tomaras GD, Haynes BF, Pantaleo G, Fauci AS. Immune correlates of vaccine protection against HIV-1 acquisition. Science Translational Medicine. 2015 Oct 21;7(310):310rv7-310rv7.

416. Ng’uni T, Chasara C, Ndhlovu ZM. Major Scientific Hurdles in HIV Vaccine Development: Historical Perspective and Future Directions. Front Immunol [Internet]. 2020 Oct 28 [cited 2020 Dec 26];11. Available from: https://www.ncbi.nlm.nih.gov/pmc/articles/PMC7655734/

417. Haynes BF, Wiehe K, Borrrow P, Saunders KO, Korber B, Wagh K, et al. Strategies for HIV-1 vaccines that induce broadly neutralizing antibodies. Nat Rev Immunol. 2022 Aug 12;1–17.

418. Katz IT, Ehrenkranz P, El-Sadr W. The Global HIV Epidemic: What Will It Take to Get to the Finish Line? JAMA. 2018 Mar 20;319(11):1094–5.

419. Alrubayyi A, Rowland-Jones S, Peppa D. Natural killer cells during acute HIV-1 infection: clues for HIV-1 prevention and therapy. AIDS. 2022 Jul 11;

420. Alrubayyi A, Ogbe A, Moreno Cubero E, Peppa D. Harnessing Natural Killer Cell Innate and Adaptive Traits in HIV Infection. Front Cell Infect Microbiol [Internet]. 2020 [cited 2020 Sep 6];10. Available from: https://www.frontiersin.org/articles/10.3389/fcimb.2020.00395/full

421. Alter G, Heckerman D, Schneidewind A, Fadda L, Kadie CM, Carlson JM, et al. HIV-1 adaptation to NK-cell-mediated immune pressure. Nature. 2011 Aug;476(7358):96–100.

422. Gray JI, Farber DL. Tissue-Resident Immune Cells in Humans. Annual Review of Immunology. 2022;40(1):195–220.

423. Vanhamel J, Bruggemans A, Debyser Z. Establishment of latent HIV-1 reservoirs: what do we really know? J Virus Erad. 2019 Jan 1;5(1):3–9.

424. Van Rompay, A KK. Tackling HIV and AIDS: contributions by non-human primate models. Lab Anim. 2017 Jun;46(6):259–70.

425. Muccio L, Falco M, Bertaina A, Locatelli F, Frassoni F, Sivori S, et al. Late Development of FcεRγneg Adaptive Natural Killer Cells Upon Human Cytomegalovirus Reactivation in Umbilical Cord Blood Transplantation Recipients. Front Immunol. 2018;9:1050.

426. Brownlie D, Scharenberg M, Mold JE, Hård J, Kekäläinen E, Buggert M, et al. Expansions of adaptive-like NK cells with a tissue-resident phenotype in human lung and blood. PNAS [Internet]. 2021 Mar 16 [cited 2021 Mar 19];118(11). Available from: https://www.pnas.org/content/118/11/e2016580118

427. Yang H, Rei M, Brackenridge S, Brenna E, Sun H, Abdulhaqq S, et al. HLA-E-restricted, Gag-specific CD8+ T cells can suppress HIV-1 infection, offering vaccine opportunities. Sci Immunol. 2021 Mar 25;6(57).

428. Peppa D. Entering a new era of harnessing natural killer cell responses in HIV infection. EBioMedicine. 2019 Jun;44:26–7.

429. Cooper MA, Fehniger TA, Colonna M. Is There Natural Killer Cell Memory and Can It Be Harnessed by Vaccination? Cold Spring Harb Perspect Biol. 2018 Oct;10(10):a029512.

430. Sharpe HR, Bowyer G, Brackenridge S, Lambe T. HLA-E: exploiting pathogen-host interactions for vaccine development. Clinical and Experimental Immunology. 2019 May 1;196(2):167–77.

431. Hansen SG, Wu HL, Burwitz BJ, Hughes CM, Hammond KB, Ventura AB, et al. Broadly targeted CD8$^+$ T cell responses restricted by major histocompatibility complex E. Science. 2016 Feb 12;351(6274):714–20.

432. Li D, Brackenridge S, Walters LC, Swanson O, Harlos K, Rozbesky D, et al. Mouse and human antibodies bind HLA-E-leader peptide complexes and enhance NK cell cytotoxicity. Commun Biol. 2022 Mar 28;5(1):1–17.

433. Board NL, Moskovljevic M, Wu F, Siliciano RF, Siliciano JD. Engaging innate immunity in HIV-1 cure strategies. Nat Rev Immunol. 2021 Nov 25;1–14.

434. Ndung'u T, McCune JM, Deeks SG. Why and where an HIV cure is needed and how it might be achieved. Nature. 2019 Dec;576(7787):397–405.

435. Mikulak J, Oriolo F, Zaghi E, Di Vito C, Mavilio D. Natural Killer cells in HIV-1 infection and therapy. AIDS. 2017 Nov 13;31(17):2317–30.

436. Ward AR, Mota TM, Jones RB. Immunological approaches to HIV cure. Seminars in Immunology. 2021 Jan 1;51:101412.

437. Myers JA, Miller JS. Exploring the NK cell platform for cancer immunotherapy. Nat Rev Clin Oncol. 2021 Feb;18(2):85–100.

438. Siliciano JD, Kajdas J, Finzi D, Quinn TC, Chadwick K, Margolick JB, et al. Long-term follow-up studies confirm the stability of the latent reservoir for HIV-1 in resting CD4+ T cells. Nat Med. 2003 Jun;9(6):727–8.

439. Ho YC, Shan L, Hosmane NN, Wang J, Laskey SB, Rosenbloom DIS, et al. Replication-competent noninduced proviruses in the latent reservoir increase barrier to HIV-1 cure. Cell. 2013 Oct 24;155(3):540–51.

440. Hosmane NN, Kwon KJ, Bruner KM, Capoferri AA, Beg S, Rosenbloom DIS, et al. Proliferation of latently infected CD4+ T cells carrying replication-competent HIV-1: Potential role in latent reservoir dynamics. J Exp Med. 2017 Apr 3;214(4):959–72.

441. Archin NM, Sung JM, Garrido C, Soriano-Sarabia N, Margolis DM. Eradicating HIV-1 infection: seeking to clear a persistent pathogen. Nat Rev Microbiol. 2014 Nov;12(11):750–64.

442. Kim Y, Anderson JL, Lewin SR. Getting the 'Kill' into 'Shock and Kill': Strategies to Eliminate Latent HIV. Cell Host Microbe. 2018 Jan 10;23(1):14–26.

443. Olesen R, Vigano S, Rasmussen TA, Søgaard OS, Ouyang Z, Buzon M, et al. Innate Immune Activity Correlates with CD4 T Cell-Associated HIV-1 DNA Decline during Latency-Reversing Treatment with Panobinostat. Journal of Virology. 2015 Oct 15;89(20):10176–89.

444. Hua S, Vigano S, Tse S, Zhengyu O, Harrington S, Negron J, et al. Pegylated Interferon-α-Induced Natural Killer Cell Activation Is Associated With Human Immunodeficiency Virus-1 DNA Decline in Antiretroviral Therapy-Treated HIV-1/Hepatitis C Virus-Coinfected Patients. Clin Infect Dis. 2018 01;66(12):1910–7.

445. Bruel T, Guivel-Benhassine F, Amraoui S, Malbec M, Richard L, Bourdic K, et al. Elimination of HIV-1-infected cells by broadly neutralizing antibodies. Nat Commun. 2016 Mar 3;7:10844.

446. Mujib S, Liu J, Rahman AKMNU, Schwartz JA, Bonner P, Yue FY, et al. Comprehensive Cross-Clade Characterization of Antibody-Mediated Recognition, Complement-Mediated Lysis, and Cell-Mediated Cytotoxicity of HIV-1 Envelope-Specific Antibodies toward Eradication of the HIV-1 Reservoir. J Virol. 2017 Aug 15;91(16):e00634-17.

447. Bredow B von, Arias JF, Heyer LN, Moldt B, Le K, Robinson JE, et al. Comparison of Antibody-Dependent Cell-Mediated Cytotoxicity and Virus Neutralization by HIV-1 Env-Specific Monoclonal Antibodies. Journal of Virology [Internet]. 2016 Apr 27 [cited 2022 Jan 6]; Available from: https://journals.asm.org/doi/abs/10.1128/JVI.00347-16

448. Nishimura Y, Gautam R, Chun TW, Sadjadpour R, Foulds KE, Shingai M, et al. Early antibody therapy can induce long-lasting immunity to SHIV. Nature. 2017 Mar 23;543(7646):559–63.

449. Hessell AJ, Hangartner L, Hunter M, Havenith CEG, Beurskens FJ, Bakker JM, et al. Fc receptor but not complement binding is important in antibody protection against HIV. Nature. 2007 Sep 6;449(7158):101–4.

450. Asokan M, Dias J, Liu C, Maximova A, Ernste K, Pegu A, et al. Fc-mediated effector function contributes to the in vivo antiviral effect of an HIV neutralizing antibody. Proc Natl Acad Sci U S A. 2020 Aug 4;117(31):18754–63.

451. Moog C, Dereuddre-Bosquet N, Teillaud JL, Biedma ME, Holl V, Van Ham G, et al. Protective effect of vaginal application of neutralizing and nonneutralizing inhibitory antibodies against vaginal SHIV challenge in macaques. Mucosal Immunol. 2014 Jan;7(1):46–56.

452. Hessell AJ, Shapiro MB, Powell R, Malherbe DC, McBurney SP, Pandey S, et al. Reduced Cell-Associated DNA and Improved Viral Control in Macaques following Passive Transfer of a Single Anti-V2 Monoclonal Antibody and Repeated Simian/Human Immunodeficiency Virus Challenges. J Virol. 2018 Jun 1;92(11):e02198-17.

453. Santra S, Tomaras GD, Warrier R, Nicely NI, Liao HX, Pollara J, et al. Human Non-neutralizing HIV-1 Envelope Monoclonal Antibodies Limit the Number of Founder Viruses during SHIV Mucosal Infection in Rhesus Macaques. PLoS Pathog. 2015 Aug;11(8):e1005042.

454. Liu LL, Béziat V, Oei VYS, Pfefferle A, Schaffer M, Lehmann S, et al. Ex Vivo Expanded Adaptive NK Cells Effectively Kill Primary Acute Lymphoblastic Leukemia Cells. Cancer Immunol Res. 2017;5(8):654–65.

455. Garrido C, Abad-Fernandez M, Tuyishime M, Pollara JJ, Ferrari G, Soriano-Sarabia N, et al. Interleukin-15-Stimulated Natural Killer Cells Clear HIV-1-Infected Cells following Latency Reversal Ex Vivo. J Virol. 2018 15;92(12).

456. Romee R, Rosario M, Berrien-Elliott MM, Wagner JA, Jewell BA, Schappe T, et al. Cytokine-induced memory-like natural killer cells exhibit enhanced responses against myeloid leukemia. Sci Transl Med. 2016 21;8(357):357ra123.

457. Kazer SW. Evolution and Diversity of Immune Responses during Acute HIV Infection. OPEN ACCESS. 2020 Nov 17;17.

458. Buchbinder SP, Mehrotra DV, Duerr A, Fitzgerald DW, Mogg R, Li D, et al. Efficacy assessment of a cell-mediated immunity HIV-1 vaccine (the Step Study): a double-blind, randomised, placebo-controlled, test-of-concept trial. Lancet. 2008 Nov 29;372(9653):1881–93.

459. Hammer SM, Sobieszczyk ME, Janes H, Karuna ST, Mulligan MJ, Grove D, et al. Efficacy Trial of a DNA/rAd5 HIV-1 Preventive Vaccine. N Engl J Med. 2013 Nov 28;369(22):2083–92.

460. Barouch DH, O'Brien KL, Simmons NL, King SL, Abbink P, Maxfield LF, et al. Mosaic HIV-1 vaccines expand the breadth and depth of cellular immune responses in rhesus monkeys. Nat Med. 2010 Mar;16(3):319–23.

461. Santra S, Liao HX, Zhang R, Muldoon M, Watson S, Fischer W, et al. Mosaic vaccines elicit CD8+ T lymphocyte responses that confer enhanced immune coverage of diverse HIV strains in monkeys. Nat Med. 2010 Mar;16(3):324–8.

462. Yang OO, Ali A, Kasahara N, Faure-Kumar E, Bae JY, Picker LJ, et al. Short conserved sequences of HIV-1 are highly immunogenic and shift immunodominance. J Virol. 2015 Jan 15;89(2):1195–204.

463. Barouch DH, Tomaka FL, Wegmann F, Stieh DJ, Alter G, Robb ML, et al. Evaluation of a Mosaic HIV-1 Vaccine in a Randomized, Double-Blinded, Placebo-Controlled Phase I/IIa Clinical Trial and in Rhesus Monkeys. Lancet. 2018 Jul 21;392(10143):232–43.

464. Borthwick N, Lin Z, Akahoshi T, Llano A, Silva-Arrieta S, Ahmed T, et al. Novel, in-natural-infection subdominant HIV-1 CD8+ T-cell epitopes revealed in human recipients of conserved-region T-cell vaccines. PLoS One. 2017;12(4):e0176418.

465. Hayes P, Fernandez N, Ochsenbauer C, Dalel J, Hare J, King D, et al. Breadth of CD8 T-cell mediated inhibition of replication of diverse HIV-1 transmitted-founder isolates correlates with the breadth of recognition within a comprehensive HIV-1 Gag, Nef, Env and Pol potential T-cell epitope (PTE) peptide set. PLoS ONE [Internet]. 2021 [cited 2023 Feb 2];16(11). Available from: https://www.ncbi.nlm.nih.gov/pmc/articles/PMC8598018/

466. Moretta A, Marcenaro E, Parolini S, Ferlazzo G, Moretta L. NK cells at the interface between innate and adaptive immunity. Cell Death Differ. 2008 Feb;15(2):226–33.

467. Raulet DH. Interplay of natural killer cells and their receptors with the adaptive immune response. Nat Immunol. 2004 Oct;5(10):996–1002.

468. Pallmer K, Oxenius A. Recognition and Regulation of T Cells by NK Cells. Frontiers in Immunology [Internet]. 2016 [cited 2023 Jan 26];7. Available from: https://www.frontiersin.org/articles/10.3389/fimmu.2016.00251

469. Peppa D, Gill US, Reynolds G, Easom NJW, Pallett LJ, Schurich A, et al. Up-regulation of a death receptor renders antiviral T cells susceptible to NK cell–mediated deletion. J Exp Med. 2013 Jan 14;210(1):99–114.

470. Chung AW, Alter G. Systems serology: profiling vaccine induced humoral immunity against HIV. Retrovirology. 2017 Dec;14(1):57.

471. Nelde A, Bilich T, Heitmann JS, Maringer Y, Salih HR, Roerden M, et al. SARS-CoV-2-derived peptides define heterologous and COVID-19-induced T cell recognition. Nat Immunol. 2021 Jan;22(1):74–85.

472. Swadling L, Diniz MO, Schmidt NM, Amin OE, Chandran A, Shaw E, et al. Pre-existing polymerase-specific T cells expand in abortive seronegative SARS-CoV-2. Nature. 2022 Jan;601(7891):110–7.

473. Bortolotti D, Gentili V, Rizzo S, Rotola A, Rizzo R. Sars-Cov-2 Spike 1 protein control Natural killer cells activation via HLA-E/NKG2A pathway. [Internet]. In Review; 2020 May [cited 2020 Sep 6]. Available from: https://www.researchsquare.com/article/rs-31860/v1

474. Chen X, Rostad CA, Anderson LJ, Sun HY, Lapp SA, Stephens K, et al. The development and kinetics of functional antibody-dependent cell-mediated cytotoxicity (ADCC) to SARS-CoV-2 spike protein. Virology. 2021 Jul;559:1–9.

475. Richardson SI, Manamela NP, Motsoeneng BM, Kaldine H, Ayres F, Makhado Z, et al. SARS-CoV-2 Beta and Delta variants trigger Fc effector function with increased cross-reactivity. CR Med [Internet]. 2022 Feb 15 [cited 2023 Jan 3];3(2). Available from: https://www.cell.com/cell-reports-medicine/abstract/S2666-3791(22)00003-9

476. Hansen SG, Hancock MH, Malouli D, Marshall EE, Hughes CM, Randall KT, et al. Myeloid cell tropism enables MHC-E-restricted CD8+ T cell priming and vaccine efficacy by the RhCMV/SIV vaccine. Sci Immunol. 2022 Jun 24;7(72):eabn9301.

477. Wu HL, Wiseman RW, Hughes CM, Webb GM, Abdulhaqq SA, Bimber BN, et al. The Role of MHC-E in T Cell Immunity Is Conserved among Humans, Rhesus Macaques, and Cynomolgus Macaques. J Immunol. 2018 Jan 1;200(1):49–60.